Climate-driven modelling of the spread and control of West Nile virus and Usutu virus in Germany

Cumulative Dissertation

to obtain the doctoral degree of natural sciences

Dr. rer. nat.

Universität Hamburg

Faculty of Mathematics, Informatics and Natural Sciences

Department of Biology

submitted by

Pride Duve

Hamburg, 2026

Acknowledgements

First and foremost, I give thanks to the Almighty God, whose grace, strength, and guidance have carried me through every stage of this journey. In moments of uncertainty and challenge, I found reassurance in His presence, and it is through His blessing that I have been able to reach this milestone.

This journey has not been mine alone. Behind every late night, every moment of doubt, and every small victory, stood a family whose unwavering support made it all possible. To my beloved wife, ***Minenhle***, and my daughter, ***Alma***, thank you for your patience, love, and understanding, especially during times when my attention was divided and my schedule demanding. You have been my greatest source of motivation and joy.

I am equally grateful to my siblings, ***Pacifier, Takalani, Tumelo, Thabhelo, and Innocentia***, and to my parents, ***Zodwa*** and ***Aramu***. Your encouragement, guidance, and constant belief in me have been a steady foundation throughout my life, and this achievement is as much yours as it is mine.

Moving from a purely mathematical background into the world of mosquito ecology was both challenging and exciting, and I was fortunate to be guided by the best supervisors. I would like to express my deepest appreciation to my Personal Instructor, ***Dr. Renke Lühken***, for the opportunity to undertake this PhD under his supervision. His support, trust, and openness to my ideas created an environment in which I could grow both academically and personally. I am also sincerely thankful to ***Dr. Felix Sauer***, whose mentorship, insightful feedback, and careful review of my work greatly improved the quality of this research.

I would further like to thank ***Prof. Dr. med. Dr. med. habil. Jonas Schmidt-Chanasit*** for fostering a supportive and inspiring research environment, and for his valuable input during Arbovirologie seminars, which enriched my perspective and understanding.

Finally, I am grateful to my colleagues, ***Leif, Kristopher, Sara, Paula, Amrei, and Magdalena***, and to all those who shared in this journey through discussions, collaborations, summer schools, lunch in the kitchen, PhD seminars, or simple words of encouragement, each of you contributed in your own way to making this experience memorable.

"***Thank you very much - Vielen Dank - Ngiyabonga - Maita basa.***"

List of Publications

1. **Duve, P.**, Sauer, F. G. and Lühken, R., 2026. *Modelling the impact of temperature and bird migration on the spread of West Nile virus.* *One Health*
2. **Duve, P.**, Sauer, F. G. and Lühken, R., 2026. *Modelling the control of West Nile virus using mosquito reduction methods, vaccination of equids, and human behavioural adoption to the usage of personal protective equipment.* *Ecological Modelling*
3. Rauhöft L., **Duve P.**, Martins Afonso S. M., Jöst H., Şulesco T., Sauer F. G., Lühken R., 2026. *A process-based model simulating the life cycle of Culex pipiens s.s./Cx. torrentium in Germany.* *Parasites & Vectors*
4. **Duve, P.**, Sauer, F. G. and Lühken, R., 2026. *A temperature-driven diffusion model of Usutu virus spread in Germany with spillover into neighbouring countries.* *Preprint*

Universität Hamburg
DER FORSCHUNG | DER LEHRE | DER BILDUNG

FACULTY
OF MATHEMATICS, INFORMATICS
AND NATURAL SCIENCES

Declaration about personal contribution to manuscripts/publications in a cumulative thesis (please submit one form per manuscript/publication)

Candidate's name: Pride Duve

Manuscript (including all authors, title, and if applicable journal, year; mark all first authors with asterisk):

Modelling the impact of temperature and bird migration on the spread of West Nile virus

Pride Duve*, Felix Gregor Sauer, Renke Lühken

One Health journal

Link to publication (if published):

https://www.sciencedirect.com/science/article/pii/S2352771426000704

Detailed description of own contribution to this manuscript

Conceptualization and planning of project:

The study design were developed by the candidate, including the formulation of the research objectives and modelling framework, under the scientific guidance of the supervisor.

Method development:

The candidate designed and developed the mathematical model, and its computational framework.

Data generation and analyses (including contribution to specific figures):

The candidate performed all data processing, model simulations, and analyses. All figures and visualisations presented in the manuscript were simulated by the candidate.

Writing and editing of manuscript:

The original manuscript was written by the candidate. The supervisor contributed through critical review, feedback, and editing of the manuscript.

I confirm that the above information is accurate

Candidate

HH, 03/06/2026 

Place, date Signature of candidate

Supervisor name:

Prof. Dr. med. Dr. med. habil. Jonas Schmidt-Chanasit

HH, 05.06.26 Jonas Schmidt-Chanasit

Place, date Signature of supervisor

Universität Hamburg
DER FORSCHUNG | DER LEHRE | DER BILDUNG

FACULTY
OF MATHEMATICS, INFORMATICS
AND NATURAL SCIENCES

Declaration about personal contribution to manuscripts/publications in a cumulative thesis (please submit one form per manuscript/publication)

Candidate's name: Pride Duve

Manuscript (including all authors, title, and if applicable journal, year; mark all first authors with asterisk):
Modelling the control of West Nile virus using mosquito reduction methods, vaccination of equids, and human behavioural adaptation to the usage of personal protective equipment

Pride Duve*, Felix Gregor Sauer, Renke Lühken

Ecological Modelling

Link to publication (if published):

https://www.sciencedirect.com/science/article/pii/S0304380026001341

Detailed description of own contribution to this manuscript

Conceptualization and planning of project:

The study design were developed by the candidate, including the formulation of the research objectives and modelling framework, under the scientific guidance of the supervisor.

Method development:

The candidate designed and developed the mathematical model, and its computational framework.

Data generation and analyses (including contribution to specific figures):

The candidate performed all data processing, model simulations, and analyses. All figures and visualisations presented in the manuscript were simulated by the candidate.

Writing and editing of manuscript:

The original manuscript was written by the candidate. The supervisor contributed through critical review, feedback, and editing of the manuscript.

I confirm that the above information is accurate

Candidate

HH, 03/06/2026 
Place, date Signature of candidate

Supervisor name:
Prof. Dr. med. Dr. med. habil. Jonas Schmidt-Chanasit

HH, 05.06.26 Jonas Schmidt-Chanasit
Place, date Signature of supervisor

Universität Hamburg
DER FORSCHUNG | DER LEHRE | DER BILDUNG

FACULTY
OF MATHEMATICS, INFORMATICS
AND NATURAL SCIENCES

Declaration about personal contribution to manuscripts/publications in a cumulative thesis (please submit one form per manuscript/publication)

Candidate's name: Pride Duve

Manuscript (including all authors, title, and if applicable journal, year; mark all first authors with asterisk):

A process-based model simulating the life cycle of Culex pipiens s.s./Cx. torrentium in Germany

Rauhöft L*., Duve P*., Martins Afonso S.M., Jöst H., Sulesco T., Sauer F.G., Lühken R

Parasites & Vectors

Link to publication (if published):

https://link.springer.com/article/10.1186/s13071-026-07410-4

Detailed description of own contribution to this manuscript

Conceptualization and planning of project:

The candidate contributed to the conceptualization and design of the model, together with the co-authors.

Method development:

The candidate contributed in the model formulation, sensitivity analysis, validation, writing and reviewing the inital draft.

Data generation and analyses (including contribution to specific figures):

The candidate contributed to the analysis that simulated Figures 1 and 8.

Writing and editing of manuscript:

Part of the model formulation, sensitivity analysis, validation and the initial draft of the model were written by the candidate.

I confirm that the above information is accurate

Candidate

HH, 03/06/2026 

Place, date Signature of candidate

Supervisor name:

Prof. Dr. med. Dr. med. habil. Jonas Schmidt-Chanasit

HH, 05.06.26 Jonas Schmidt-Chanasit

Place, date Signature of supervisor

Universität Hamburg
DER FORSCHUNG | DER LEHRE | DER BILDUNG

FACULTY
OF MATHEMATICS, INFORMATICS
AND NATURAL SCIENCES

Declaration about personal contribution to manuscripts/publications in a cumulative thesis (please submit one form per manuscript/publication)

Candidate's name: Pride Duve

Manuscript (including all authors, title, and if applicable journal, year; mark all first authors with asterisk):

A temperature-driven diffusion model of Usutu virus spread in Germany with spillover into neighbouring countries

Pride Duve*, Dániel Cadar, Norbert Becker, Jonas Schmidt-Chanasit, Felix Gregor Sauer, and Renke Lühken

Link to publication (if published): (Preprint)

https://arxiv.org/pdf/2605.03146

Detailed description of own contribution to this manuscript

Conceptualization and planning of project:

The study design were developed by the candidate, including the formulation of the research objectives and modelling framework, under the scientific guidance of the supervisor.

Method development:

The candidate designed and developed the mathematical model, and its computational framework.

Data generation and analyses (including contribution to specific figures):

The candidate performed model simulations, and analyses. All figures and visualisations presented in the manuscript were simulated by the candidate.

Writing and editing of manuscript:

The original manuscript was written by the candidate. The supervisor contributed through critical review, feedback, and editing of the manuscript.

I confirm that the above information is accurate

Candidate

HH, 03/06/2026 
Place, date Signature of candidate

Supervisor name:
Prof. Dr. med. Dr. med. habil. Jonas Schmidt-Chanasit

HH, 05.06.26 Jonas Schmidt-Chanasit
Place, date Signature of supervisor

Thesis Reviewers:

Professor Dr. med. Dr. med. habil. Jonas Schmidt-Chanasit
Dr. Renke Lühken

Date of Disputation: 09 October 2026

Eidesstattliche Versicherung | *Declaration on Oath*

Hiermit versichere ich an Eides statt, die vorliegende Dissertationsschrift selbst verfasst und keine anderen als die angegebenen Hilfsmittel und Quellen benutzt zu haben. Sofern im Zuge der Erstellung der vorliegenden Dissertationsschrift generative Künstliche Intelligenz (gKI) basierte elektronische Hilfsmittel verwendet wurden, versichere ich, dass meine eigene Leistung im Vordergrund stand und dass eine vollständige Dokumentation aller verwendeten Hilfsmittel gemäß der Guten wissenschaftlichen Praxis vorliegt. Ich trage die Verantwortung für eventuell durch die gKI generierte fehlerhafte oder verzerrte Inhalte, fehlerhafte Referenzen, Verstöße gegen das Datenschutz- und Urheberrecht oder Plagiate.

I hereby declare and affirm that this doctoral dissertation is my own work and that I have not used any aids and sources other than those indicated. If electronic resources based on generative artificial intelligence (gAI) were used in the course of writing this dissertation, I confirm that my own work was the main and value-adding contribution and that complete documentation of all resources used is available in accordance with good scientific practice. I am responsible for any erroneous or distorted content, incorrect references, violations of data protection and copyright law or plagiarism that may have been generated by the gAI.

Hamburg, 03/06/2026

Ort, den | City, date



Unterschrift | Signature

Abstract

Mosquito-borne flaviviruses remain a significant public health and ecological concern, influenced by climate change, environmental variability, and the range expansion of entomologically relevant mosquito vectors. In recent years, West Nile virus (WNV) and Usutu virus (USUV) have become endemic in parts of Europe, including Germany, posing risks to birds, humans, and other vertebrate hosts. Despite increasing surveillance, important questions remain about the factors driving their spatial spread, seasonal outbreaks, and the success of intervention strategies.

This PhD thesis investigates the transmission and spread of mosquito-borne flaviviruses through mechanistic modelling frameworks that integrate mosquito ecology, eco-epidemiological processes, and environmental variables. Initially, a process-based ordinary differential equation (ODE) model was developed to simulate the population dynamics of *Culex pipiens* s.s./*Cx. torrentium*, the primary vectors of WNV and USUV in Germany. The model incorporated temperature-, rainfall-, and photoperiod-dependent processes governing mosquito development, mortality, reproduction, and overwintering. Validation against mosquito surveillance data from 106 sampling sites demonstrated good agreement between simulated and observed mosquito phenology, with temperature as the primary driver of mosquito seasonal dynamics.

Building on these insights, ODE and partial differential equation (PDE)-based eco-epidemiology models were developed to investigate the transmission dynamics and spatial spread of WNV and USUV. These models incorporated temperature-dependent transmission processes, spatial diffusion to represent local dispersal, and advection to capture directional movement associated with migratory birds. Furthermore, optimal control theory was applied to evaluate the timing, intensity, and cost-effectiveness of intervention strategies, including mosquito control, equid vaccination, and personal protective measures.

Results obtained show that temperature is also a key variable influencing seasonal transmission patterns and regional differences in WNV and USUV infection risk. Transmission remains mainly localised, driven by environmental conditions and vector abundance, with eastern Germany and the Upper Rhine Valley identified as consistently high-risk areas for both viruses. Simulations that include migratory bird movements indicate that changes in mosquito feeding behaviour towards migratory hosts may significantly accelerate WNV spread, supporting the hypothesis that migratory birds

might facilitate its long-distance dispersal. Conversely, USUV spread appears to be driven mainly by short-range processes involving highly vulnerable resident bird species, especially the Eurasian blackbird (*Turdus merula*), which is consistent with its relatively slower spatial spread during the early years of endemicity.

Optimal control analyses suggest that mosquito control efforts started in early spring and intensified in early May may reduce the August peak in the infectious bird population. Furthermore, a combined approach of mosquito control methods, human PPE adoption, and equid vaccination could be the most effective strategy for both human and equid hosts. These results further indicate that targeting overwintering mosquito populations can lessen the intensity of interventions needed during the transmission season. To aid decision-making, a free and open-source web application has been developed, allowing users to explore the impact of different control strategies under various temperature projections, such as low-mitigation (SSP126), intermediate (SSP245), and high-emission (SSP585) scenarios.

Although WNV and USUV differ in their public health implications, the models highlight their shared ecological transmission pathway, driven by common vector species. This suggests that integrated control strategies can simultaneously reduce the impact of both viruses. The general findings of this thesis advance the understanding of the ecological and climatic factors influencing arbovirus transmission in Germany and provide a quantitative basis for developing climate-informed surveillance and control strategies.

Zusammenfassung

Durch Stechmücken übertragene Flaviviren stellen ein zunehmendes Problem für die öffentliche Gesundheit und die Ökologie dar, das durch den Klimawandel, Umweltveränderungen und die Ausbreitung entomologisch relevanter Stechmückenvektoren beeinflusst wird. In den letzten Jahren sind das West-Nil-Virus (WNV) und das Usutu-Virus (USUV) in Teilen Europas, darunter auch in Deutschland, endemisch geworden und stellen ein Risiko für Vögel, Menschen und andere Wirbeltierwirte dar. Trotz verstärkter Überwachung bleiben wichtige Fragen zu den Faktoren offen, die ihre räumliche Ausbreitung, saisonalen Ausbrüche und die Wirksamkeit von Interventionsstrategien bestimmen.

Diese Dissertation untersucht die Übertragung und Ausbreitung von durch Stechmücken übertragenen Flaviviren mithilfe mechanistischer Modellierungsansätze, die Stechmückenökologie, öko-epidemiologische Prozesse und Umweltvariablen integrieren. Zunächst wurde ein prozessbasiertes Modell auf Grundlage gewöhnlicher Differentialgleichungen (ODE) entwickelt, um die Populationsdynamik von *Culex pipiens* s.s./*Cx. torrentium*, den wichtigsten Vektoren von WNV und USUV in Deutschland, zu simulieren. Das Modell berücksichtigt temperatur-, niederschlags- und photoperiodenabhängige Prozesse, welche die Entwicklung, Mortalität, Reproduktion und Überwinterung der Stechmücken steuern. Die Validierung anhand von Überwachungsdaten aus 106 Fangstandorten zeigte eine gute Übereinstimmung zwischen simulierten und beobachteten Phänologiemustern, wobei sich die Temperatur als der wichtigste Treiber der saisonalen Stechmückendynamik erwies.

Aufbauend auf diesen Erkenntnissen wurden ODE- und PDE-basierte öko-epidemiologische Modelle entwickelt, um die Übertragungsdynamik und räumliche Ausbreitung von WNV und USUV zu untersuchen. Die Modelle berücksichtigen temperaturabhängige Übertragungsprozesse, räumliche Diffusion zur Beschreibung lokaler Ausbreitung sowie Advektion zur Erfassung gerichteter Bewegungen von Zugvögeln. Darüber hinaus wurde die Theorie der optimalen Steuerung angewendet, um den Zeitpunkt, die Intensität und die Kosteneffizienz verschiedener Interventionsstrategien, darunter Stechmückenbekämpfung, Impfung von Equiden und persönliche Schutzmaßnahmen, zu bewerten.

Die Ergebnisse zeigen, dass die Temperatur ein zentraler Faktor für saisonale Übertragungsmuster und regionale Unterschiede im Infektionsrisiko von WNV und USUV ist.

Die Übertragung bleibt überwiegend lokal begrenzt und wird durch Umweltbedingungen sowie die Vektorhäufigkeit bestimmt, wobei Ostdeutschland und das Oberrheintal als Gebiete mit dauerhaft erhöhtem Risiko für beide Viren identifiziert wurden. Simulationen unter Berücksichtigung von Zugvogelbewegungen deuten darauf hin, dass Veränderungen im Wirtswahlverhalten von Stechmücken zugunsten von Zugvögeln die Ausbreitung von WNV erheblich beschleunigen können und damit die Hypothese unterstützen, dass Zugvögel zur Ausbreitung des Virus über große Entfernungen beitragen. Im Gegensatz dazu scheint die Ausbreitung von USUV hauptsächlich durch kurzreichweitige Prozesse bestimmt zu werden, an denen besonders anfällige resident lebende Vogelarten beteiligt sind, insbesondere die Amsel (*Turdus merula*), was mit ihrer vergleichsweise langsameren räumlichen Ausbreitung während der frühen Phase der Endemizität übereinstimmt.

Analysen zur optimalen Steuerung legen nahe, dass Maßnahmen zur Stechmückenbekämpfung, die bereits im frühen Frühjahr beginnen und Anfang Mai intensiviert werden, den Höhepunkt der infektiösen Vogelpopulation im August reduzieren können. Darüber hinaus erwies sich ein kombinierter Ansatz aus Stechmückenbekämpfung, persönlichem Schutz und der Impfung von Equiden als die wirksamste Strategie zum Schutz menschlicher und equiner Wirte. Die Ergebnisse zeigen ferner, dass die Bekämpfung überwinternder Stechmückenpopulationen die Intensität der während der Übertragungssaison erforderlichen Maßnahmen verringern kann. Zur Unterstützung von Entscheidungsträgern wurde eine frei verfügbare Open-Source-Webanwendung entwickelt, mit der die Auswirkungen verschiedener Bekämpfungsstrategien unter unterschiedlichen Temperaturszenarien - darunter SSP126, SSP245 und SSP585 - untersucht werden können.

Obwohl sich WNV und USUV hinsichtlich ihrer Bedeutung für die öffentliche Gesundheit unterscheiden, verdeutlichen die Modelle ihren gemeinsamen ökologischen Übertragungsweg über dieselben Vektorarten. Dies legt nahe, dass integrierte Bekämpfungsstrategien die Auswirkungen beider Viren gleichzeitig reduzieren können. Die Ergebnisse dieser Dissertation tragen zu einem besseren Verständnis der ökologischen und klimatischen Faktoren bei, welche die Übertragung von Arboviren in Deutschland beeinflussen, und liefern eine quantitative Grundlage für die Entwicklung klimaorientierter Überwachungs- und Bekämpfungsstrategien.

Contents

Acknowledgements i

List of Publications ii

List of Figures xv

List of Tables xvi

List of Abbreviations xvii

1 Introduction 1
- 1.1 Mosquito-borne diseases . . . 1
- 1.2 Arboviruses . . . 2
- 1.3 West Nile virus epidemiology . . . 2
- 1.4 Usutu virus epidemiology . . . 4
- 1.5 Mosquito control methods . . . 5
  - 1.5.1 Control of aquatic stages . . . 6
  - 1.5.2 Adult control . . . 6
- 1.6 Organisation of the PhD thesis . . . 8

2 State of the art 9
- 2.1 Processes-based models for mosquito seasonal dynamics . . . 9
- 2.2 Mechanistic models of West Nile virus . . . 10
- 2.3 Mechanistic models of Usutu virus . . . 13
- 2.4 Summary . . . 14
- 2.5 Objectives of the PhD project . . . 15

3 Discussions and conclusions 16
- 3.1 Methodological framework . . . 16
  - 3.1.1 *Culex pipiens* s.s./*Cx. torrentium* process-based model . . . 16
  - 3.1.2 WNV-ODE-based models . . . 17
  - 3.1.3 WNV & USUV PDE-based models . . . 18
- 3.2 Environmental forcing . . . 19
- 3.3 Historical temperature trends in Germany . . . 20
- 3.4 Impact of temperature on the basic reproductive number . . . 22
- 3.5 Spreading pattern of West Nile virus in Germany . . . 27

3.6 Spreading pattern of Usutu virus in Germany 28
3.7 Control of West Nile virus and Usutu virus 28
3.8 Conclusion 30
3.9 Take-home message 32

List of References **34**

4 Appendix **57**
4.1 **Publication 1**: *Modelling the impact of temperature and bird migration on the spread of West Nile virus* 57
4.2 **Publication 2**: *Modelling the control of West Nile virus using mosquito reduction methods, vaccination of equids, and human behavioural adaptation to the usage of personal protective equipment* 82
4.3 **Publication 3**: *A process-based model simulating the life-cycle of Culex pipiens s.s./Cx. torrentium (Diptera: Culicidae) in Germany* 105
4.4 **Publication 4**: *A temperature-driven diffusion model of Usutu virus spread in Germany with spillover into neighbouring countries* 122

List of Figures

3.1 Overview of the modelling frameworks used in this thesis. ODE models were employed to examine the temporal dynamics of *Culex* vectors responsible for transmitting WNV, and WNV transmission dynamics, optimal control strategies, and the web-based Shiny App. The PDE model provided a spatially explicit representation of both the WNV and USUV models under the influence of diffusion, advection, and temperature forcing. 19
3.2 Number of decade heat wave events observed in the period 1965-2024. . . . 21
3.3 Number of heat wave events observed in the period 1972-2024, in selected stations in Berlin, Halle, Hamburg, Mannheim. 21
3.4 Onset of theoretical mosquito activity season based on ($T \geq 12^{\circ}C$ for 10 consecutive days 1965-2024), with r=-0.45. 22
3.5 Basic reproductive number for WNV and USUV, for the period 1972-2024. . . 26
3.6 Decadal WNV basic reproduction number $R_0(x)$ for the period 1946-2025. . . 26
3.7 Decadal USUV basic reproduction number $R_0(x)$ for the period 1946-2025. . 27

List of Tables

3.1 Definition and values of WNV and USUV parameters for simulating the basic reproductive numbers. 25

List of Abbreviations

- **Arboviruses**: Arthropod-borne viruses
- **CHIKV**: Chikungunya virus
- **ODE**: Ordinary differential equation
- **PDE**: Partial differential equation
- **PPE**: Personal protective equipment
- R_0: Basic reproduction number
- **SEIR model**: Susceptible-Exposed-Infected/Infectious-Recovered/Removed
- **USUV**: Usutu virus
- **SSP126:** Shared Socioeconomic Pathway 1-2.6 (low-emissions scenario)
- **SSP245:** Shared Socioeconomic Pathway 2-4.5 (intermediate-emissions scenario)
- **SSP585:** Shared Socioeconomic Pathway 5-8.5 (high-emissions scenario)
- **WHO**: World Health Organization
- **WNV**: West Nile virus

1 Introduction

1.1 Mosquito-borne diseases

Despite decades of progress in medicine, public health, and disease control technologies, mosquito-borne diseases remain a growing public health concern and impose substantial global epidemiological and economic burdens. Factors such as climate change, rapid urbanisation, land-use changes, socio-economic shifts, and increased international travel have been linked to the spread and re-emergence of various mosquito-borne disease pathogens (Franklinos et al., 2019; Tatem et al., 2006; Zayed, 2020). These factors affect mosquito survival, biting frequency, gonotrophic cycles, the extrinsic incubation period (Brugger and Rubel, 2009; Rubel et al., 2008), and particularly the distribution of vectors and pathogens, ultimately influencing the force of infection (Anderson and May, 1991; Shocket et al., 2020). To date, more than half of the world's population lives in areas at risk of mosquito-borne infections (Moura-Neto et al., 2019; Ross et al., 2022; Varghese et al., 2023; World Health Organization, 2025), as various mosquito species keep spreading into regions that were once considered low-risk (Baker et al., 2021; Ryan et al., 2017).

Over 3,500 mosquito species have been identified worldwide, found on every continent except Antarctica, with only a few being medically relevant (Hawkes and Hopkins, 2021). *Anopheles gambiae* is regarded as the most deadly mosquito species due to its high vector capacity, driven by its strong anthropophily, high survival rate, frequent human biting, and high vector competence for *Plasmodium* parasites (Garrett-Jones and Shidrawi, 1969; Takken et al., 2024; Wamae et al., 2015). Mosquitoes of the *Aedes* genus are also significant vectors because of their substantial high global disease burden. This burden results from their role in causing large outbreaks of dengue, Zika, chikungunya, and yellow fever, leading to increased morbidity and socioeconomic impacts worldwide (Powell et al., 2018; Powell, 2018).

Mosquito-borne diseases are caused by diverse pathogens, including viruses, bacteria and protozoan parasites. Among these, arthropod-borne viruses (arboviruses) constitute a distinct subgroup characterised by transmission via infected mosquitoes, such as *Aedes* and *Culex* species (Schulz and Becker, 2018). These viruses usually circulate in complex enzootic cycles involving mosquito vectors and vertebrate hosts, and they may cause symptoms ranging from mild febrile illness to severe neurological or haemorrhagic disease (Franklinos et al., 2019; Huang et al., 2019).

1.2 Arboviruses

Recent centuries have seen a worldwide rise in arbovirus infections, with every continent except Antarctica experiencing at least one outbreak. To date, various arboviruses have been documented globally, including dengue fever, chikungunya, Zika, yellow fever, Oropouche, West Nile, Usutu, and St. Louis encephalitis. Dengue is considered as the most widespread arbovirus, causing the highest number of cases in the Americas, with cyclical epidemics occurring every three to five years (Center for Disease Control, 2025; World Health Organization, 2023). In 2024 alone, over 13 million dengue cases were reported across North, Central, and South America, as well as the Caribbean, with the risk remaining high in these regions (Center for Disease Control, 2025; Haider et al., 2025). Notably, in 2024, Europe reported more than 300 locally acquired dengue cases, surpassing the total number of cases recorded over the previous 15 years, highlighting the threat this virus is posing in temperate regions.

Chikungunya virus is another globally distributed arbovirus that has a significant impact on human populations. Outbreaks of chikungunya have occurred in Africa, the Americas, Asia, Europe, and islands in the Indian and Pacific Oceans. The Americas have continued to bear the heaviest burden of chikungunya for several years (de Souza et al., 2024). Several vaccines have been approved worldwide for specific arboviruses. For example, at least one human vaccine has been approved for yellow fever, Japanese encephalitis, dengue, tick-borne encephalitis, and chikungunya virus (Center for Disease Control, 2025). However, challenges related to arboviruses still remain. Key setbacks include restrictions for certain groups and settings, limited access and coverage, among others, leaving large susceptible populations unprotected (World Health Organization, 2019; Weber et al., 2024).

Among these arboviruses are West Nile virus and Usutu virus, two closely related mosquito-borne flaviviruses that share similar transmission cycles involving *Culex* mosquitoes and avian amplifying hosts. Originally endemic to Africa, both viruses have expanded their geographic range in recent decades, establishing sustained, recurring transmissions in large parts of Europe.

1.3 West Nile virus epidemiology

WNV is a mosquito-borne virus of the *Flavivirus* genus in the *Flaviviridae* family of the Japanese encephalitis antigenic complex (Calisher et al., 1989). It circulates between mosquitoes and birds (Petersen et al., 2013), with humans and other mammals considered incidental dead-end hosts. *Culex* mosquitoes are the dominant vectors, while several bird species are susceptible to the virus. WNV was first isolated in 1937

from the blood of a febrile patient in the West Nile district of Uganda, after which it was named (Smithburn et al., 1940).

Historical WNV outbreaks occurred in Israel during the mid-20th century and again in 1980 (Katz et al., 2001; Marberg et al., 1956). Subsequently, between 1997 and 1998, the virus was associated with the deaths of thousands of domestic geese, prompting large-scale culling measures to limit further transmission (Giladi et al., 2001). In Europe, the first major outbreak of the West Nile disease occurred in Romania in 1996, resulting in a significant number of human cases and marking the emergence of WNV as a major public health concern on the continent (Tsai et al., 1998). By 1999, the virus had spread to the Western Hemisphere, arriving in New York City (Giladi et al., 2001). Genetic analysis revealed that the New York isolates shared over 99.8% genetic identity with the virus isolated from the brain tissue of an Israeli goose in 1998 (Lanciotti et al., 1999), highlighting the impact of vector and host movement in spreading arboviruses. The virus then spread swiftly across North America, reaching Canada, the Caribbean and Latin America within a few years (Dauphin et al., 2004; Hayes et al., 2005; Komar and Clark, 2006). It was considered the leading cause of mosquito-borne encephalitis in the United States (Gould et al., 2025). WNV outbreaks were frequently reported in southern and eastern Europe during the early and mid-2010s, including in Hungary (Frank et al., 2022). Resident birds are believed to be responsible for WNV amplification, while infected migratory birds are thought to facilitate the long-distance spread of the virus (Semenza et al., 2016).

In 2018, Europe faced its worst outbreak of WNV cases, with 2,000 confirmed human infections and a notable increase in WNV infections in horses and birds, reaching regions previously free of WNV (Aberle et al., 2018; Camp and Nowotny, 2020). That year was marked by a prolonged and unusually warm summer (Aberle et al., 2018; Semenza and Suk, 2017), indicating the impact of climate variability in amplifying mosquito populations and speeding up viral replication. Since then, the virus has been detected annually, with expanding geographic spread and increasing case numbers in birds, horses, and humans, underscoring the need for urgent action to better understand the complex mechanisms behind WNV transmission and spread (Tóth et al., 2025).

To date, WNV vaccines are only licensed for equids (Cendejas and Goodman, 2024), while preventive measures for humans primarily rely on recommendations to use equipment that minimises contact with mosquitoes, along with mosquito reduction methods (Bellini et al., 2014). By the year 2025, WNV continued to cause human fatalities across Europe, with surveillance data reporting approximately 63 confirmed deaths continent-wide. Italy was the most affected country, with 48 human deaths as of 3 October 2025, and several hundred human cases (European Centre for Disease

Prevention and Control (ECDC) and European Food Safety Authority (EFSA), 2025).

1.4 Usutu virus epidemiology

Usutu virus (USUV) is another emerging mosquito-borne zoonotic virus belonging to the *Flaviviridae* family in the Japanese encephalitis serocomplex (Gaibani and Rossini, 2017; Weissenböck et al., 2002). The virus is closely related to other significant human pathogens, including Japanese encephalitis, dengue, yellow fever, Saint Louis encephalitis, and WNV (Kuno et al., 1998; Poidinger et al., 1996; Weissenböck et al., 2002). USUV was first isolated in 1959 from mosquitoes in South Africa near the Usutu river, after which it was named (Woodall, 1964). The virus was initially confined to sub-Saharan Africa, but has extended its range to the European continent (Weissenböck et al., 2013). In 2001, a massive die-off of common blackbirds (*Turdus merula*) in Vienna, Austria, provided the first evidence of the successful introduction of USUV into Europe (Weissenböck et al., 2002). However, retrospective testing later revealed that USUV had already reached Europe by the mid-1990s (Weissenböck et al., 2013), when the virus RNA was detected in archived blackbird tissues from the Tuscany region of Italy in 1996.

Since then, several European countries have experienced repeated epizootics in wild and captive birds, mainly driven by summer temperatures (Rubel et al., 2008). In Germany, USUV was first detected only in 2010 in a pool of *Culex pipiens* mosquitoes captured in Weinheim (Upper Rhine valley) as part of a mosquito-based surveillance program (Vilibic-Cavlek et al., 2020). In the following year, 2011, the virus caused a mass die-off among the blackbird population (*Turdus merula*), in the Upper Rhine valley (south-west of Germany) and surrounding areas (Lühken et al., 2017; Ziegler et al., 2016). This marked the first major USUV-induced avian epizootic in Germany. The circulating USUV lineage confirmed in Germany was suspected to have been imported from Italy, rather than Austria (Engel et al., 2016), demonstrating the ability of the virus to to reach distant regions.

In 2014, more USUV cases were detected in western Germany, specifically in the city of Bonn (Ziegler et al., 2016). These two outbreaks confirmed that USUV had successfully established a local transmission cycle in Germany, facilitated by native mosquito vectors and the highly susceptible blackbird population. The virus continued circulating in Germany after 2014. Its local expansion remained confined to the south-west and western regions of Germany between 2011 and 2015, with occasional isolated cases towards the north, involving wild and zoo birds. In 2016, a new USUV case was documented in two captive juvenile owls at the Berlin Zoological Garden (north-eastern Germany). From 2016 onwards, USUV activity increased significantly. Surveillance

data from 2016 to 2018 reported many more USUV-positive wild and captive birds, including not only blackbirds, but also great grey owls in zoos (Störk et al., 2021). Since then, the virus has spread to much larger parts of Germany, and was described as endemic in many regions by 2018 (Cadar et al., 2017; Störk et al., 2021; Ziegler et al., 2016).

It is evident that USUV circulation among birds and mosquitoes is generally high, yet reported human cases remain relatively low. This discrepancy is likely due to under-detection, as many infections are asymptomatic, as indicated by higher seroprevalence in blood donor studies (Ashraf et al., 2015; Störk et al., 2021). The first severe human neuro-invasive case in Europe was documented in Italy in 2009, involving a woman with meningoencephalitis (Ashraf et al., 2015; Pecorari et al., 2009). Since then, approximately 105 laboratory-confirmed infections have been reported in EU/EEA countries including Austria, Croatia, Czechia, France, Germany, Hungary, Italy, and the Netherlands from 2012 to 2021 (Angeloni et al., 2023). In 2025, Europe recorded its first fatal case of autochthonous USUV infection in a 61-year-old immunocompromised woman from Hungary (Szabó et al., 2025). She developed severe neuro-invasive disease and died after 37 days, with USUV detected in multiple body tissues. This case further illustrates that USUV can be fatal in vulnerable patients (Szabó et al., 2025).

Several factors contribute to the emergence and continued spread of USUV and WNV. There is no doubt that USUV receives less attention compared to WNV due to its rarer and milder human cases, making its current surveillance largely dependent on avian mortality rather than human clinical disease. Climate warming in Europe has further extended the duration and severity of summers by increasing the number of days with suitable temperatures for transmission, increasing mosquito populations, and reducing the extrinsic incubation period (Brugger and Rubel, 2009; Rubel et al., 2008). Vegetation, land use changes, different host species, and other unknown ecological factors also influence the geographical distribution of the viruses in Europe (Engel et al., 2016; Krol et al., 2023). Continued climate change, bird migration, and shifts in vector ecology are likely to affect the future spread of USUV and WNV, underscoring the importance of coordinated surveillance for early detection and risk assessment.

1.5 Mosquito control methods

Mosquito control remains the most essential intervention against mosquito-borne diseases (Bellini et al., 2014). Because no single intervention offers a complete solution, effective management relies heavily on an integrated framework that targets various stages of the mosquito life cycle (Achee et al., 2019; Bellini et al., 2014). Despite their broader application, mosquito control efforts often face challenges such as vector

diversity, uncontrolled urbanisation, and growing resistance to insecticides (Silva et al., 2018), reducing their overall effectiveness.

1.5.1 Control of aquatic stages

Mosquito eggs, larvae and pupae can be suppressed through the removal or modification of aquatic breeding sites, including the elimination of standing water (World Health Organization, 2013). This method is crucial for mosquito control because many breeding sites are man-made, predictable, and can be managed through environmental changes (Gu et al., 2006; Kloter, 1983). Efforts include removing or modifying stagnant water in urban and peri-urban areas, such as catch basins, storm water drains, rain barrels, irrigation channels, and poorly maintained sewage systems. These actions reduce larval populations and, may consequently, reduce the risk of mosquito-borne disease outbreaks (Carlson et al., 2004; Howard, 1911). Gu et al. (2006) noted that source reduction not only reduces aquatic habitats but also delays vectors' ability to locate oviposition sites, thereby prolonging the gonotrophic cycle.

Despite its benefits, source reduction has notable limitations. One main challenge is public perception of environmental modification (Dale and Knight, 2017), as mosquitoes often breed and develop in economically vital wetlands, leading to political debates (Floore, 2006; Webb, 2021). Moreover, *Cx. pipiens* commonly breed in storm drains, catch basins, sewer systems, and other difficult-to-access aquatic habitats, which can limit the effectiveness of source reduction through habitat removal or modification (Becker et al., 2012; Liu et al., 2019; Minakawa et al., 1999). Larviciding involves the regular application of biological or chemical insecticides to stagnant water bodies (Floore, 2006; Howard, 1911; Tusting, 2014). An integrated approach combining source reduction and larviciding ensures that breeding sites that cannot be modified can still be treated with larvicides. Various types of larvicides are already available, such as *Bacillus thuringiensis* subsp. *israelensis (Bti)*, *Bacillus sphaericus*, spinosad, methoprene, pyriproxyfen, and diflubenzuron (Su, 2022). However, these larvicides often face challenges such as resistance and the need for frequent reapplication across different environments, their effects on non-target species, etc., further reducing their effectiveness (Rumbos and Athanassiou, 2020; Ser and Cetin, 2015; Su, 2022).

1.5.2 Adult control

Adult control methods refer to techniques aimed at killing mosquitoes during their aerial stage. The most common method is the use of pyrethroids (Floore, 2006). Adulticides have been of great use over the past years, but they are known for their adverse effect on non-target species such as pollinators and aquatic invertebrates, raising ecological

and environmental concerns (Yadav et al., 2023). In Europe, adulticides are commonly used in many European countries, however, their usage is highly regulated and can only be employed in emergencies (Chaskopoulou et al., 2011). For example, in Greece, recent experimental aerial spraying of deltamethrin and d-phenothrin against WNV mosquitoes was conducted during a WNV outbreak (Bellini et al., 2014; Chaskopoulou et al., 2011). Other adult mosquito control methods include mass trapping. For example, host-seeking female mosquitoes can be targeted using carbon dioxide-baited traps, such as BG-Sentinel and CDC light traps, while gravid traps can be used to capture ovipositing females (Becker et al., 2020; Benelli et al., 2016; Jaffal et al., 2023; Seelig). Although mosquito traps are mainly used for surveillance, strategic deployment at high densities can help reduce populations, especially in confined or semi-urban areas (Barrera, 2016, 2022; Jaffal et al., 2023; Pontifes et al., 2024; Poulin et al., 2017).

The World Health Organization emphasizes the importance of using non-chemical strategies to control mosquito populations (Bouyer, 2024). This has motivated scientists to develop alternative methods such as the Sterile Insect Technique (SIT) and the *Wolbachia* Incompatible Insect Technique (IIT). SIT is a species-specific approach that involves releasing large numbers of irradiated, sterile male mosquitoes, which mate with wild females and reduce the number of viable offspring (Bouyer, 2024). This ultimately leads to a decline in mosquito populations. One large-scale SIT release trial was conducted in Havana, Cuba, to control *Aedes aegypti*. Approximately 1.27 million sterile males were released into a 50-hectare treatment area over 20 weeks, where they demonstrated excellent mating success and caused significant sterility among the wild population. By the final weeks, ovitrap indices and egg counts dropped significantly, confirming that the sterile males effectively suppressed the natural vector population (Gato et al., 2021).

An alternative to the SIT is the *Wolbachia* method, which introduces naturally occurring endosymbiotic bacteria into mosquitoes (Zug and Hammerstein, 2012). This bacterium is considered eco-friendly and safe and can disrupt the mosquito's ability to transmit viruses, although outcomes vary depending on the specific host-symbiont pairing (Benelli et al., 2016; Minwuyelet et al., 2023). There are two main approaches: population replacement and population suppression. In the replacement strategy, male and female mosquitoes carrying the bacteria are released into the environment. When these mosquitoes breed with wild ones, the *Wolbachia* spreads through subsequent generations until nearly all local mosquitoes carry the bacteria. The resulting *Wolbachia*-infected mosquitoes effectively block the replication and transmission of viruses, without necessarily killing the mosquito, thereby reducing the risk of disease transmission (Moreira et al., 2009). In contrast, the suppression strategy involves

releasing only *Wolbachia*-infected males that induce cytoplasmic incompatibility when they mate with uninfected females, leading to non-viable offspring and eventually, a decline in the mosquito population (Lees et al., 2015). The *Wolbachia* method provides a sustainable, chemical-free solution that effectively transforms mosquitoes into a tool for public health control (Moretti et al., 2025). Several large-scale field trials have demonstrated significant success with *Wolbachia* methods. In Niterói and Rio de Janeiro, Brazil, large-scale releases resulted in huge public health benefits, with Niterói experiencing a 69% reduction in dengue cases, a 56 % reduction in chikungunya, and a 37% reduction in Zika cases across treated areas (Pinto et al., 2021). In Yogyakarta, Indonesia, a rigorous cluster randomised controlled trial achieved a 77% reduction in dengue incidence and an 86% decrease in dengue-related hospitalisations (Utarini et al., 2021). A study by Ong et al. (2022) further cements that combining the SIT with *Wolbachia* IIT reduced the *Aedes aegypti* population by 98% and dengue incidence by 88%.

1.6 Organisation of the PhD thesis

This PhD thesis is structured as follows:

- **Chapter 1** presents the background of the study.
- **Chapter 2** discusses the relevant state of the art and literature review of mechanistic models for WNV and USUV, which formed the backbone of this thesis.
- **Chapter 3** is the discussions and conclusions.
- **Appendix** has the list of published papers that make up this PhD thesis.

2 State of the art

Mathematical models of mosquito-borne infections have advanced since their early development in the twentieth century (Reiner et al., 2013). More than a century ago, Sir. Ronald Ross developed the first model of malaria transmission (Ross, 1911, 1923). About fifty years later, MacDonald expanded and operationalised this framework during the era of Global Malaria Eradication (Macdonald, 1950, 1952a,b, 1956). The extended version became famously known as the Ross-MacDonald theory, which forms the basis of many modern studies on vector-borne disease modelling today. The evolution has ranged from deterministic models to modern spatially explicit approaches, shaping much of today's quantitative epidemiology and ecological modelling of mosquito-borne diseases.

Progress in computational modelling and software developments has further supported the application of mathematical models to real-world scenarios. Nonetheless, variations in assumptions, parameter sources, and model formulations continue to produce divergent conclusions across studies. Modern research on mosquito-borne disease modelling has considered incorporating temperature-dependent parameters, heterogeneous landscapes, and mobility processes to better represent mosquito dynamics in large-scale predictions (Barman et al., 2025; Tuff et al., 2016). Despite these advances, uncertainties remain regarding long-range spread, seasonal re-emergence, and the influence of environmental forcing on outbreak trajectories. This chapter reviews the key theoretical developments, modelling approaches, and analytical tools that are the backbone of the work presented in this thesis.

2.1 Processes-based models for mosquito seasonal dynamics

Process-based models have become important tools for understanding mosquito population dynamics and their responses to environmental conditions by explicitly representing mosquito life stages and the biological processes governing development, survival, and reproduction. Early mosquito population models employed stage-structured systems of ODE-based models to link mosquito abundance to climatic variables such as temperature and precipitation (Bhowmick et al., 2025; Cailly et al., 2012; Ezanno et al., 2015; Tran et al., 2013). For *Culex* species, several mechanistic models have been developed to investigate seasonal population dynamics and their implications for

arbovirus transmission. For example, Yu et al. (2018) developed a temperature-driven ODE model for the West Nile virus vectors *Cx. pipiens* and *Cx. restuans* in southern Ontario, incorporating temperature-dependent development, mortality, and diapause processes. Validation against mosquito surveillance data demonstrated that the model successfully reproduced observed seasonal abundance patterns and could serve as a forecasting tool for mosquito surveillance and control.

A broader approach was proposed by Ezanno et al. (2015), who developed a generic weather-driven mechanistic model for mosquito species in the genera *Anopheles*, *Culex*, and *Aedes* in southern France. By incorporating environmental drivers such as temperature and precipitation, the model reproduced observed abundance patterns and highlighted the importance of weather conditions in shaping mosquito population dynamics. More recently, Frantz et al. (2024) extended mechanistic modelling approaches using an age-structured PDE framework that explicitly incorporated mosquito age and developmental stage. Their formulation enabled tracking of mosquito abundance across developmental and reproductive stages, producing realistic seasonal abundance patterns and providing a more detailed representation of mosquito population structure than traditional stage-structured ODE models.

2.2 Mechanistic models of West Nile virus

Multiple models for WNV dynamics have been developed and extensively studied. Bergsman et al. (2016) developed a mathematical model for the transmission of WNV involving resident and migratory bird populations, along with the mosquito population. The model's properties were analysed mathematically, and the basic reproductive number was calculated. The interaction of WNV in both resident and migratory bird species was examined using the American Crow (*Corvus brachyrhynchos*) as the resident bird and the American Robin (*Turdus migratorius*) as the migratory bird. Results from the model showed that seasonal outbreaks depended primarily on the number of susceptible migrant birds entering the local population each season. Additionally, the early growth rates of seasonal outbreaks were more strongly affected by the migratory bird population than by the resident bird population.

Research further highlights that the link between vector activity and viral spread overlaps but is not identical (Bhowmick et al., 2023). While temperature significantly affects mosquito abundance, especially through its impact on the extrinsic incubation period, and mosquito feeding behaviour, environmental factors alone cannot fully explain where and how the virus spreads across different areas. Other researchers point out that spread results from a mix of climatic conditions and biological factors such as vector competence, natural habitat suitability, feeding preferences, and bird

movement routes (Bhowmick et al., 2023; Ferraguti et al., 2023). For this reason, Bhowmick et al. (2023) developed a meta-population, network-based model to describe the regional spread of WNV. The model uses separate movement kernels for mosquitoes and birds, fitting their different dispersal ranges, including short-range movement for vectors and long-range migration for birds. This approach helps simulations reflect both local survival and long-distance jumps, which are often seen in real-world WNV outbreaks.

More studies support the hypothesis of WNV spread through avian movement, e.g., (Owen et al., 2006; Zhang et al., 2018; Zhuang and Wang, 2021). Zhang et al. (2018) developed a two-patch model for the spread of WNV between two distinct geographical regions. The model incorporated the mobility process, which describes how contact transmission occurs between individuals from and between these regions. The basic reproductive number was calculated assuming that host birds can migrate between regions, but mosquitoes cannot. Numerical simulations showed that WNV becomes endemic in both patches when birds move back and forth between the regions. However, multi-group and multi-patch models are inherently discrete, often dividing the system into parts based on different locations, with disease dynamics in each location described by an ODE sub-system (Zhuang and Wang, 2021). This leads to large systems of ordinary differential equations (van den Driessche, 2008), which can be expensive to solve.

This limitation of ODE-based multi-population models can be addressed by partial differential equation (PDE)-based models, which are continuous in nature. Maidana and Yang (2009) proposed one of the first PDE models for WNV propagation. The model, which consists of a system of reaction-diffusion-advection terms, is analysed, and travelling-wave solutions are determined. Results from the study indicate that the virus propagated from New York City to California as a consequence of bird migration and advection. Since then, several PDE-based models have been studied to expand knowledge of the spread of WNV, for example, Lin and Zhu (2017) and Wang et al. (2019).

Laperriere et al. (2011) developed the first environmental temperature-driven process-based model for WNV comprising 19 compartments: 4 for mosquitoes and 5 for each for birds, humans and equids. The model was simulated for 2002-2009, driven solely by environmental temperature. Simulated incidences are mainly determined by host and vector population dynamics, virus transmission, and herd immunity, respectively. Monthly cases for birds, equids, and humans in the Minneapolis metropolitan area were used to fit the model. The model accurately captured the major peaks in the observed time series for each species.

Building on the biological foundation introduced by Laperriere et al. (2011), Mbaoma et al. (2024) developed another ODE-based WNV model with 28 compartments, specifically designed for Germany. The framework includes 13 mosquito compartments, 10 of which describe the general mosquito life cycle driven by climatic variables. This model divided the bird population into residential and migratory groups, consistent with suspected dissemination pathways of WNV (Bergsman et al., 2016; Lelli et al., 2011; Lord and Calisher, 1970; Owen et al., 2006). Parameters for the bird species considered most vulnerable in Germany were estimated in this study. The model successfully generated spatially and temporally explicit maps of the basic reproductive number, illustrating the dynamics of WNV occurrences across Germany and showing that these were closely linked to deviations from daily climatic means, indicating the influence of climate change on vector-borne disease dynamics. The results provided evidence that WNV could spread rapidly towards western Germany following rapid increases in temperature and amplifying host birds, particularly short-distance migratory birds.

Bhowmick et al. (2020) formulated and studied a dynamic model to describe the spreading process of WNV in the presence of migratory birds in Germany. The model, which includes recurring presence of migratory birds through a mechanistic ODE-based system, indicated that after introducing WNV into Germany, the basic reproduction number remains above the critical value in many regions of Germany. While understanding the WNV transmission dynamics is essential for anticipating risk, prevention ultimately depends on strategic intervention. To date, at least three anti-WNV vaccines have been licensed and approved for use in horses (Seino et al., 2007). However, no vaccine exists for humans or birds. As a result, mosquito control remains the most frequently used method for WNV management. Various control measures have been examined in the literature, with the most common mosquito control strategies being source reduction methods, adulticiding, and larviciding (Becker et al., 2010; Bhowmick et al., 2025, 2024; Mahyoub et al., 2016).

Mathematical models have played a big role in quantifying and guiding mosquito control efforts. Models enable these interventions to be tested under realistic ecological and climatic scenarios prior to field deployment, identifying where, when, how and for how long controls should be applied for maximum effectiveness. The theory of optimal control has formed the foundation of most WNV models developed to date. Abdelrazec et al. (2015) developed a model to evaluate the impact of adulticide, larvicide and human protection measures. Numerical simulations of their optimal control problem indicated that larviciding was the most effective strategy for managing an ongoing WNV epidemic. Other studies further reinforce the idea that mosquito reduction efforts are more effective than human protective measures (Blayneh et al., 2010). Moreover, Bwman et al. (2005) stated that WNV can be eradicated from the mosquito-bird cycle

and dead-end hosts, provided that the chosen strategy can reduce the reproductive number below 1.

WNV research available so far has laid a solid groundwork for understanding WNV epidemiology and for developing and testing intervention strategies. However, a lot of questions regarding the spreading patterns, spatial dynamics and climate-host interactions are still open, and this study seeks to provide answers to some of them.

2.3 Mechanistic models of Usutu virus

Despite its high mortality in the avian population, the epidemiology of USUV remains understudied (Cheng et al., 2018) compared to WNV. This is evidenced by the fact that many parameters, such as the extrinsic incubation rate for USUV, remain inconclusively derived to date (Lühken et al., 2017), despite the virus arriving in Europe more than 23 years ago. Using the available data, many models rely on WNV parameters, as the two viruses are closely related. Rubel et al. (2008) developed the first mechanistic model for USUV. The model comprises vector-host compartments, along with weather-driven mosquito parameters. It was simulated using air-temperature data for Vienna, Austria, from 2001 to 2005, corresponding to the years when USUV emerged in Austria. Results from the model aligned with observed dead-bird data, including the peaks in the number of infections, during those years. Since this study, several extensions have been introduced.

Brugger and Rubel (2009) used the model of Rubel et al. (2008) with four different climate-warming scenarios defined by the Intergovernmental Panel on Climate Change, IPCC, with 20 different model-scenario combinations. The simulations predicted that USUV would persist in the host population after the 2003 epidemic peak. The time-series plots of USUV-specific annual blackbird mortality predicted that outbreak frequency would increase from the beginning to the end of the century. Results of the worst-case scenario identified an endemic equilibrium with a decline of the blackbird population of about 24%. Moreover, the annually averaged basic reproduction number for the period 1901-2100 suggested that undetected major outbreaks before 2000 were unlikely, whereas USUV is likely to become endemic after 2040.

Assuming random variation in temperature data, reproduction data of birds, and the number of birds found to be infected, Reiczigel et al. (2009) extended the deterministic model by Rubel et al. (2008) to a hierarchical Bayes model. This hierarchical Bayes approach proved fruitful in transforming the deterministic model into a stochastic version. It enabled Bayesian point and interval estimation and the quantification of prediction uncertainty, while also enhancing model fit.

Some studies have highlighted the importance of combining ecological suitability models with mechanistic transmission dynamics when evaluating USUV risks (Cheng et al., 2018; Meineri et al., 2014). A similar model analyses by Cheng et al. (2018) showed that a Maxent niche model and a temperature-driven SEIR framework produce overlapping yet distinct risk maps across Europe. While the Maxent model more accurately reflected observed distribution patterns, its correlation-based design may underestimate future spread in new areas. In contrast, the SEIR model replicated known outbreak sites but was highly sensitive to temperature, resulting in high predicted R_0 values even in regions lacking evidence of real transmission. These findings emphasize that relying on a single model for assessing vector-borne disease risks may result in incomplete conclusions.

Some studies also considered the formulation and analysis of population-level USUV models (Cheng et al., 2018; Rubel et al., 2008). In addition, other researchers have approached USUV modelling differently by developing multi-scale models that also examine the virus's in-host dynamics (Heitzman-Breen et al., 2024). In the study by Heitzman-Breen et al. (2024), a multi-scale modelling framework was utilised to model USUV transmission and epidemiology by integrating within-host infection processes, bird-to-vector transmission, and population-level epidemiological dynamics. The study combined laboratory inoculation experiments with dynamical models to estimate incidence in birds and mosquitoes using within-host viral load measurements and mosquito infection proportions. A key finding was that prediction uncertainty at one biological scale propagates into subsequent scales, affecting epidemiological forecasts. Their work also proposed optimal experimental designs and recommended types of experiments to enhance model identifiability at the transmission scale, thereby increasing the robustness of epidemiological predictions.

2.4 Summary

Indeed, significant progress has been made in understanding WNV and USUV transmission through mathematical modelling. Existing models have identified key mechanisms, including temperature-driven seasonal dynamics, invasion thresholds, density-dependent phenology, and overwintering effects, while providing baseline and refined temperature-dependent mosquito parameters that shape modern mosquito-borne disease models. However, ODE models in the literature assume localised dynamics and fail to capture the spatial heterogeneity of Germany, which affects the spread of WNV and USUV. Although ODE-based models offer a more convenient framework for understanding the primary interactions of a virus and testing control strategies, no existing models in the literature address optimal control strategies in Germany for either virus.

Furthermore, existing spatially explicit models assess virus suitability based on the reproductive number and temperature, and discuss migratory birds as dispersers of WNV to previously uninfected regions. However, these models do not incorporate the known seasonal flyways of migratory birds, to better understand virus spread. This thesis seeks to fill these gaps and advance scientific knowledge by providing PDE-based models that complement existing ODE-based models discussed here. Additionally, the control methods are modelled and explored in a web-based application that is publicly accessible even to non-scientific audiences, in line with modern scientific practices of making science accessible to all.

2.5 Objectives of the PhD project

The objectives of this PhD project are to:

1. Develop a weather-driven process-based model for the seasonal dynamics of *Culex pipiens* s.s./*Cx. torrentium* in Germany.

2. Develop and analyse a spatially explicit reaction-diffusion PDE model for WNV transmission in Germany, incorporating migratory bird movement, and temperature forcing, in order to quantify the location, speed, and spatial extent of viral spread.

3. Develop and analyse a spatial PDE model of USUV transmission in Germany and neighbouring countries, characterising its regional spread.

4. Study optimal control strategies for WNV, including vector reduction methods, human protective measures, and equid vaccination, using scenario-based modelling and sensitivity analysis.

5. Develop a free, open-source web-based Shiny application that transforms model outputs into an interactive decision-support tool, since mosquito control efforts like source reduction and larval treatments often rely on citizen support.

3 Discussions and conclusions

Given the increasing threat of mosquito-borne diseases, it is essential to understand their spreading patterns (Colón-González et al., 2021). To do this, models that explicitly include spatial heterogeneity, temporal patterns, climatic factors, and vector-host interactions are needed. This chapter discusses results of this PhD thesis based on these factors. Initially, the modelling frameworks from a methodological standpoint are examined, highlighting how temperature influences the epidemic spread at both temporal and spatial level. This also supports the selection of the modelling approaches used here. Next, the main scientific findings from all the published studies are examined, along with their biological and epidemiological implications. Finally, the chapter concludes with remarks on the overall contribution of this PhD thesis and offers suggestions for future research.

3.1 Methodological framework

In this PhD thesis, ODE-based models are used to investigate mosquito seasonal dynamics, WNV transmission patterns, and the effectiveness of control strategies, while PDE-based models are employed to study the transmission dynamics and spatial spread of WNV and USUV. The mosquito-related parameters are primarily temperature-dependent and were obtained from published studies, including (Cailly et al., 2012; Ezanno et al., 2015; Tran et al., 2013; Heidecke et al., 2025; Laperriere et al., 2011; Mbaoma et al., 2024; Rubel et al., 2008), while several others were assumed values within biologically plausible ranges when empirical estimates were unavailable. Due to limited experimental data, parameter values describing host populations were similarly adapted from the existing literature.

3.1.1 *Culex pipiens* s.s./*Cx. torrentium* process-based model

Process-based mosquito population models provide a mechanistic framework for describing the seasonal dynamics of mosquito vectors by explicitly representing the biological processes governing development, survival, reproduction, and overwintering. Unlike epidemiological models that focus on pathogen transmission between hosts and vectors, process-based models are primarily concerned with the ecological drivers of vector abundance (Bhowmick et al., 2025; Cailly et al., 2012; Ezanno et al., 2015; Lutambi et al., 2013; Tran et al., 2013). In this PhD thesis, a process-based model

was developed for *Culex pipiens* s.s./*Cx. torrentium*, the principal vectors of WNV and USUV in Germany. The model incorporated temperature-, rainfall-, and photoperiod-dependent processes to describe mosquito development, mortality, reproduction, and diapause, thereby enabling realistic simulation of seasonal mosquito phenology under temperate climatic conditions.

A major advantage of process-based mosquito models is their explicit representation of the mosquito life cycle and the environmental processes governing stage transitions. By dividing the population into their life stages, such as eggs, larvae, pupae, adults, and overwintering individuals, the model provides mechanistic insights into seasonal mosquito dynamics. This stage structure is also highly relevant for vector control, as different interventions target different life stages (Lutambi et al., 2013). Consequently, the model can be used not only to investigate the environmental drivers of mosquito abundance but also to identify life stages that may be most effective to target for population suppression.

Despite these advantages, process-based mosquito models do not explicitly represent pathogen transmission between mosquitoes and hosts and therefore cannot directly quantify infection dynamics or disease risk. While they provide valuable ecological insights into vector abundance, seasonality, and overwintering behaviour, additional modelling frameworks are required to investigate the epidemiological consequences of these ecological processes. The seasonal mosquito dynamics characterised by process-based models therefore motivated the development of eco-epidemiological ODE models to investigate the transmission dynamics of WNV and USUV.

3.1.2 WNV-ODE-based models

An ODE-based model was developed to investigate the transmission dynamics and control of WNV, capturing transmission between mosquitoes and birds together with spillover infections in humans and equids. The compartmental framework consisted of susceptible, exposed, infectious, recovered, and disease-induced mortality classes, enabling the analysis of transmission pathways, epidemic potential, and intervention strategies over time. This approach enables the systematic examination of the underlying transmission mechanisms and facilitates the derivation of threshold quantities and equilibrium points that define epidemic potential (Hethcote, 2000; Hoang and Ehrhardt, 2025). In particular, the application of ODE frameworks in this work allowed for clear interpretation of epidemiological parameters and supported comparative analyses of the basic reproductive numbers for WNV.

One key advantage of ODE-based models is their flexibility in formulating and analysing optimal control strategies (Bussell et al., 2019). The relatively simple mathemati-

cal structure of ODE systems provides a convenient setting for incorporating time-dependent interventions and applying established optimal control techniques such as Pontryagin's Maximum/Minimum Principle (Lenhart and Workman, 2007a,b). This facilitated the exploration of control timing, intensity, and trade-off, providing the necessary conditions for the existence of optimal control, which is more challenging to explore within more complex modelling frameworks. Moreover, the computational efficiency of ODE models enabled extensive scenario exploration and sensitivity analyses, thereby supporting robust assessment of parameter uncertainty and model behaviour.

Despite these advantages, ODE-based models often struggle to accurately represent spatial heterogeneity and localised transmission processes, which are crucial for understanding the spread of mosquito-borne diseases. The implicit assumption of homogeneous mixing in population-averaged ODE model limits their capacity to account for spatial variation in vector abundance, and the environmental conditions.

3.1.3 WNV & USUV PDE-based models

To address the limitations of ODE models, PDE-based models were used to expand understanding of WNV and USUV transmission beyond dynamics confined to predefined population-aggregated units. This was achieved by including diffusion and advection terms, allowing for the random and directed movement of specimens across heterogeneous landscapes. This thesis uses PDE models to determine whether observed spatial patterns can be explained solely by the random dispersal of birds and mosquitoes or if directed transport is necessary. Furthermore, this spatially explicit approach is essential for capturing temperature-driven spread patterns, which ODE-based models fail to capture (Sego et al., 2021).

Even at the spatial level, the temperature-dependent mosquito parameters were integrated into the model, given that changes in temperature often affect regions where the infection is most likely to establish and become endemic. Such a formulation enables the study of temperature-dependent wave-like invasion fronts and spatial gradients in infection intensity as examined in (Maidana and Yang, 2009), which are key features of WNV and USUV propagation. These features arise naturally from the model structure rather than being imposed through predefined connectivity or regional coupling, such as in meta-population, cellular automata, and multi-patch models.

Although PDE-based epidemic models have several strengths, they also have notable limitations. For instance, diffusion and advection coefficients represent effective population-level transport processes that cannot be directly measured in the field. Their estimation thus depends on indirect validation through spatial patterns rather than direct data collection. Moreover, PDE models assume spatial smoothness, which

may oversimplify ecological boundaries. The limited amount of observed data also affects the validation process, as PDE solutions are continuous in nature while observed data are usually discrete. This discrepancy further complicates the validation of PDE models with observed spatial and discrete data. A summary of the modelling frameworks used in this thesis is shown in Figure (3.1).

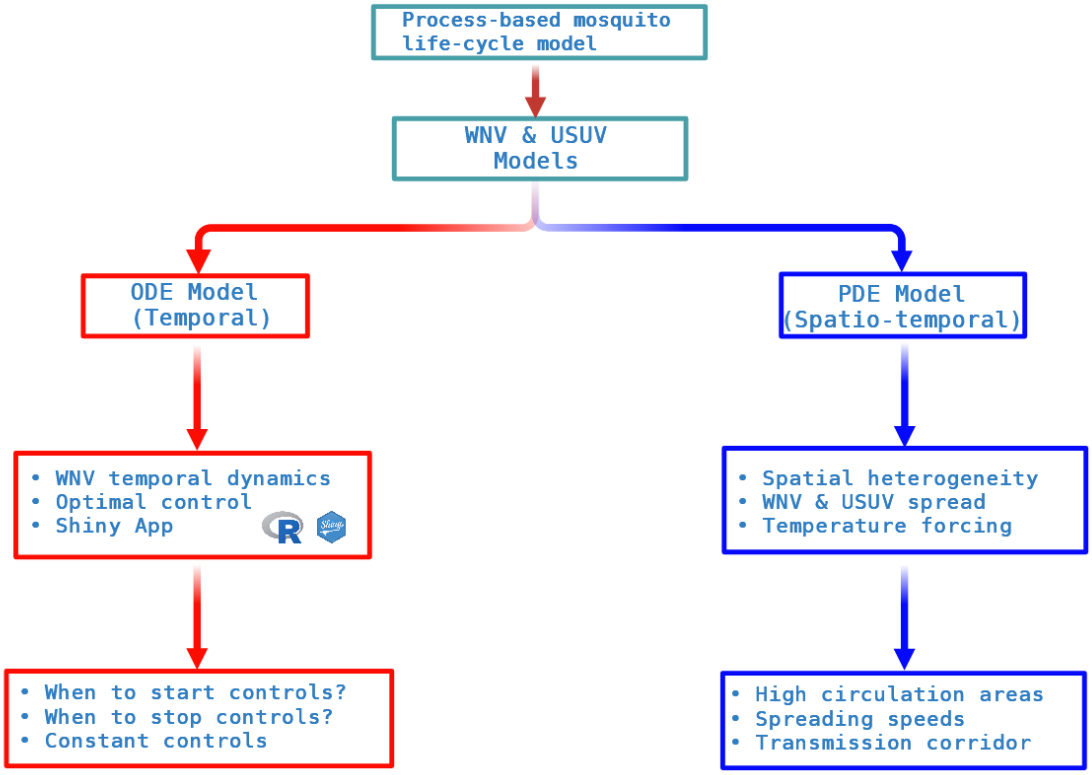


Figure 3.1: Overview of the modelling frameworks used in this thesis. ODE models were employed to examine the temporal dynamics of Culex vectors responsible for transmitting WNV, and WNV transmission dynamics, optimal control strategies, and the web-based Shiny App. The PDE model provided a spatially explicit representation of both the WNV and USUV models under the influence of diffusion, advection, and temperature forcing.

3.2 Environmental forcing

Environmental forcing was incorporated into the process-based mosquito model through temperature, rainfall, and photoperiod, as these variables are known to be among the principal environmental drivers influencing the life cycle of *Culex* mosquitoes (Ciota et al., 2014; Farooq et al., 2023; Groen et al., 2017). Temperature governs key physiological processes such as development, survival, reproduction, and diapause termination, while rainfall/precipitation influences the availability and persistence of aquatic breeding habitats required for immature mosquito stages (Ciota et al., 2014; Ezanno et al., 2015). Photoperiod plays a crucial role in regulating diapause induction and seasonal activity, particularly in temperate regions where overwintering is an im-

portant component of the mosquito life cycle (Ezanno et al., 2015). Climate data used to parametrise the model were obtained from publicly available meteorological datasets and interpolated to provide continuous environmental forcing throughout the simulation period. During the model simulation, temperature-dependent functions were used to describe developmental, mortality, and reproductive rates, whereas rainfall was incorporated through its effects on the carrying capacity. Photoperiod-dependent functions regulated the induction and termination of diapause, thereby controlling the transition between active and overwintering populations.

3.3 Historical temperature trends in Germany

Daily gridded temperature data were obtained from the E-OBS datasets in the Copernicus Climate Data Store (Cornes, 2020), which provides Europe-wide meteorological derived from quality-controlled in-situ station observations. The datasets span the period from 1965 to 2024. Daily minimum (tn), mean (tg), and maximum (tx) air temperatures were extracted at a spatial resolution of 0.1° × 0.1°. From these datasets, climate indicators such as the spatial distribution of the number of heatwave events in Germany and the timing of early mosquito-favourable seasons, indicating the premature onset of mosquito activity over the years, were explored.

As also defined by Tomczyk and Sulikowska (2017), a heatwave is characterised as a period of at least three consecutive days with maximum air temperatures reaching or exceeding 30°C. The spatial distribution of heatwave events across Germany between 1965 and 2024 is shown in Figure (3.2). During the early decades (1965-1984), fewer than 22 events were observed. Since then, the number of heatwave events has increased across the country. The last decade recorded a more significant rise in events, surpassing 38 events (Figure 3.2). The most affected regions include the Upper Rhine Valley and the eastern parts of Germany. Interestingly, these are the regions where USUV and WNV were isolated in 2011 and 2018, respectively (Lühken et al., 2017; Ziegler et al., 2016, 2019).

Using station-based datasets obtained from the German Weather Service (DWD) (Deutscher Wetterdienst, 2024), selected weather stations in Hamburg, Berlin, Halle, and near Weinheim were examined from 1972 to 2024. In Hamburg, the Fühlsbuttel station (ID: 01975) was chosen for its consistent reporting of minimum, mean and maximum daily temperatures during this period. The same criteria applied to the Berlin-Dahlem (FU) station (ID: 00403). Since no DWD station is located in Weinheim, where USUV was first isolated in Germany, this station is represented by Mannheim station (ID: 05906), which is closer to Weinheim. Similarly, Halle (Saale), where WNV was first detected, is represented by the Leipzig airport station (ID: 02932). Using this

data, a high number of heatwave events occurred in the decade 2012-2021 (Figure 3.3). Berlin experienced the highest number of heatwave events in a single year, with five in 2018. These increasing heat events which promote mosquito activity in Germany correlate and highlight the rising risk of arboviruses in recent decades.

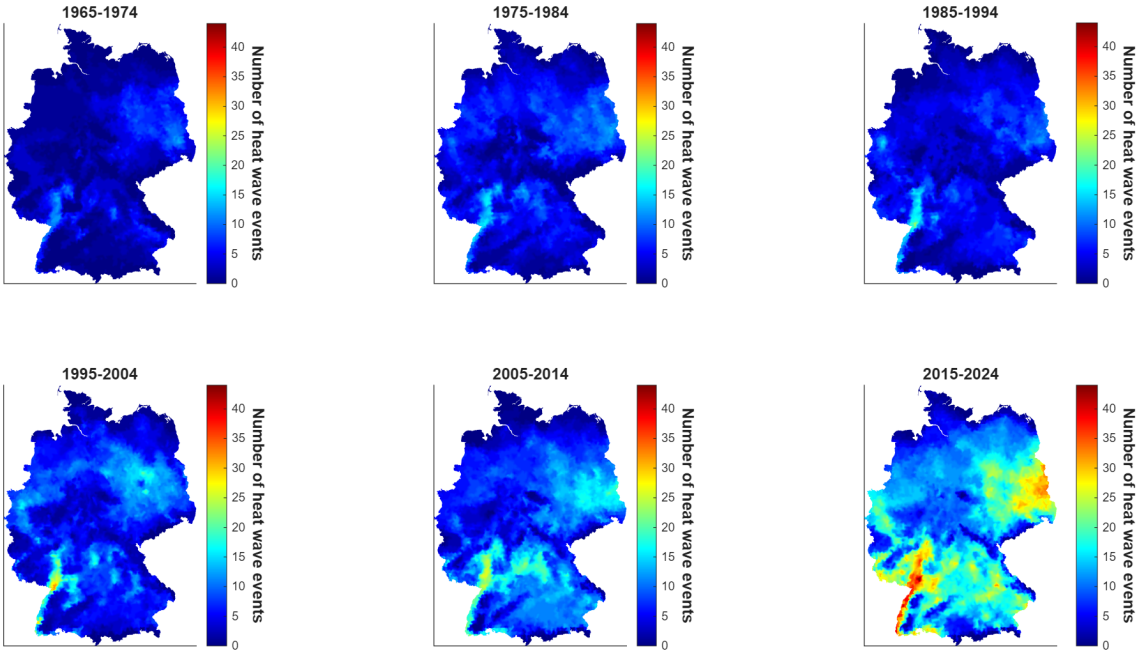


Figure 3.2: Number of decade heat wave events observed in the period 1965-2024.

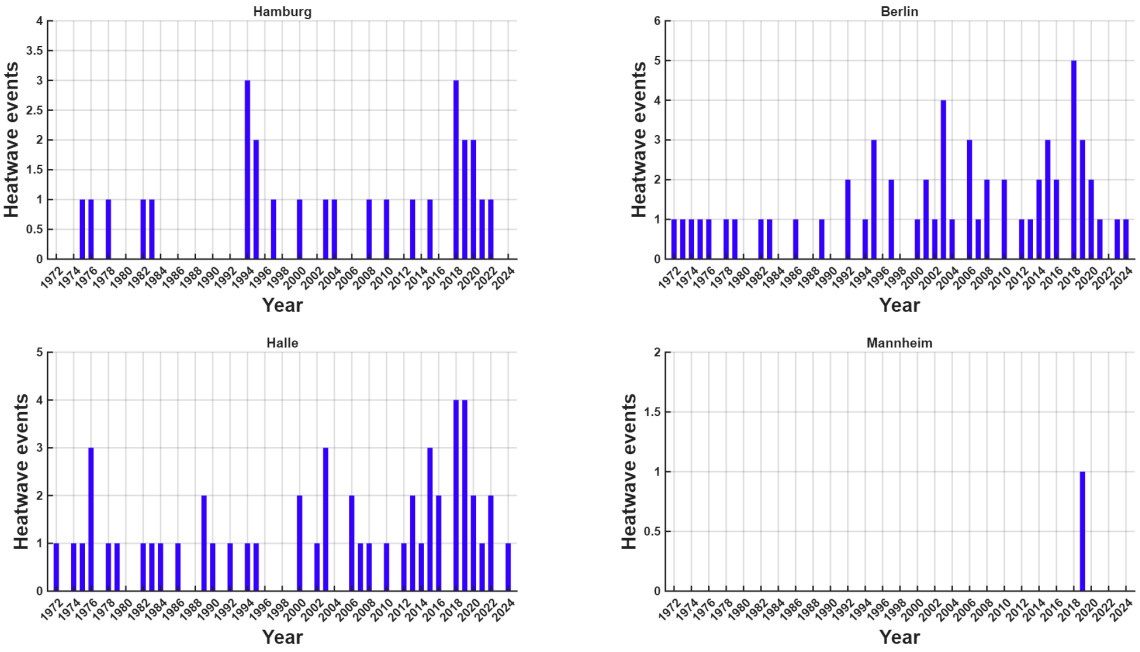


Figure 3.3: Number of heat wave events observed in the period 1972-2024, in selected stations in Berlin, Halle, Hamburg, Mannheim.

Climate change also affects spring temperatures, which, together with photoperiod, define the onset and end of the mosquito favourable seasons (Rauhöft et al., 2026).

Although no studies have established a temperature threshold for the onset of *Culex* mosquito season in Germany, many studies often rely on models and collected mosquito data. Moreover, laboratory experiments on *Cx. pipiens* demonstrate that larval development and survival to adulthood are not possible at $7°C$, while it can be achieved at $10°C$ (Almirón and Brewer, 1996; Ewing et al., 2016; Loetti et al., 2011; Mbaoma et al., 2024). Accordingly, it is reasonable to assume a minimum temperature threshold of $12°C$ sustained for a period of ten consecutive days as the start of *Culex* development-favourable window. The requirement of at least ten consecutive days above the temperature threshold ensures that an isolated single-day or short temperature spikes are not classified as heatwaves. Data from 1965-2024 (Figure 3.4) show a negative correlation trend suggesting that earlier years experienced minimum thresholds for a sustained period of $10°C$, in late May, compared to recent years. The earliest onset within this period was observed on the 29th of April 2018, the year WNV was detected in Germany for the first time.

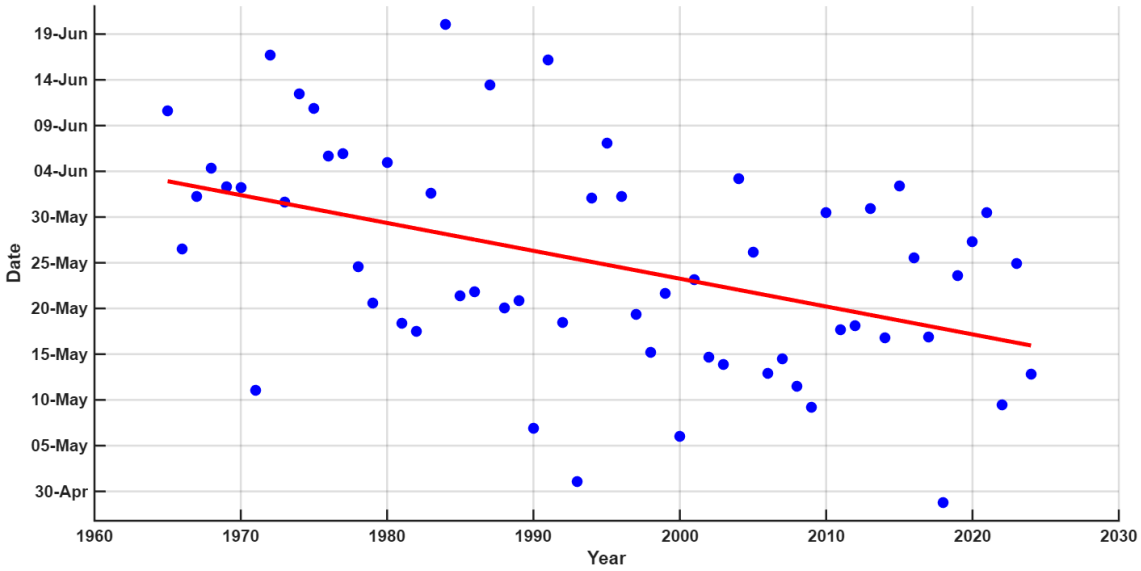


Figure 3.4: Onset of theoretical mosquito activity season based on ($T \geq 12°C$ for 10 consecutive days 1965-2024), with r=-0.45.

3.4 Impact of temperature on the basic reproductive number

The basic reproduction number (R_0) was calculated using the next-generation matrix for the WNV and USUV models described in equations (3.1 and 3.2). Since both viruses are transmitted by the same mosquito species, their mosquito parameters (biting rate, extrinsic incubation rate and mortality rate) are assumed to be identical. However, significant differences in susceptibility and mortality among bird species have been documented (Mbaoma et al., 2024). Blackbirds (*Turdus merula*) are highly susceptible

to USUV, with a high mortality rate. Conversely, WNV is considered primarily amplified by various bird species, including both resident and migratory species (Ain-Najwa et al., 2020; Bergsman et al., 2016; Mbaoma et al., 2024; Rubel et al., 2008). Following Mbaoma et al. (2024), resident and migratory birds were represented respectively by the northern goshawk (*Accipiter gentilis*) and the hooded crow (*Corvus cornix*), chosen because of their high susceptibility to the WNV. Specifically, the northern goshawk was selected to represent resident birds because of its largely sedentary behaviour and high WNV mortality, which limits its role in sustained transmission but makes it a valuable sentinel for detecting active circulation. In contrast, the hooded crow was chosen as a short-distance migratory bird species because of its broad distribution in Germany, partial migratory behaviour, urban colonisation, and documented capacity to develop viraemia while experiencing relatively low WNV-induced mortality (Mbaoma et al., 2024).

In contrast, USUV shows strong host specificity, with the highest susceptibility consistently observed in Eurasian blackbirds (*Turdus merula*), which are widely considered the primary sentinel and amplifying host in Europe (Weissenböck et al., 2002). Large-scale mortality events in blackbirds were first recorded during the 2001 outbreak in Austria (Rubel et al., 2008; Weissenböck et al., 2002) and have since been repeatedly observed across Germany, the Netherlands, Belgium, Switzerland, southeast England and Italy, where USUV is now endemic (Schilling et al., 2025; Vilibic-Cavlek et al., 2020). Experimental and field studies indicate that blackbirds develop high viraemia and severe systemic infection, often leading to rapid death, making them highly sensitive indicators of local USUV transmission. Other bird species, including house sparrows (*Passer domesticus*), common starlings (*Sturnus vulgaris*), canaries (*Serinus canaria*), great grey owls (*Strix nebulosa*), and common kingfishers (*Alcedo atthis*), have also been shown to be susceptible to USUV infection (Becker et al., 2012). Compared with Eurasian blackbirds which experiences consistently high mortality during USUV outbreaks (Musto et al., 2022), these species generally exhibit lower or less frequent infection-related mortality, with many infections remaining subclinical or identified primarily through surveillance rather than mass die-offs. Therefore, USUV epidemiology in Germany is dominated by high susceptibility and mortality in European blackbirds, supporting their role as the most crucial species for surveillance and early detection of the virus (Becker et al., 2012; Ziegler et al., 2016). The temporal and spatial trend for the basic reproductive numbers for the WNV and USUV were compared over the period 1972-2024 (equations 3.1, 3.2), and (Figure 3.5), using parameters defined in Table (3.1).

An increasing trend in the (R_0) values is observed over the years (Figure 3.5), with 2018 showing the highest risk for both viruses. Notably, this was the year when WNV was

first confirmed in Germany, and USUV was detected across nearly the entire country, correlating with rising temperatures over the years. R_0 values for WNV are higher than those for USUV, partly because of the WNV huge dependence in temperature, compared to USUV (Figure 3.5-3.7). Additionally, multiple bird species, such as Northern goshawks and other birds of prey, are highly susceptible to WNV compared to USUV, which circulates only in blackbirds. In addition, WNV shows a more widespread pattern and has a much larger impact on human health, attracting greater attention and surveillance than USUV (Zannoli and Sambri, 2019).

At the spatial level, the decadal reproductive number for WNV remains higher than that for USUV (Figures 3.6 and 3.7). The risk is low during the initial decades, namely 1965-1995. However, recent decades show an increased risk, with the last decade exhibiting the highest risk, as indicated by the elevated R_0 values (Figures 3.6 and 3.7). Spatial patterns of the basic reproduction number reveal heterogeneity in environmental suitability driven by temperature. Using identical mosquito demography and temperature-dependent vector traits, both USUV and WNV displayed broadly similar spatial gradients, with higher risk concentrated mainly in eastern Germany, as well as in western and southwestern regions. This presents a similar transmission corridor for WNV and USUV (Zannoli and Sambri, 2019), highlighting regions with a greater likelihood of repeated seasonal transmissions. In the event of implementing control measures, these regions should be prioritised.

The basic reproductive number R_0 for WNV is given by:

$$R_0(\boldsymbol{x}) = \sqrt{R_0^{Res} + R_0^{Mig}}, \tag{3.1}$$

$$\text{where} \quad R_0^{Res} = \frac{\gamma_V \phi \beta p_{rV} p_{Vr} \gamma_{rB}}{\mu_V(\alpha_{rB} + \mu_{rB})(\gamma_{rB} + \mu_{rB})(\gamma_V + \mu_V)\left[1 + \frac{K_{mB}\left(1 - \frac{\mu_{mB}}{b_{mB}}\right)}{K_{rB}\left(1 - \frac{\mu_{rB}}{b_{rB}}\right)}\right]^2}$$

$$\text{and} \quad R_0^{Mig} = \frac{\gamma_V \phi \beta p_{mV} p_{Vm} \gamma_{mB}}{\mu_V(\alpha_{mB} + \mu_{mB})(\gamma_{mB} + \mu_{mB})(\gamma_V + \mu_V)\left[1 + \frac{K_{rB}\left(1 - \frac{\mu_{rB}}{b_{rB}}\right)}{K_{mB}\left(1 - \frac{\mu_{mB}}{b_{mB}}\right)}\right]^2}.$$

while that for USUV is given by:

$$R_0 = \sqrt{\frac{\beta p_b \gamma_V}{(\gamma_V + \mu_V)\mu_V} \times \frac{\beta p_v \gamma_B}{(\gamma_B + \mu_B)(\alpha_B + \mu_B)}}. \tag{3.2}$$

Table 3.1: Definition and values of WNV and USUV parameters for simulating the basic reproductive numbers.

Parameter	Definition	Pathogen	Value	Source
$b_V(\boldsymbol{x})$	birth rate of mosquitoes	WNV	0.0666	(Bergsman et al., 2016)
$b_{rB}(\boldsymbol{x})$	birth rate of resident birds	WNV	0.00342	(Rubel et al., 2008)
$b_{mB}(\boldsymbol{x})$	birth rate of migratory birds	WNV	0.0014	(Bergsman et al., 2016)
$\mu_V(T,\boldsymbol{x})$	natural mortality rate of mosquitoes	WNV&USUV	$f(T)$	(Rubel et al., 2008)
$\mu_{rB}(\boldsymbol{x})$	natural mortality rate of resident birds	WNV	0.0005	(Mbaoma et al., 2024)
$\mu_{mB}(\boldsymbol{x})$	natural mortality rate of migratory birds	WNV	0.00023	(Mbaoma et al., 2024)
$\gamma_V(T,\boldsymbol{x})$	latency rate on mosquitoes	WNV&USUV	$f(T)$	(Heidecke et al., 2024)
$\gamma_{rB}(\boldsymbol{x})$	latency rate on resident birds	WNV	0.196	(Mbaoma et al., 2024)
$\gamma_{mB}(\boldsymbol{x})$	latency rate on migratory birds	WNV	0.285	(Mbaoma et al., 2024)
$\alpha_{rB}(\boldsymbol{x})$	removal rate of infectious resident birds	WNV	0.867	(Mbaoma et al., 2024)
$\alpha_{mB}(\boldsymbol{x})$	removal rate of infectious migratory birds	WNV	0.4	(Mbaoma et al., 2024)
$\nu_{rB}(\boldsymbol{x})$	proportion of dead resident birds	WNV	0.655	(Mbaoma et al., 2024)
$\nu_{mB}(\boldsymbol{x})$	proportion of dead migratory birds	WNV	0.103	(Mbaoma et al., 2024)
$p_{Vr}(\boldsymbol{x})$	probability of a new resident bird infection	WNV	0.97	(Mbaoma et al., 2024)
$p_{Vm}(\boldsymbol{x})$	probability of a new migratory bird infection	WNV	0.9	(Mbaoma et al., 2024)
$p_{rV}(\boldsymbol{x})$	probability of a new mosquito infection from a resident bird	WNV	0.4	(Mbaoma et al., 2024)
$p_{mV}(\boldsymbol{x})$	probability of a new mosquito infection from a migratory bird	WNV	0.7	(Mbaoma et al., 2024)
$\beta(T,\boldsymbol{x})$	mosquito biting rate	WNV&USUV	$f(T)$	(Rubel et al., 2008)
$\phi(\boldsymbol{x})$	mosquito to resident bird ratio	WNV&USUV	varies	assumed
$\gamma_B(\boldsymbol{x})$	latency rate of birds	USUV	0.667	(Rubel et al., 2008)
$\alpha_B(\boldsymbol{x})$	removal rate of birds	USUV	0.0182	(Rubel et al., 2008)
$\nu_B(\boldsymbol{x})$	fraction of birds dying due to the infection	USUV	0.3	(Rubel et al., 2008)
$\mu_B(\boldsymbol{x})$	mortality rate of birds	USUV	0.0012	(Rubel et al., 2008)
$p_v(\boldsymbol{x})$	probability of virus transmission by infectious birds	USUV	0.125	(Rubel et al., 2008)
$p_b(\boldsymbol{x})$	probability of virus transmission by infectious mosquitoes	USUV	1.000	(Rubel et al., 2008)
K_V	environmental carrying capacity of mosquitoes	WNV&USUV	2×10^9	assumed
K_{rB}	carrying capacity of resident birds	WNV	110×10^6	assumed
K_{mB}	carrying capacity of migratory birds	WNV	110×10^6	assumed
K_B	environmental carrying capacity of birds	USUV	110×10^6	assumed

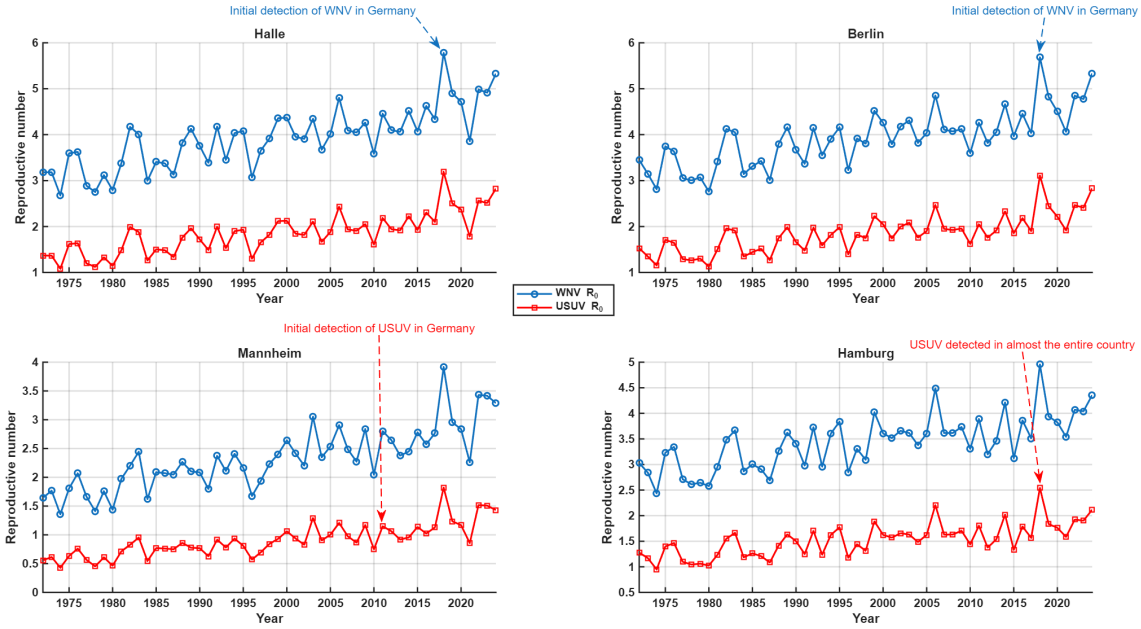


Figure 3.5: Basic reproductive number for WNV and USUV, for the period 1972-2024.

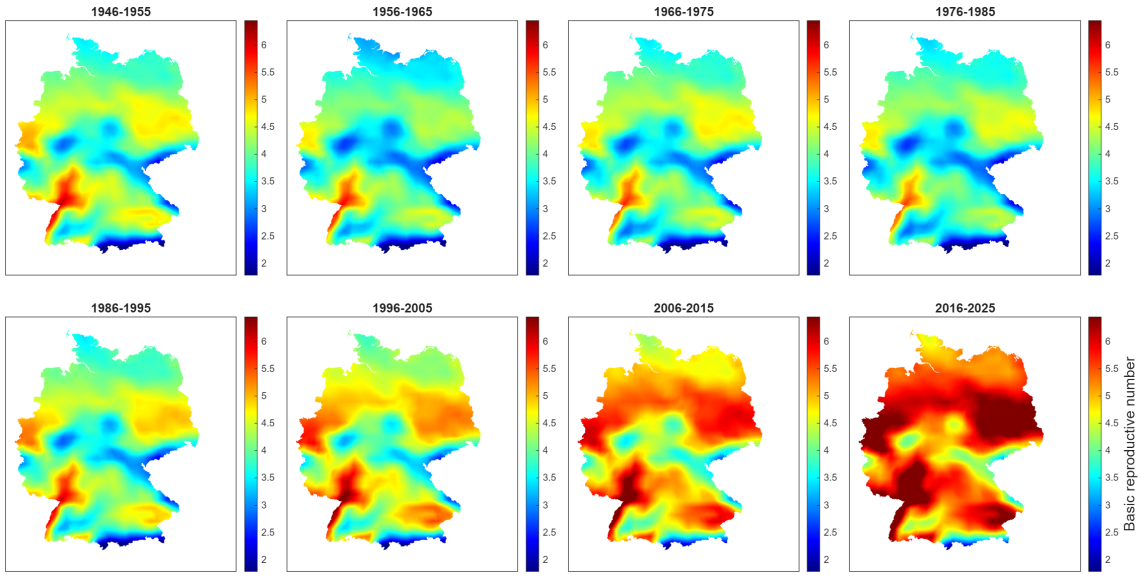


Figure 3.6: Decadal WNV basic reproduction number $R_0(x)$ for the period 1946-2025.

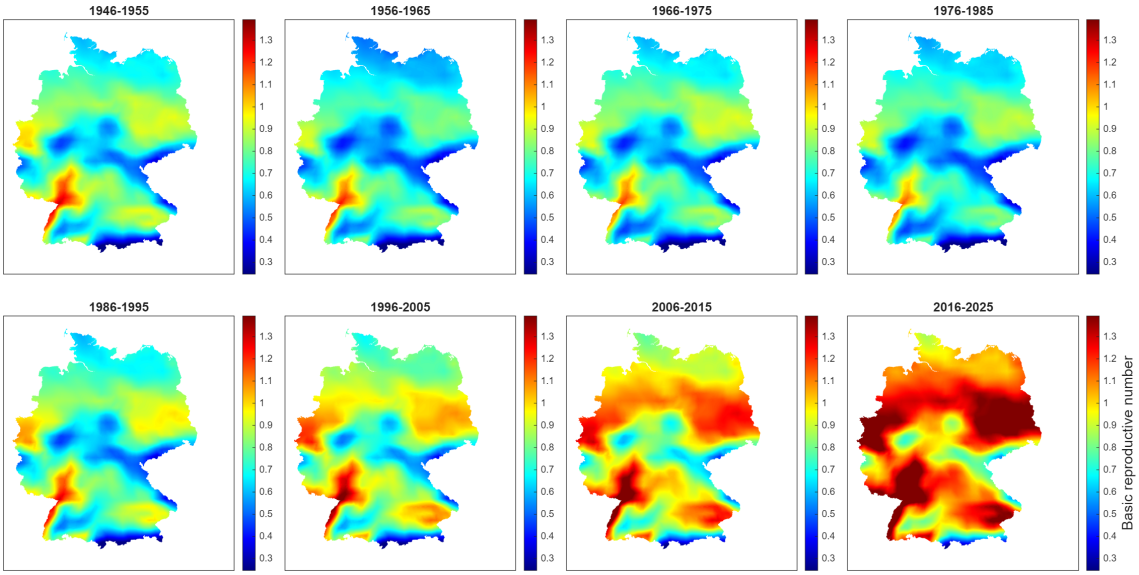


Figure 3.7: Decadal USUV basic reproduction number $R_0(x)$ for the period 1946-2025.

3.5 Spreading pattern of West Nile virus in Germany

WNV presents a unique spatio-temporal spreading pattern influenced by the combined effects of temperature suitability, host movement, and landscape heterogeneity. Following its initial establishment in Halle (Saale) in 2018, the virus has expanded across nearly the entire country, with persistent high circulation areas emerging in regions that favour high mosquito activity. These areas then serve as sources for further spread, demonstrating that WNV propagation in Germany is not uniform but rather occurs through local amplification followed by gradual dispersal into surrounding areas. In addition to seasonal fluctuations, the spatial expansion in Germany mainly follows an anti-clockwise pattern. This pattern indicates that host movement, including that of migratory bird species, plays a vital role in facilitating long-distance dispersal beyond initial establishment sites.

Results obtained from the simulation of the WNV PDE model highlighted that when mosquito bites meant for residential birds are channelled to migratory birds, then WNV spreads faster than the case when bites are biased towards resident birds. This spreading mechanism may explain the observed pattern of gradual geographic expansion marked by sporadic emergence of new infection regions that were previously uninfected. Identifying high circulation areas may help support targeted screening of organ, tissue and blood donors, given that WNV transmission through transplantation has been documented and associated with severe clinical outcomes (Anesi and Silveira, 2019; Frank et al., 2022; Sambri, 2016; Soto et al., 2022).

3.6 Spreading pattern of Usutu virus in Germany

In contrast, USUV showed a different geographic distribution and progressed more slowly. It generally remained localised, especially from 2011 to 2015, with recurrent activity in areas where it was already present. Similar to WNV, the spread of USUV is strongly affected by seasonal variation, with transmission mainly occurring during periods that favour mosquito activity and viral development (Ziegler et al., 2019, 2020). As a result, the spatial persistence of USUV in localised regions during the initial years of infection led the model to focus on resident birds only, influenced by the diffusion process. This aligns with the biology of USUV, given its high viraemia in Eurasian blackbirds that are considered less migratory (Lühken et al., 2017; Rubel et al., 2008).

Over the years, USUV and WNV exhibited contrasting spreading patterns: USUV mainly expanded clockwise, while WNV spread anticlockwise across Germany. The model simulations showed that these differences resulted from the viruses being introduced at different locations and times, which shaped their spreading directions. Despite this, both viruses follow similar major infection routes, largely governed by temperature suitability, which favours *Culex* mosquito activity and virus amplification.

3.7 Control of West Nile virus and Usutu virus

Control of WNV in Germany typically depends on integrated One Health surveillance efforts that include vector monitoring, dead-bird surveillance, veterinary reports, and human diagnostics (Frank et al., 2022). The virus mainly persists through a complex mosquito-bird enzootic cycle, in which birds serve as amplifying hosts, while *Culex* mosquitoes are the primary vectors. This enzootic cycle is difficult to break, given the widespread distribution of *Culex* vector species and the bird migration (Marino et al., 2025). Surveillance of mosquitoes and birds often detects WNV activity weeks before human and equid cases emerge (Eidson et al., 2001; Tsioka et al., 2025), reinforcing the importance of increased bird and mosquito testing as early warning tools for WNV.

As a result, a model for the control of WNV was developed and used to examine the role of awareness and educational campaigns against WNV, based on bird infections. These campaigns aim to promote the early adoption of personal protective equipment (PPE), thereby reducing mosquito-human contact. The simulation results indicate that if humans begin using PPE immediately after WNV detections in birds, the incidence of human infections can be prevented or minimised. This timing allows for effective public health interventions before the virus spillover into humans, as supported by some surveillance studies (Eidson et al., 2001; Tsioka et al., 2025).

Conversely, PPE are primarily designed for humans and may not serve as a practical means of protection for equids against mosquito exposure. Thus, for equids, vaccination remains the main and approved preventive measure against WNV infection (Cendejas and Goodman, 2024). Incorporating vaccination into the model, the effect of increasing vaccine coverage on equine infection dynamics was examined. A consistent decrease in equid infections was observed as coverage increased. This outcome reflects the reduction in the force of infection during periods of active viral circulation when equids are vaccinated. Although equids are dead-end hosts and do not contribute to onward transmission, lowering their infection rates is epidemiologically and clinically relevant, as equid cases form a substantial disease burden and may serve as important sentinel indicators of local transmission intensity (Chevalier et al., 2025; Monath et al., 1985; Ward and Scheurmann, 2008).

While PPE and vaccination reduce disease risk in humans and equids, respectively, neither intervention directly targets the underlying enzootic transmission cycle sustained by mosquitoes and birds. Consequently, control strategies aimed at mosquito populations remain central to reducing overall transmission intensity. In the model presented here, interventions that decrease mosquito abundance, such as physical removal and destruction of potential breeding sites, the use of larvicides, and the application of adult mosquito controls, were examined. These control measures were modelled using an adjoint system to determine the optimal timing and duration based on the temperature data. Findings from this analysis indicated that breeding site removal and larviciding should commence in early spring and continue through mid-summer, stopping entirely before the end of July. This aligns with other research emphasising spring temperatures as crucial for WNV phenology, e.g., (Farooq et al., 2023), and studies advocating early mosquito suppression prior to emergence (Morreale et al., 2024). Since mosquito populations are at their lowest in spring, it is logical to begin control efforts early to curb population growth before summer amplification, thus reducing the effort required later. Delaying mosquito control until mid-summer usually shifts the focus towards more expensive strategies, as mosquitoes and breeding sites become more widespread and dispersed. Bellver-Arnau et al. (2025) further supports this argument by suggesting that, for optimal results, mosquito controls should be preventive rather than reactive, aligning with the findings from the optimal control model presented in this thesis.

Adult mosquito control methods focus on strategies that target mosquitoes during their adult phase. These strategies directly reduce the vector population and include actions such as modifying or treating overwintering sites with adulticides. Although adulticide spraying has traditionally been used during human WNV outbreaks and has yielded positive results (Carney et al., 2008), its use is increasingly discouraged

due to documented negative impacts on non-target species, ecosystem health, and the development of insecticide resistance. The optimal control analysis presented in this thesis shows that controlling adult mosquitoes is the most effective and cost-efficient method when performed before the peak transmission season.

The model suggests that winter or late-winter interventions may be particularly effective because *Culex* mosquitoes often overwinter in sheltered and relatively predictable habitats, such as in cellars, basements, tunnels, and other underground structures. Targeting these overwintering populations before spring emergence could reduce the number of infected mosquitoes available to initiate transmission in the following season (Dörge et al., 2020; Sauer et al., 2023). However, this hypothesis remains theoretical and requires further investigation. If applied successfully, such control efforts could reduce the number of adult mosquitoes emerging in the subsequent spring, thereby lowering early-season vector abundance and delaying seasonal amplification. Additionally, limiting vector populations at the start of the transmission season might help decrease disease burden the following season (Field et al., 2022; Kobayashi et al., 2012; Liu et al., 2016; Peffers et al., 2021; Romiti et al., 2025; Sauer et al., 2022; Thomas et al., 2009).

USUV and WNV share similar enzootic transmission cycles involving *Culex* mosquitoes and bird hosts, often co-circulating in the same ecological and climatic zones (Zannoli and Sambri, 2019). Consequently, vector control measures targeting WNV, like larval source management, adult mosquito control, and mosquito and bird surveillance, are also effective for USUV without needing major modifications. This overlap offers an opportunity for integrated, cost-effective vector control strategies that could reduce transmission of both viruses, especially in areas where both viruses co-circulate.

3.8 Conclusion

Understanding the spatio-temporal dynamics and control of mosquito-borne flaviviruses is essential for protecting human and animal health. Results from the process-based model demonstrated that the seasonal phenology of *Culex pipiens* s.s./*Cx. torrentium* in Germany can be realistically reproduced using temperature-, rainfall-, and photoperiod-dependent processes. The reliance on environmental data including the predicted data that are routinely available suggests that the model could support early-warning systems by forecasting periods of increased mosquito abundance and informing targeted vector surveillance and control activities.

An important question examined in this thesis is when mosquito control measures are most effective. The optimal control analyses indicated that interventions targeting

mosquito populations could be most beneficial when implemented early, particularly in late winter or early spring, before large-scale vector amplification occurs. Conversely, control measures taken during peak summer transmission require more effort and cost to achieve similar infection reductions. These findings support the hypothesis that targeting and modifying mosquito overwintering sites provides a valuable opportunity for targeted off-season interventions, potentially reducing the need for intensive control during the transmission season (Cox et al., 2025). Additionally, this strategy can also help prevent outbreaks at the beginning of the mosquito season.

The temperature-dependent PDE models in this study show that WNV and USUV transmission in Germany heterogeneously distributed, influenced by local temperature conditions that impact vector populations and virus incubation. This demonstrates that spatially explicit PDE models capture heterogeneity missed by non-spatial models, emphasising the need to adopt spatially explicit approaches for developing region-specific interventions.

Results obtained here demonstrate that movement processes such as diffusion and advection are important for understanding how mosquito-borne viruses spread across regions. Diffusion models the local dispersal of vectors and hosts (Fick, 1855), resulting in local expansion of infections. In contrast, advection describes long-distance transport capturing the directed movement of species by a known velocity field (Boyd, 2001). Migratory birds, for instance, act as effective carriers of flaviviruses, facilitating the rapid spread along migration routes for migratory birds and transporting disease pathogens to distant locations (Dusek et al., 2009; Lord and Calisher, 1970; Rappole et al., 2000). This interaction between local diffusion, long-range advection, and temperature-dependent mosquito parameters connects small-scale transmission with regional spread, providing insights into how new hotspots may emerge in previously unaffected areas.

Although WNV and USUV differ in their public health impacts and surveillance levels, the modelling results here show that both viruses follow similar ecological transmission pathways as they are amplified by the same vectors. This indicates that vector control strategies designed for WNV could also be effective against USUV, particularly targeting the vectors themselves. The lower risk associated with USUV, as indicated by the basic reproductive number, should therefore, not discourage proactive control efforts, especially considering its widespread occurrence in bird populations.

Effective intervention strategies should focus on both local transmission hotspots and the larger pathways that facilitate virus spread. Specifically, control and surveillance efforts need to be extended along major migratory bird flyways, which may significantly contribute to the long-distance dissemination of mosquito-borne flaviviruses. Resources

should also prioritise high-risk hotspots identified in the eastern regions and in the northern, western, and southwestern (Upper Rhine Valley) areas, where ecological conditions and vector populations consistently support virus transmission. Focusing on these critical corridors and hotspots can improve early detection, reduce geographic spread, and enhance the efficiency of control measures by directing resources to where they will be most effective.

Like any modelling study, this research has limitations that must be acknowledged. The models developed in this study use parameter values from the literature, which can differ across regions and years. Although the spatial framework accounts for large-scale heterogeneity, it does not explicitly include finer details such as micro-habitat variability, human behaviour, and local control measures, which are all important in ecological models. Uncertainty in climate forecasts and surveillance data can also affect long-term risk assessments. Additionally, Germany lacks systematic arbovirus surveillance, so models rely on sparse data from sporadic or incidental citizen-reported cases. For example, the lack of any USUV cases in Germany between the years 2011-2015 could also be partly attributed to under reporting of cases, and not necessarily ecological factors. These limitations point to areas for future improvement, which will help better understand the mechanisms behind the global spread of mosquito-borne diseases.

3.9 Take-home message

1. Environmental forcing can forecast seasonal mosquito abundance and arbovirus risk, supporting early-warning systems and targeted control.
2. Climate change is increasing the suitability of Germany for WNV and USUV transmission by extending favourable conditions for mosquito survival, development, and seasonal activity.
3. Transmission risk is spatially heterogeneous, highlighting the importance of region-specific surveillance and intervention strategies.
4. Spatial diffusion and advection processes provide a realistic representation of how infected vectors and hosts contribute to disease spread across landscapes.
5. Migratory birds may facilitate the long-distance introduction and dispersal of WNV into previously unaffected regions.
6. Seasonal transmission periods alone can sustain WNV and USUV circulation in temperate environments.
7. Early-season mosquito control may be more effective than delayed interventions

in reducing peak infections.

8. Climate change influences not only the magnitude of outbreaks but also their timing and geographical distribution.

9. Integrating mosquito ecology, climate drivers, and spatial transmission processes within a PDE framework enables realistic prediction of arbovirus emergence and spread.

10. The modelling frameworks developed in this thesis can support climate-informed surveillance, risk assessment, and control of mosquito-borne diseases in Germany and beyond.

Bibliography

Abdelrazec, A., Lenhart, S. and Zhu, H. Dynamics and optimal control of a West Nile virus model with seasonality. *Canadian Appl Math Quarterly*, 23(4):12–33, 2015.

Aberle, S.W., Kolodziejek, J., Jungbauer, C., Stiasny, K., Aberle, J.H., Zoufaly, A., Hourfar, M.K., Weidner, L. and Nowotny, N. Increase in human West Nile and Usutu virus infections, Austria, 2018. *Eurosurveillance*, 23(43), October 2018. https://doi.org/10.2807/1560-7917.es.2018.23.43.1800545.

Achee, N.L., Grieco, J.P., Vatandoost, H., Seixas, G., Pinto, J., Ching-NG, L., Martins, A.J., Juntarajumnong, W., Corbel, V., Gouagna, C., David, J.P., Logan, J.G., Orsborne, J., Marois, E., Devine, G.J. and Vontas, J. Alternative strategies for mosquito-borne arbovirus control. *PLOS Neglected Tropical Diseases*, 13(1):e0006822, January 2019. https://doi.org/10.1371/journal.pntd.0006822.

Ain-Najwa, M.Y., Yasmin, A.R., Omar, A.R., Arshad, S.S., Abu, J., Mohammed, H.O., Kumar, K., Loong, S.K., Rovie-Ryan, J.J. and Mohd-Kharip-Shah, A.K. Evidence of West Nile virus infection in migratory and resident wild birds in West Coast of Peninsular Malaysia. *One Health*, 10:100134, December 2020. https://doi.org/10.1016/j.onehlt.2020.100134.

Almirón, W.R. and Brewer, M.E. Winter biology of *Culex pipiens quinquefasciatus* say, (diptera: *Culicidae*) from Córdoba, Argentina. *Memórias do Instituto Oswaldo Cruz*, 91(5):649–654, October 1996. https://doi.org/10.1590/s0074-02761996000500019.

Anderson, R.M. and May, R.M. *Infectious diseases of humans: dynamics and control*. Oxford university press, 1991.

Anesi, J.A. and Silveira, F.P. Arenaviruses and West Nile virus in solid organ transplant recipients: Guidelines from the American Society of Transplantation Infectious Diseases Community of Practice. *Clinical Transplantation*, 33(9), May 2019. https://doi.org/10.1111/ctr.13576.

Angeloni, G., Bertola, M., Lazzaro, E., Morini, M., Masi, G., Sinigaglia, A., Trevisan, M., Gossner, C.M., Haussig, J.M., Bakonyi, T., Capelli, G. and Barzon, L. Epidemiology, surveillance and diagnosis of Usutu virus infection in the EU/EEA, 2012 to 2021. *Eurosurveillance*, 28(33), August 2023. https://doi.org/10.2807/1560-7917.es.2023.28.33.2200929.

Ashraf, U., Ye, J., Ruan, X., Wan, S., Zhu, B. and Cao, S. Usutu virus: An emerging Flavivirus in Europe. *Viruses*, 7(1):219–238, January 2015. https://doi.org/10.3390/v7010219.

Baker, R.E., Mahmud, A.S., Miller, I.F., Rajeev, M., Rasambainarivo, F., Rice, B.L., Takahashi, S., Tatem, A.J., Wagner, C.E., Wang, L.F., Wesolowski, A. and Metcalf, C.J.E. Infectious disease in an era of global change. *Nature Reviews Microbiology*, 20 (4):193–205, October 2021. https://doi.org/10.1038/s41579-021-00639-z.

Barman, S., Semenza, J.C., Singh, P., Sjödin, H., Rocklöv, J. and Wallin, J. A climate and population dependent diffusion model forecasts the spread of *Aedes Albopictus* mosquitoes in Europe. *Communications Earth & Environment*, 6(1), April 2025. doi: 10.1038/s43247-025-02199-z. http://dx.doi.org/10.1038/s43247-025-02199-z.

Barrera, R. Control of container *Aedes* mosquito vectors using trapping devices. In *2016 International Congress of Entomology*, ice2016. Entomological Society of America, 2016. https://doi.org/10.1603/ice.2016.93065.

Barrera, R. New tools for *Aedes* control: mass trapping. *Current Opinion in Insect Science*, 52:100942, August 2022. https://doi.org/10.1016/j.cois.2022.100942.

Becker, N., Petric, D., Zgomba, M., Boase, C., Madon, M., Dahl, C. and Kaiser, A. *Mosquitoes and Their Control*. Springer Berlin Heidelberg, 2010. ISBN 9783540928744. https://doi.org/10.1007/978-3-540-92874-4.

Becker, N., Jöst, A. and Weitzel, T. The *Culex pipiens* complex in Europe. *Journal of the American Mosquito Control Association*, 28(4s):53–67, December 2012. https://doi.org/10.2987/8756-971x-28.4s.53.

Becker, N., Petrić, D., Zgomba, M., Boase, C., Madon, M.B., Dahl, C. and Kaiser, A. *Mosquitoes: Identification, Ecology and Control*. Springer International Publishing, 2020. ISBN 9783030116231. https://doi.org/10.1007/978-3-030-11623-1.

Bellini, R., Zeller, H. and Van Bortel, W. A review of the vector management methods to prevent and control outbreaks of West Nile virus infection and the challenge for Europe. *Parasites and Vectors*, 7(1):323, 2014. https://doi.org/10.1186/1756-3305-7-323.

Bellver-Arnau, J., Blanco-Sierra, L., Escartin, S., Mariani, S. and Bartumeus, F. Climate-responsive vector control strategies for *Aedes albopictus*. *Parasites and Vectors*, 18(1), May 2025. https://doi.org/10.1186/s13071-025-06791-2.

Benelli, G., Jeffries, C. and Walker, T. Biological control of mosquito vectors: Past, present, and future. *Insects*, 7(4):52, October 2016. https://doi.org/10.3390/insects7040052.

Bergsman, L.D., Hyman, J.M. and Manore, C.A. A mathematical model for the spread of West Nile virus in migratory and resident birds. *Mathematical Biosciences and Engineering*, 13(2):401–424, 2016. https://doi.org/10.3934/mbe.2015009.

Bhowmick, S., Gethmann, J., Conraths, F.J., Sokolov, I.M. and Lentz, H.H. Locally temperature-driven mathematical model of West Nile virus spread in Germany. *Journal of Theoretical Biology*, 488:110117, March 2020. https://doi.org/10.1016/j.jtbi.2019.110117.

Bhowmick, S., Gethmann, J., Conraths, F.J., Sokolov, I.M. and Lentz, H.H. Seir-metapopulation model of potential spread of West Nile virus. *Ecological Modelling*, 476:110213, February 2023. https://doi.org/10.1016/j.ecolmodel.2022.110213.

Bhowmick, S., Fritz, M.L. and Smith, R.L. Host-feeding preferences and temperature shape the dynamics of West Nile virus: A mathematical model to predict the impacts of vector-host interactions and vector management on R0. *Acta Tropica*, 258:107346, 2024.

Bhowmick, S., Irwin, P., Lopez, K., Fritz, M.L. and Smith, R.L. A weather-driven mathematical model of *culex* population abundance and the impact of vector control interventions. *Ecological Informatics*, 89:103163, November 2025. https://doi.org/10.1016/j.ecoinf.2025.103163.

Blayneh, K.W., Gumel, A.B., Lenhart, S. and Clayton, T. Backward bifurcation and optimal control in transmission dynamics of West Nile virus. *Bulletin of Mathematical Biology*, 72(4):1006–1028, January 2010. https://doi.org/10.1007/s11538-009-9480-0.

Bouyer, J. Current status of the sterile insect technique for the suppression of mosquito populations on a global scale. *Infectious Diseases of Poverty*, 13(1), September 2024. https://doi.org/10.1186/s40249-024-01242-z.

Boyd, J.P. *Chebyshev and Fourier spectral methods*. Courier Corporation, 2001.

Brugger, K. and Rubel, F. Simulation of climate-change scenarios to explain Usutu-virus dynamics in Austria. *Preventive Veterinary Medicine*, 88(1):24–31, January 2009. https://doi.org/10.1016/j.prevetmed.2008.06.023.

Bussell, E.H., Dangerfield, C.E., Gilligan, C.A. and Cunniffe, N.J. Applying optimal control theory to complex epidemiological models to inform real-world disease management. *Philosophical Transactions of the Royal Society B: Biological Sciences*, 374 (1776):20180284, May 2019. https://doi.org/10.1098/rstb.2018.0284.

Bwman, C., Gumel, A., van Den Driessche, P., Wu, J. and Zhu, H. A mathematical model for assessing control strategies against West Nile virus. *Bulletin of Mathematical Biology*, 67(5):1107–1133, September 2005. https://doi.org/10.1016/j.bulm.2005.01.002.

Cadar, D., Lühken, R., van der Jeugd, H., Garigliany, M., Ziegler, U., Keller, M., Lahoreau, J., Lachmann, L., Becker, N., Kik, M., Oude Munnink, B.B., Bosch, S., Tannich, E., Linden, A., Schmidt, V., Koopmans, M.P., Rijks, J., Desmecht, D., Groschup, M.H., Reusken, C. and Schmidt-Chanasit, J. Widespread activity of multiple lineages of Usutu virus, western Europe, 2016. *Eurosurveillance*, 22(4), January 2017. https://doi.org/10.2807/1560-7917.es.2017.22.4.30452.

Cailly, P., Tran, A., Balenghien, T., L'Ambert, G., Toty, C. and Ezanno, P. A climate-driven abundance model to assess mosquito control strategies. *Ecological Modelling*, 227:7–17, February 2012. ISSN 0304-3800. doi: 10.1016/j.ecolmodel.2011.10.027. http://dx.doi.org/10.1016/j.ecolmodel.2011.10.027.

Calisher, C.H., Karabatsos, N., Dalrymple, J.M., Shope, R.E., Porterfield, J.S., Westaway, E.G. and Brandt, W.E. Antigenic relationships between flaviviruses as determined by cross-neutralization tests with polyclonal antisera. *Journal of General Virology*, 70 (1):37–43, January 1989. https://doi.org/10.1099/0022-1317-70-1-37.

Camp, J.V. and Nowotny, N. The knowns and unknowns of West Nile virus in europe: what did we learn from the 2018 outbreak? *Expert Review of Anti-infective Therapy*, 18(2):145–154, January 2020. https://doi.org/10.1080/14787210.2020.1713751.

Carlson, J.C., Byrd, B.D. and Omlin, F.X. Field assessments in western Kenya link malaria vectors to environmentally disturbed habitats during the dry season. *BMC Public Health*, 4(1), August 2004. https://doi.org/10.1186/1471-2458-4-33.

Carney, R.M., Husted, S., Jean, C., Glaser, C. and Kramer, V. Efficacy of aerial spraying of mosquito adulticide in reducing incidence of West Nile virus, California, 2005. *Emerging Infectious Diseases*, 14(5):747–754, May 2008. https://doi.org/10.3201/eid1405.071347.

Cendejas, P.M. and Goodman, A.G. Vaccination and control methods of West Nile

virus infection in equids and humans. *Vaccines*, 12(5):485, May 2024. https://doi.org/10.3390/vaccines12050485.

Center for Disease Control. Current dengue outbreak. httpss://www.cdc.gov/dengue/outbreaks/2024/index.html#:~:text=Dengue%20is%20the%20most%20common,of%20infected%20Aedes%20species%20mosquitoes., 2025. Accessed: 10 December 2025.

Center for Disease Control. Vaccines licensed for use in the united states. httpss://www.fda.gov/vaccines-blood-biologics/vaccines/vaccines-licensed-use-united-states, 2025. Accessed: 10 December 2025.

Chaskopoulou, A., Latham, M.D., Pereira, R.M., Connelly, R., Bonds, J.A.S. and Koehler, P.G. Efficacy of aerial ultra-low volume applications of two novel water-based formulations of unsynergized pyrethroids against riceland mosquitoes in Greece. *Journal of the American Mosquito Control Association*, 27(4):414–422, December 2011. https://doi.org/10.2987/11-6177.1.

Cheng, Y., Tjaden, N.B., Jaeschke, A., Lühken, R., Ziegler, U., Thomas, S.M. and Beierkuhnlein, C. Evaluating the risk for Usutu virus circulation in Europe: comparison of environmental niche models and epidemiological models. *International Journal of Health Geographics*, 17(1), October 2018. https://doi.org/10.1186/s12942-018-0155-7.

Chevalier, N., Migné, C.V., Mariteragi-Helle, T., Dumarest, M., De Mas, M., Chevrier, M., Queré, E., Marcillaud-Pitel, C., Lupo, C., Bigeard, C., Touzet, T., Leblond, A., Durand, B., Depecker, M. and Gonzalez, G. Seroprevalence of West Nile, Usutu and tick-borne encephalitis viruses in equids from south-western France in 2023. *Veterinary Research*, 56(1), April 2025. doi: 10.1186/s13567-025-01508-w. http://dx.doi.org/10.1186/s13567-025-01508-w.

Ciota, A.T., Matacchiero, A.C., Kilpatrick, A.M. and Kramer, L.D. The effect of temperature on life history traits of *Culex* mosquitoes. *Journal of Medical Entomology*, 51(1): 55–62, January 2014. https://doi.org/10.1603/me13003.

Colón-González, F.J., Sewe, M.O., Tompkins, A.M., Sjödin, H., Casallas, A., Rocklöv, J., Caminade, C. and Lowe, R. Projecting the risk of mosquito-borne diseases in a warmer and more populated world: a multi-model, multi-scenario intercomparison modelling study. *The Lancet Planetary Health*, 5(7):e404–e414, July 2021. https://doi.org/10.1016/s2542-5196(21)00132-7.

Cornes, v.d.S.G.v.d.B.E.J.M.J.P. E-obs daily gridded meteorological data for Europe from 1950 to present derived from in-situ observations., 2020. https://doi.org/

10.24381/cds.151d3ec6. Ensemble mean; grid resolution 0.1°; variables: daily minimum, mean and maximum temperature.

Cox, V.M., Tiley, K., Rosa, R., Pugliese, A., Angelini, P., Carrieri, M., Bhatt, S., Tamba, M., Marini, G., Calzolari, M. and Dorigatti, I. Meteorological and environmental drivers of West Nile virus prevalence in *Culex pipiens* mosquitoes in Emilia-Romagna, Italy in 2013 to 2022. *PLOS Pathogens*, 21(12):e1013753, December 2025. https://doi.org/10.1371/journal.ppat.1013753.

Dale, P. and Knight, J. Mosquito control: Perspectives on current issues and challenges. *Annals of Community Medicine and Practice*, 3(2):1023, 2017.

Dauphin, G., Zientara, S., Zeller, H. and Murgue, B. West Nile: worldwide current situation in animals and humans. *Comparative Immunology, Microbiology and Infectious Diseases*, 27(5):343–355, September 2004. https://doi.org/10.1016/j.cimid.2004.03.009.

de Souza, W.M., Ribeiro, G.S., de Lima, S.T., de Jesus, R., Moreira, F.R., Whittaker, C., Sallum, M.A.M., Carrington, C.V., Sabino, E.C., Kitron, U., Faria, N.R. and Weaver, S.C. Chikungunya: a decade of burden in the Americas. *The Lancet Regional Health - Americas*, 30:100673, February 2024. https://doi.org/10.1016/j.lana.2023.100673.

Deutscher Wetterdienst. Climate Data Center (CDC): Historical daily climate observations in Germany, 2024. httpss://www.dwd.de/EN/climate_environment/cdc/cdc_node.html. Accessed: 2024-08-01.

Dusek, R.J., McLean, R.G., Kramer, L.D., Ubico, S.R., Dupuis, A.P., Ebel, G.D. and Guptill, S.C. Prevalence of West Nile virus in migratory birds during spring and fall migration. *The American Journal of Tropical Medicine and Hygiene*, 81(6):1151–1158, December 2009. https://doi.org/10.4269/ajtmh.2009.09-0106.

Duve, P., Cadar, D., Becker, N., Schmidt-Chanasit, J., Sauer, F.G. and Lühken, R. A temperature-driven diffusion model of Usutu virus spread in Germany with spillover into neighbouring countries. *arXiv preprint arXiv:2605.03146*, 2026a.

Duve, P., Sauer, F.G. and Lühken, R. Modelling the control of West Nile virus using mosquito reduction methods, equid vaccination, and human behavioural adoption of personal protective equipment. *Ecological Modelling*, 517:111605, 2026b. ISSN 0304-3800. doi: 10.1016/j.ecolmodel.2026.111605. http://dx.doi.org/10.1016/j.ecolmodel.2026.111605.

Duve, P., Sauer, F.G. and Lühken, R. Modelling the impact of temperature and bird migration on the spread of West Nile virus. *One Health*, 22:101386, 2026c. ISSN 2352-7714. doi: 10.1016/j.onehlt.2026.101386. http://dx.doi.org/10.1016/j.onehlt.2026.101386.

Dörge, D.D., Cunze, S., Schleifenbaum, H., Zaenker, S. and Klimpel, S. An investigation of hibernating members from the *Culex pipiens* complex (diptera, *Culicidae*) in subterranean habitats of central Germany. *Scientific Reports*, 10(1), June 2020. https://doi.org/10.1038/s41598-020-67422-7.

Eidson, M., Kramer, L., Stone, W., Hagiwara, Y. and Schmit, K. Dead bird surveillance as an early warning system for West Nile virus. *Emerging Infectious Diseases*, 7(4): 631–635, August 2001. https://doi.org/10.3201/eid0704.040405.

Engel, D., Jöst, H., Wink, M., Börstler, J., Bosch, S., Garigliany, M.M., Jöst, A., Czajka, C., Lühken, R., Ziegler, U., Groschup, M.H., Pfeffer, M., Becker, N., Cadar, D. and Schmidt-Chanasit, J. Reconstruction of the evolutionary history and dispersal of Usutu virus, a neglected emerging arbovirus in Europe and Africa. *mBio*, 7(1), March 2016. https://doi.org/10.1128/mbio.01938-15.

European Centre for Disease Prevention and Control (ECDC) and European Food Safety Authority (EFSA). Surveillance of West Nile virus infections in humans and animals in Europe, monthly report – data submitted up to 3 october 2025. *EFSA Journal*, 23 (10), October 2025. https://doi.org/10.2903/j.efsa.2025.9715.

Ewing, D., Cobbold, C., Purse, B., Nunn, M. and White, S. Modelling the effect of temperature on the seasonal population dynamics of temperate mosquitoes. *Journal of Theoretical Biology*, 400:65–79, July 2016. https://doi.org/10.1016/j.jtbi.2016.04.008.

Ezanno, P., Aubry-Kientz, M., Arnoux, S., Cailly, P., L'Ambert, G., Toty, C., Balenghien, T. and Tran, A. A generic weather-driven model to predict mosquito population dynamics applied to species of *Anopheles*, *Culex* and *Aedes* genera of southern France. *Preventive Veterinary Medicine*, 120(1):39–50, 2015. ISSN 0167-5877. doi: 10.1016/j.prevetmed.2014.12.018. http://dx.doi.org/10.1016/j.prevetmed.2014.12.018.

Farooq, Z., Sjödin, H., Semenza, J.C., Tozan, Y., Sewe, M.O., Wallin, J. and Rocklöv, J. European projections of West Nile virus transmission under climate change scenarios. *One Health*, 16:100509, June 2023. https://doi.org/10.1016/j.onehlt.2023.100509.

Ferraguti, M., Dimas Martins, A. and Artzy-Randrup, Y. Quantifying the invasion risk of West Nile virus: Insights from a multi-vector and multi-host seir model. *One Health*, 17:100638, December 2023. https://doi.org/10.1016/j.onehlt.2023.100638.

Fick, A. Ueber diffusion. *Annalen der Physik*, 170(1):59–86, January 1855. https://doi.org/10.1002/andp.18551700105.

Field, E.N., Shepard, J.J., Clifton, M.E., Price, K.J., Witmier, B.J., Johnson, K., Boze, B., Abadam, C., Ebel, G.D., Armstrong, P.M., Barker, C.M. and Smith, R.C. Semi-field and surveillance data define the natural diapause timeline for *Culex pipiens* across the United States. *Communications Biology*, 5(1), November 2022. https://doi.org/10.1038/s42003-022-04276-x.

Floore, T.G. Mosquito larval control practices: Past and present. *Journal of the American Mosquito Control Association*, 22(3):527–533, September 2006. https://doi.org/10.2987/8756-971x(2006)22[527:mlcppa]2.0.co;2.

Frank, C., Schmidt-Chanasit, J., Ziegler, U., Lachmann, R., Preußel, K. and Offergeld, R. West Nile virus in Germany: An emerging infection and its relevance for transfusion safety. *Transfusion Medicine and Hemotherapy*, 49(4):192–204, 2022. https://doi.org/10.1159/000525167.

Franklinos, L.H.V., Jones, K.E., Redding, D.W. and Abubakar, I. The effect of global change on mosquito-borne disease. *The Lancet Infectious Diseases*, 19(9):e302–e312, September 2019. https://doi.org/10.1016/s1473-3099(19)30161-6.

Frantz, R.M., Godinez, H., Martinez, K., Cuello, W.S. and Manore, C. Age structured partial differential equations model for *Culex* mosquito abundance. *Ecological Modelling*, 494:110764, August 2024. ISSN 0304-3800. doi: 10.1016/j.ecolmodel.2024.110764. http://dx.doi.org/10.1016/j.ecolmodel.2024.110764.

Gaibani, P. and Rossini, G. An overview of Usutu virus. *Microbes and Infection*, 19(7–8): 382–387, July 2017. https://doi.org/10.1016/j.micinf.2017.05.003.

Garrett-Jones, C. and Shidrawi, G. Malaria vectorial capacity of a population of *anopheles gambiae*: an exercise in epidemiological entomology. *Bulletin of the World Health Organization*, 40(4):531, 1969.

Gato, R., Menéndez, Z., Prieto, E., Argilés, R., Rodríguez, M., Baldoquín, W., Hernández, Y., Pérez, D., Anaya, J., Fuentes, I., Lorenzo, C., González, K., Campo, Y. and Bouyer, J. Sterile insect technique: Successful suppression of an aedes aegypti field population in Cuba. *Insects*, 12(5):469, May 2021. https://doi.org/10.3390/insects12050469.

Giladi, M., Metzkor-Cotter, E., Martin, D.A., Siegman-Igra, Y., Korczyn, A.D., Rosso, R., Berger, S.A., Campbell, G.L. and Lanciotti, R.S. West Nile encephalitis in Israel, 1999: The New York connection. *Emerging Infectious Diseases*, 7(4):659–661, August 2001. https://doi.org/10.3201/eid0704.017410.

Gould, C.V., Staples, J.E., Guagliardo, S.A.J., Martin, S.W., Lyons, S., Hills, S.L., Nett, R.J. and Petersen, L.R. West Nile virus: a review. *JAMA*, 2025.

Groen, T.A., L'Ambert, G., Bellini, R., Chaskopoulou, A., Petric, D., Zgomba, M., Marrama, L. and Bicout, D.J. Ecology of West Nile virus across four European countries: empirical modelling of the *Culex pipiens* abundance dynamics as a function of weather. *Parasites and Vectors*, 10(1), October 2017. https://doi.org/10.1186/s13071-017-2484-y.

Gu, W., Regens, J.L., Beier, J.C. and Novak, R.J. Source reduction of mosquito larval habitats has unexpected consequences on malaria transmission. *Proceedings of the National Academy of Sciences*, 103(46):17560–17563, November 2006. https://doi.org/10.1073/pnas.0608452103.

Haider, N., Hasan, M.N., Onyango, J., Billah, M., Khan, S., Papakonstantinou, D., Paudyal, P. and Asaduzzaman, M. Global dengue epidemic worsens with record 14 million cases and 9000 deaths reported in 2024. *International Journal of Infectious Diseases*, 158:107940, September 2025. https://doi.org/10.1016/j.ijid.2025.107940.

Hawkes, F.M. and Hopkins, R.J. *The mosquito*, page 16–31. Routledge, September 2021. ISBN 9781003056034. doi: 10.4324/9781003056034-3. https://doi.org/10.4324/9781003056034-3.

Hayes, E.B., Komar, N., Nasci, R.S., Montgomery, S.P., O'Leary, D.R. and Campbell, G.L. Epidemiology and transmission dynamics of West Nile virus disease. *Emerging Infectious Diseases*, 11(8):1167–1173, August 2005. https://doi.org/10.3201/eid1108.050289a.

Heidecke, J., Wallin, J., Fransson, P., Singh, P., Sjödin, H., Stiles, P., Treskova, M. and Rocklöv, J. Disclosing temperature sensitivity of West Nile virus transmission: novel computational approaches to mosquito-pathogen trait responses. September 2024. doi: 10.1101/2024.09.16.613097. http://dx.doi.org/10.1101/2024.09.16.613097.

Heidecke, J., Wallin, J., Fransson, P., Singh, P., Sjödin, H., Stiles, P.C., Treskova, M. and Rocklöv, J. Uncovering temperature sensitivity of West Nile virus transmission:

Novel computational approaches to mosquito-pathogen trait responses. *PLOS Computational Biology*, 21(3):e1012866, March 2025. https://doi.org/10.1371/journal.pcbi.1012866.

Heitzman-Breen, N., Liyanage, Y.R., Duggal, N., Tuncer, N. and Ciupe, S.M. The effect of model structure and data availability on Usutu virus dynamics at three biological scales. *Royal Society Open Science*, 11(2), February 2024. https://doi.org/10.1098/rsos.231146.

Hethcote, H.W. The mathematics of infectious diseases. *SIAM Review*, 42(4):599–653, January 2000. https://doi.org/10.1137/s0036144500371907.

Hoang, M.T. and Ehrhardt, M. Differential equation models for infectious diseases: Mathematical modeling, qualitative analysis, numerical methods and applications. *SeMA Journal*, August 2025. https://doi.org/10.1007/s40324-025-00404-9.

Howard, L.O. *Remedies and preventives against mosquitoes*. Number 444. US Government Printing Office, 1911.

Huang, Y.J.S., Higgs, S. and Vanlandingham, D.L. Arbovirus-mosquito vector-host interactions and the impact on transmission and disease pathogenesis of arboviruses. *Frontiers in Microbiology*, 10, January 2019. https://doi.org/10.3389/fmicb.2019.00022.

Jaffal, A., Fite, J., Baldet, T., Delaunay, P., Jourdain, F., Mora-Castillo, R., Olive, M.M. and Roiz, D. Current evidences of the efficacy of mosquito mass-trapping interventions to reduce *Aedes aegypti* and *Aedes albopictus* populations and *Aedes-borne* virus transmission. *PLOS Neglected Tropical Diseases*, 17(3):e0011153, March 2023. https://doi.org/10.1371/journal.pntd.0011153.

Katz, G., Rannon, L., Nili, E. and Danon, Y. West Nile fever-occurrence in a new endemic site in the Negev. *Israel Journal of Medical Sciences*, 25(1):39–41, August 2001.

Kloter, K.O. Manual on environmental management for mosquito control with special emphasis on malaria vectors: 283 pages. World Health Organization, Geneva (WHO offset publication no. 66). 1982. sw. fr. 22.-. *The American Journal of Tropical Medicine and Hygiene*, 32(3):635–636, May 1983. https://doi.org/10.4269/ajtmh.1983.32.635.

Kobayashi, M., Kasai, S., Isawa, H., Hayashi, T., Sawabe, K. and Tsuda, Y. Overwintering site of *Culex pipiens pallens* in an urban environment of Saitama Prefecture in Japan.

Medical Entomology and Zoology, 63(4):319–323, 2012. https://doi.org/10.7601/mez.63.319.

Komar, N. and Clark, G.G. West Nile virus activity in Latin America and the Caribbean. *Revista Panamericana de Salud Pública*, 19(2):112–117, February 2006. https://doi.org/10.1590/s1020-49892006000200006.

Krol, L., Blom, R., Dellar, M., van der Beek, J.G., Stroo, A.C., van Bodegom, P.M., Geerling, G.W., Koenraadt, C.J. and Schrama, M. Interactive effects of climate, land use and soil type on *Culex pipiens/torrentium* abundance. *One Health*, 17:100589, December 2023. https://doi.org/10.1016/j.onehlt.2023.100589.

Kuno, G., Chang, G.J.J., Tsuchiya, K.R., Karabatsos, N. and Cropp, C.B. Phylogeny of the genus *Flavivirus*. *Journal of Virology*, 72(1):73–83, January 1998. https://doi.org/10.1128/jvi.72.1.73-83.1998.

Lanciotti, R.S., Roehrig, J.T., Deubel, V., Smith, J., Parker, M., Steele, K., Crise, B., Volpe, K.E., Crabtree, M.B., Scherret, J.H., Hall, R.A., MacKenzie, J.S., Cropp, C.B., Panigrahy, B., Ostlund, E., Schmitt, B., Malkinson, M., Banet, C., Weissman, J., Komar, N., Savage, H.M., Stone, W., McNamara, T. and Gubler, D.J. Origin of the West Nile virus responsible for an outbreak of encephalitis in the Northeastern United States. *Science*, 286(5448):2333–2337, December 1999. https://doi.org/10.1126/science.286.5448.2333.

Laperriere, V., Brugger, K. and Rubel, F. Simulation of the seasonal cycles of bird, equine and human West Nile virus cases. *Preventive Veterinary Medicine*, 98(2–3):99–110, February 2011. https://doi.org/10.1016/j.prevetmed.2010.10.013.

Lees, R.S., Gilles, J.R., Hendrichs, J., Vreysen, M.J. and Bourtzis, K. Back to the future: the sterile insect technique against mosquito disease vectors. *Current Opinion in Insect Science*, 10:156–162, August 2015. https://doi.org/10.1016/j.cois.2015.05.011.

Lelli, R., Calistri, P., Bruno, R., Monaco, F., Savini, G., Di Sabatino, D., Corsi, I. and Pascucci, I. West Nile transmission in resident birds in italy: West Nile transmission in resident birds. *Transboundary and Emerging Diseases*, 59(5):421–428, December 2011. https://doi.org/10.1111/j.1865-1682.2011.01287.x.

Lenhart, S. and Workman, J.T. *Optimal Control Applied to Biological Models*. Chapman and Hall/CRC, May 2007a. ISBN 9781420011418. https://doi.org/10.1201/9781420011418.

Lenhart, S. and Workman, J.T. An introduction to optimal control applied to immunology problems, 2007b. https://doi.org/10.1090/psapm/064/2359650.

Lin, Z. and Zhu, H. Spatial spreading model and dynamics of West Nile virus in birds and mosquitoes with free boundary. *Journal of Mathematical Biology*, 75(6–7): 1381–1409, April 2017. https://doi.org/10.1007/s00285-017-1124-7.

Liu, L., Zhang, B., Cheng, P., Wang, H., Guo, X., Zhang, C., Wang, H., Zhao, Y. and Gong, M. Overwintering of *Culex pipiens pallens* (diptera: *Culicidae*) in Shandong, China. *Journal of Entomological Science*, 51(4):314–320, October 2016. https://doi.org/10.18474/jes15-38.1.

Liu, X., Baimaciwang, Yue, Y., Wu, H., Pengcuociren, Guo, Y., Cirenwangla, Ren, D., Danzenggongga, Dazhen, Yang, J., Zhaxisangmu, Li, J., Cirendeji, Zhao, N., Sun, J., Li, J., Wang, J., Cirendunzhu and Liu, Q. Breeding site characteristics and associated factors of *Culex pipiens* complex in Lhasa, Tibet, P. R. China. *International Journal of Environmental Research and Public Health*, 16(8):1407, April 2019. https://doi.org/10.3390/ijerph16081407.

Loetti, V., Schweigmann, N. and Burroni, N. Development rates, larval survivorship and wing length of *Culex pipiens* (diptera: *Culicidae*) at constant temperatures. *Journal of Natural History*, 45(35–36):2203–2213, September 2011. https://doi.org/10.1080/00222933.2011.590946.

Lord, R.D. and Calisher, C.H. Further evidence of southward transport of arboviruses by migratory birds. *American Journal of Epidemiology*, 92(1):73–78, July 1970. https://doi.org/10.1093/oxfordjournals.aje.a121181.

Lorenzon, A., Granata, M., Verzelloni, P., Tommasi, L., Palandri, L., Malavolti, M., Bargellini, A., Righi, E., Vinceti, M., Paduano, S. and Filippini, T. Effect of climate change on West Nile virus transmission in Italy: A systematic review. *Public Health Reviews*, 46, April 2025. doi: 10.3389/phrs.2025.1607444. http://dx.doi.org/10.3389/phrs.2025.1607444.

Lutambi, A.M., Penny, M.A., Smith, T. and Chitnis, N. Mathematical modelling of mosquito dispersal in a heterogeneous environment. *Mathematical Biosciences*, 241 (2):198–216, February 2013. ISSN 0025-5564. doi: 10.1016/j.mbs.2012.11.013. http://dx.doi.org/10.1016/j.mbs.2012.11.013.

Lühken, R., Jöst, H., Cadar, D., Thomas, S.M., Bosch, S., Tannich, E., Becker, N., Ziegler, U., Lachmann, L. and Schmidt-Chanasit, J. Distribution of Usutu virus in Germany and its effect on breeding bird populations. *Emerging Infectious Diseases*, 23(12): 1994–2001, December 2017. https://doi.org/10.3201/eid2312.171257.

Macdonald, G. The analysis of infection rates in diseases in which superinfection occurs. *Tropical Diseases Bulletin*, 47(10):907–915, October 1950.

Macdonald, G. The analysis of the sporozoite rate. *Tropical Diseases Bulletin*, 49(6): 569–586, June 1952a.

Macdonald, G. The analysis of equilibrium in malaria. *Tropical diseases bulletin*, 49(9): 813–829, 1952b.

Macdonald, G. Epidemiological basis of malaria control. *Bulletin of the World Health Organization*, 15(3-5):613, 1956.

Mahyoub, J.A., Alsobhi, A.S., Al-Ghamdi, K., Khatter, N.A., Aziz, A.T., Al-Shami, S.A., Panneerselvam, C., Murugan, K., Nicoletti, M., Canale, A. and Benelli, G. Effectiveness of seven mosquito larvicides against the West Nile vector *Culex pipiens (L.)* in Saudi Arabia. *Asian Pacific Journal of Tropical Disease*, 6(5):361–365, May 2016. https://doi.org/10.1016/s2222-1808(15)61048-9.

Maidana, N.A. and Yang, H.M. Spatial spreading of West Nile virus described by traveling waves. *Journal of Theoretical Biology*, 258(3):403–417, June 2009. https://doi.org/10.1016/j.jtbi.2008.12.032.

Marberg, K., Goldblum, N., Sterk, V.V., Jasinska-Klingberg, W. and Klingberg, M.A. The natural history of West Nile fever. clinical observations during an epidemic in Israel. *American Journal of Epidemiology*, 64(3):259–269, November 1956. https://doi.org/10.1093/oxfordjournals.aje.a119838.

Marino, A., Vitale, E., Maniaci, A., La Via, L., Moscatt, V., Spampinato, S., Senia, P., Venanzi Rullo, E., Restivo, V., Cacopardo, B. and Nunnari, G. West Nile virus: Insights into microbiology, epidemiology, and clinical burden. *Acta Microbiologica Hellenica*, 70(4):44, November 2025. https://doi.org/10.3390/amh70040044.

Mbaoma, O.C., Thomas, S.M. and Beierkuhnlein, C. Spatiotemporally explicit epidemic model for West Nile virus outbreak in Germany: An inversely calibrated approach. *Journal of Epidemiology and Global Health*, 14(3):1052–1070, July 2024. https://doi.org/10.1007/s44197-024-00254-0.

Meineri, E., Deville, A., Grémillet, D., Gauthier-Clerc, M. and Béchet, A. Combining correlative and mechanistic habitat suitability models to improve ecological compensation. *Biological Reviews*, 90(1):314–329, May 2014. https://doi.org/10.1111/brv.12111.

Minakawa, N., Mutero, C.M., Githure, J.I., Beier, J.C. and Yan, G. Spatial distribution and habitat characterization of Anopheline mosquito larvae in Western Kenya. *The American journal of tropical medicine and hygiene*, 61(6):1010–1016, December 1999. https://doi.org/10.4269/ajtmh.1999.61.1010.

Minwuyelet, A., Petronio, G.P., Yewhalaw, D., Sciarretta, A., Magnifico, I., Nicolosi, D., Di Marco, R. and Atenafu, G. Symbiotic *Wolbachia* in mosquitoes and its role in reducing the transmission of mosquito-borne diseases: updates and prospects. *Frontiers in Microbiology*, 14, October 2023. doi: 10.3389/fmicb.2023.1267832. http://dx.doi.org/10.3389/fmicb.2023.1267832.

Monath, T.P., Pauli, R., Bowen, G.S., Mitchell, C.J., Daffner, J.F., Cropp, C.B. and Sabattini, M.S. Arbovirus investigations in Argentina, 1977—1980: Iv. serologic surveys and sentinel equine program. *The American Journal of Tropical Medicine and Hygiene*, 34(5):966–975, September 1985. doi: 10.4269/ajtmh.1985.34.966. http://dx.doi.org/10.4269/ajtmh.1985.34.966.

Moreira, L.A., Iturbe-Ormaetxe, I., Jeffery, J.A., Lu, G., Pyke, A.T., Hedges, L.M., Rocha, B.C., Hall-Mendelin, S., Day, A., Riegler, M., Hugo, L.E., Johnson, K.N., Kay, B.H., McGraw, E.A., van den Hurk, A.F., Ryan, P.A. and O'Neill, S.L. A *Wolbachia* symbiont in *Aedes aegypti* limits infection with dengue, chikungunya, and plasmodium. *Cell*, 139(7):1268–1278, December 2009. https://doi.org/10.1016/j.cell.2009.11.042.

Moretti, R., Lim, J.T., Ferreira, A.G.A., Ponti, L., Giovanetti, M., Yi, C.J., Tewari, P., Cholvi, M., Crawford, J., Gutierrez, A.P., Dobson, S.L. and Ross, P.A. Exploiting *Wolbachia* as a tool for mosquito-borne disease control: Pursuing efficacy, safety, and sustainability. *Pathogens*, 14(3):285, March 2025. https://doi.org/10.3390/pathogens14030285.

Morreale, R., Stenhouse, S., Carvalho, D.O., Hahn, D.A., Bourtzis, K., Lloyd, A., Gale, T.W. and Hoel, D.F. Seasonal insights for integrative mosquito management from multi-year baseline entomological data on *Aedes aegypti* in Lee County, Florida. *PLOS ONE*, 19(10):e0311407, October 2024. https://doi.org/10.1371/journal.pone.0311407.

Moura-Neto, J.A., Braga Silva, C.A., Moura, A.F. and Rocco Suassuna, J.H. Emergent arboviruses and renal transplantation: A global challenge. *Kidney International Reports*, 4(5):647–655, May 2019. https://doi.org/10.1016/j.ekir.2019.02.013.

Musto, C., Tamba, M., Calzolari, M., Torri, D., Marzani, K., Cerri, J., Bonilauri, P. and Delogu, M. Usutu virus in blackbirds (*Turdus merula*) with clinical signs, a case study from northern Italy. *European Journal of Wildlife Research*, 68(2), March 2022. https://doi.org/10.1007/s10344-022-01572-z.

Ong, J., Ho, S.H., Soh, S.X.H., Wong, Y., Ng, Y., Vasquez, K., Lai, Y.L., Setoh, Y.X., Chong, C.S., Lee, V., Wong, J.C.C., Tan, C.H., Sim, S., Ng, L.C. and Lim, J.T. Assessing

the efficacy of male *Wolbachia*-infected mosquito deployments to reduce dengue incidence in Singapore: study protocol for a cluster-randomized controlled trial. *Trials*, 23(1), December 2022. https://doi.org/10.1186/s13063-022-06976-5.

Owen, J., Moore, F., Panella, N., Edwards, E., Bru, R., Hughes, M. and Komar, N. Migrating birds as dispersal vehicles for West Nile virus. *EcoHealth*, 3(2):79–85, May 2006. https://doi.org/10.1007/s10393-006-0025-9.

Pecorari, M., Longo, G., Gennari, W., Grottola, A., Sabbatini, A.M., Tagliazucchi, S., Savini, G., Monaco, F., Simone, M.L., Lelli, R. and Rumpianesi, F. First human case of Usutu virus neuroinvasive infection, Italy, August-September 2009. *Eurosurveillance*, 14(50), December 2009. https://doi.org/10.2807/ese.14.50.19446-en.

Peffers, C.S., Pomeroy, L.W. and Meuti, M.E. Critical photoperiod and its potential to predict mosquito distributions and control medically important pests. *Journal of Medical Entomology*, 58(4):1610–1618, April 2021. https://doi.org/10.1093/jme/tjab049.

Petersen, L.R., Brault, A.C. and Nasci, R.S. West Nile virus: Review of the literature. *JAMA*, 310(3):308, July 2013. https://doi.org/10.1001/jama.2013.8042.

Pinto, S.B., Riback, T.I.S., Sylvestre, G., Costa, G., Peixoto, J., Dias, F.B.S., Tanamas, S.K., Simmons, C.P., Dufault, S.M., Ryan, P.A., O'Neill, S.L., Muzzi, F.C., Kutcher, S., Montgomery, J., Green, B.R., Smithyman, R., Eppinghaus, A., Saraceni, V., Durovni, B., Anders, K.L. and Moreira, L.A. Effectiveness of *Wolbachia*-infected mosquito deployments in reducing the incidence of dengue and other *Aedes*-borne diseases in Niterói, Brazil: A quasi-experimental study. *PLOS Neglected Tropical Diseases*, 15(7): e0009556, July 2021. https://doi.org/10.1371/journal.pntd.0009556.

Poidinger, M., Hall, R.A. and Mackenzie, J.S. Molecular characterization of the *japanese encephalitis* serocomplex of the *Flavivirus* genus. *Virology*, 218(2):417–421, April 1996. https://doi.org/10.1006/viro.1996.0213.

Pontifes, P.A., Ferre, J., Lavergne, J., Sidos, N. and Roiz, D. Evaluation of a mass trapping strategy to prevent mosquito nuisance in campsites of southern France. *Medical and Veterinary Entomology*, 38(4):592–598, July 2024. https://doi.org/10.1111/mve.12740.

Poulin, B., Lefebvre, G., Muranyi-Kovacs, C. and Hilaire, S. Mosquito traps: An innovative, environmental friendly technique to control mosquitoes. March 2017. https://doi.org/10.20944/preprints201703.0128.v1.

Powell, J.R. Mosquito-borne human viral diseases: Why *Aedes Aegypti*? *The American Journal of Tropical Medicine and Hygiene*, 98(6):1563–1565, June 2018. https://doi.org/10.4269/ajtmh.17-0866.

Powell, J.R., Gloria-Soria, A. and Kotsakiozi, P. Recent history of *Aedes Aegypti*: Vector genomics and epidemiology records. *BioScience*, 68(11):854–860, October 2018. https://doi.org/10.1093/biosci/biy119.

Rappole, J.H., Derrickson, S.R. and Hubálek, Z. Migratory birds and spread of West Nile virus in the Western hemisphere. *Emerging Infectious Diseases*, 6(4):397–400, August 2000. https://doi.org/10.3201/eid0604.000401.

Rauhöft, L., Duve, P., Martins-Afonso, S.M., Hanna, J., Şuleşco, T., Sauer, F.G. and Lühken, R. A process-based model simulating the life-cycle of culex pipiens s.s./cx. torrentium (diptera: Culicidae) in germany. *Parasites & Vectors*, 19(1), May 2026. doi: 10.1186/s13071-026-07410-4. http://dx.doi.org/10.1186/s13071-026-07410-4.

Reiczigel, J., Brugger, K., Rubel, F., Solymosi, N. and Lang, Z. Bayesian analysis of a dynamical model for the spread of the Usutu virus. *Stochastic Environmental Research and Risk Assessment*, 24(3):455–462, August 2009. https://doi.org/10.1007/s00477-009-0333-z.

Reiner, R.C., Perkins, T.A., Barker, C.M., Niu, T., Chaves, L.F., Ellis, A.M., George, D.B., Le Menach, A., Pulliam, J.R.C., Bisanzio, D., Buckee, C., Chiyaka, C., Cummings, D.A.T., Garcia, A.J., Gatton, M.L., Gething, P.W., Hartley, D.M., Johnston, G., Klein, E.Y., Michael, E., Lindsay, S.W., Lloyd, A.L., Pigott, D.M., Reisen, W.K., Ruktanonchai, N., Singh, B.K., Tatem, A.J., Kitron, U., Hay, S.I., Scott, T.W. and Smith, D.L. A systematic review of mathematical models of mosquito-borne pathogen transmission: 1970–2010. *Journal of The Royal Society Interface*, 10(81):20120921, April 2013. https://doi.org/10.1098/rsif.2012.0921.

Romiti, F., Casini, R., Del Lesto, I., Magliano, A., Ermenegildi, A., Droghei, S., Tofani, S., Scicluna, M.T., Pichler, V., Augello, A., Censi, F., Scaringella, P.L., Mastrobuoni, G., Bacciotti, D., Nencetti, A. and De Liberato, C. Characterization of overwintering sites (hibernacula) of the West Nile vector *Culex pipiens* in Central Italy. *Parasites and Vectors*, 18(1), February 2025. https://doi.org/10.1186/s13071-025-06710-5.

Ross, P.A., Robinson, K.L., Yang, Q., Callahan, A.G., Schmidt, T.L., Axford, J.K., Coquilleau, M.P., Staunton, K.M., Townsend, M., Ritchie, S.A., Lau, M.J., Gu, X. and Hoffmann, A.A. A decade of stability for *wMel Wolbachia* in natural *Aedes*

aegypti populations. *PLOS Pathogens*, 18(2):e1010256, February 2022. https://doi.org/10.1371/journal.ppat.1010256.

Ross, R. The mathematics of malaria. *BMJ*, 1(2626):1023–1023, April 1911. doi: 10.1136/bmj.1.2626.1023. https://doi.org/10.1136/bmj.1.2626.1023.

Ross, R. Malaria and *Anopheles funestus* in Mauritius. *Nature*, 112(2826):935–936, December 1923. https://doi.org/10.1038/112935a0.

Rubel, F., Brugger, K., Hantel, M., Chvala-Mannsberger, S., Bakonyi, T., Weissenböck, H. and Nowotny, N. Explaining Usutu virus dynamics in Austria: Model development and calibration. *Preventive Veterinary Medicine*, 85(3–4):166–186, July 2008. https://doi.org/10.1016/j.prevetmed.2008.01.006.

Rumbos, C.I. and Athanassiou, C.G. Assessment of selected larvicides for the control of *Culex pipiens* biotype *pipiens* and *Culex pipiens* biotype *molestus* under laboratory and semi-field conditions. *Pest Management Science*, 76(11):3568–3576, 2020. https://doi.org/10.1002/ps.5847.

Ryan, S.J., Carlson, C.J., Mordecai, E.A. and Johnson, L.R. Global expansion and redistribution of *Aedes*-borne virus transmission risk with climate change. August 2017. doi: 10.1101/172221. http://dx.doi.org/10.1101/172221.

Sambri, V. Seroprevalence of West Nile virus-specific antibodies in a cohort of blood donors in Northeastern Italy after five years. March 2016. https://doi.org/10.26226/morressier.56d5ba29d462b80296c9649c.

Sauer, F.G., Timmermann, E., Lange, U., Lühken, R. and Kiel, E. Effects of hibernation site, temperature, and humidity on the abundance and survival of overwintering *Culex pipiens pipiens* and *Anopheles messeae* (diptera: *Culicidae*). *Journal of Medical Entomology*, 59(6):2013–2021, September 2022. https://doi.org/10.1093/jme/tjac139.

Sauer, F.G., Lange, U., Schmidt-Chanasit, J., Kiel, E., Wiatrowska, B., Myczko, L. and Lühken, R. Overwintering *Culex torrentium* in abandoned animal burrows as a reservoir for arboviruses in Central Europe. *One Health*, 16:100572, June 2023. https://doi.org/10.1016/j.onehlt.2023.100572.

Schilling, M., Lawson, B., Spiro, S., Jagdev, M., Vaux, A.G.C., Bruce, R.C., Johnston, C.J., Abbott, A.J., Wrigglesworth, E., Pearce-Kelly, P., Cunningham, A.A., Medlock, J.M., Johnson, N. and Folly, A.J. Vertical transmission in field-caught mosquitoes identifies a mechanism for the establishment of Usutu virus in a temperate country. *Scientific Reports*, 15(1), July 2025. https://doi.org/10.1038/s41598-025-09335-x.

Schulz, C. and Becker, S.C. *Mosquitoes as Arbovirus Vectors: From Species Identification to Vector Competence*, page 163–212. Springer International Publishing, 2018. ISBN 9783319940755. https://doi.org/10.1007/978-3-319-94075-5_9.

Seelig, F. Guidelines for mosquito control in built-up areas in Europe.

Sego, T.J., Aponte-Serrano, J.O., Gianlupi, J.F. and Glazier, J.A. Generation of multicellular spatiotemporal models of population dynamics from ordinary differential equations, with applications in viral infection. *BMC Biology*, 19(1), September 2021. https://doi.org/10.1186/s12915-021-01115-z.

Seino, K.K., Long, M.T., Gibbs, E.P.J., Bowen, R.A., Beachboard, S.E., Humphrey, P.P., Dixon, M.A. and Bourgeois, M.A. Comparative efficacies of three commercially available vaccines against West Nile Virus (WNV) in a short-duration challenge trial involving an equine WNV encephalitis model. *Clinical and Vaccine Immunology*, 14 (11):1465–1471, November 2007. https://doi.org/10.1128/cvi.00249-07.

Semenza, J.C. and Suk, J.E. Vector-borne diseases and climate change: a European perspective. *FEMS Microbiology Letters*, 365(2), November 2017. https://doi.org/10.1093/femsle/fnx244.

Semenza, J.C., Tran, A., Espinosa, L., Sudre, B., Domanovic, D. and Paz, S. Climate change projections of West Nile virus infections in Europe: implications for blood safety practices. *Environmental Health*, 15(S1), March 2016. https://doi.org/10.1186/s12940-016-0105-4.

Ser, O. and Cetin, H. Toxicity of mosquito larvicides on non-target mosquito predator insect, backswimmer (*Notonecta* sp.). *Fres Environ Bull*, 24:311–316, 2015.

Shocket, M.S., Verwillow, A.B., Numazu, M.G., Slamani, H., Cohen, J.M., El Moustaid, F., Rohr, J., Johnson, L.R. and Mordecai, E.A. Transmission of West Nile and five other temperate mosquito-borne viruses peaks at temperatures between 23°c and 26°c. *eLife*, 9, September 2020. https://doi.org/10.7554/elife.58511.

Silva, J.V., Lopes, T.R., Oliveira-Filho, E.F.d., Oliveira, R.A., Durães-Carvalho, R. and Gil, L.H. Current status, challenges and perspectives in the development of vaccines against yellow fever, dengue, Zika and chikungunya viruses. *Acta Tropica*, 182: 257–263, June 2018. https://doi.org/10.1016/j.actatropica.2018.03.009.

Smithburn, K.C., Hughes, T.P., Burke, A.W. and Paul, J.H. A neurotropic virus isolated from the blood of a native of Uganda. *The American Journal of Tropical Medicine*, s1-20 (4):471–492, July 1940. https://doi.org/10.4269/ajtmh.1940.s1-20.471.

Soto, R.A., McDonald, E., Annambhotla, P., Velez, J.O., Laven, J., Panella, A.J., Machesky, K.D., White, J.L., Hyun, J., Freuck, E., Habel, J., Oh, D., Levi, M., Hasz, R., Eidbo, E., Staples, J.E., Basavaraju, S.V. and Gould, C.V. West Nile virus transmission by solid organ transplantation and considerations for organ donor screening practices, United States. *Emerging Infectious Diseases*, 28(2):403–406, February 2022. https://doi.org/10.3201/eid2802.211697.

Störk, T., de le Roi, M., Haverkamp, A.K., Jesse, S.T., Peters, M., Fast, C., Gregor, K.M., Könenkamp, L., Steffen, I., Ludlow, M., Beineke, A., Hansmann, F., Wohlsein, P., Osterhaus, A.D.M.E. and Baumgärtner, W. Analysis of avian Usutu virus infections in Germany from 2011 to 2018 with focus on dsrna detection to demonstrate viral infections. *Scientific Reports*, 11(1), December 2021. https://doi.org/10.1038/s41598-021-03638-5.

Su, T. Resistance and resistance management of biorational larvicides for mosquito control. *Journal of the Florida Mosquito Control Association*, 69(1), March 2022. https://doi.org/10.32473/jfmca.v69i1.130641.

Szabó, B.G., Nagy, A., Nagy, O., Koroknai, A., Csonka, N., Korózs, D., Jeszenszky, K., Hardi, A., Deézsi-Magyar, N., Sztikler, J., Bódi, Z., Cadar, D., Tóth, G.E., Veres, L., Barcsay, E., Takács, M. and Sinkó, J. First documented case of a fatal autochthonous Usutu virus infection in an immunocompromised patient in Hungary: a clinical-virological report and implications from the literature. *Virology Journal*, 22(1), July 2025. https://doi.org/10.1186/s12985-025-02890-9.

Takken, W., Charlwood, D. and Lindsay, S.W. The behaviour of adult *Anopheles gambiae*, sub-Saharan Africa's principal malaria vector, and its relevance to malaria control: a review. *Malaria Journal*, 23(1), May 2024. https://doi.org/10.1186/s12936-024-04982-3.

Tatem, A., Rogers, D. and Hay, S. *Global Transport Networks and Infectious Disease Spread*, page 293–343. Elsevier, 2006. ISBN 9780120317622. doi: 10.1016/s0065-308x(05)62009-x. http://dx.doi.org/10.1016/s0065-308x(05)62009-x.

Thomas, D., Weedermann, M., Billings, L., Hoffacker, J. and Washington-Allen, R.A. When to spray: a time-scale calculus approach to controlling the impact of West Nile virus. *Ecology and Society*, 14(2), 2009. https://doi.org/10.5751/es-03006-140221.

Tomczyk, A.M. and Sulikowska, A. Heat waves in lowland Germany and their circulation-related conditions. *Meteorology and Atmospheric Physics*, 130(5):499–515, September 2017. https://doi.org/10.1007/s00703-017-0549-2.

Tran, A., L'Ambert, G., Lacour, G., Benoît, R., Demarchi, M., Cros, M., Cailly, P., Aubry-Kientz, M., Balenghien, T. and Ezanno, P. A rainfall- and temperature-driven abundance model for *Aedes albopictus* populations. *International Journal of Environmental Research and Public Health*, 10(5):1698–1719, April 2013. ISSN 1660-4601. doi: 10.3390/ijerph10051698. http://dx.doi.org/10.3390/ijerph10051698.

Tsai, T., Popovici, F., Cernescu, C., Campbell, G. and Nedelcu, N. West Nile encephalitis epidemic in southeastern Romania. *The Lancet*, 352(9130):767–771, September 1998. https://doi.org/10.1016/s0140-6736(98)03538-7.

Tsioka, K., Stoikou, K., Antalis, V., Charizani, E., Pappa, S., Gewehr, S., Kalaitzopoulou, S., Mourelatos, S. and Papa, A. Detection of West Nile virus, Usutu virus and insect-specific bunyaviruses in *Culex spp.* mosquitoes, Greece, 2024. *Viruses*, 17(11):1414, October 2025. https://doi.org/10.3390/v17111414.

Tuff, K.T., Tuff, T. and Davies, K.F. A framework for integrating thermal biology into fragmentation research. *Ecology Letters*, 19(4):361–374, February 2016. https://doi.org/10.1111/ele.12579.

Tusting, L.S. Larval source management: A supplementary measure for malaria control. *Outlooks on Pest Management*, 25(1):41–43, February 2014. https://doi.org/10.1564/v25_feb_13.

Tóth, G.E., Petersen, M., Chevenet, F., Sikora, M., Tomazatos, A., Bialonski, A., Baum, H., Horváth, B., Siriyasatien, P., Heitmann, A., Jansen, S., Offergeld, R., Lachmann, R., Schmidt, M., Schmidt-Chanasit, J. and Cadar, D. Blood donors as sentinels for genomic surveillance of West Nile virus in Germany using a sensitive amplicon-based sequencing approach. *Journal of Infection*, 91(5):106647, November 2025. doi: 10.1016/j.jinf.2025.106647. http://dx.doi.org/10.1016/j.jinf.2025.106647.

Utarini, A., Indriani, C., Ahmad, R.A., Tantowijoyo, W., Arguni, E., Ansari, M.R., Supriyati, E., Wardana, D.S., Meitika, Y., Ernesia, I., Nurhayati, I., Prabowo, E., Andari, B., Green, B.R., Hodgson, L., Cutcher, Z., Rancès, E., Ryan, P.A., O'Neill, S.L., Dufault, S.M., Tanamas, S.K., Jewell, N.P., Anders, K.L. and Simmons, C.P. Efficacy of *Wolbachia*-infected mosquito deployments for the control of dengue. *New England Journal of Medicine*, 384(23):2177–2186, June 2021. https://doi.org/10.1056/nejmoa2030243.

van den Driessche, P. *Spatial Structure: Patch Models*, page 179–189. Springer Berlin Heidelberg, 2008. ISBN 9783540789116. https://doi.org/10.1007/978-3-540-78911-6_7.

Varghese, J., De Silva, I. and Millar, D.S. Latest advances in arbovirus diagnostics. *Microorganisms*, 11(5):1159, April 2023. https://doi.org/10.3390/microorganisms11051159.

Vilibic-Cavlek, T., Petrovic, T., Savic, V., Barbic, L., Tabain, I., Stevanovic, V., Klobucar, A., Mrzljak, A., Ilic, M., Bogdanic, M., Benvin, I., Santini, M., Capak, K., Monaco, F., Listes, E. and Savini, G. Epidemiology of Usutu virus: The European scenario. *Pathogens*, 9(9):699, August 2020. https://doi.org/10.3390/pathogens9090699.

Wamae, P., Githeko, A., Otieno, G., Kabiru, E. and Duombia, S. Early biting of the *Anopheles gambiae s.s.* and its challenges to vector control using insecticide treated nets in Western Kenya highlands. *Acta Tropica*, 150:136–142, October 2015. https://doi.org/10.1016/j.actatropica.2015.07.008.

Wang, Z., Nie, H. and Du, Y. Spreading speed for a West Nile virus model with free boundary. *Journal of Mathematical Biology*, 79(2):433–466, April 2019. https://doi.org/10.1007/s00285-019-01363-2.

Ward, M.P. and Scheurmann, J.A. The relationship between equine and human West Nile virus disease occurrence. *Veterinary Microbiology*, 129(3–4):378–383, June 2008. doi: 10.1016/j.vetmic.2007.11.022. http://dx.doi.org/10.1016/j.vetmic.2007.11.022.

Webb, J.L. *The long arc of mosquito control*, page 49–60. Routledge, September 2021. ISBN 9781003056034. https://doi.org/10.4324/9781003056034-6.

Weber, W.C., Streblow, D.N. and Coffey, L.L. Chikungunya virus vaccines: A review of ixchiq and pxvx0317 from pre-clinical evaluation to licensure. *BioDrugs*, 38(6):727–742, September 2024. https://doi.org/10.1007/s40259-024-00677-y.

Weissenböck, H., Kolodziejek, J., Url, A., Lussy, H., Rebel-Bauder, B. and Nowotny, N. Emergence of Usutu virus, an african mosquito-borne *flavivirus* of the *japanese encephalitis* virus group, central europe. *Emerging Infectious Diseases*, 8(7):652–656, July 2002. https://doi.org/10.3201/eid0807.020094.

Weissenböck, H., Bakonyi, T., Rossi, G., Mani, P. and Nowotny, N. Usutu virus, Italy, 1996. *Emerging Infectious Diseases*, 19(2):274–277, February 2013. https://doi.org/10.3201/eid1902.121191.

Woodall, J. The viruses isolated from arthropods at the East African Virus Research Institute in the 26 years ending december 1963. *Proc E Afr Acad*, 2:141–146, 1964.

World Health Organization. Larval source management: a supplementary malaria vector control measure: an operational manual. 2013.

World Health Organization. Dengue vaccine: WHO position paper, September 2018 – recommendations. *Vaccine*, 37(35):4848 – 4849, 2019. https://www.sciencedirect.com/science/article/pii/S0264410X18313392.

World Health Organization. Dengue - Global situation. https://www.who.int/emergencies/disease-outbreak-news/item/2023-DON498, 2023. Accessed: 10 December 2025.

World Health Organization. WHO fact sheet: Dengue. https://www.who.int/news-room/fact-sheets/detail/dengue-and-severe-dengue, 2025. Accessed: 10 December 2025.

Yadav, R., Shinde, N.G., Patil, K.T., Kote, A. and Kadam, P. Deltamethrin toxicity: Impacts on non-target organisms and the environment. *Environment and Ecology*, 41 (3D):2039–2043, September 2023. https://doi.org/10.60151/envec/vfht1065.

Yu, D., Madras, N. and Zhu, H. Temperature-driven population abundance model for *Culex pipiens* and *Culex restuans* (diptera: Culicidae). *Journal of Theoretical Biology*, 443:28–38, April 2018. ISSN 0022-5193. doi: 10.1016/j.jtbi.2018.01.024. http://dx.doi.org/10.1016/j.jtbi.2018.01.024.

Zannoli, S. and Sambri, V. West Nile virus and Usutu virus co-circulation in Europe: Epidemiology and implications. *Microorganisms*, 7(7):184, June 2019. https://doi.org/10.3390/microorganisms7070184.

Zayed, A. Vector-borne disease problems in rapid urbanization. *QJM: An International Journal of Medicine*, 113(Supplement 1), March 2020. doi: 10.1093/qjmed/hcaa060.002. http://dx.doi.org/10.1093/qjmed/hcaa060.002.

Zhang, J., Cosner, C. and Zhu, H. Two-patch model for the spread of West Nile virus. *Bulletin of Mathematical Biology*, 80(4):840–863, February 2018. https://doi.org/10.1007/s11538-018-0404-8.

Zhuang, Q. and Wang, J. A spatial epidemic model with a moving boundary. *Infectious Disease Modelling*, 6:1046–1060, 2021. https://doi.org/10.1016/j.idm.2021.08.005.

Ziegler, U., Fast, C., Eiden, M., Bock, S., Schulze, C., Hoeper, D., Ochs, A., Schlieben, P., Keller, M., Zielke, D.E., Luehken, R., Cadar, D., Walther, D., Schmidt-Chanasit, J. and Groschup, M.H. Evidence for an independent third Usutu virus introduction

into Germany. *Veterinary Microbiology*, 192:60–66, August 2016. https://doi.org/10.1016/j.vetmic.2016.06.007.

Ziegler, U., Lühken, R., Keller, M., Cadar, D., van der Grinten, E., Michel, F., Albrecht, K., Eiden, M., Rinder, M., Lachmann, L., Höper, D., Vina-Rodriguez, A., Gaede, W., Pohl, A., Schmidt-Chanasit, J. and Groschup, M.H. West Nile virus epizootic in Germany, 2018. *Antiviral Research*, 162:39–43, February 2019. https://doi.org/10.1016/j.antiviral.2018.12.005.

Ziegler, U., Santos, P.D., Groschup, M.H., Hattendorf, C., Eiden, M., Höper, D., Eisermann, P., Keller, M., Michel, F., Klopfleisch, R., Müller, K., Werner, D., Kampen, H., Beer, M., Frank, C., Lachmann, R., Tews, B.A., Wylezich, C., Rinder, M., Lachmann, L., Grünewald, T., Szentiks, C.A., Sieg, M., Schmidt-Chanasit, J., Cadar, D. and Lühken, R. West Nile virus epidemic in Germany triggered by epizootic emergence, 2019. *Viruses*, 12(4):448, April 2020. https://doi.org/10.3390/v12040448.

Zug, R. and Hammerstein, P. Still a host of hosts for *Wolbachia*: Analysis of recent data suggests that 40% of terrestrial arthropod species are infected. *PLoS ONE*, 7(6): e38544, June 2012. https://doi.org/10.1371/journal.pone.0038544.

4 Appendix

This appendix contains copies of the peer-reviewed publications that form the basis of this cumulative PhD thesis (Duve et al., 2026b,c; Rauhöft et al., 2026). The articles are included as PDF files in their published form and have not been edited or reformatted. They provide the methodological and scientific foundation for the analyses and findings presented in the main chapters of this thesis. In addition, the manuscript Duve et al. (2026a), which is currently under review, is included as a preprint.

4.1 Publication 1: *Modelling the impact of temperature and bird migration on the spread of West Nile virus*

One Health 22 (2026) 101386

Contents lists available at ScienceDirect

One Health

journal homepage: www.elsevier.com/locate/onehlt

Modelling the impact of temperature and bird migration on the spread of West Nile virus☆

Pride Duve*, Felix Gregor Sauer, Renke Lühken

Bernhard Nocht Institute for Tropical Medicine, Hamburg, Germany

ARTICLE INFO

Keywords:
West Nile virus
Diffusion
Advection
Spread
Mosquitoes
Migratory birds
Resident birds

ABSTRACT

West Nile virus (WNV) is a climate-sensitive mosquito-borne arbovirus that circulates between mosquitoes of the genus *Culex* and birds, with potential spillover to humans and other mammals. Recent trends in climatic change, characterised by early and/or prolonged summer seasons, increased temperatures, and above-average rainfall, are likely to have facilitated the spread of WNV in Europe. In this work, we formulate a spatial WNV model as a system of parabolic partial differential equations (PDEs), incorporating diffusion, advection, and temperature-dependent parameters, namely the mosquito birth rate, mosquito biting rate, extrinsic incubation rate, and mortality rate. Diffusion represents the random movement of both mosquitoes and birds across space, while advection captures the directed movement of migratory birds. The model is first studied mathematically, and we show that it has non-negative, unique, and bounded solutions in time and space. Numerical simulations of the PDE model are performed using temperature data for Germany (2019–2025). The simulation results showed strong agreement with the reported WNV cases among birds and equids in Germany. The observed spread patterns throughout the years were mainly driven by the combination of temperature, diffusion processes of hosts and vectors, and the biting preference of mosquitoes between resident and migratory birds. The model better explained the observed WNV spreading pattern, including distant, isolated cases in Germany, when more bites were allocated to migratory birds than to resident birds.

1. Introduction

West Nile virus (WNV) is an arbovirus of the Japanese encephalitis antigenic complex of the *Flaviviridae* family. It was first detected in a febrile patient from the West Nile district of Northern Uganda in 1937 [1], but is now considered the most geographically widespread arbovirus worldwide [2]. The virus circulates in an enzootic cycle between *Culex (Cx.)* mosquitoes and birds, with regular spillovers to humans, equids, and other mammals [3–5]. Birds are considered amplifying hosts because they develop sufficient viremia, allowing infection of mosquitoes, whereas humans, equids, and other mammals are considered dead-end hosts [6]. Most humans infected with WNV are asymptomatic, but a few may develop fever, headache, rash, among others [7], including the risk of a fatal outcome [8]. Infected equids often exhibit ataxia, lethargy, and weakness as signs of the infection [9]. Multiple theories have been proposed to explain the introduction of new WNV cases in a previously unaffected region. There is evidence that migratory birds play an important role in the spread of the pathogen [6]. For example, birds captured during their seasonal migration have tested positive for WNV in Israel [10–13]. Migratory birds likely spread the virus to stopover sites in Europe as they travel from the south to the north [4,14]. In contrast, considering the speed and duration of migratory birds' flights, along with the duration of viremia, other researchers argued that the short-distance movements of resident birds better explain the spread pattern of WNV [6].

Several mathematical models for WNV have been formulated. Many models emphasise the role of climatic conditions in the dynamics of WNV, as temperature plays a critical role in mosquito life-history traits and virus replication. Thereby, temperature-dependent functions are used to model mosquito and virus development rates [15–17]. These are included in ordinary differential equations (ODEs) to analyse the dynamics of WNV. However, local transmission dynamics are generally modelled within the vector and host populations, without accounting for geographic spread. Fesce et al. [18] estimated the basic reproductive number of the WNV infection and used it to quantify the infection spread in mosquitoes and birds, to classify areas with temperatures suitable for the outbreak of WNV. Other studies focus on controlling WNV, e.g., Bowman et al. [19]

☆ This article is part of a Special issue entitled: 'One Health framework for Inf Disease Modelling' published in One Health.

* Corresponding author.
E-mail address: pride.duve@bnitm.de (P. Duve).

https://doi.org/10.1016/j.onehlt.2026.101386
Received 19 August 2025; Received in revised form 13 February 2026; Accepted 8 March 2026
Available online 11 March 2026
2352-7714/© 2026 The Authors. Published by Elsevier B.V. This is an open access article under the CC BY license (http://creativecommons.org/licenses/by/4.0/).

simulated mosquito-reduction methods and personal protective measures. A potential spill-over from birds to equids and humans was modelled by Laperriere et al. [16] using temperature-driven parameters and providing values for parameters governing development and transitions between compartments. Other models analysed differences in seasonal trends using sinusoidal (trigonometric) functions to represent seasonal variations of the WNV disease dynamics [20–22]. Such models typically show seasons when mosquitoes are most likely to be active without accounting for climatic factors.

Different modelling frameworks also include the role of migratory birds in WNV transmission. Bergsman et al. [23] formulated an ODE model that investigates the interplay of WNV in both resident and migratory hosts. The model considers the yearly seasonal outbreaks that depend primarily on the number of susceptible migrant birds entering the local population each season, demonstrating that the early growth rates of seasonal outbreaks are more influenced by the migratory than the resident bird population. For Germany, Mbaoma et al. [17] recently developed an ODE model for WNV by incorporating the complete life cycle of *Cx. pipiens* as a vector, and resident birds, migratory birds, and humans as hosts. The study concluded that short-distance migratory birds such as the hooded crow were identified as important hosts in maintaining the enzootic transmission cycle of WNV in Germany. These ecological patterns for bird migration provide the fundamental biological basis for incorporating migratory birds into our model. This is mainly because bird movement patterns may determine where the virus can be introduced and how quickly it can spread during transmission seasons.

Although ODE-based models allow us to understand the transmission dynamics of WNV, they generally do not consider the spatial movement of hosts and vectors across different regions without incorporating additional mechanisms, such as those in multi-patch models or distance-dispersal kernels. For example, Bhowmick et al. [24] used an ODE-based modelling approach in combination with different distance dispersal kernels to describe the spreading process of WNV through migratory birds in Germany. As a promising alternative, researchers have incorporated spatial variation and disease spread across different geographical regions into ODE-based models using partial differential equation (PDE) methods. Lin and Zhu [25] developed a reaction–diffusion PDE model for the spatial spread of WNV in mosquitoes and birds in North America using free-boundary conditions. Another study of WNV propagation was conducted by Maidana and Yang [26], who proposed a spatial model to analyse WNV spread across the USA and calculated the travelling wave speed. The model considers a system of PDEs that describes the movement of mosquito and avian populations through diffusion and advection. Results from this study show that mosquito movements do not play a major role in the spread, while bird advection is an important factor for lower mosquito biting rates.

Maidana and Yang [27,28] also made significant contributions to the spatial modelling of WNV using PDE models, and their framework is the basis of this study. Unlike previous WNV PDE models in the literature, our model considers not only resident birds but also migratory birds as hosts, thereby capturing seasonal changes in WNV transmission patterns driven by bird migration. Furthermore, we simulate the model in Germany, accounting for spatial heterogeneity, identifying high circulation areas, and giving theoretical insights into the contribution of migratory birds to WNV spread. In Germany, WNV was first detected in August 2018 in birds from the Southeastern region of Berlin [29]. Since then, WNV has been established in Germany and has spread. Germany lies along migration routes of birds between Europe, the Mediterranean, and Africa [30]. A study conducted by Nussbaumer et al. [31] indicates that most migratory birds arrive in the northeastern region of Germany during spring and leave the country in early autumn via the southwestern direction. First WNV strains confirmed in Germany were closely related to strains previously detected in Austria and the Czech Republic [29], indicating a potential route of introduction, and their ability to overwinter in *Cx. pipiens* [32] allows the virus to persist in the long term.

2. Model formulation

Building on ODE-based models developed by Laperriere et al. [16] and Mbaoma et al. [17], we formulate a model for the spatial spread of WNV in Germany for the years 2019-2025, using 2018 data as initial distribution pattern. Our spatial model consists of a system of semi-linear parabolic PDEs that account for diffusion, advection, and reaction processes, together with temperature-dependent mosquito biting, latency, and mortality rates. In addition, our model includes the populations of mosquitoes and resident and migratory birds. The population of mosquitoes at time t and geographic location $\boldsymbol{x} = (x, y)$, is divided into three compartments: susceptible $S_V(t, \boldsymbol{x})$, exposed $E_V(t, \boldsymbol{x})$ and infectious $I_V(t, \boldsymbol{x})$, with the total population given by $N_V(t, \boldsymbol{x}) = S_V(t, \boldsymbol{x}) + E_V(t, \boldsymbol{x}) + I_V(t, \boldsymbol{x})$. Mosquitoes are recruited into the susceptible class via a logistic recruitment term: $b_V N_V \left[1 - \frac{N_V}{K_V}\right]$ governed by the environmental carrying capacity K_V.

In the susceptible state, mosquitoes get infected by biting an infectious resident bird I_{rB} and/or migratory bird I_{mB} at a temperature-dependent mosquito biting rate

$$\beta(T, \boldsymbol{x}) = \frac{0.344}{1 + 1.231e^{-0.184(T-20)}}, \tag{1}$$

and a probability of acquiring the infection of p_{rV} and p_{mV} (Table 1), from resident and migratory birds respectively. When multiple bird host types are present, mosquito bites are distributed among the hosts based on host density and biting preferences. Because of this, we here introduce bite-allocation fractions q_r and q_m, which represent the proportions of mosquito bites on resident and migratory birds, respectively. Under a density-dependent assumption, these fractions are defined as proportional to local host abundance, such that $q_r = \frac{N_{rB}}{N_{rB} + cN_{mB}}$ and $q_m = \frac{cN_{mB}}{N_{rB} + cN_{mB}}$, where $N_{rB} = S_{rB} + E_{rB} + I_{rB} + R_{rB}$ and $N_{mB} = S_{mB} + E_{mB} + I_{mB} + R_{mB}$ are the total resident and migratory bird populations. $c > 0$ is the host-preference parameter that controls how mosquito bites are divided between resident and migratory birds. When $c > 1$, migratory birds are more attractive, leading to a higher proportion of bites on them. Conversely, when $0 < c < 1$, the attractiveness of migratory birds is reduced, resulting in more bites on resident birds. When $c = 1$, bites are split based on host availability, which corresponds to density-dependent allocation without a specific feeding preference [23].

The force of infection on mosquitoes is therefore given by

$$\lambda_{BV}(T, \boldsymbol{x}) = \lambda_{r_V} + \lambda_{m_V} = \frac{q_r p_{rV} \beta(T, \boldsymbol{x}) I_{rB}}{N_{rB}} + \frac{q_m p_{mM} \beta(T, \boldsymbol{x}) I_{mB}}{N_{mB}}.$$

A successful contact between infectious birds and susceptible mosquitoes at location $\boldsymbol{x}$ and time t sends susceptible mosquitoes to the exposed class. The latency rate on mosquitoes was fitted in [15], and is given by

$$\gamma_V(T, \boldsymbol{x}) = \frac{1}{e^{-0.09T + 5.36}}. \tag{2}$$

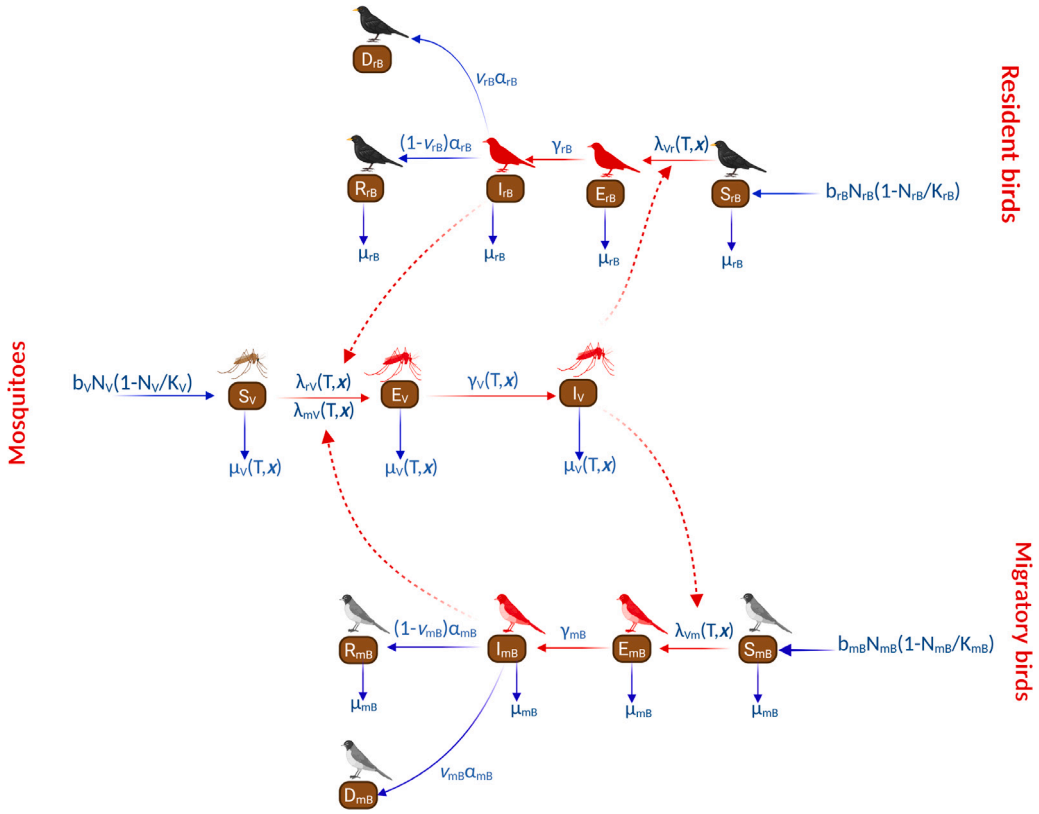


Fig. 1. Flow chart diagram describing the transmission dynamics of WNV in Germany. Solid arrows represent transitions between compartments, while dotted lines represent interactions between different states. *Image created in BioRender, with the licence: Arbovirologie (2025) https://BioRender.com/8a0gfj1. Content not licensed under the Creative Commons Attribution (CC BY) license.*

and from the exposed stage, mosquitoes progress to the infectious class (I_V). Mosquitoes die at temperature-dependent natural mortality rate of $\mu_V(T,\boldsymbol{x})$, where

$$\mu_V(T,\boldsymbol{x}) = \frac{0.0025T^2 - 0.094T + 1.0257}{10} \tag{3}$$

defined in [45]. Spatial and temporal plots of the thermal functions (Eqs. (1), (2), and (3)) are presented in Section S1 of the Suplementary material. The host population consists of resident and migratory birds. This population is divided into susceptible S_j, exposed E_j, infected I_j, recovered R_j, and dead D_j hosts, with $j = rB, mB$, and for easier readability, we denote resident birds by subscript (rB), and migratory birds by (mB). The recruitment into the susceptible bird populations is modelled using a logistic growth with density-dependent recruitment: $b_j N_j \left[1 - \frac{N_j}{K_j}\right]$, following Bhowmick et al. [33]. Susceptible resident and migratory birds get infected by interacting with infectious mosquitoes, with a biting rate $\beta(T,\boldsymbol{x})$ defined in Eq. (1), and a probability of acquiring the infection of p_{Vr} and p_{Vm} respectively.

In mosquito-borne disease models, the mosquito-to-bird ratio is crucial because it determines the per-bird biting pressure [16,17,33], which influences the disease burden. Vogels et al. [34] argued that mosquito abundance is limited by the availability of host blood meals, and bird density directly impacts mosquito feeding success. As a result, the number of bites an individual bird receives mainly depends on the ratio of mosquitoes to birds, rather than solely on mosquito or bird density. Because of this, we introduce the mosquito-to-bird ratio parameter ϕ for resident and migratory birds.

For simplicity of the model, this ratio is considered as an effective seasonal measure of mosquito biting pressure per host, instead of a population count over time. In WNV models, Bhowmick et al. [33] simulated their ODE model with a mosquito-to-bird ratio ranging from 10 to 30, while Laperriere et al. [16] used a ratio of 30. Another study by de Freitas Costa et al. [35], which aimed to investigate the conditions necessary for the circulation of WNV in Germany and the Netherlands, found that larger proportions of susceptible birds and higher vector–host ratios were required. The study showed that WNV circulation in the Netherlands was rarely sustained when vector–host ratios fell below approximately 1:100. We here inferred different yearly ratios whose values ranged between 30 and 60 (Table 2). The force of infection on resident birds is thus given by

$$\lambda_{Vr}(T,\boldsymbol{x}) = \frac{q_r \phi p_{Vr} \beta(T,\boldsymbol{x}) I_V(t,\boldsymbol{x})}{N_V}, \tag{4}$$

while that of migratory birds is

$$\lambda_{Vm}(T,\boldsymbol{x}) = \frac{q_m \phi p_{Vm} \beta(T,\boldsymbol{x}) I_V(t,\boldsymbol{x})}{N_V}. \tag{5}$$

The latency rates on resident and migratory birds are given by γ_{rB} and γ_{mB} respectively, while their recovery rates are given by α_{rB} and α_{mB}. Proportions $1 - \nu_{rB}$ of resident birds and $1 - \nu_{mB}$ of migratory birds recover from the infection, while the proportions ν_{rB} and ν_{mB} die at the rates α_{rB}, and α_{mB} respectively. Resident and migratory bird species can also die naturally at rates μ_{rB} and μ_{mB}.

2.1. Diffusion and advection processes

Diffusion describes the process by which matter is transported from one part of a system to another due to random molecular motions [36]. The concept of diffusion dates back to the 19th century, when Fick [37] recognised the transfer of heat by conduction driven by random molecular motions and quantified this process using the heat-conduction equation previously derived by baron de Fourier [38]. To date, the diffusion process has attracted significant attention, especially in mathematical biology. In ecological modelling, diffusion is used to describe the random movement of species from areas of higher concentration to areas of lower concentration [39], influencing their spatial distribution patterns. On the other hand, the advection process refers to the directional flow of a substance by a known velocity vector field [40]. The combined effects of diffusion and advection, along with the ODE terms, form an advection–diffusion–reaction PDE system that models how a phenomenon spreads over time and space. Reaction terms govern local transmission at each location, while diffusion and advection model the movement of species, including infectious ones.

In this study, we define diffusion for mosquitoes and for both resident and migratory birds as they move locally in search of resting/breeding sites, food, and other needs. The advection process is defined for migratory birds only, as we can account for their seasonal directional migration patterns. Diffusion is denoted by the Laplacian operator (Δ), with diffusion coefficients for mosquitoes, resident, and migratory birds denoted by D_1, D_2, D_3 in km^2/day respectively. Furthermore, we set the diffusion coefficients so that mosquito diffusion is lower than that of resident and migratory birds, as mosquitoes are considered insects with a small radius of action [26,41,42]. A lower diffusion coefficient is assigned to resident birds compared to migratory birds to highlight the greater mobility of migratory birds. To improve the interpretability of diffusion coefficients, we define the root-mean-square displacement (RMSD). The RMSD describes the dispersal distance species move from the initial source under diffusion alone after a time τ [43,44], and it is calculated using the formula:

$$\text{RMSD} = \sqrt{2pD\tau},$$

where $p = 2$ is the spatial dimension, D is the diffusion coefficient and τ is the time step. We denote the advection term by the gradient operator (∇), with a velocity $\boldsymbol{A} = [v_x, v_y]$ km/day, in a two-dimensional plane. The schematic diagram of our PDE model and the governing system of equations are shown in Fig. 1 and system (6).

$$
\begin{aligned}
\text{Mosquito population:}\quad & \begin{cases}
\frac{\partial S_V}{\partial t} &= D_1\Delta S_V + b_V N_V\left[1-\frac{N_V}{K_V}\right] - [\lambda_{rV}(T,\boldsymbol{x}) + \lambda m V(T,\boldsymbol{x}) + \mu_V(T,\boldsymbol{x})]S_V,\\
\frac{\partial E_V}{\partial t} &= D_1\Delta E_V + [\lambda_{rV}(T,\boldsymbol{x}) + \lambda m V(T,\boldsymbol{x})]S_V - \left[\gamma_V(T,\boldsymbol{x}) + \mu_V(T,\boldsymbol{x})\right]E_V,\\
\frac{\partial I_V}{\partial t} &= D_1\Delta I_V + \gamma_V(T,\boldsymbol{x})E_V - \mu_V(T,\boldsymbol{x})I_V,
\end{cases}\\
\text{Resident birds:}\quad & \begin{cases}
\frac{\partial S_{rB}}{\partial t} &= D_2\Delta S_{rB} + b_{rB}N_{rB}\left[1-\frac{N_{rB}}{K_{rB}}\right] - \left[\lambda_{Vr}(T,\boldsymbol{x}) + \mu_{rB}\right]S_{rB},\\
\frac{\partial E_{rB}}{\partial t} &= D_2\Delta E_{rB} + \lambda_{Vr}(T,\boldsymbol{x})S_{rB} - [\gamma_{rB} + \mu_{rB}]E_{rB},\\
\frac{\partial I_{rB}}{\partial t} &= D_2\Delta I_{rB} + \gamma_{rB}E_{rB} - [\alpha_{rB} + \mu_{rB}]I_{rB},\\
\frac{\partial R_{rB}}{\partial t} &= D_2\Delta R_{rB} + (1-\nu_{rB})\alpha_{rB}I_{rB} - \mu_{rB}R_{rB},\\
\frac{\partial D_{rB}}{\partial t} &= \alpha_{rB}\nu_{rB}I_{rB},
\end{cases}\\
\text{Migratory birds:}\quad & \begin{cases}
\frac{\partial S_{mB}}{\partial t} &= D_3\Delta S_{mB} - \boldsymbol{A}\cdot\nabla S_{mB} + b_{mB}N_{mB}\left[1-\frac{N_{mB}}{K_{mB}}\right] - \left[\lambda_{Vm}(T,\boldsymbol{x}) + \mu_{mB}\right]S_{mB},\\
\frac{\partial E_{mB}}{\partial t} &= D_3\Delta E_{mB} - \boldsymbol{A}\cdot\nabla E_{mB} + \lambda_{Vm}(T,\boldsymbol{x})S_{mB} - [\gamma_{mB} + \mu_{mB}]E_{mB},\\
\frac{\partial I_{mB}}{\partial t} &= D_3\Delta I_{mB} - \boldsymbol{A}\cdot\nabla I_{mB} + \gamma_{mB}E_{mB} - [\alpha_{mB} + \mu_{mB}]I_{mB},\\
\frac{\partial R_{mB}}{\partial t} &= D_3\Delta R_{mB} - \boldsymbol{A}\cdot\nabla R_{mB} + (1-\nu_{mB})\alpha_{mB}I_{mB} - \mu_{mB}R_{mB},\\
\frac{\partial D_{mB}}{\partial t} &= \nu_{mB}\alpha_{mB}I_{mB}.
\end{cases}
\end{aligned}
\tag{6}
$$

The total populations of mosquitoes, resident birds and migratory birds are given by $N_V = S_V + E_V + I_V$, $N_{rB} = S_{rB} + E_{rB} + I_{rB} + R_{rB}$, $N_{mB} = S_{mB} + E_{mB} + I_{mB} + R_{mB}$, while the initial conditions are given by:

$S_V(0,\boldsymbol{x}) = \psi_1(\boldsymbol{x})$, $E_V(0) = \psi_2(\boldsymbol{x})$, $I_V(0) = \psi_3(\boldsymbol{x})$, $S_{rB}(0,\boldsymbol{x}) = \psi_4(\boldsymbol{x})$, $E_{rB}(0,\boldsymbol{x}) = \psi_5(\boldsymbol{x})$, $I_{rB}(0,\boldsymbol{x}) = \psi_6(\boldsymbol{x})$, $R_{rB}(0,\boldsymbol{x}) = \psi_7(\boldsymbol{x})$, $D_{rB}(0) \geq 0$, $S_{mB}(0,\boldsymbol{x}) = \psi_8(\boldsymbol{x})$, $E_{mB}(0,\boldsymbol{x}) = \psi_9(\boldsymbol{x})$, $I_{mB}(0,\boldsymbol{x}) = \psi_{10}(\boldsymbol{x})$, $R_{mB}(0,\boldsymbol{x}) = \psi_{11}(\boldsymbol{x})$, $D_{mB}(0) \geq 0$, where,

$$\boldsymbol{x} = (x,y) \in \Omega, \quad \Delta = \frac{\partial^2(\cdot)}{\partial x^2} + \frac{\partial^2(\cdot)}{\partial y^2}, \quad \nabla = \left[\frac{\partial(\cdot)}{\partial x}, \frac{\partial(\cdot)}{\partial y}\right].$$

We assume the system moves in a region $\Omega \subset \mathbb{R}^2$, with a smooth boundary $\partial\Omega$ according to Fick's law [37], so that in the initial conditions, $\boldsymbol{x} \in \Omega$, where $\psi_i \in C^2(\Omega) \cap C(\bar{\Omega})$ and subject to the homogeneous Neumann boundary conditions:

$$\frac{\partial S_V}{\partial n} = \frac{\partial E_V}{\partial n} = \frac{\partial I_V}{\partial n} = \frac{\partial S_{rB}}{\partial n} = \frac{\partial E_{rB}}{\partial n} = \frac{\partial I_{rB}}{\partial n} = \frac{\partial R_{rB}}{\partial n} = \frac{\partial S_{mB}}{\partial n} = \frac{\partial E_{mB}}{\partial n} = \frac{\partial I_{mB}}{\partial n} = \frac{\partial R_{mB}}{\partial n} = 0,$$

for $\boldsymbol{x} \in \partial\Omega$, $t > 0$, and n is the unit outer normal to Ω. The state variables and initial conditions are summarised in Table (S1) of the Supplementary material, while model parameters are shown in Table 1.

Table 1
Definition of parameters used in system (6).

Parameter	Definition	Value	Source
$b_V(\boldsymbol{x})$	Birth rate of mosquitoes	0.0666	[23]
$b_{rB}(\boldsymbol{x})$	Birth rate of resident birds	0.00342	[45]
$b_{mB}(\boldsymbol{x})$	Birth rate of migratory birds	0.0014	[23]
$\mu_V(T,\boldsymbol{x})$	Natural mortality rate of mosquitoes	Eq. (3)	[16]
$\mu_{rB}(\boldsymbol{x})$	Natural mortality rate of resident birds	0.0005	[17]
$\mu_{mB}(\boldsymbol{x})$	Natural mortality rate of migratory birds	0.00023	[17]
$\gamma_V(T,\boldsymbol{x})$	Latency rate on mosquitoes	Eq. (2)	[15]
$\gamma_{rB}(\boldsymbol{x})$	Latency rate on resident birds	0.196	[17]
$\gamma_{mB}(\boldsymbol{x})$	Latency rate on migratory birds	0.285	[17]
$\alpha_{rB}(\boldsymbol{x})$	Removal rate of infectious resident birds	0.867	[17]
$\alpha_{mB}(\boldsymbol{x})$	Removal rate of infectious migratory birds	0.4	[17]
$\nu_{rB}(\boldsymbol{x})$	Proportion of dead resident birds	0.655	[17]
$\nu_{mB}(\boldsymbol{x})$	Proportion of dead migratory birds	0.103	[17]
$p_{Vr}(\boldsymbol{x})$	Probability of a new resident bird infection	0.97	[17]
$p_{Vm}(\boldsymbol{x})$	Probability of a new migratory bird infection	0.9	[17]
$p_{rV}(\boldsymbol{x})$	Probability of a new mosquito infection from a resident bird	0.4	[17]
$p_{mV}(\boldsymbol{x})$	Probability of a new mosquito infection from a migratory bird	0.7	[17]
$\beta(T,\boldsymbol{x})$	Mosquito biting rate	Eq. (1)	[45]
$\phi(\boldsymbol{x})$	Mosquito to resident bird ratio	Table 2	Assumed
$D_1(\boldsymbol{x})$	Diffusion coefficient of mosquitoes	Table 2	Inferred from the data
$D_2(\boldsymbol{x})$	Diffusion coefficient of resident birds	Table 2	Inferred from the data
$D_3(\boldsymbol{x})$	Diffusion coefficient of migratory birds	Table 2	Inferred from the data
$\boldsymbol{A}(t,\boldsymbol{x})=[v_x;v_y]$	Advection vector for migratory birds (in km/day)	[1;1] & [−1;−1]	Estimated Section 5

3. Mathematical properties of the model

The mathematical proofs for the positivity, uniqueness, boundedness and well-posedness of the model and its solution are shown in Section S3 of the Supplementary material.

4. Steady states and the reproductive number

The PDE system (6) admits a non-trivial WNV-free equilibrium point $\mathscr{E}^0$ such that

$$\left(S_V^0, E_V^0, I_V^0, S_{rB}^0, E_{rB}^0, I_{rB}^0, R_{rB}^0, D_{rB}^0, S_{mB}^0, E_{mB}^0, I_{mB}^0, R_{mB}^0, D_{mB}^0\right)$$
$$= \left(K_V\left[1-\frac{\mu_V}{b_V}\right], 0, 0, K_{rB}\left[1-\frac{\mu_{rB}}{b_{rB}}\right], 0, 0, 0, 0, K_{mB}\left[1-\frac{\mu_{mB}}{b_{mB}}\right], 0, 0, 0, 0\right).$$

$\mathscr{E}^0$ is positive if and only if $b_j > \mu_j$, for $j = V, rB, mB$. The uniqueness of $\mathscr{E}^0$ can be verified using [[46], Lemma 2.1]. The basic reproductive number of the deterministic part of our model is computed following [47], as follows:

Let $\mathscr{F}$, be the matrix of new infections, and $\mathscr{V}$, the matrix of transitions, then

$$\mathscr{F} = \begin{bmatrix} (\lambda_{rV}+\lambda_{Vm})S_V \\ 0 \\ \lambda_{Vr}S_{rB} \\ 0 \\ \lambda_{Vm}S_{mB} \\ 0 \end{bmatrix}, \quad \mathscr{V} = \begin{bmatrix} (\gamma_V+\mu_V)E_V \\ -\gamma_V E_V + \mu_V I_V \\ (\gamma_{rB}+\mu_{rB})E_{rB} \\ -\gamma_{rB}E_{rB} + (\alpha_{rB}+\mu_{rB})I_{rB} \\ (\gamma_{mB}+\mu_{mB})E_{mB} \\ -\gamma_{mB}E_{mB} + (\alpha_{mB}+\mu_{mB})I_{mB} \end{bmatrix}.$$

Partial derivatives evaluated at the WNV-free equilibrium point yield:

$$F = \begin{bmatrix} 0 & 0 & 0 & \frac{\phi\beta p_{rV}S_V^0}{S_{rB}^0+S_{mB}^0} & 0 & \frac{\phi\beta p_{mV}S_V^0}{S_{rB}^0+S_{mB}^0} \\ 0 & 0 & 0 & 0 & 0 & 0 \\ 0 & \frac{\beta p_{Vr}S_{rB}^0}{S_V^0(S_{rB}^0+S_{mB}^0)} & 0 & 0 & 0 & 0 \\ 0 & 0 & 0 & 0 & 0 & 0 \\ 0 & \frac{\beta p_{Vm}S_{mB}^0}{S_V^0(S_{rB}^0+S_{mB}^0)} & 0 & 0 & 0 & 0 \\ 0 & 0 & 0 & 0 & 0 & 0 \end{bmatrix},$$

and

$$V = \begin{bmatrix} -\gamma_V - \mu_V & 0 & 0 & 0 & 0 & 0 \\ \gamma_V & -\mu_V & 0 & 0 & 0 & 0 \\ 0 & 0 & -\gamma_{rB} - \mu_{rB} & 0 & 0 & 0 \\ 0 & 0 & \gamma_{rB} & -\alpha_{rB} - \mu_{rB} & 0 & 0 \\ 0 & 0 & 0 & 0 & -\gamma_{mB} - \mu_{mB} & 0 \\ 0 & 0 & 0 & 0 & \gamma_{mB} & -\alpha_{mB} - \mu_{mB} \end{bmatrix}.$$

The basic reproductive number $R_0(\boldsymbol{x})$ is thus given by the spectral radius of FV^{-1}, which gives

$$R_0(\boldsymbol{x}) = \sqrt{R_0^{Res} + R_0^{Mig}}, \tag{7}$$

where $$R_0^{Res} = \frac{\gamma_V \phi \beta p_{rV} p_{Vr} \gamma_{rB}}{\mu_V(\alpha_{rB} + \mu_{rB})(\gamma_{rB} + \mu_{rB})(\gamma_V + \mu_V)\left[1 + \frac{K_{mB}\left(1 - \frac{\mu_{mB}}{b_{mB}}\right)}{K_{rB}\left(1 - \frac{\mu_{rB}}{b_{rB}}\right)}\right]^2}$$

and $$R_0^{Mig} = \frac{\gamma_V \phi \beta p_{mV} p_{Vm} \gamma_{mB}}{\mu_V(\alpha_{mB} + \mu_{mB})(\gamma_{mB} + \mu_{mB})(\gamma_V + \mu_V)\left[1 + \frac{K_{rB}\left(1 - \frac{\mu_{rB}}{b_{rB}}\right)}{K_{mB}\left(1 - \frac{\mu_{mB}}{b_{mB}}\right)}\right]^2}.$$

Since all parameters of the model are positive, and the equilibrium point is also positive, then R_0^{Res} and R_0^{Mig} are non-negative. The basic reproductive number $R_0(\boldsymbol{x})$ is plotted for the entire country and compared with observed data for 2018–2025 (Fig. 2). $R_0(\boldsymbol{x})$ shows high circulation areas in the eastern parts of Germany, with other regions in the southeastern and northern parts also showing circulation, which is in agreement with the observed data. Moreover, we also included the 2025 case data to evaluate whether our $R_0(\boldsymbol{x})$ risk map can predict regions where future cases may occur. Indeed, as of March 2026, 2025 WNV cases were observed in the east, north, and southwest of Germany, regions previously flagged as high-risk by $R_0(\boldsymbol{x})$. This result is important because it allows potential high-risk regions to be identified before seasonal outbreaks occur.

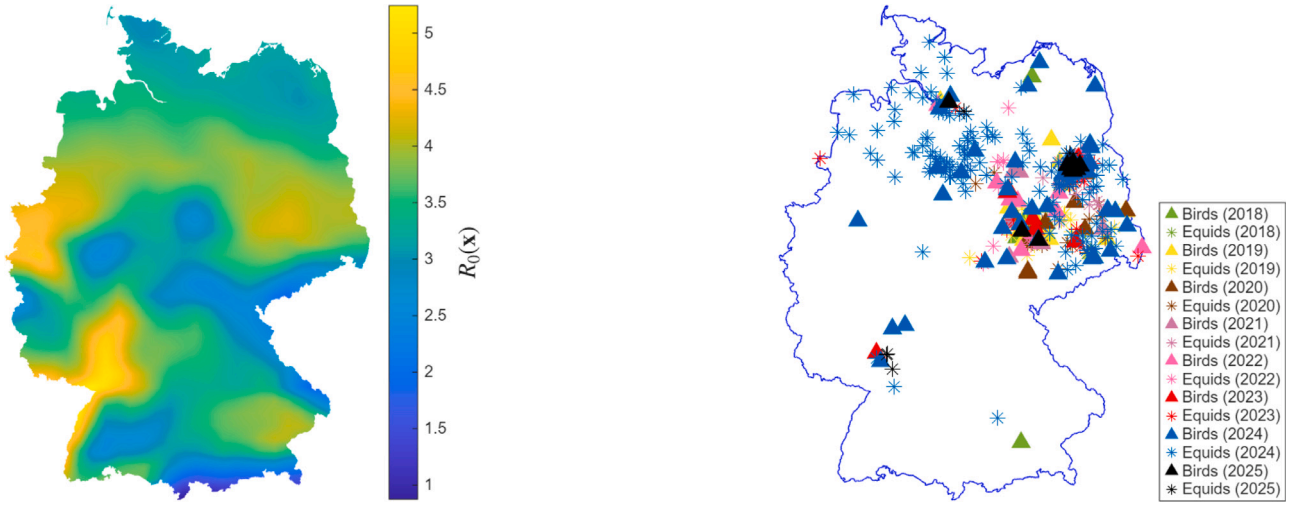


Fig. 2. The basic reproductive number $R_0(\boldsymbol{x})$ compared to observed data.

5. Simulation framework

Based on available WNV data in Germany, birds of the Accipitridae family were the most affected species in 2018 [17,48]. Therefore, as also done by Mbaoma et al. [17], we used parameters associated with northern goshawks and raptors for the resident bird, both of which fall under the Accipitridae family. Migratory birds in the model represent species that move over short to long distances, particularly along the northeast to southwest seasonal migratory routes. Parameters for these birds are based on those observed in corvids, as they are among the most frequently reported WNV-positive birds, second only to raptors and tits [17]. For a detailed derivation of these parameters, we refer the reader to [17] and the references therein.

Initial population densities of infectious birds and mosquitoes are estimated to be high in Halle (Saale), the main WNV hot spot in 2018, followed by Berlin, and, lastly, lower densities in Laage, Poing, and Plessa, as indicated by the 2018 WNV observed case data [49]. On the other hand, initial densities of susceptible hosts and mosquitoes are assumed to be spatially homogeneously distributed across the entire country. A 2-dimensional Gaussian function of the form

$$f(t, \boldsymbol{x}) = e^{-\frac{(x - x_0)^2 + (y - y_0)^2}{2\sigma^2}}$$

is used to define the initial condition peaks. (x_0, y_0) are the central coordinates specifying the nodes of the infected regions, and σ is the standard deviation. $\sigma = 40$ km in Berlin and Halle Saale (main hotspot regions), and 20 km in other infected areas.

The effect of host-specific feeding allocation is first examined using a baseline scenario with $c = 1$, in which mosquito feeding preference depends solely on bird densities. This scenario is used to infer diffusion coefficients and compare model predictions with observed data. Two additional scenarios are then defined: scenario 1, with $c = 0.4$, in which mosquitoes primarily feed on resident birds; and scenario 2, with $c = 3$, in which mosquitoes prefer migratory birds.

The model runs on a daily time step from 1 March to 30 November each year, spanning 2019 to 2025. Each year, the final solution for that year is saved and used as the initial condition for the next, but starting with zero exposed and infectious birds. Such an initialisation reflects the short duration of WNV viremia in birds, which lasts only a few days [50–52], and may be cleared before the next spring. The only reservoirs considered in this work are mosquitoes, which overwinter with infected specimens carrying the virus into spring [32,53]. These start and end dates are chosen because WNV activity is known to be high in summer. Spring and autumn are included to account for the seasonal bird migrations into Germany in spring and out in autumn. This choice also enables the incorporation of new data from ongoing WNV surveillance activities. For instance, the initial conditions for 2020 were updated when a new WNV case was confirmed in Hamburg, north of Germany, which may have influenced subsequent spread patterns observed in the north.

In the process, we use inverse modelling to infer the diffusion and advection coefficients that may have influenced the observed spreading pattern. This is done by running the model with different coefficients and visually comparing the model output to the observed data. The final coefficients are selected based on their ability to replicate the observed pattern, while respecting the biological constraints of the magnitudes, i.e., $D_1 < D_2 < D_3$. This approach is primarily used because the available data are limited and sparse; therefore, our main goal is to explain the observed qualitative spread pattern of WNV.

Temperature strongly influences the activity of *Cx. pipiens* including their ability to transmit WNV [54]. This motivated us to model mosquito parameters using temperature-dependent functions, namely: mosquito biting rate $\beta(T, \boldsymbol{x})$, latency rate $\gamma_V(T, \boldsymbol{x})$, and mortality rate $\mu_V(T, \boldsymbol{x})$. ERA5 reanalysis data on single levels from 1940 to present are downloaded from the Copernicus Climate Data Store [55]. The data is first cleaned, and the years 2019–2025 are subsequently extracted for interpolation onto the mesh and used to compute the temperature-space dependent mosquito functions. During the simulation process, $\beta(T, \boldsymbol{x}), \gamma_V(T, \boldsymbol{x})$ and $\mu(T, \boldsymbol{x})$ are dynamically updated based on the temperatures at different locations in Germany. Advection, representing the directed movement of migratory birds, is fixed throughout the years. The spring-to-early summer movement is described by the vector field $[v_x; v_y] = [1; 1]$ while the late summer-to-autumn movement is described by $[v_x; v_y] = [-1; -1]$ in km per day. To solve our PDE model, we use the MATLAB PDE Toolbox [56], which uses the finite element method. The toolbox solves PDEs of the form:

$$m\frac{\partial^2 u}{\partial t^2} + d\frac{\partial u}{\partial t} - \nabla \cdot (c\nabla u) + au = f, \tag{8}$$

In our case, $m = 0$, $d = 1$, and $a = 0$. Matrices c and f represent the diffusion coefficients and reaction terms, respectively, and are included in Section S4 of the Supplementary material, along with the pseudo-code for the simulation procedure. The map of Germany is downloaded as a shapefile from [57] and simplified using MapShaper [58]. The observed data indicate presence only, as no absence data are available, and for this reason, we qualitatively present our results on a Low-High scale for better interpretation.

6. Model fitting

To fit our model predictions, we compared simulated cases with observed data. The observed data comprises bird and equid infection cases, as well as mortality, obtained from the World Organisation for Animal Health (WOAH) [59]. Due to the lack of systematic WNV surveillance in Germany, many dead birds go undetected, while others are discovered at decomposed stages, which can affect PCR tests. Domesticated equids are usually easier to diagnose because owners often report sick animals. Given that birds are the amplifying hosts, it is reasonable to assume that, before equid cases are reported, an amplifying host was infected first and might have gone undetected. Moreover, our observed bird data is dominated by dead birds, while the equid data is dominated by infected equids. Because of this, our model fitting compares merged WNV-related events observed in birds and equids, with the compartment of dead resident birds, given the high WNV-related deaths observed in birds of the Accipitridae family [17,48]. Firstly, we aggregate both the simulated and observed data within the GADM (Database of Global Administrative Areas) level-2 administrative units of Germany (N = 356) [57], comprising both rural districts (Landkreise) and urban districts (kreisfreie Städte). The PDE solution $u(x, y, t_f)$ is extracted at the final time step, and the domain Ω is divided into 356 sub domains $\{\Omega_i\}_{i=1}^{N}$ corresponding to the GADM level-2 administrative units, such that $\Omega = \bigcup_{i=1}^{N} \Omega_i$. For each Ω_i, the mean simulated number of cases is given by $\frac{1}{|\Omega_i|}\int_{\Omega_i} u(x, y, t_f)\, dA$, where $|\Omega_i|$ is the area of the region Ω_i.

Observed cases are aggregated using the formula $\sum_{j=1}^{N_{\text{obs}}} \mathbf{1}_{\Omega_i}(x_j, y_j, t_f)$, where $\mathbf{1}_{\Omega_i}(x_j, y_j, t_f)$ is the indicator function equal to 1 if the observed point lies within Ω_i, and 0 otherwise, and N_{obs} is the number of observed points per region.

Boundaries are shrunk inwards using the `polybuffer` function [56] from the toolbox to prevent misclassification near borders. The `isinterior` operator [56] is then applied to prevent double-counting elements located on regional borders. Thus, only points lying strictly within the interior of a polygon are counted as belonging to that region.

Lastly, Spearman's rank correlation coefficient (ρ) [60] is applied to quantify the degree of spatial correspondence between simulated and observed patterns in each district. Spearman's (ρ) is calculated using the formula:

$$\rho = 1 - \frac{6\sum_{i=1}^{N} d_i^2}{N(N^2 - 1)}, \tag{9}$$

where d_i is the difference between the rank of the simulated and observed points, and N is the number of administrative units. A positive ρ indicates that locations with a high density of simulated cases correspond to locations with a high density of observed points. Conversely, a negative ρ implies that high values in one pattern correspond to low values in the other, indicating an opposite relationship. A ρ close to zero suggests the absence of a monotonic spatial relationship [60]. P-values are computed to assess whether the observed correlation occurred by chance, with smaller p-values (< 0.05) indicating that the correlation is unlikely to have occurred by chance.

Table 2
Summary values for the diffusion coefficients (D_1, D_2, D_3), in km^2 per day; RMSD for each species in km; Spearman's correlation coefficient and P-values, for the case $c = 1$, corresponding to density-dependent bite allocation proportional to host availability.

Year	D_1	D_2	D_3	$RMSD_1$	$RMSD_2$	$RMSD_3$	ϕ_V	ρ	P-value
2019	1.0	3.0	10.0	33.2	57.4	104.9	60	0.42	5.9×10^{-16}
2020	1.0	3.0	10.0	33.2	57.4	104.9	30	0.49	2.3×10^{-25}
2021	1.0	3.0	10.0	33.2	57.4	104.9	40	0.48	3.4×10^{-23}
2022	2.0	4.0	10.0	46.9	66.3	104.9	50	0.50	1.3×10^{-22}
2023	1.0	3.0	10.0	33.2	57.4	104.9	50	0.44	1.0×10^{-17}
2024	1.0	3.0	10.0	33.2	57.4	104.9	30	0.42	1.1×10^{-16}
2025	1.0	3.0	10.0	33.2	57.4	104.9	30	0.43	4.9×10^{-17}

7. Results

For all scenarios, the model is initialised with 2018 WNV cases data. Under the baseline scenario, where mosquito biting is solely influenced by host availability, a strong visual agreement between the simulated and observed patterns is evident throughout the 2019–2025 simulation period (Fig. 3). The model's main strength lies in its ability to identify high circulation areas that were initially localised in 2018. The RMSD estimates indicate that WNV-mosquito infections reached an average annual dispersal range of 46.9 km in 2022, and 33.2 km for all other years. However, resident birds dispersed an average range of 66.3 km in 2022 and 57.4 km in all other years. In migratory birds, an annual RMSD of 104.9 km was observed over the years (Table 2). The RMSD for mosquitoes remained lower than that for resident and migratory birds, while the RMSD for resident birds was lower than that for migratory birds, reflecting the greater mobility of avian hosts compared to mosquito species. Still under the baseline scenario, Spearman's correlation coefficients (ρ) were all statistically significant with values greater than 0.4 (Table 2, Fig. 4).

In 2023, the model accurately predicted an isolated case in the northwestern region (next to the Dutch border) and another isolated case in the southwestern region close to the Upper Rhine valley (Fig. 3(f)). This suggests the model's ability to anticipate under-reported spread patterns mainly driven by temperature, mosquito, and bird movements.

When mosquito preference is biased towards resident birds (scenario 1, c=0.4), the model predicts a slower spatial expansion of WNV (Fig. 7). Although resident birds may experience increased local transmission, the reduced infection probability among migratory birds limits long-range dissemination of the virus. Only in 2025 did the model manage to detect the isolated case observed in 2023 along the Upper Rhine valley. This outcome suggests that local amplification alone is insufficient to reproduce the observed national-scale spread and highlights the critical role of migratory-mediated dispersal, which can involve either short or long-distance migration, in shaping WNV spreading patterns.

In contrast, when mosquitoes bite migratory birds instead of resident birds (scenario 3, c=3), the spread of WNV becomes rapid (Fig. 6). This occurs when mosquito bites that might have gone to resident birds are instead taken by migratory birds. It is clear that by the year 2022, cases observed in 2024 were already being predicted by the model. Due to their directional dispersal patterns, infected migratory birds could serve as long-range carriers, establishing the virus in new locations beyond primary endemic areas. Therefore, host-specific feeding behaviour might play a crucial role in long-distance transmission dynamics.

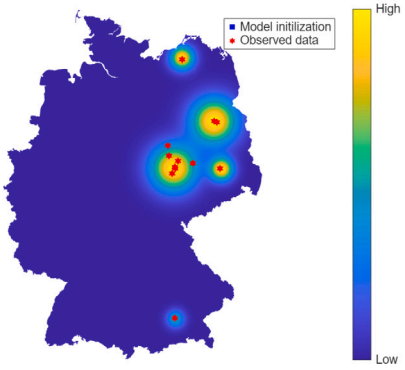
8. Discussions and conclusions

Understanding the WNV spreading pattern allows early detection of WNV outbreaks. Identifying high-circulation areas also supports early planning and resource allocation for preventive measures. At the same time, implementing systematic surveillance programs to understand the spread of WNV is costly. Therefore, in this study, we modelled the spread of WNV in Germany using a temperature-driven PDE model with advection and diffusion processes. We proved that our model has non-negative, bounded, and unique solutions, and that the system (6) is well-posed.

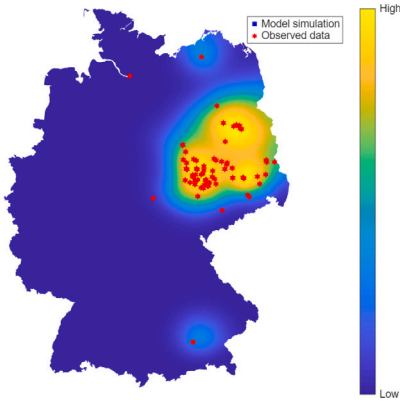
In agreement with previous studies [17,23,33], at the temporal level, the basic reproductive number ($R_0(\boldsymbol{x})$) indicates that the presence of migratory birds increases the number of amplifying local hosts. At the spatial scale, $R_0(\boldsymbol{x})$ identified low-high risk regions of public health interest, which agreed with the observed WNV cases in birds and equids, and other temperature-driven WNV models, e.g., by Mbaoma et al. [17]. The reproductive number identified regions in the eastern parts of Germany as high circulation areas, a result similar to that obtained in [17,24]. In addition, $R_0(\boldsymbol{x})$ flagged regions in the north, south and southwest of Germany as new circulation areas. Our approach explains the drivers of WNV spread in Germany and infers estimates of spreading speeds. In particular, from the simulation of our PDE model, we computed the annual RMSD, which estimates the average displacement of the infection over a given period, and due to a lack of real host movement data, we chose diffusion coefficients that best matched the observed data.

Scenario analyses comparing the model with different mosquito biting preferences between resident and migratory birds were explored. Results indicated that when a large proportion of bites is allocated to resident birds, WNV spread is very localised (Fig. 7). In contrast, when migratory birds receive more bites, a more rapid spread is observed (Fig. 6) and the model detected 2023, 2024, and 2025 cases as early as in 2022 (Fig. 6(e)). While this comparison is based on limited, sparse data, the alignment between simulated spreading pathways and known migratory bird flyways is consistent with the hypothesis that long-range, directed bird migration may contribute to WNV dissemination. This observation is also supported by a recent study by Tóth et al. [61]. Our results suggest that migratory birds may still have played a role in shaping the WNV spread pattern in Germany, even if they may not be the primary source of infection. Thus, effective surveillance and prevention efforts of WNV may also be implemented at key stopover sites, where migratory birds are likely to rest and interact with local mosquitoes.

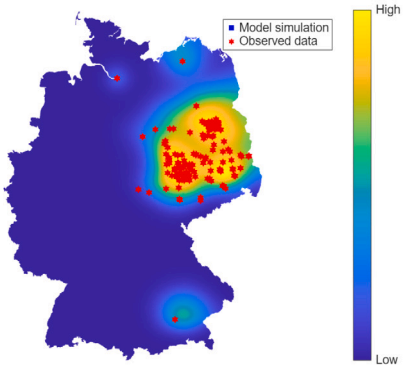
The 2023 data showed an isolated WNV case near the Dutch border (Fig. 3(f)). That year, no WNV cases were reported directly across the Dutch border, suggesting that the German case may have resulted from internal dispersal rather than immediate cross-border importation. However, given regional differences in surveillance intensity and reporting, the absence of reported cases may not necessarily indicate the absence of infection. Therefore, while the spatial agreement is promising, results near national boundaries should be interpreted with caution, given our modelling assumptions on homogeneous Neumann boundary conditions, which prevent cross-border inflows. Notably, in 2023, the model identified a region between the Dutch border and parts of the north of Germany as a possible high-circulation area, a finding confirmed by the observational data for the year 2024 (Fig. 2 and Fig. 3(f)).



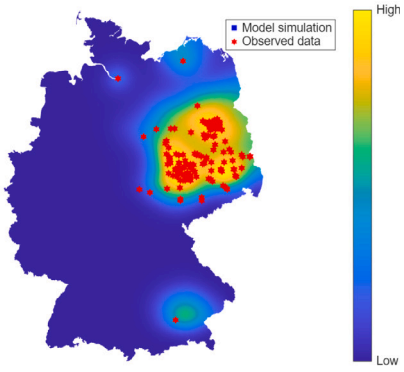
(a) 2018 cases.



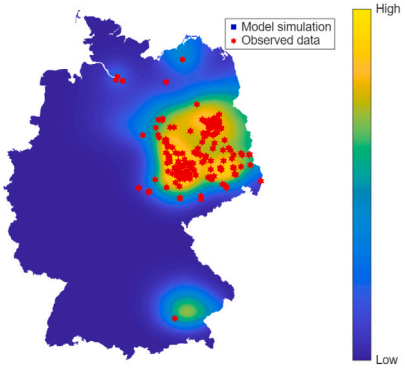
(b) 2018-2019 cases.



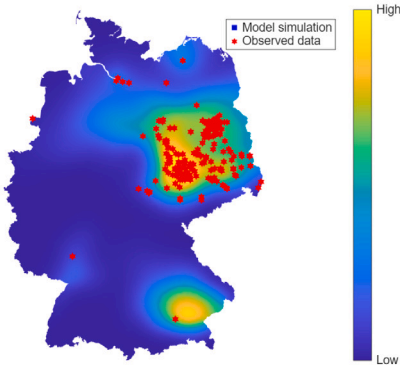
(c) 2018-2020 cases.



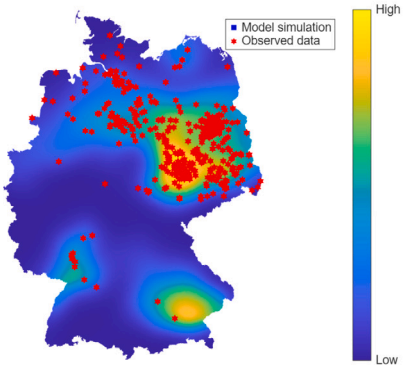
(d) 2018-2021 cases.



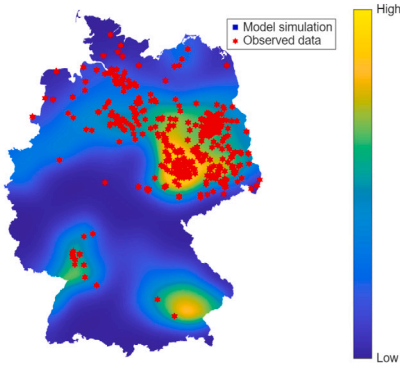
(e) 2018-2022 cases.



(f) 2018-2023 cases.

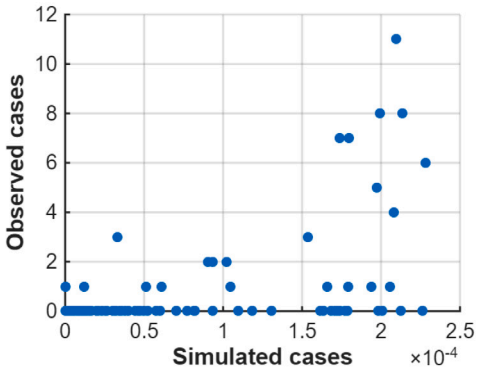


(g) 2018-2024 cases.

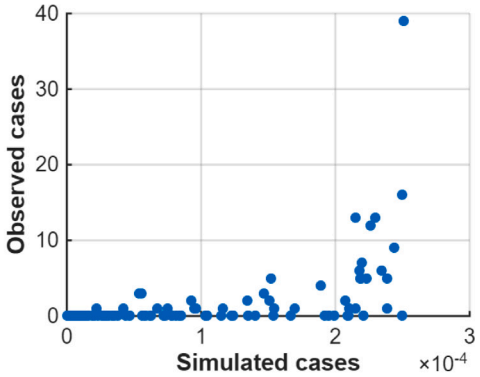


(h) 2018-2025 cases.

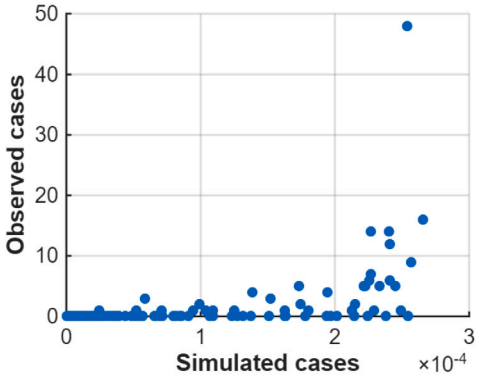
Fig. 3. Model simulation compared to observed data of WNV in Germany between the years 2019–2025, for the case when $c = 1$, corresponding to density-dependent bite allocation proportional to host availability.



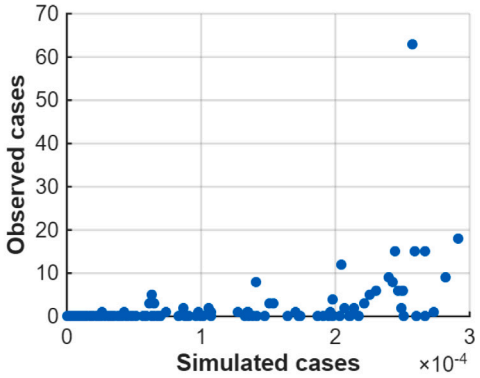
(a) 2018-2019 cases.



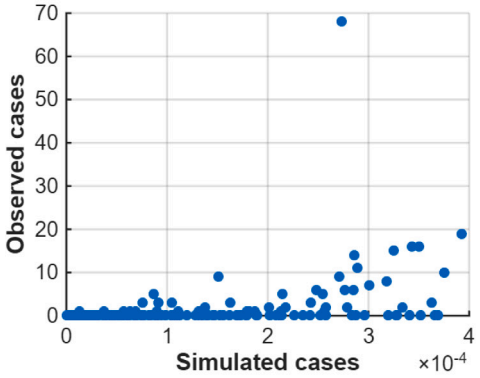
(b) 2018-2020 cases.



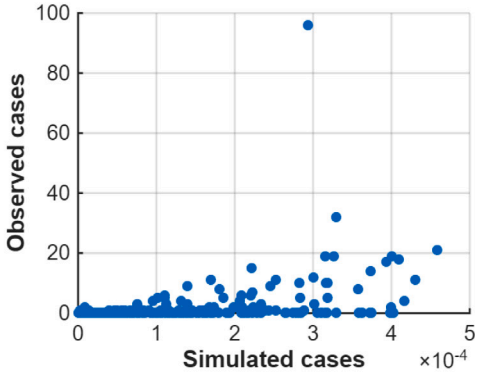
(c) 2018-2021 cases.



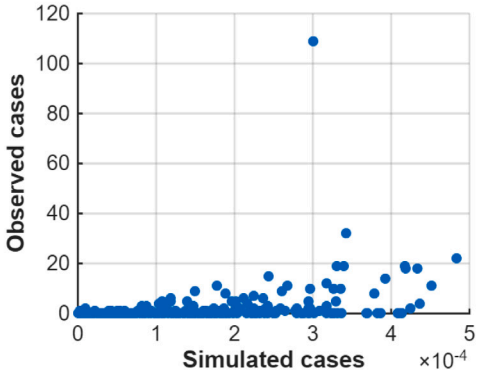
(d) 2018-2022 cases.



(e) 2018-2023 cases.



(f) 2018-2024 cases.



(g) 2018-2025 cases.

Fig. 4. Scatter plots for Spearman's rank correlation showing the monotonic relationship between model predictions and observed data for the case $c = 1$, corresponding to density-dependent bite allocation proportional to host availability.

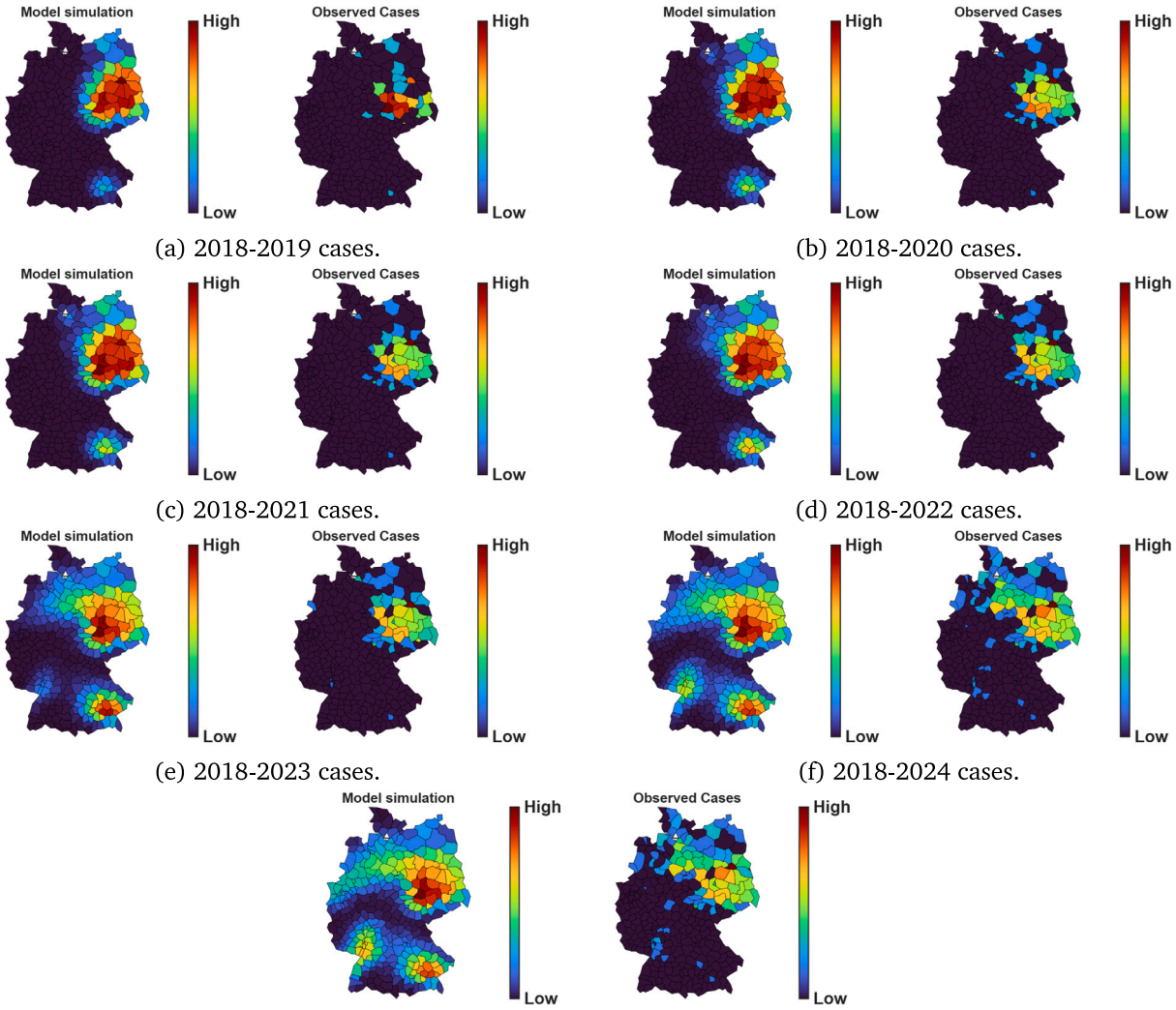


Fig. 5. Spatial comparison between simulated and observed WNV cases in Germany (2019–2025), on a $\log_{10}$ scale.

Our model uncovers a transmission corridor for WNV that spreads from the east in an anticlockwise direction, likely reflecting the temperature gradient suitable for mosquito activity. Interestingly, the circulation areas identified in our model agree with those in the study by Di Pol et al. [62], which aimed at modelling the temperature suitability for the risk of WNV establishment in European *Cx. pipiens* populations. As of March 2026, WNV bird and equid cases for 2025 had been reported in the eastern, northern, and southwestern regions, regions that were previously flagged as circulation areas in previous years (Fig. 2, right). This is an indication of seasonal recurrence supported by empirical evidence from North America and Southern Europe WNV events that show that once introduced into ecologically suitable regions, WNV tends to establish persistent seasonal transmission with annual reemergence [7,63]. The overwintering of WNV-infected *Culex* mosquitoes likely plays an important role for the local persistence of the virus [32].

Results from our spatially explicit PDE model suggest that temperature, mosquito-feeding preference, together with species movement through diffusion and advection, play a significant role in the spread of WNV in Germany. However, while our model successfully simulates WNV dispersal in Germany, limitations exist. For instance, factors such as land use influence the overall spatiotemporal distribution of mosquito populations [64], which is important for modelling mosquito abundance. Additionally, we used only temperature as the weather variable to account for heterogeneity in mosquito parameters, whereas precipitation, wind speed, and wind direction also affect mosquito distribution and activity [65]. If spatially resolved datasets for all these factors are accessible, they can be considered to improve the spatial heterogeneity of our PDE model. Estimating diffusion and advection coefficients through inverse modelling may introduce uncertainty and potential identifiability issues, as different parameter combinations can yield similar model outputs [66,67]. Even if our diffusion coefficients were estimated within a biologically plausible range consistent with previous studies and known dispersal behaviour of species, exploratory simulations (not presented here) indicated that the qualitative model behaviour remained reasonable even for different combinations, and thus values chosen here represent one plausible scenario. Future work could address this limitation by adopting more systematic estimation frameworks, such as Bayesian approaches [68]. To better capture spatial heterogeneity, another step could be to use spatially varying diffusion coefficients, since movement patterns are not constant in reality.

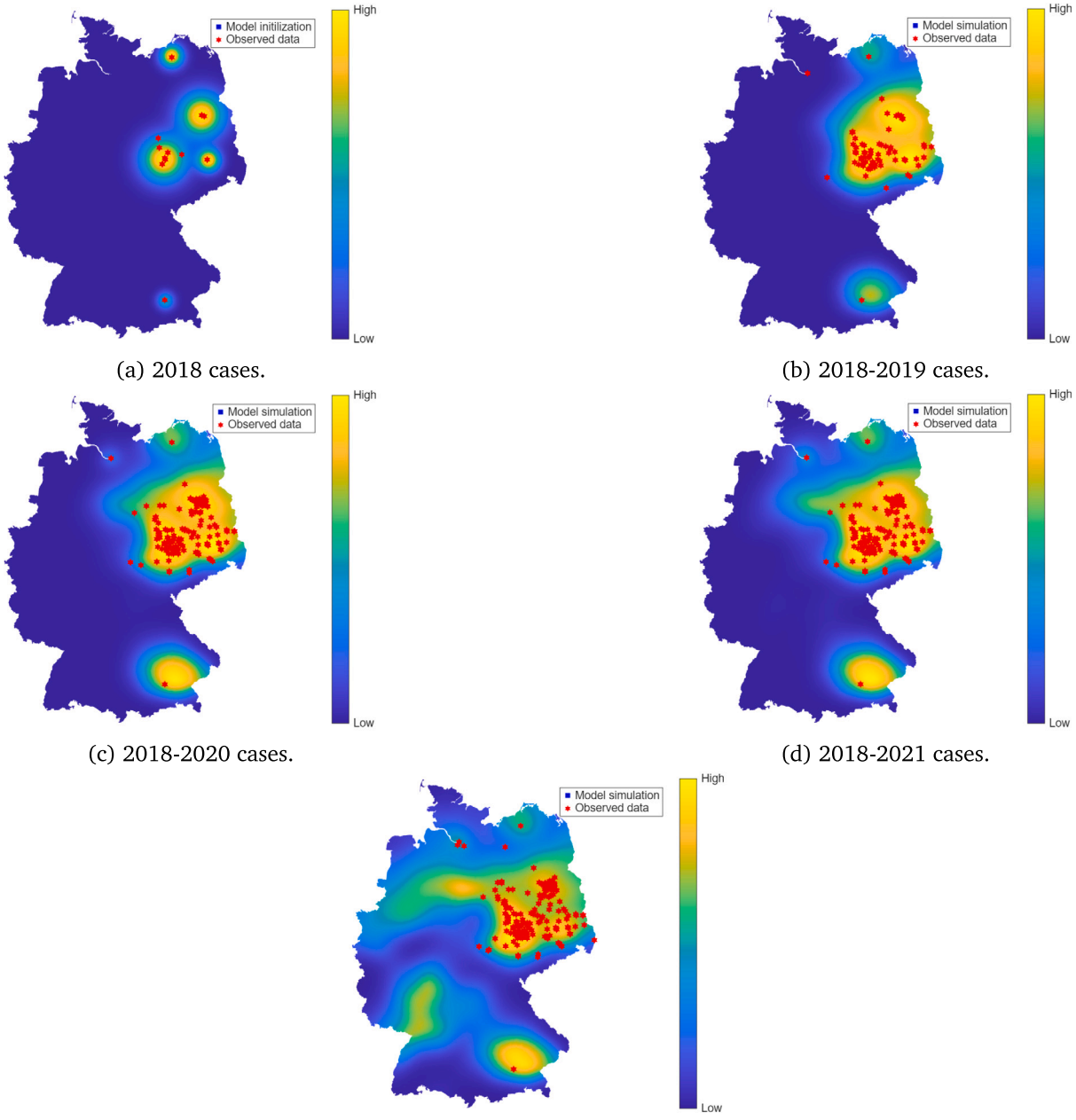
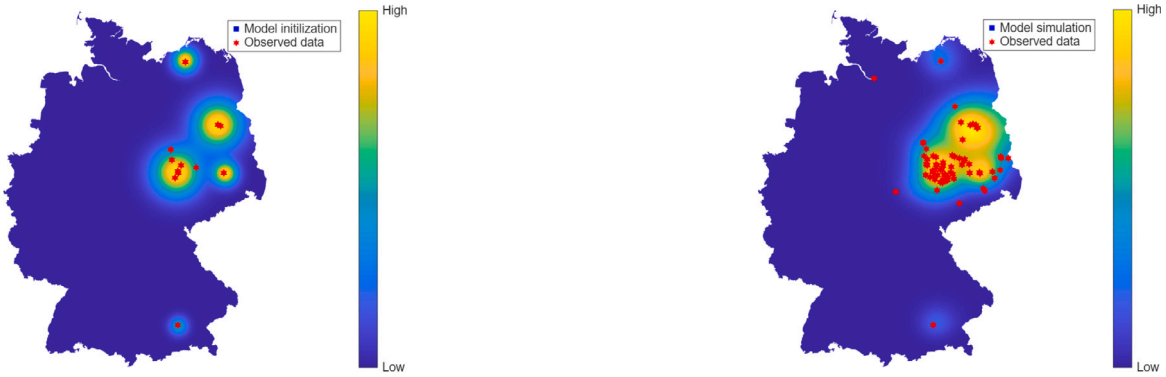


Fig. 6. Model simulations compared with observed WNV cases in Germany (2019–2022) under Scenario 3: $c = 3$, representing preferential biting of migratory birds.

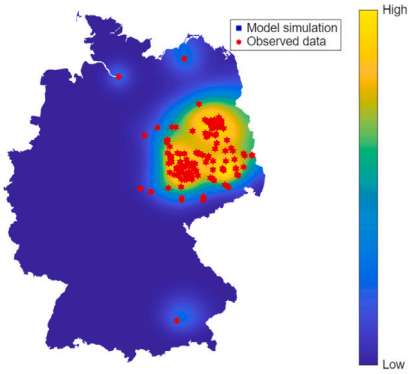
Moreover, our PDE model could also be extended to a stochastic PDE system to incorporate additional random effects that deterministic PDEs cannot model.

The low correlation coefficients observed in model fitting may have partly resulted from the sparse and discrete nature of the reported observational data. Future work incorporating higher-resolution surveillance data could improve the model's calibration accuracy. Furthermore, the choropleth maps presented in Fig. 5 indicate that the model overestimates cases in some towns, where no WNV cases were confirmed. Although this could be true given the continuous nature of the PDE model, the lack of systematic surveillance might also lead to under-reporting of observed cases. This is evidenced by the fact that most data arises from incidental or passive detection rather than systematic monitoring [69], and thus our simulation results should be viewed as minimum estimates rather than representing the full WNV situation.

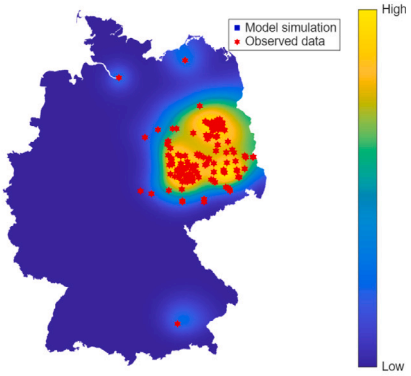


(a) 2018 cases.

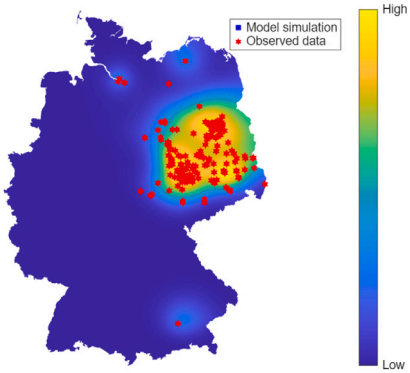
(b) 2018-2019 cases.



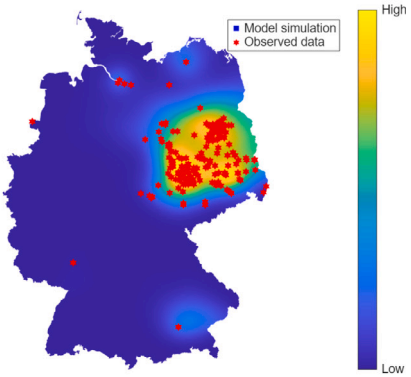
(c) 2018-2020 cases.



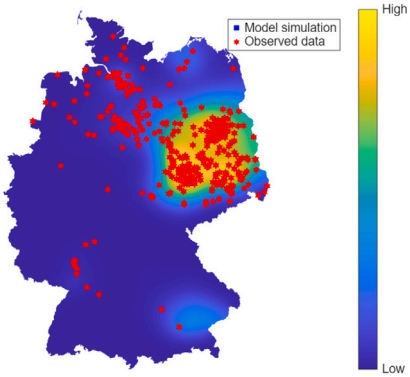
(d) 2018-2021 cases.



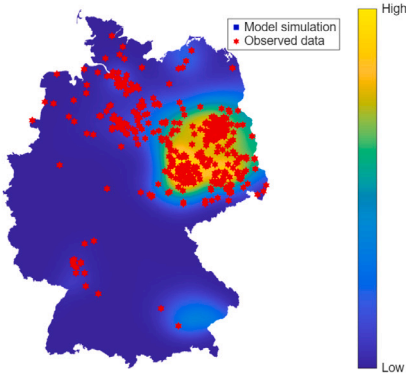
(e) 2018-2022 cases.



(f) 2018-2023 cases.



(g) 2018-2024 cases.



(h) 2018-2025 cases.

Fig. 7. Model simulation compared to observed data of WNV in Germany between the years 2019–2025, for the case when $c = 0.4$, corresponding to the case when resident birds are preferred, and there is a reduced mosquito feeding on migratory birds.

CRediT authorship contribution statement

Pride Duve: Writing – review & editing, Conceptualization, Methodology, Formal analysis, Software, Validation, Writing – original draft. **Felix Gregor Sauer:** Writing – review & editing, Writing – original draft, Supervision, Conceptualization. **Renke Lühken:** Writing – review & editing, Writing – original draft, Supervision, Conceptualization.

Declaration of competing interest

The authors declare that they have no known competing financial interests or personal relationships that could have influenced the work reported in this paper.

Acknowledgements

The authors would like to thank the Federal Ministry of Education and Research of Germany (BMBF) under the project NEED (Grant Number 01Kl2022), the Federal Ministry for the Environment, Nature Conservation, Nuclear Safety and Consumer Protection (Grant Number 3721484020), and the German Research Foundation (JO 1276/51) for funding this project. The authors are also grateful to the National Research Platform for Zoonosen for funding the research visit of Pride Duve to Prof. Dr. Reinhard Racke's lab, at the University of Konstanz. Furthermore, we would like to acknowledge and thank Reinhard Racke, Nicolas Schlosser, and Stefanie Frei from the University of Konstanz for the discussions, consultations, and support.

Appendix A. Supplementary data

Supplementary material related to this article can be found online at https://doi.org/10.1016/j.onehlt.2026.101386.

Data availability

The MATLAB codes used to reproduce the simulations presented in this study, together with the cleaned WNV datasets used for model fitting, are archived at Zenodo and can be accessed from Duve et al. [70]. The codes may also be adapted to investigate transmission dynamics in other regions. The original datasets can be obtained from the World Organisation for Animal Health (WOAH) [59] website.

References

[1] K.C. Smithburn, T.P. Hughes, A.W. Burke, J.H. Paul, A neurotropic virus isolated from the blood of a native of Uganda, Am. J. Trop. Med. (ISSN: 0096-6746) s1-20 (4) (1940) 471–492, http://dx.doi.org/10.4269/ajtmh.1940.s1-20.471.
[2] Alexander T. Ciota, West Nile virus and its vectors, Curr. Opin. Insect Sci. (ISSN: 2214-5745) 22 (2017) 28–36, http://dx.doi.org/10.1016/j.cois.2017.05.002.
[3] C.H. Calisher, N. Karabatsos, J.M. Dalrymple, R.E. Shope, J.S. Porterfield, E.G. Westaway, W.E. Brandt, Antigenic relationships between flaviviruses as determined by cross-neutralization tests with polyclonal antisera, J. Gen. Virol. (ISSN: 1465-2099) 70 (1) (1989) 37–43, http://dx.doi.org/10.1099/0022-1317-70-1-37.
[4] Zdenek Hubálek, Jirí Halouzka, West Nile fever–a reemerging mosquito-borne viral disease in Europe, Emerg. Infect. Dis. (ISSN: 1080-6059) 5 (5) (1999) 643–650, http://dx.doi.org/10.3201/eid0505.990505.
[5] Laura D. Kramer, Linda M. Styer, Gregory D. Ebel, A global perspective on the epidemiology of West Nile virus, Annu. Rev. Entomol. (ISSN: 1545-4487) 53 (1) (2008) 61–81, http://dx.doi.org/10.1146/annurev.ento.53.103106.093258.
[6] J.H. Rappole, Z. Hubálek, Migratory birds and West Nile virus: Migratory birds and west nile virus, J. Appl. Microbiol. (ISSN: 1364-5072) 94 (2003) 47–58, http://dx.doi.org/10.1046/j.1365-2672.94.s1.6.x.
[7] Lyle R. Petersen, Aaron C. Brault, Roger S. Nasci, West Nile virus: review of the literature, Jama (ISSN: 0098-7484) 310 (3) (2013) 308, http://dx.doi.org/10.1001/jama.2013.8042.
[8] Grant L. Campbell, Anthony A. Marfin, Robert S. Lanciotti, Duane J. Gubler, West Nile virus, Lancet Infect. Dis. (ISSN: 1473-3099) 2 (9) (2002) 519–529, http://dx.doi.org/10.1016/s1473-3099(02)00368-7.
[9] Patricia Salazar, Josie L. Traub-Dargatz, Paul S. Morley, Delwin D. Wilmot, David J. Steffen, Wayne E. Cunningham, M.D. Salman, Outcome of equids with clinical signs of West Nile virus infection and factors associated with death, J. Am. Vet. Med. Assoc. (ISSN: 0003-1488) 225 (2) (2004) 267–274, http://dx.doi.org/10.2460/javma.2004.225.267.
[10] E. Ernek, O. Kozuch, J. Nosek, J. Teplan, C. Folk, Arboviruses in birds captured in Slovakia, 1977.
[11] Mertyn Malkinson, Caroline Banet, Yoram Weisman, Shimon Pokamunski, Roni King, Vincent Deubel, Introduction of West Nile virus in the Middle East by migrating white storks, Emerg. Infect. Dis. (ISSN: 1080-6059) 8 (4) (2002) 392–397, http://dx.doi.org/10.3201/eid0804.010217.
[12] Yehuda Nir, Robert Goldwasser, Yehuda Lasowski, Amiel Avivi, Isolation of arboviruses from wild birds in Israeli, Am. J. Epidemiol. (ISSN: 0002-9262) 86 (2) (1967) 372–378, http://dx.doi.org/10.1093/oxfordjournals.aje.a120747.
[13] G.E. Watson, R.E. Shope, M.N. Kaiser, An ectoparasite and virus survey of migratory birds in the eastern Mediterranean, in: Transcontinental connections of migratory birds and their role in the distribution of arboviruses, Nauka, Novosibirsk, 1972, pp. 176–180.
[14] Claude Hannoun, Berhard Corniou, Jean Mouchet, Role of migrating birds in arbovirus transfer between Africa and Europe, in: Transcontinental connections of migratory birds and their role in the distribution of arboviruses, Nauka Novosibirsk, Russia, 1972, pp. 167–172.
[15] Julian Heidecke, Jonas Wallin, Peter Fransson, Pratik Singh, Henrik Sjödin, Pascale Claire Stiles, Marina Treskova, Joacim Rocklöv, Uncovering temperature sensitivity of West Nile virus transmission: Novel computational approaches to mosquito-pathogen trait responses, PLoS Comput. Biol. (ISSN: 1553-7358) 21 (3) (2025) e1012866, http://dx.doi.org/10.1371/journal.pcbi.1012866.
[16] Vincent Laperriere, Katharina Brugger, Franz Rubel, Simulation of the seasonal cycles of bird, equine and human West Nile virus cases, Prev. Vet. Med. (ISSN: 0167-5877) 98 (2–3) (2011) 99–110, http://dx.doi.org/10.1016/j.prevetmed.2010.10.013.
[17] Oliver Chinonso Mbaoma, Stephanie Margarete Thomas, Carl Beierkuhnlein, Spatiotemporally explicit epidemic model for West Nile virus outbreak in Germany: An inversely calibrated approach, J. Epidemiol. Glob. Health (ISSN: 2210-6014) 14 (3) (2024) 1052–1070, http://dx.doi.org/10.1007/s44197-024-00254-0.
[18] Elisa Fesce, Giovanni Marini, Roberto Rosà, Davide Lelli, Monica Pierangela Cerioli, Mario Chiari, Marco Farioli, Nicola Ferrari, Understanding West Nile Virus Spread: Mathematical Modelling to Determine the Mechanisms with the Most Influence on Infection Dynamics, Cold Spring Harbor Laboratory, 2022, http://dx.doi.org/10.1101/2022.02.15.480483.
[19] C. Bowman, A. Gumel, P. van den Driessche, J. Wu, H. Zhu, A mathematical model for assessing control strategies against West Nile virus, Bull. Math. Biol. (ISSN: 0092-8240) 67 (5) (2005) 1107–1133, http://dx.doi.org/10.1016/j.bulm.2005.01.002.
[20] Ahmed Abdelrazec, Suzanne Lenhart, Huaiping Zhu, Dynamics and optimal control of a West Nile virus model with seasonality, Can. Appl. Math. Q. 23 (4) (2015) 12–33.
[21] Gustavo Cruz-Pacheco, Lourdes Esteva, Cristobal Vargas, Seasonality and outbreaks in West Nile virus infection, Bull. Math. Biol. (ISSN: 1522-9602) 71 (6) (2009) 1378–1393, http://dx.doi.org/10.1007/s11538-009-9406-x.

[22] P. Moschini, D. Bisanzio, A. Pugliese, A seasonal model for West Nile virus, Math. Model. Nat. Phenom. (ISSN: 1760-6101) 12 (2) (2017) 58–83, http://dx.doi.org/10.1051/mmnp/201712205.

[23] Louis Bergsman, James M. Hyman, Carrie A. Manore, A mathematical model for the spread of West Nile virus in migratory and resident birds, Math. Biosci. Eng. (ISSN: 1551-0018) 13 (2) (2016) 401–424, http://dx.doi.org/10.3934/mbe.2015009.

[24] Suman Bhowmick, Jörn Gethmann, Franz J. Conraths, Igor M. Sokolov, Hartmut H.K. Lentz, SEIR-Metapopulation model of potential spread of West Nile virus, Ecol. Model. (ISSN: 0304-3800) 476 (2023) 110213, http://dx.doi.org/10.1016/j.ecolmodel.2022.110213.

[25] Zhigui Lin, Huaiping Zhu, Spatial spreading model and dynamics of West Nile virus in birds and mosquitoes with free boundary, J. Math. Biol. (ISSN: 1432-1416) 75 (6–7) (2017) 1381–1409, http://dx.doi.org/10.1007/s00285-017-1124-7.

[26] Norberto Aníbal Maidana, Hyun Mo Yang, Spatial spreading of West Nile virus described by traveling waves, J. Theoret. Biol. (ISSN: 0022-5193) 258 (3) (2009) 403–417, http://dx.doi.org/10.1016/j.jtbi.2008.12.032.

[27] Norberto A. Maidana, Hyun M. Yang, Assessing the spatial propagation of West Nile virus, in: Biomat 2007, World Scientific, 2008, pp. 259–273, http://dx.doi.org/10.1142/9789812812339_0013.

[28] Norberto Anibal Maidana, Hyun Mo Yang, How do bird migrations propagate the West Nile virus, Math. Popul. Stud. (ISSN: 1547-724X) 20 (4) (2013) 192–207, http://dx.doi.org/10.1080/08898480.2013.831709.

[29] Ute Ziegler, Renke Lühken, Markus Keller, Daniel Cadar, Elisabeth van der Grinten, Friederike Michel, Kerstin Albrecht, Martin Eiden, Monika Rinder, Lars Lachmann, Dirk Höper, Ariel Vina-Rodriguez, Wolfgang Gaede, Andres Pohl, Jonas Schmidt-Chanasit, Martin H. Groschup, West Nile virus epizootic in Germany, 2018, Antiviral Res. (ISSN: 0166-3542) 162 (2019) 39–43, http://dx.doi.org/10.1016/j.antiviral.2018.12.005.

[30] Federica Musitelli, Fernando Spina, Anders Pape Møller, Diego Rubolini, Franz Bairlein, Stephen R. Baillie, Jacquie A. Clark, Boris P. Nikolov, Chris du Feu, Robert A. Robinson, Nicola Saino, Roberto Ambrosini, Representing migration routes from re-encounter data: a new method applied to ring recoveries of Barn swallows (hirundo rustica) in Europe, J. Ornithol. (ISSN: 2193-7206) 160 (1) (2018) 249–264, http://dx.doi.org/10.1007/s10336-018-1612-6.

[31] Raphaël Nussbaumer, Silke Bauer, Lionel Benoit, Grégoire Mariethoz, Felix Liechti, Baptiste Schmid, Quantifying year-round nocturnal bird migration with a fluid dynamics model, J. R. Soc. Interface (ISSN: 1742-5662) 18 (179) (2021) 20210194, http://dx.doi.org/10.1098/rsif.2021.0194.

[32] Helge Kampen, Birke Andrea Tews, Doreen Werner, First evidence of West Nile virus overwintering in mosquitoes in Germany, Viruses (ISSN: 1999-4915) 13 (12) (2021) 2463, http://dx.doi.org/10.3390/v13122463.

[33] Suman Bhowmick, Jörn Gethmann, Franz J. Conraths, Igor M. Sokolov, Hartmut H.K. Lentz, Locally temperature-driven mathematical model of West Nile virus spread in Germany, J. Theoret. Biol. (ISSN: 0022-5193) 488 (2020) 110117, http://dx.doi.org/10.1016/j.jtbi.2019.110117.

[34] Chantal B.F. Vogels, Nienke Hartemink, Constantianus J.M. Koenraadt, Modelling West Nile virus transmission risk in Europe: effect of temperature and mosquito biotypes on the basic reproduction number, Sci. Rep. (ISSN: 2045-2322) 7 (1) (2017) http://dx.doi.org/10.1038/s41598-017-05185-4.

[35] Eduardo de Freitas Costa, Kiki Streng, Mariana Avelino de Souza Santos, Michel Jacques Counotte, The effect of temperature on the boundary conditions of West Nile virus circulation in Europe, PLOS Negl. Trop. Dis. (ISSN: 1935-2735) 18 (5) (2024) e0012162, http://dx.doi.org/10.1371/journal.pntd.0012162.

[36] John Crank, The Mathematics of Diffusion, Oxford University Press, 1979.

[37] Adolf Fick, Ueber diffusion, Ann. Phys., Lpz. (ISSN: 1521-3889) 170 (1) (1855) 59–86, http://dx.doi.org/10.1002/andp.18551700105.

[38] Jean Baptiste Joseph baron de Fourier, Théorie analytique de la chaleur, Firmin Didot, 1822.

[39] James D. Murray, Mathematical Biology: I. An Introduction, vol. 17, Springer Science & Business Media, 2007.

[40] John P. Boyd, Chebyshev and Fourier Spectral Methods, Courier Corporation, 2001.

[41] Laura C. Harrington, Thomas W. Scott, Kriangkrai Lerdthusnee, Russell C. Coleman, Adriana Costero, Gary G. Clark, James J. Jones, Sangvorn Kitthawee, Pattamaporn Kittayapong, Ratana Sithiprasasna, John D. Edman, Dispersal of the dengue vector *Aedes Aegypti* within and between rural communities, Am. J. Trop. Med. Hyg. (ISSN: 0002-9637) 72 (2) (2005) 209–220, http://dx.doi.org/10.4269/ajtmh.2005.72.209.

[42] Piet F.M. Verdonschot, Anna A. Besse-Lototskaya, Flight distance of mosquitoes *(Culicidae)*: A metadata analysis to support the management of barrier zones around rewetted and newly constructed wetlands, Limnologica (ISSN: 0075-9511) 45 (2014) 69–79, http://dx.doi.org/10.1016/j.limno.2013.11.002.

[43] A. Einstein, 00DCber die von der molekularkinetischen theorie der W00e4rme geforderte bewegung von in ruhenden Fl00FCssigkeiten suspendierten teilchen, Ann. Phys., Lpz. (ISSN: 1521-3889) 322 (8) (1905) 549–560, http://dx.doi.org/10.1002/andp.19053220806.

[44] Soeren Metelmann, Development of Climate-Driven Models for Mosquito-Borne Disease Risk in the UK, The University of Liverpool (United Kingdom), 2019.

[45] Franz Rubel, Katharina Brugger, Michael Hantel, Sonja Chvala-Mannsberger, Tamás Bakonyi, Herbert Weissenböck, Norbert Nowotny, Explaining usutu virus dynamics in Austria: Model development and calibration, Prev. Vet. Med. (ISSN: 0167-5877) 85 (3–4) (2008) 166–186, http://dx.doi.org/10.1016/j.prevetmed.2008.01.006.

[46] Xueying Wang, Xiao-Qiang Zhao, Jin Wang, A cholera epidemic model in a spatiotemporally heterogeneous environment, J. Math. Anal. Appl. (ISSN: 0022-247X) 468 (2) (2018) 893–912, http://dx.doi.org/10.1016/j.jmaa.2018.08.039.

[47] P. van den Driessche, James Watmough, Reproduction numbers and sub-threshold endemic equilibria for compartmental models of disease transmission, Math. Biosci. (ISSN: 0025-5564) 180 (1–2) (2002) 29–48, http://dx.doi.org/10.1016/s0025-5564(02)00108-6.

[48] Ute Ziegler, Felicitas Bergmann, Dominik Fischer, Kerstin Müller, Cora M. Holicki, Balal Sadeghi, Michael Sieg, Markus Keller, Rebekka Schwehn, Maximilian Reuschel, Luisa Fischer, Oliver Krone, Monika Rinder, Karolin Schütte, Volker Schmidt, Martin Eiden, Christine Fast, Anne Günther, Anja Globig, Franz J. Conraths, Christoph Staubach, Florian Brandes, Michael Lierz, Rüdiger Korbel, Thomas W. Vahlenkamp, Martin H. Groschup, Spread of West Nile virus and usutu virus in the German bird population, 201920132020, Microorganisms (ISSN: 2076-2607) 10 (4) (2022) 807, http://dx.doi.org/10.3390/microorganisms10040807.

[49] Ute Ziegler, Pauline Dianne Santos, Martin H. Groschup, Carolin Hattendorf, Martin Eiden, Dirk Höper, Philip Eisermann, Markus Keller, Friederike Michel, Robert Klopfleisch, Kerstin Müller, Doreen Werner, Helge Kampen, Martin Beer, Christina Frank, Raskit Lachmann, Birke Andrea Tews, Claudia Wylezich, Monika Rinder, Lars Lachmann, Thomas Grünewald, Claudia A. Szentiks, Michael Sieg, Jonas Schmidt-Chanasit, Daniel Cadar, Renke Lühken, West Nile virus epidemic in Germany triggered by epizootic emergence, 2019, Viruses (ISSN: 1999-4915) 12 (4) (2020) 448, http://dx.doi.org/10.3390/v12040448.

[50] Aaron C. Brault, Stanley A. Langevin, Richard A. Bowen, Nicholas A. Panella, Brad J. Biggerstaff, Barry R. Miller, Nicholas Komar, Differential virulence of West Nile strains for American crows, Emerg. Infect. Dis. (ISSN: 1080-6059) 10 (12) (2004) 2161–2168, http://dx.doi.org/10.3201/eid1012.040486.

[51] Nicholas Komar, Stanley Langevin, Steven Hinten, Nicole Nemeth, Eric Edwards, Danielle Hettler, Brent Davis, Richard Bowen, Michel Bunning, Experimental infection of North American birds with the New York 1999 strain of West Nile virus, Emerg. Infect. Dis. (ISSN: 1080-6059) 9 (3) (2003) 311–322, http://dx.doi.org/10.3201/eid0903.020628.

[52] Nicole Nemeth, Daniel Gould, Richard Bowen, Nicholas Komar, Natural and experimental West Nile virus infection in five raptor species, J. Wildl. Dis. (ISSN: 0090-3558) 42 (1) (2006) 1–13, http://dx.doi.org/10.7589/0090-3558-42.1.1.

[53] Georgios Balatsos, Stavroula Beleri, Nikolaos Tegos, Marina Bisia, Vasileios Karras, Evangelia Zavitsanou, Dimitrios P. Papachristos, Nikos T. Papadopoulos, Antonios Michaelakis, Eleni Patsoula, Overwintering West Nile Virus in Active *Culex Pipiens* Mosquito Populations in Greece, Springer Science and Business Media LLC, 2024, http://dx.doi.org/10.21203/rs.3.rs-4205818/v1.

[54] Alexander T. Ciota, Amy C. Matacchiero, A. Marm Kilpatrick, Laura D. Kramer, The effect of temperature on life history traits of *Culex* mosquitoes, J. Med. Entomol. (ISSN: 1938-2928) 51 (1) (2014) 55–62, http://dx.doi.org/10.1603/me13003.

[55] Hans Hersbach, Bill Bell, Paul Berrisford, Giovanni Biavati, András Horányi, Joaquín Muñoz Sabater, Jean Nicolas, Christophe Peubey, Radu Radu, Ivan Rozum, Dennis Schepers, Adrian Simmons, Claudia Soci, Dick Dee, Jean-Noël Thépaut, ERA5 Monthly Averaged Data on Single Levels from 1940 to Present, Copernicus Climate Change Service (C3S) Climate Data Store (CDS), 2023, http://dx.doi.org/10.24381/cds.f17050d7, (Accessed 09 April 2025).

[56] MathWorks, Inc., Partial Differential Equation Toolbox™ User's Guide, The MathWorks, Inc., Natick, Massachusetts, 2025b, Available at: https://www.mathworks.com/help/pde/.

[57] Global Administrative Areas, GADM database of Global Administrative Areas (version 4.1), University of California, Berkeley, 2024, Available online: https://gadm.org. (Accessed 20 October 2025). (digital geospatial data).

[58] M. Harrower, M. Bloch, MapShaper.org: a map generalization web service, IEEE Comput. Graph. Appl. (ISSN: 0272-1716) 26 (4) (2006) 22–27, http://dx.doi.org/10.1109/mcg.2006.85.

[59] World Organisation for Animal Health (WOAH), WAHIS (animal disease events), 2018 - 2024, Retrieved on (2024-11-11) from (https://wahis.woah.org/#/event-management). Data extracted by (Pride Duve/BNITM). Reproduced with permission. "The World Organisation for Animal Health (WOAH) bears no responsibility for the integrity or accuracy of the data contained herein, but not limited to, any deletion, manipulation, or reformatting of data that may have occurred beyond its control.".

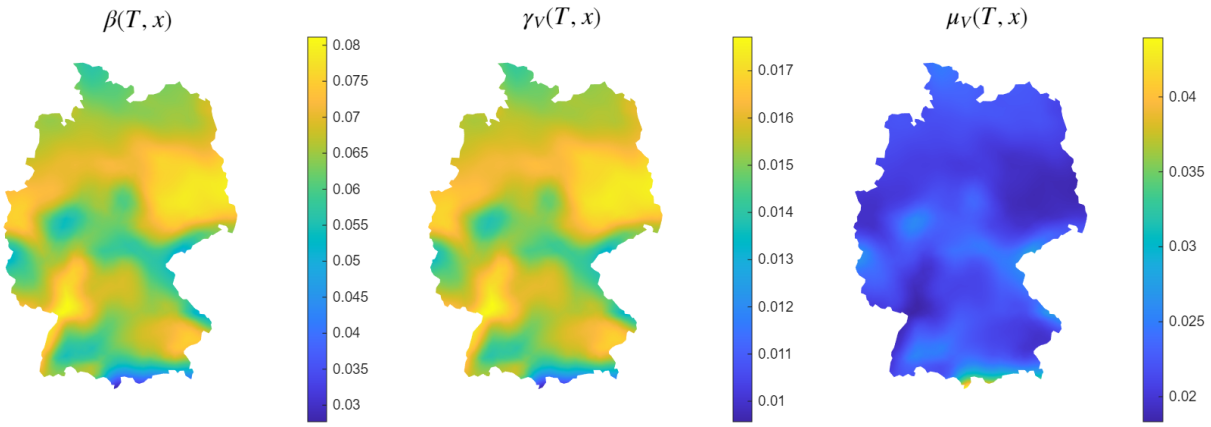
[60] C. Spearman, The proof and measurement of association between two things, Am. J. Psychol. (ISSN: 0002-9556) 15 (1) (1904) 72, http://dx.doi.org/10.2307/1412159.
[61] Gábor Endre Tóth, Marike Petersen, Francois Chevenet, Marcy Sikora, Alexandru Tomazatos, Alexandra Bialonski, Heike Baum, Balázs Horváth, Padet Siriyasatien, Anna Heitmann, Stephanie Jansen, Ruth Offergeld, Raskit Lachmann, Michael Schmidt, Jonas Schmidt-Chanasit, Dániel Cadar, Blood Donors as Sentinels for Genomic Surveillance of West Nile Virus in Germany (2020–2024) Using a Sensitive Amplicon-Based Sequencing Approach, Cold Spring Harbor Laboratory, 2025, http://dx.doi.org/10.1101/2025.06.24.25329984.
[62] Gabriella Di Pol, Matteo Crotta, Rachel A. Taylor, Modelling the temperature suitability for the risk of West Nile virus establishment in European *Culex pipiens* populations, Transbound. Emerg. Dis. (ISSN: 1865-1682) 69 (5) (2022) http://dx.doi.org/10.1111/tbed.14513.
[63] Paolo Calistri, Armando Giovannini, Zdenek Hubalek, Aurelia Ionescu, Federica Monaco, Giovanni Savini, Rossella Lelli, Epidemiology of West Nile in Europe and in the Mediterranean basin, Open Virol. J. 4 (2010) 29, http://dx.doi.org/10.2174/1874357901004010029.
[64] Matthew J. Watts, Victor Sarto i Monteys, P. Graham Mortyn, Panagiota Kotsila, The rise of West Nile virus in Southern and Southeastern Europe: A spatial-temporal analysis investigating the combined effects of climate, land use and economic changes, One Health (ISSN: 2352-7714) 13 (2021) 100315, http://dx.doi.org/10.1016/j.onehlt.2021.100315.
[65] E. Ducheyne, R. De Deken, S. Bécu, B. Codina, K. Nomikou, O. Mangana-Vougiaki, G. Georgiev, B.V. Purse, G. Hendrickx, Quantifying the wind dispersal of *Culicoides* species in Greece and Bulgaria, Geospatial Health (ISSN: 1827-1987) 1 (2) (2007) 177, http://dx.doi.org/10.4081/gh.2007.266.
[66] Yue Liu, Kevin Suh, Philip K. Maini, Daniel J. Cohen, Ruth E. Baker, Parameter identifiability and model selection for partial differential equation models of cell invasion, J. R. Soc. Interface (ISSN: 1742-5662) 21 (212) (2024) http://dx.doi.org/10.1098/rsif.2023.0607.
[67] Matthew J. Simpson, Ruth E. Baker, Sean T. Vittadello, Oliver J. Maclaren, Practical parameter identifiability for spatio-temporal models of cell invasion, J. R. Soc. Interface (ISSN: 1742-5662) 17 (164) (2020) 20200055, http://dx.doi.org/10.1098/rsif.2020.0055.
[68] D.A. Barajas-Solano, A.M. Tartakovsky, Approximate Bayesian model inversion for PDEs with heterogeneous and state-dependent coefficients, J. Comput. Phys. (ISSN: 0021-9991) 395 (2019) 247–262, http://dx.doi.org/10.1016/j.jcp.2019.06.010.
[69] Orianne Constant, Patricia Gil, Jonathan Barthelemy, Karine Bolloré, Vincent Foulongne, Caroline Desmetz, Agnès Leblond, Isabelle Desjardins, Sophie Pradier, Aurélien Joulié, Alain Sandoz, Rayane Amaral, Michel Boisseau, Ignace Rakotoarivony, Thierry Baldet, Albane Marie, Benoît Frances, Florence Reboul Salze, Bachirou Tinto, Philippe Van de Perre, Sara Salinas, Cécile Beck, Sylvie Lecollinet, Serafin Gutierrez, Yannick Simonin, One health surveillance of West Nile and Usutu viruses: a repeated cross-sectional study exploring seroprevalence and endemicity in southern France, 2016 to 2020, Eurosurveillance (ISSN: 1560-7917) 27 (25) (2022) http://dx.doi.org/10.2807/1560-7917.es.2022.27.25.2200068.
[70] Pride Duve, Felix. G. Sauer, Renke Lühken, Codes and data for the paper: Modelling the impact of temperature and bird migration on the spread of West Nile virus, 2026, Archived in Zenodo (Version 1.0). Available at (https://doi.org/10.5281/zenodo.18996831).

Supplementary File: Modelling the impact of temperature and bird migration on the spread of West Nile virus

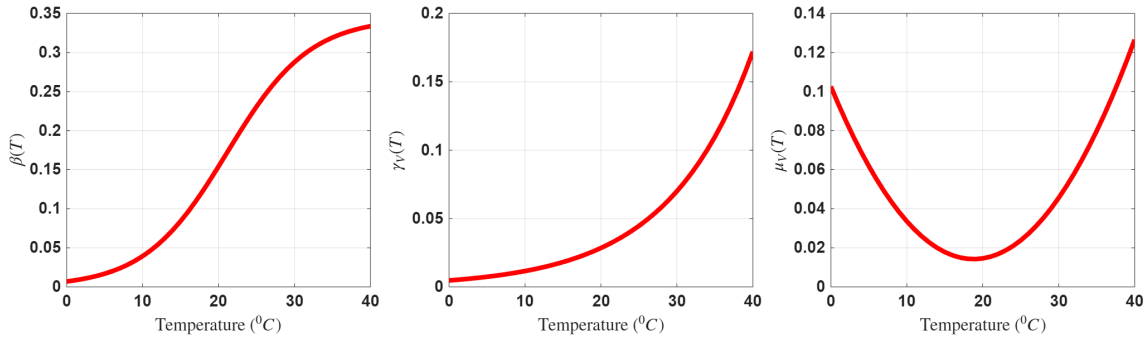
Pride Duve*, Felix Gregor Sauer, and Renke Lühken

Bernhard Nocht Institute for Tropical Medicine, Hamburg, Germany

S1 Plots for mosquito parameters



(a) Space-dependent thermal mosquito parameters for the year 2024.



(b) Temperature evolution for mosquito parameters.

Figure S1: Spatio-temporal mosquito parameters used in the model. The parameters $\beta(T,x)$ and $\mu_V(T,x)$ are adapted from [1], while $\gamma_V(T,x)$ from [2].

S2 Initial conditions

Unlike ODE-based models that rely on total population counts, spatially explicit PDE models interpret state variables as population densities, typically measured in individuals per unit area. Thus, it is important to convert the ODE-based initial conditions in Table (S1) into population densities per

*Corresponding author: pride.duve@bnitm.de

unit area by dividing susceptible classes by the total area of our mesh (cleaned map of Germany). From the mesh, we obtained a total domain area of approximately A = 356,280 km^2 for mainland Germany. The other compartments are localized around the infection points for 2018, and thus they are only divided by the total area around the infection, which we denote B.

Table S1: Definition of variables used in system (6), as defined by the authors.

Variable	Definition	Value	Units
$S_V(0,\boldsymbol{x})$	susceptible mosquitoes	20×10^9/A	mosquitoes/m^2
$E_V(0,\boldsymbol{x})$	exposed mosquitoes	10,000/B	mosquitoes/m^2
$I_V(0,\boldsymbol{x})$	infectious mosquitoes	10,000/B	mosquitoes/m^2
$S_{rB}(0,\boldsymbol{x})$	susceptible resident birds	110×10^6/A	birds/m^2
$E_{rB}(0,\boldsymbol{x})$	exposed resident birds	10,000/B	birds/m^2
$I_{rB}(0,\boldsymbol{x})$	infectious resident birds	10,000/B	birds/m^2
$R_{rB}(0,\boldsymbol{x})$	recovered resident birds	10,000/B	birds/m^2
$D_{rB}(0,\boldsymbol{x})$	dead resident birds	10,000/B	birds/m^2
$S_{mB}(0,\boldsymbol{x})$	susceptible migratory birds	5×10^5/A	birds/m^2
$E_{mB}(0,\boldsymbol{x})$	exposed migratory birds	10,000/B	birds/m^2
$I_{mB}(0,\boldsymbol{x})$	infectious migratory birds	10,000/B	birds/m^2
$R_{mB}(0,\boldsymbol{x})$	recovered migratory birds	10,000/B	birds/m^2
$D_{mB}(0,\boldsymbol{x})$	dead migratory birds	10,000/B	birds/m^2

S3 Mathematical properties of the model

Theorem 1. *System (6) has non-negative and unique solutions that are bounded in* $[0,\infty)$.

Proof. We write system (6) together with the corresponding initial conditions, in the Banach space of continuous functions that include the boundary, $\mathscr{B} = C(\bar{\Omega})$, as follows [3]:

$$\begin{cases} \dfrac{\partial X(t,\boldsymbol{x})}{\partial t} = & \mathscr{L}X(t,\boldsymbol{x}) + f(X(t,\boldsymbol{x})),\ t>0, \\ X(t,0) = & X_0 \geq 0_{\mathbb{R}^{11}}, \end{cases} \tag{S1}$$

where

$$X(t,\boldsymbol{x})=\begin{bmatrix} S_V(t,\boldsymbol{x}) \\ E_V(t,\boldsymbol{x}) \\ I_V(t,\boldsymbol{x}) \\ S_{rB}(t,\boldsymbol{x}) \\ E_{rB}(t,\boldsymbol{x}) \\ I_{rB}(t,\boldsymbol{x}) \\ R_{rB}(t,\boldsymbol{x}) \\ S_{mB}(t,\boldsymbol{x}) \\ E_{mB}(t,\boldsymbol{x}) \\ I_{mB}(t,\boldsymbol{x}) \\ R_{mB}(t,\boldsymbol{x}) \end{bmatrix}, X(0,\boldsymbol{x})=\begin{bmatrix} S_V(0,\boldsymbol{x}) \\ E_V(0,\boldsymbol{x}) \\ I_V(0,\boldsymbol{x}) \\ S_{rB}(0,\boldsymbol{x}) \\ E_{rB}(0,\boldsymbol{x}) \\ I_{rB}(0,\boldsymbol{x}) \\ R_{rB}(0,\boldsymbol{x}) \\ S_{mB}(0,\boldsymbol{x}) \\ E_{mB}(0,\boldsymbol{x}) \\ I_{mB}(0,\boldsymbol{x}) \\ R_{mB}(0,\boldsymbol{x}) \end{bmatrix}, \mathscr{L}X(t,\boldsymbol{x})=\begin{bmatrix} D_1\Delta S_V(t,\boldsymbol{x}) \\ D_1\Delta E_V(t,\boldsymbol{x}) \\ D_1\Delta I_V(t,\boldsymbol{x}) \\ D_2\Delta S_{rB}(t,\boldsymbol{x}) \\ D_2\Delta E_{rB}(t,\boldsymbol{x}) \\ D_2\Delta I_{rB}(t,\boldsymbol{x}) \\ D_2\Delta R_{rB}(t,\boldsymbol{x}) \\ D_3\Delta S_{mB}(t,\boldsymbol{x})-\boldsymbol{A}\cdot\nabla S_{mB}(t,\boldsymbol{x}) \\ D_3\Delta E_{mB}(t,\boldsymbol{x})-\boldsymbol{A}\cdot\nabla E_{mB}(t,\boldsymbol{x}) \\ D_3\Delta I_{mB}(t,\boldsymbol{x})-\boldsymbol{A}\cdot\nabla I_{mB}(t,\boldsymbol{x}) \\ D_3\Delta R_{mB}(t,\boldsymbol{x})-\boldsymbol{A}\cdot\nabla R_{mB}(t,\boldsymbol{x}) \end{bmatrix},$$

and

$$f=\begin{cases} f_1= & b_V N_V\left[1-\dfrac{N_V}{K_V}\right]-[\lambda_{rV}(T)+\lambda mV(T)+\mu_V]S_V, \\ f_2= & [\lambda_{rV}(T)+\lambda mV(T)]S_V-(\gamma_V+\mu_V)E_V, \\ f_3= & \gamma_V E_V-\mu_V I_V, \\ f_4= & b_{rB}N_{rB}\left[1-\dfrac{N_{rB}}{K_{rB}}\right]-[\lambda_{Vr}(T)+\mu_{rB}]S_{rB}, \\ f_5= & \lambda_{Vr}(T)S_{rB}-[\gamma_{rB}+\mu_{rB}]E_{rB}, \\ f_6= & \gamma_{rB}E_{rB}-[\alpha_{rB}+\mu_{rB}]I_{rB}, \\ f_7= & (1-\nu_{rB})\alpha_{rB}I_{rB}-\mu_{rB}R_{rB}, \\ f_8= & b_{mB}N_{mB}\left[1-\dfrac{N_{mB}}{K_{mB}}\right]-[\lambda_{Vm}(T)+\mu_{mB}]S_{mB}, \\ f_9= & \lambda_{Vm}(T)S_{mB}-[\gamma_{mB}+\mu_{mB}]E_{mB}, \\ f_{10}= & \gamma_{mB}E_{mB}-[\alpha_{mB}+\mu_{mB}]I_{mB}, \\ f_{11}= & (1-\nu_{mB})\alpha_{mB}I_{mB}-\mu_{mB}R_{mB}. \end{cases}$$

Next, we show that f is locally Lipschitz in $\mathscr{B}$. Thus we show that

$$\forall\, K\subset\mathscr{B},\ \exists L:\quad \|f(X_1)-f(X_2)\|_\infty\le L\|X_1-X_2\|_\infty,\ \forall X_1,X_2\in K,$$

where L is the Lipschitz constant.

We observe that for $\Lambda_V=b_V N_V\left[1-\dfrac{N_V}{K_V}\right]$, $\Lambda_{rB}=b_{rB}N_{rB}\left[1-\dfrac{N_{rB}}{K_{rB}}\right]$ and $\Lambda_{mB}=b_{mB}N_{mB}\left[1-\dfrac{N_{mB}}{K_{mB}}\right]$,

$$X_1 - X_2 = \begin{bmatrix} \left[\Lambda_{V_1} - \Lambda_{V_2}\right] - \left[\lambda_{rV_1} S_{V_1} - \lambda_{rV_2} S_{V_2}\right] - \left[\lambda_{mV_1} S_{V_1} - \lambda_{mV_2} S_{V_2}\right] - \mu_V (S_{V_1} - S_{V_2}) \\ \left[\lambda_{rV_1} S_{V_1} - \lambda_{rV_2} S_{V_2}\right] + \left[\lambda_{mV_1} S_{V_1} - \lambda_{mV_2} S_{V_2}\right] - (\gamma_V + \mu_V)[E_{V_1} - E_{V_2}] \\ \gamma_V [E_{V_1} - E_{V_2}] - \mu_V [I_{V_1} - I_{V_2}] \\ [\Lambda_{rB_1} - \Lambda_{rB_2}] - (\lambda_{Vr_1} S_{rB_1} - \lambda_{Vr_2} S_{rB_2}) - \mu_{rB} [S_{rB_1} - S_{rB_2}] \\ \lambda_{Vr_1} S_{rB_1} - \lambda_{Vr_2} S_{rB_2} - (\gamma_{rB} + \mu_{rB})[E_{rB_1} - E_{rB_2}] \\ \gamma_{rB} [E_{rB_1} - E_{rB_2}] - (\alpha_{rB} + \mu_{rB})[I_{rB_1} - I_{rB_2}] \\ (1 - \nu_{rB}) \alpha_{rB} [I_{rB_1} - I_{rB_2}] - \mu_{rB} [R_{rB_1} - R_{rB_2}] \\ [\Lambda_{mB_1} - \Lambda_{mB_2}] - [\lambda_{Vm_1} S_{mB_1} - \lambda_{Vm_2} S_{mB_2}] - \mu_{mB} [S_{mB_1} - S_{mB_2}] \\ \lambda_{Vm_1} S_{mB_1} - \lambda_{Vm_2} S_{mB_2} - (\gamma_{mB} + \mu_{mB})[E_{mB_1} - E_{mB_2}] \\ \gamma_{mB} [E_{mB_1} - E_{mB_2}] - (\alpha_{mB} + \mu_{mB})[I_{mB_1} - I_{mB_2}] \\ (1 - \nu_{mB}) \alpha_{mB} [I_{mB_1} - I_{mB_2}] - \mu_{mB} [R_{mB_1} - R_{mB_2}] \end{bmatrix}.$$

Simplifying, we obtain $\|f(X_1) - f(X_2)\|_\infty =$

$$\begin{aligned} &= \sup_{x \in \bar{\Omega}} \left| \left[\Lambda_{V_1} - \Lambda_{V_2}\right] - S_{V_1} [\lambda_{rV_1} - \lambda_{rV_2}] \right| \\ &\vee \sup_{x \in \bar{\Omega}} \left| -\lambda_{rV_2} [S_{V_1} - S_{V_2}] - S_{V_1} [\lambda_{mV_1} - \lambda_{mV_2}] - \lambda_{mV_2} [S_{V_1} - S_{V_2}] - \mu_V (S_{V_1} - S_{V_2}) \right| \\ &\vee \sup_{x \in \bar{\Omega}} \left| \gamma_V [E_{V_1} - E_{V_2}] - \mu_V [I_{V_1} - I_{V_2}] \right| \\ &\vee \sup_{x \in \bar{\Omega}} \left| [\Lambda_{rB_1} - \Lambda_{rB_2}] - \lambda_{Vr_1} [S_{rB_1} - S_{rB_2}] - S_{rB_2} [\lambda_{Vr_1} - \lambda_{Vr_2}] - \mu_{rB} [S_{rB_1} - S_{rB_2}] \right| \\ &\vee \sup_{x \in \bar{\Omega}} \left| \lambda_{Vr_1} [S_{rB_1} - S_{rB_2}] + S_{rB_2} [\lambda_{Vr_1} - \lambda_{Vr_2}] - (\gamma_{rB} + \mu_{rB})[E_{rB_1} - E_{rB_2}] \right| \\ &\vee \sup_{x \in \bar{\Omega}} \left| \gamma_{rB} [E_{rB_1} - E_{rB_2}] - (\alpha_{rB} + \mu_{rB})[I_{rB_1} - I_{rB_2}] \right| \\ &\vee \sup_{x \in \bar{\Omega}} \left| (1 - \nu_{rB}) \alpha_{rB} [I_{rB_1} - I_{rB_2}] - \mu_{rB} [R_{rB_1} - R_{rB_2}] \right| \\ &\vee \sup_{x \in \bar{\Omega}} \left| [\Lambda_{mB_1} - \Lambda_{mB_2}] - \lambda_{Vm_1} [S_{mB_1} - S_{mB_2}] - S_{mB_2} [\lambda_{Vm_1} - \lambda_{Vm_2}] - \mu_{mB} [S_{mB_1} - S_{mB_2}] \right| \\ &\vee \sup_{x \in \bar{\Omega}} \left| \lambda_{Vm_1} [S_{mB_1} - S_{mB_2}] + S_{mB_2} [\lambda_{Vm_1} - \lambda_{Vm_2}] - (\gamma_{mB} + \mu_{mB})[E_{mB_1} - E_{mB_2}] \right| \\ &\vee \sup_{x \in \bar{\Omega}} \left| \gamma_{mB} [E_{mB_1} - E_{mB_2}] - (\alpha_{mB} + \mu_{mB})[I_{mB_1} - I_{mB_2}] \right| \\ &\vee \sup_{x \in \bar{\Omega}} \left| (1 - \nu_{mB}) \alpha_{mB} [I_{mB_1} - I_{mB_2}] - \mu_{mB} [R_{mB_1} - R_{mB_2}] \right|. \end{aligned} \tag{S2}$$

By the triangular inequality, and some simplifications, we arrive at

$$\|f(X_1) - f(X_2)\|_\infty \leq (\mu_V + \nu_{rB} \alpha_{rB} + \nu_{mB} \alpha_{mB}) \|X_1 - X_2\|_\infty,$$

and thus f is locally Lipschitz in $\mathscr{B}$. By [[4], Theorem B.17], [5], and [[6], Theorem 14.4], there exist a local smooth and unique solution of system (6) in Ω. We observe that system (6) can be written in the form of system (14.12) in the book [6], together with initial data defined in system (14.13). By [[6], Theorem (14.14)], the solutions of system (6) are always positive. □

S3.1 Well-posedness of the model in a feasible region

Theorem 2. *System (6) is well-posed mathematically and biologically, and for any* $(S_V(0,x), E_V(0,x), I_V(0,x), S_{rB}(0,x), E_{rB}(0,x), I_{rB}(0,x), R_{rB}(0,x), S_{mB}(0,x), E_{mB}(0,x),$ $I_{mB}(0,x), R_{mB}(0,x)) \in \mathbb{X}$, *system (6) admits a unique positive solution:* $(S_V(t,x), E_V(t,x), I_V(t,x),$ $S_{rB}(t,x), E_{rB}(t,x), I_{rB}(t,x), R_{rB}(t,x), S_{mB}(t,x), E_{mB}(t,x), I_{mB}(t,x), R_{mB}(t,x)) \in \mathbb{X}$, *satisfying:* $(S_V(t,x), E_V(t,x), I_V(t,x), S_{rB}(t,x), E_{rB}(t,x), I_{rB}(t,x), R_{rB}(t,x), S_{mB}(t,x), E_{mB}(t,x), I_{mB}(t,x), R_{mB}(t,x) \in C^{1,2}((0,\infty)\times\bar{\Omega}) \times C^{1,2}((0,\infty)\times\bar{\Omega})$, *where* $\mathbb{X} := C(\bar{\Omega}) \times C(\bar{\Omega})$.

Moreover, there exist another constant $C_1 > 0$ *independent of initial data, such that the solution* $(S_V(t,x), E_V(t,x), I_V(t,x), S_{rB}(t,x), E_{rB}(t,x), I_{rB}(t,x), R_{rB}(t,x), S_{mB}(t,x), E_{mB}(t,x), I_{mB}(t,x), R_{mB}(t,x))$ *satisfies:*

$\|S_V(t,x)\|_{L^\infty(\Omega)} + \|E_V(t,x)\|_{L^\infty(\Omega)} + \|I_V(t,x)\|_{L^\infty(\Omega)} + \|S_{rB}(t,x)\|_{L^\infty(\Omega)} + \|E_{rB}(t,x)\|_{L^\infty(\Omega)} + \|I_{rB}(t,x)\|_{L^\infty(\Omega)} + \|R_{rB}(t,x)\|_{L^\infty(\Omega)} + \|S_{mB}(t,x)\|_{L^\infty(\Omega)} + \|E_{mB}(t,x)\|_{L^\infty(\Omega)} + \|I_{mB}(t,x)\|_{L^\infty(\Omega)} + \|R_{mB}(t,x)\|_{L^\infty(\Omega)} \leq C_1$, *for all* $t > T_0 > 0$.

Proof. We follow the approach presented in [7, 8]. Using the regularity theory of parabolic PDEs [9], system (6) admits a unique non-negative classical solution

$$(S_j(t,x), E_j(t,x), I_j(t,x), R_j(t,x)) \in C^{1,2}((0,T_m)\times\bar{\Omega}) \times C^{1,2}((0,T_m)\times\bar{\Omega}),$$

where T_m represents the maximal existence time of the solution. By the strong maximum principle [10], then $S_j(t,x), E_j(t,x), I_j(t,x), R_j(t,x)$, where $j = rB, mB$ are positive in $(0,T_m)\times\bar{\Omega}$.

Summing up the equations gives

$$\frac{\partial N_j}{\partial t} = D_j \Delta N_j + b_j N_j \left[1 - \frac{N_j}{K_j}\right] - \mu_j N_j - \alpha_j \nu_j I_j,$$

subject to homogeneous Neumann boundary conditions $\nabla N_j \cdot n = 0$ on $\partial\Omega$ and non-negative initial data $N_j(x,0) = N_j(x) \geq 0$. Integrating over Ω, we get

$$\frac{d}{dt}\int_\Omega N_j(x,t)\,dx = \int_\Omega \left[b_j - \mu_j\right] N_j\,dx - \int_\Omega b_j \frac{N_j}{K_j}\,dx \leq \bar{r}\int_\Omega N_j(x,t)\,dx,\ x\in\Omega,\ t>0, \bar{r} \leq b_{j,max},$$

yielding

$$\int_\Omega N_j(x,t)\,dx \leq \int_\Omega e^{t b_{j,max}} N_{j0}(x)\,dx, \quad x\in\Omega,\ t\geq 0.$$

Thus, $\|S_j(t,\cdot)\|_{L^1(\Omega)}$, $\|E_j(t,\cdot)\|_{L^1(\Omega)}$, $\|I_j(t,\cdot)\|_{L^1(\Omega)}$, and $\|R_j(t,\cdot)\|_{L^1(\Omega)}$ are bounded for all $0 < t < T_m$. By the positivity of $S_j(t,\cdot)$, $E_j(t,\cdot)$, $I_j(t,\cdot)$, $R_j(t,\cdot)$, and [[7], Lemma (3.1)], with $\sigma = p_0 = 1$, we conclude that there exist a positive constant C_1 that does not depend on initial data such that the solution S_j, E_j, I_j, R_j satisfies

$$\|S_j(t,\cdot)\|_{L^\infty(\Omega)} + \|E_j(t,\cdot)\|_{L^\infty(\Omega)} + \|I_j(t,\cdot)\|_{L^\infty(\Omega)} + \|R_j(t,\cdot)\|_{L^\infty(\Omega)} \leq C_1,\ \forall t > T_0.$$

Similar arguments can be made for the mosquito population, thus we conclude that system (6) is well-posed. □

S4 Simulation framework

The toolbox solves PDEs of the form

$$m\frac{\partial^2 u}{\partial t^2} + d\frac{\partial u}{\partial t} - \nabla \cdot (c\nabla u) + au = f, \tag{S3}$$

and in our case, $m = 0, d = 1$, $a = 0$, and matrices c and f are given by:

$$c = [D_1; D_1; D_1; D_2; D_2; D_2; D_2; 0; D_3; D_3; D_3; D_3; 0],$$

while

$$f = \begin{cases} \mu_V(T,\boldsymbol{x})N_V - [\lambda_{rV}(T,\boldsymbol{x}) + \lambda m V(T,\boldsymbol{x}) + \mu_V(T,\boldsymbol{x})]S_V, \\ [\lambda_{rV}(T,\boldsymbol{x}) + \lambda m V(T,\boldsymbol{x})]S_V - [\gamma_V(T,\boldsymbol{x}) + \mu_V(T,\boldsymbol{x})]E_V, \\ \gamma_V(T,\boldsymbol{x})E_V - \mu_V(T,\boldsymbol{x})I_V, \\ \mu_{rB}N_{rB} - [\lambda_{Vr}(T,\boldsymbol{x}) + \mu_{rB}]S_{rB}, \\ \lambda_{Vr}(T,\boldsymbol{x})S_{rB} - [\gamma_{rB} + \mu_{rB}]E_{rB}, \\ \gamma_{rB}E_{rB} - [\alpha_{rB} + \mu_{rB}]I_{rB}, \\ (1-\nu_{rB})\alpha_{rB}I_{rB} - \mu_{rB}R_{rB}, \\ \alpha_{rB}\nu_{rB}I_{rB}, \\ \mu_{mB}N_{mB} - [\lambda_{Vm}(T,\boldsymbol{x}) + \mu_{mB}]S_{mB} - \boldsymbol{A}\cdot\nabla S_{mB}, \\ \lambda_{Vm}(T,\boldsymbol{x})S_{mB} - [\gamma_{mB} + \mu_{mB}]E_{mB} - \boldsymbol{A}\cdot\nabla E_{mB}, \\ \gamma_{mB}E_{mB} - [\alpha_{mB} + \mu_{mB}]I_{mB} - \boldsymbol{A}\cdot\nabla I_{mB}, \\ (1-\nu_{mB})\alpha_{mB}I_{mB} - \mu_{mB}R_{mB} - \boldsymbol{A}\cdot\nabla R_{mB}, \\ \nu_{mB}\alpha_{mB}I_{mB}. \end{cases} \tag{S4}$$

The matrix c consists of the diffusion coefficients, while f stores reaction and advection terms. The model is solved as follows [11]:

Algorithm S1 Pseudo-code for solving system (7) using Matlab's `PDEToolbox`

Step 1: Create the PDE model with N equations

`model` ← `createpde(N)`

Step 2: Define the geometry

`geometryFromEdges(model,g)`

Step 3: Generate a mesh for the geometry

`gm` ← `generateMesh(model)`

Step 4: Add boundary conditions to the PDEModel

`applyBoundaryCondition(_)`

Step 5: Specify coefficients of the PDE model

`specifyCoefficients(model,"m",0,"d",1,"c",c,"a",0,"f",f)`

Step 6: Give initial conditions or initial solution

`setInitialConditions(model,initial_value_vector)`

Step 7: Solve the PDE system

`results` ← `solvepde(model)`

Step 8: Extract the solution

`Sol` ← `results.NodalSolution`

Step 9: Plot the solution

Plot `Sol` using `pdeplot()`

The map of Germany is downloaded as a shape file from (https://gadm.org/download_country_v3.html) and simplified using mapshaper [12]. Matlab codes for the full implementation and the data are freely available in our Zenodo repository [13] and they can be used to extend our model, or adopt for any country.

References

[1] Vincent Laperriere, Katharina Brugger, and Franz Rubel. Simulation of the seasonal cycles of bird, equine and human west nile virus cases. *Preventive Veterinary Medicine*, 98(2–3):99–110, February 2011. ISSN 0167-5877. https://dx.doi.org/10.1016/j.prevetmed.2010.10.013.

[2] Julian Heidecke, Jonas Wallin, Peter Fransson, Pratik Singh, Henrik Sjödin, Pascale Claire Stiles, Marina Treskova, and Joacim Rocklöv. Uncovering temperature sensitivity of west nile virus transmission: Novel computational approaches to mosquito-pathogen trait responses. *PLOS Computational Biology*, 21(3):e1012866, March 2025. ISSN 1553-7358. doi: 10.1371/journal.pcbi.1012866. URL http://dx.doi.org/10.1371/journal.pcbi.1012866.

[3] Hamadjam Abboubakar, Reinhard Racke, and Nicolas Schlosser. A reaction-diffusion model for the transmission dynamics of the coronavirus pandemic with reinfection and vaccination process. 2023.

[4] Vincenzo Capasso. *Mathematical Structures of Epidemic Systems*. Springer Berlin Heidelberg, 1993. ISBN 9783540705147. https://dx.doi.org/10.1007/978-3-540-70514-7.

[5] Xavier Mora. Semilinear parabolic problems define semiflows on c k spaces. *Transactions of the American Mathematical Society*, 278(1):21, July 1983. ISSN 0002-9947. https://dx.doi.org/10.2307/1999300.

[6] Joel Smoller. *Shock Waves and Reaction—Diffusion Equations*. Springer US, 1983. ISBN 9781468401523. https://dx.doi.org/10.1007/978-1-4684-0152-3.

[7] Rui Peng and Xiao-Qiang Zhao. A reaction–diffusion sis epidemic model in a time-periodic environment. *Nonlinearity*, 25(5):1451–1471, April 2012. ISSN 1361-6544. https://dx.doi.org/10.1088/0951-7715/25/5/1451.

[8] Jianpeng Wang and Binxiang Dai. Qualitative analysis on a reaction-diffusion host-pathogen model with incubation period and nonlinear incidence rate. *Journal of Mathematical Analysis and Applications*, 514(2):126322, October 2022. ISSN 0022-247X. https://dx.doi.org/10.1016/j.jmaa.2022.126322.

[9] C. V. Pao. *Nonlinear parabolic and elliptic equations*. Springer US, 1993. ISBN 9781461530343. https://dx.doi.org/10.1007/978-1-4615-3034-3.

[10] Murray H. Protter and Hans F. Weinberger. *Maximum principles in differential equations*. Springer New York, 1984. ISBN 9781461252825. https://dx.doi.org/10.1007/978-1-4612-5282-5.

[11] The MathWorks, Inc. *MATLAB*. Natick, Massachusetts, United States, 2024. Available from https://www.mathworks.com/help/pde/pde-problem-setup.html?s_tid=CRUX_topnav.

[12] M. Harrower and M. Bloch. Mapshaper.org: a map generalization web service. *IEEE Computer Graphics and Applications*, 26(4):22–27, July 2006. ISSN 0272-1716. doi: 10.1109/mcg.2006.85. URL http://dx.doi.org/10.1109/mcg.2006.85.

[13] Pride Duve, Felix. G. Sauer, and Renke Lühken. Codes and data for the paper: Modelling the impact of temperature and bird migration on the spread of West Nile Virus, June 2025. URL https://doi.org/10.5281/zenodo.18996831. Version 1.0.

4.2 Publication 2: *Modelling the control of West Nile virus using mosquito reduction methods, vaccination of equids, and human behavioural adaptation to the usage of personal protective equipment*

Ecological Modelling 517 (2026) 111605

Contents lists available at ScienceDirect

Ecological Modelling

journal homepage: www.elsevier.com/locate/ecolmodel

Modelling the control of West Nile virus using mosquito reduction methods, equid vaccination, and human behavioural adoption of personal protective equipment

Pride Duve *, Felix Gregor Sauer, Renke Lühken

Bernhard Nocht Institute for Tropical Medicine, Hamburg, Germany

ARTICLE INFO

Dataset link: https://github.com/Pride1234/West-Nile-virus-control

Keywords:
West Nile virus
Temperature
Mosquito control
Behavioural dynamics
Equid vaccination
Control app

ABSTRACT

West Nile virus (WNV) is a mosquito-borne virus in the genus *Flavivirus* that circulates between mosquitoes and birds, whereas humans, equids, and other mammals are dead-end hosts. Since its emergence in Germany in 2018, the virus has spread across the country, highlighting the need for effective intervention strategies. However, it remains unclear how different strategies should be combined and timed to effectively reduce WNV transmission under temperature-driven dynamics. In this study, we develop a temperature-dependent, process-based model to evaluate the effectiveness of WNV control strategies, such as mosquito reduction methods, equid vaccination, and the use of personal protective equipment (PPE). Human behavioural responses to infection risk are incorporated through imitation dynamics that capture how individuals adopt PPE based on perceived infection risk and social influence. An optimal control problem has been formulated and studied to determine the seasonal timing of mosquito controls under temperature forcing. Results suggest that mosquito controls initiated in early spring and intensified in early May, may reduce the August peak in the infectious bird population. Moreover, a combined scenario of mosquito control methods, human PPE adoption, and equid vaccination could be the best strategy among dead-end hosts. The analysis of various combinations of constant controls is available as an interactive application, allowing users to explore intervention strategies under different temperature projections corresponding to the low-mitigation (SSP126), intermediate (SSP245), and high-emission (SSP585) scenarios.

1. Introduction

The circulation of West Nile virus (WNV) in Europe has been observed for several decades (Sambri et al., 2013). Today, many countries in Southern and Southeastern Europe have confirmed cases in birds, equids, humans, and other mammals, while several other countries remain at risk of WNV (Bakonyi and Haussig, 2020). Climate warming has a significant role in the establishment and spread of WNV globally, including Europe (Erazo et al., 2024), posing a substantial public health and economic challenge (Paz, 2015; Watts et al., 2021; Ziegler et al., 2019a,b, 2020). The enzootic cycle involves different *Culex* species and birds, with a risk of spillover to humans, equids, and other mammals (Vogels et al., 2016, 2017).

Mammals are dead-end hosts as they do not develop viremia high enough to infect mosquitoes, while birds are considered the amplifying host (Nemeth et al., 2007). Most cases in humans are asymptomatic, but mild symptoms may include vomiting, or skin rash, headache, or confusion, among others, and in some cases, the infection can be fatal (Petersen et al., 2013; Sambri et al., 2013). Symptoms in equids include ataxia, weakness, depression, dysphagia, and frequent stumbling (Salazar et al., 2004; Schuler et al., 2004). WNV symptoms in birds vary by species, but some species are at risk of developing ataxia, abnormal head posture, and rapid death (Phalen and Dahlhausen, 2004).

In Germany, the first case of WNV was reported in August 2018, in a bird from Eastern Germany (Ziegler et al., 2019a,b, 2020). Over the following years, annual circulation was observed, particularly in central-eastern Germany (Fig. 1). To date, there is no specific cure for WNV, and treatment only relies on managing symptoms (Colpitts et al., 2012), while vaccines are only available for equids (Sambri et al., 2013). Thus, preventive measures for humans rely mainly on recommendations to use personal protective measures that reduce contact between mosquitoes and humans (Petersen et al., 2013; European Centre for Disease Prevention and Control, 2024), and most importantly, on measures to reduce mosquito populations (Bellini et al., 2014). Thereby, several

* Corresponding author.
E-mail address: pride.duve@bnitm.de (P. Duve).

https://doi.org/10.1016/j.ecolmodel.2026.111605
Received 13 November 2025; Received in revised form 16 March 2026; Accepted 11 April 2026
Available online 27 April 2026
0304-3800/© 2026 The Authors. Published by Elsevier B.V. This is an open access article under the CC BY license (http://creativecommons.org/licenses/by/4.0/).

mosquito control methods are available, e.g., breeding-site removal, larvicides, adulticides, and biological control methods such as the introduction of natural enemies (Cailly et al., 2012; Ferede et al., 2018; Takken and Knols, 2009). The European Centre for Disease Prevention and Control (2024) further stresses that people should consider using mosquito bed nets, sleeping in screened or air-conditioned rooms, wearing clothing that covers most of the body, or using mosquito repellents.

Several process-based models have been developed to assess various control measures and their timing for WNV. Early modelling studies focused on describing the interaction between mosquito vectors and avian hosts to understand the ecological drivers of WNV transmission (Bhowmick et al., 2024; Laperriere et al., 2011; Mbaoma et al., 2024). These models provided valuable insights into how environmental factors and host-vector interactions influence the spread of WNV. Subsequent studies then extended these frameworks by incorporating additional host populations and intervention strategies, such as mosquito control and vaccination. Bowman et al. (2005) found that adulticiding is more effective than personal protection for controlling the spread of human WNV. According to Thomas et al. (2009), mosquito spraying during autumn is more effective than in summer. Bhowmick et al. (2024) demonstrated that ultra-low volume spraying only temporarily reduces the reproductive number. The combination of bird immunisation and mosquito control approaches is the most cost-effective strategy against WNV (Malik, 2018). Blayneh et al. (2010) concluded that mosquito reduction should be prioritised over personal protection measures, and Abdelrazec et al. (2015) highlighted larviciding as the most effective ongoing strategy while emphasising the importance of seasonal timing.

Although these models have improved our understanding of WNV dynamics, many assume constant intervention strategies and do not explicitly consider how environmental factors, particularly temperature, influence the timing and effectiveness of mosquito control measures. Additionally, human behavioural responses, such as the adoption of personal protective equipment, are rarely incorporated into WNV transmission models despite their potential importance in reducing spillover infections. These limitations highlight the need for modelling frameworks that integrate environmental drivers, behavioural responses, and multiple intervention strategies to better inform WNV control.

An interdisciplinary perspective, such as the One Health approach, is particularly important for zoonotic pathogens like WNV, as it integrates knowledge from ecology, animal health, and human health to design and evaluate control strategies (Cendejas and Goodman, 2024). In this study, we analyse the effectiveness of several intervention strategies within a system of ordinary differential equations (ODEs), including larviciding, adult mosquito control, and PPE adoption. In addition, we incorporate the physical removal of mosquito breeding sites and the vaccination of equids, two interventions that have not been explicitly considered together in previous modelling studies. The model is driven by real-world temperature data for Berlin, allowing environmental conditions to influence mosquito dynamics and the effectiveness of control measures. Furthermore, we formulate and solve an optimisation problem to determine the timing of mosquito control strategies, driven by temperature. Finally, we explore constant intervention levels ranging from 0 to 90% and evaluate different combinations of controls. These scenarios are implemented in our interactive, open-access web-based application, which enables users, including non-specialists, to explore the effects of different intervention strategies and their combinations without requiring expertise in programming or mathematical modelling.

2. Model formulation

Our model consists of a system of first-order ODEs, extending the work of Laperriere et al. (2011), Mbaoma et al. (2024), and Rubel et al. (2008). We here focus on capturing control methods against WNV. Temperature-dependent parameters of the model are fitted from various datasets in Laperriere et al. (2011) and Rubel et al. (2008), and thus, for a more detailed derivation of the baseline WNV model and the thermal parameters, we refer the reader to the studies by Laperriere et al. (2011) and Rubel et al. (2008).

2.1. Mosquito population

In this study, the mosquito population is divided into four classes: mosquito larvae (L_M), susceptible adults (S_M), exposed adults (E_M), and infectious adults (I_M). The larval population increases through oviposition by adults, assuming that all adult mosquitoes under study are females. This recruitment process is proportional to the total adult mosquito population $N_M = S_M + E_M + I_M$, thereby linking larval births to adult abundance. Overwintering dynamics are modelled via a hibernation rate δ_M, which regulates the fraction of adult mosquitoes that lay eggs each year. Following Rubel et al. (2008), the fraction of non-diapausing adult mosquitoes is described by a photoperiod-dependent logistic function

$$\delta_M(D) = 1 - \frac{1}{1 + 1775.7 \times e^{(1.559(D - 18.177))}}, \tag{1}$$

where D denotes the daytime length (in hours). The photoperiod depends on calendar day d and geographic latitude ϕ through a standard astronomical relationship (see Rubel et al., 2008 for full derivation):

$$D = 7.639 \arcsin\left[\tan(\epsilon)\tan(\phi) + \frac{0.0146}{\cos(\epsilon)\cos(\phi)}\right] + 12,$$

with solar declination

$$\epsilon = 0.409 \sin\left(\frac{2\pi(d - 80)}{365}\right).$$

The geographic latitude is fixed to Berlin ($\phi = 52.52°$N), one of the WNV hotspots in Germany. Fig. 2 shows the spatio-temporal distribution of the function δ_M at selected locations to indicate its heterogeneity driven by the photoperiod over Germany.

Although photoperiod primarily regulates diapause cues in temperate regions, daylight length alone is insufficient to determine the onset and intensity of transmission activity (Eldridge, 1968; Field et al., 2022; Spielman and Wong, 1973). Temperature acts as an additional environmental variable, modulating the general activity, development, survival, and feeding behaviour of mosquitoes (Eldridge, 1968; Rubel et al., 2008). Moreover, viral replication within the mosquito vector is strongly temperature-dependent. Low temperatures prolong the extrinsic incubation period (EIP), potentially preventing mosquitoes from becoming infectious before they die. In contrast, higher temperatures accelerate viral replication and shorten the EIP, thereby increasing transmission potential (Andreadis et al., 2014; Vollans et al., 2024). As a result, we here introduce temperature-dependent larval birth rate ($b_L(T)$), mosquito development rate ($b_M(T)$), larvae mortality rate ($\mu_L(T)$), adult mortality rate ($\mu_M(T)$), biting rate ($k(T)$), and the extrinsic incubation rate ($\gamma_M(T)$), defined in Table 2. The temperature-dependent larval birth and death rates were fitted by Rubel et al. (2008) and are given by:

$$b_L(T) = \frac{0.7998}{1 + 1.231e^{-0.184(T - 20)}}, \tag{2}$$

and

$$\mu_L(T) = 0.0025T^2 - 0.094T + 1.0257 \tag{3}$$

respectively. Thus, the natural birth term of mosquito larvae governed by temperature and photoperiod is then given by:

$$(1 - \boldsymbol{u_1})b_L(T)\delta_M(D)\left[1 - \frac{L_M}{K_M}\right]N_M,$$

where $\boldsymbol{u}_1 \in [0, 1)$ represents the level of implementation effort of breeding site removal. When $\boldsymbol{u}_1 = 0$, then, the breeding site removal has

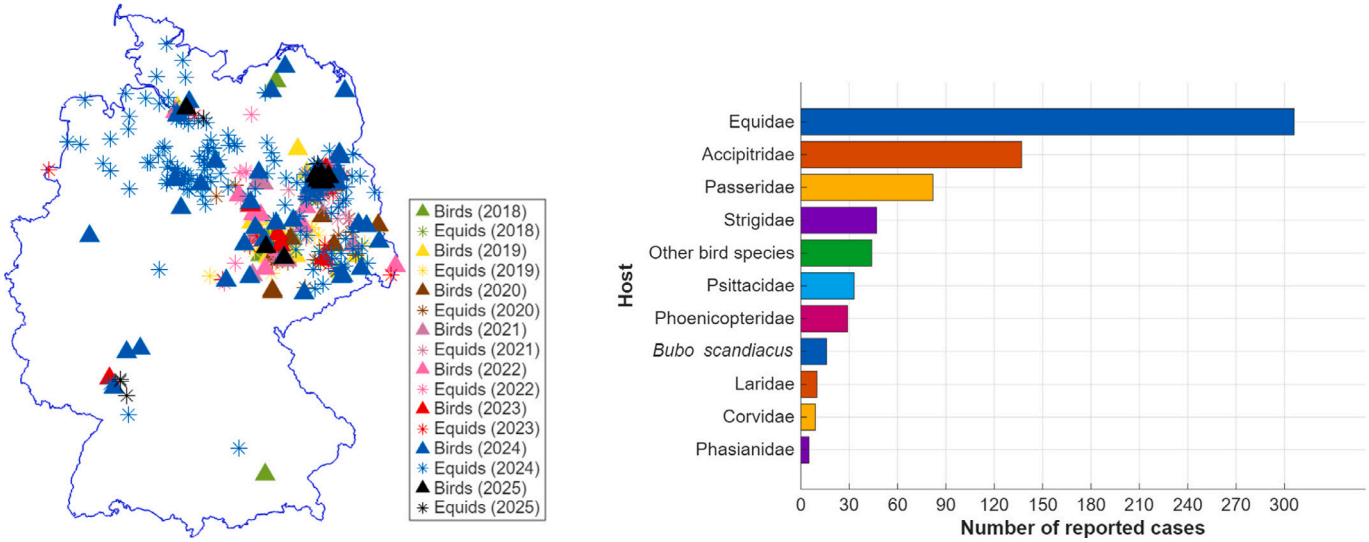


Fig. 1. Observed animal WNV cases in Germany from August 2018 to December 2025 (left) and WNV cases for the different species (right). Data obtained from World Organisation for Animal Health (WOAH) (2018 - 2025) for the period 2018–2025.

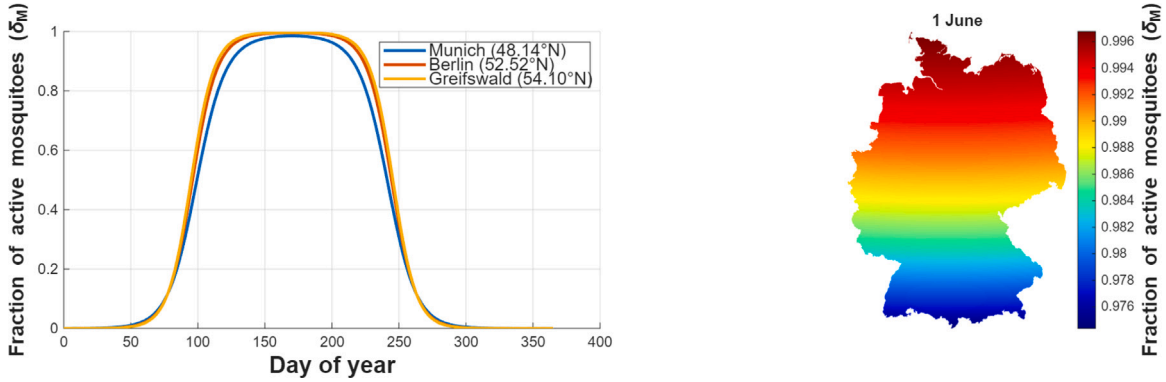


Fig. 2. Fraction of active (non-hibernating) mosquitoes driven by photoperiod at selected locations (left) and for the entire country on 1 June (right).

no impact on larval production and mortality. In contrast, $u_1 \approx 1$ corresponds to maximal effectiveness, meaning that full implementation may completely suppress larval recruitment and effectively increase its mortality. The term $\left[1 - \frac{L_M}{K_M}\right]$ is the density-dependent limiting factor in the breeding sites.

As introduced earlier, the European Centre for Disease Prevention and Control (2023) encourages the use of larvicides to increase the mortality of mosquito larvae; thus, we define a parameter $u_2 \in [0, 1)$ to represent larviciding. Mosquito larvae that survive the larval stage develop into susceptible adults class (S_M) at a temperature-dependent larval development rate:

$$b_M(T) = \frac{b_L(T)}{10}. \tag{4}$$

Susceptible mosquitoes get infected by biting infectious birds at a temperature-dependent mosquito-biting rate of

$$k(T) = \frac{0.344}{1 + 1.231e^{-0.184(T-20)}} \tag{5}$$

and a probability that a successful bite of a susceptible mosquito on an infectious bird leads to a new mosquito infection $p_B = 0.125$. The force of infection on mosquitoes is thus given by

$$\lambda_{BM}(T) = \frac{\delta_M k(T) p_B I_B}{K_B}, \tag{6}$$

while the natural mortality rate of adult mosquitoes is given by the function

$$\mu_M(T) = \frac{\mu_L(T)}{10}. \tag{7}$$

For all adult mosquitoes, we consider the use of adult control measures denoted u_3, which increase the adult mosquito mortality rate. Such measures can include adulticide sprays or traps that use mosquito lures to attract and capture adult mosquitoes, such as carbon dioxide traps, human-mimicking odours, or visual cues. Recently, Sauer et al. (2023) carried out a field study to identify overwintering sites for *Cx. torrentium* and *Cx. pipiens pipiens*. Their results indicated that *Cx. torrentium* are mainly dominant in animal burrows, while *Cx. pipiens pipiens* in human-made sites. Motivated by this overwintering behaviour of *Culex* vectors, we include the elimination of adult-overwintering sites as part of adult control methods for *Culex* mosquitoes. Although this control method has not yet been implemented in practice, it has been discussed in various studies, e.g., Kobayashi et al. (2012), Liu et al. (2016), Sauer et al. (2022), given that overwintering mosquitoes are potentially easy to target and can be detected at high concentrations in their overwintering sites. After a successful interaction between susceptible mosquitoes and infectious birds, susceptible mosquitoes move to the exposed compartment (E_M). The extrinsic incubation period in the exposed stage is given by $\frac{1}{\gamma_M(T)}$, where

$$\gamma_M(T) = \begin{cases} 0.0093T - 0.1352 & \text{if} \quad T > 15, \\ 0 & \text{otherwise}, \end{cases} \tag{8}$$

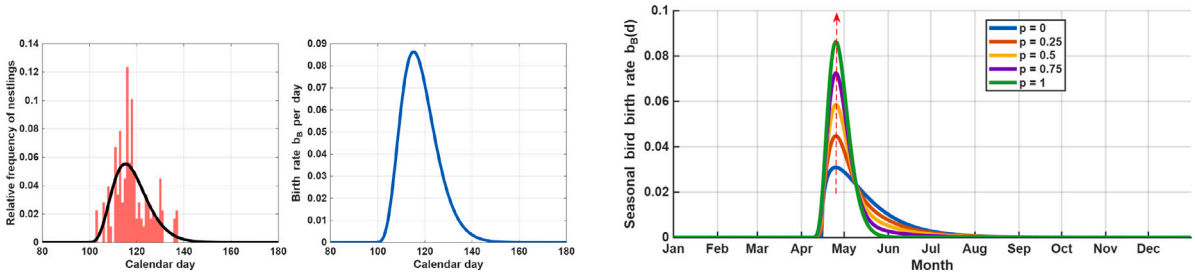


Fig. 3. Observed relative frequency of the nestlings of northern goshawks (Courtiol, 2020; Merling de Chapa et al., 2020) with fitted Gamma distribution (left) and bird birth rate as a function of the calendar day (right).

and from this stage, mosquitoes progress to the infectious class (I_M). Temperature-dependent functions are summarised in Table 2 and Fig (1) of the Supplementary material.

2.2. Bird population

The primary bird species responsible for WNV amplification in Germany remains unknown, but it is suspected that multiple species may be involved (Mbaoma et al., 2024; Michel et al., 2018; Offergeld et al., 2025). Surveillance data from Germany indicate that birds from the Accipitridae and Passeridae families were the most affected species between the years 2018–2025 (Fig. 1 and Mbaoma et al. (2024), Ziegler et al. (2019b)). The most frequently observed Accipitridae species during this period included the northern goshawk and other raptors, while the Eurasian blackbird (*Turdus merula*) were also affected (Ziegler et al., 2019b). The blackbird is one of Germany's most common breeding birds, with approximately 10 million breeding pairs reported nationwide (Gerlach et al., 2019). Considering the high population of blackbirds and the frequent WNV infections observed in northern goshawks, these two species are used in this study as representative avian hosts.

Rubel et al. (2008) modelled blackbird birth rates by fitting a Gamma distribution to the observed frequency of blackbird nestlings, based on data from Poland. The resulting curve has the form

$$b_{B_{b.b}}(d) = \frac{1.25}{10}\frac{(x/\beta)^{\alpha-1}\exp(-x/\beta)}{\beta\Gamma(\alpha)}, \quad x,\alpha,\beta > 0, \tag{9}$$

which produces a right-skewed birth-rate function with a peak in nestling frequency around day 115.

For northern goshawks, we used surveillance data from a citizen science project published by Courtiol (2020), Merling de Chapa et al. (2020). The data showed that urban goshawks breed earlier than their rural counterparts. Since our model is specific to Berlin, we extracted only Berlin urban data and fitted it to the Gamma distribution in Eq. (10), with $x = d - d_0$. This resulted in fitted parameters $\alpha = 6.867, \beta = 2.935, d_0 = 98$, with a predicted peak in nestling frequency around day 115, the same day predicted by the function by Rubel et al. (2008). Here, d_0 marks the start of the breeding season. Based on this data, the annual per-capita recruitment rate was estimated as 1.5614 offspring per adult per year, leading to an estimated birth rate function of northern goshawks:

$$b_{B_{n.g}}(d) = 1.5614\frac{(x/\beta)^{\alpha-1}\exp(-x/\beta)}{\beta\Gamma(\alpha)}, \quad x,\alpha,\beta > 0. \tag{10}$$

The seasonal recruitment of susceptible birds is then modelled as a weighted mixture of the species-specific birth functions derived for northern goshawks and blackbirds. Such a formulation accounts for the fact that multiple bird species contribute to the pool of susceptible hosts involved in the transmission cycle. The combined recruitment function is therefore expressed as

$$b_B(d) = p\, b_{B_{n.g}}(d) + (1-p)\, b_{B_{b.b}}(d), \tag{11}$$

where $b_{B_{n.g}}(d)$ and $b_{B_{b.b}}(d)$ denote the seasonal birth functions for northern goshawks and blackbirds, respectively, and d represents the day of the year. The parameter $0 \le p \le 1$ determines the bird recruitment rate to the overall seasonal recruitment pattern, based on birth rates of northern goshawks and blackbirds. We examine the sensitivity of the seasonal birth-rate function $b_B(d)$ to the mixing parameter p, illustrating how different values of p influence the timing and magnitude of seasonal recruitment (Fig. 3, right). The recruitment rate into the susceptible bird population is thus defined by

$$b_B(d)\left[1 - \frac{N_B}{K_B}\right]N_B,$$

while their natural mortality rate by $\mu_B = 0.0005$.

The population of birds is divided into susceptible (S_B), exposed (E_B), infectious (I_B), recovered (R_B), and dead birds (D_B), with $N_B = S_B + E_B + I_B + R_B$, and a force of infection between infectious mosquitoes and susceptible birds of

$$\lambda_{MB}(T) = \frac{\delta_M k(T) p_M \phi_B I_M}{K_M}. \tag{12}$$

In Eq. (12), $p_M = 1.0$ is the probability that a successful bite by an infectious mosquito on a susceptible bird leads to a new bird infection, and ϕ_B is the mosquito to bird ratio. The intrinsic incubation period of exposed birds is given by $\frac{1}{\gamma_B}$, where $\gamma_B = 0.196$, and from this stage, exposed birds progress to the infectious compartment. A proportion $\nu_B = 0.655$ of infectious birds die due to the WNV, at a rate of $\alpha_B = 0.867$, while a proportion $(1-\nu_B)$ recover from the virus at a rate of α_B. Parameter definitions and sources are summarised in Table 2.

2.3. Human population

Laperriere et al. (2011) and Mbaoma et al. (2024) modelled the human population by dividing it into susceptible (S_H), exposed (E_H), infected (I_H), recovered (R_H), and deceased (D_H) compartments. In this study, we adopt these four compartments and integrate human behavioural adoption of PPE through game-theoretic and imitation-dynamics modelling.

Bauch (2005) initially examined imitation dynamics to predict vaccination behaviour based on disease prevalence. We here use this approach to model how people may decide to start using PPE in response to WNV prevalence in birds. In this formulation, PPE use is assumed to begin once an increase in WNV cases among birds is observed, as bird infections are typically detected before human cases (Tamba et al., 2024). Thus, the proportion of humans using PPE is here defined by x, while $1-x$ are those who are unprotected at any time t, with the rate of change of x described by the equation

$$\frac{dx}{dt} = qx(1-x)\left[-r_p + r_i m I_B\right]. \tag{13}$$

In this equation, q is the imitation rate that measures how quickly people adopt PPE due to factors such as social influence, imitation, what they hear, and what they observe within their social circle. r_p measures the perceived inconvenience, frustration, or annoyance due to PPE use, r_i measures the perceived infection risk, and m indicates how much disease prevalence in birds affects PPE adoption by susceptible humans. Notably, when $r_i m I_B > r_p$, more people use

PPE, whereas when $r_i m I_B < r_p$, fewer people do. This enables us to model PPE adoption as a game in which players are susceptible humans who are undecided about adopting PPE, considering their potential impacts on people's daily socio-economic, cultural, and emotional livelihoods (Bauch, 2005; N'konzi et al., 2022). The reduced version of Eq. (13) is given by Eq. (14) and the full derivation is shown in Section S2 of the Supplementary material.

$$\frac{dx}{dt} = \kappa x(1-x)\left[-1+\omega I_B\right]. \tag{14}$$

It follows that when $x = 0$, individuals do not use any PPE, whereas when $x = 1$, the entire susceptible population adopts PPE, representing the maximum level of protective behaviour in the model.

The population of susceptible humans in Berlin is obtained from Amt für Statistik Berlin-Brandenburg (2024), which reported an estimated population of approximately 3,685,265 in 2024. This office further reported 33,749 births, and 37,686 in the Berlin-Brandenburg area (Amt für Statistik Berlin-Brandenburg, 2025a) during the same year. Additionally, Berlin is one of the major cities with high migration populations (Heider et al., 2020; Amt für Statistik Berlin-Brandenburg, 2025b), with a 2024 net migration of 27,107, as reported by Amt für Statistik Berlin-Brandenburg (2025b). Based on this data, we estimate the crude per-capita daily recruitment rate (b_H) of susceptible humans in Berlin as the sum of the crude birth rate and the crude net migration rates, yielding estimates of $b_H = 0.0000452$ per day while the natural mortality rates of humans is calculated from the crude death rates of humans in Berlin yielding $\mu_H = 0.0000280$ per day. Full calculations are presented in the Section S3 of the Supplementary material.

The force of infection on humans is given by

$$\lambda_{MH} = \frac{(1-x)\delta_M k(T) p_M \phi_H I_M}{K_M}. \tag{15}$$

Susceptible humans progress to the exposed class via the force of infection in Eq. (15). In the exposed class, the intrinsic incubation period is given by $\frac{1}{\gamma_H}$, where $\gamma_H = 0.25$. As dead-end hosts, humans do not infect mosquitoes, instead, infected humans either recover at a rate $\alpha_H = 0.5$ or die at a rate $\nu_H = 0.004$ due to WNV (Laperriere et al., 2011; Mbaoma et al., 2024). The mosquito to human ratio is assumed to be $\phi_H = 0.3 - 3$.

2.4. Equid population

The population of equids is divided into susceptible (S_E), vaccinated (V_E), exposed (E_E), infected (I_E), recovered (R_E), and dead (D_E). Official statistics from the Landesamt für Ländliche Entwicklung, Landwirtschaft und Flurneuordnung (LELF; the state of Brandenburg department responsible for rural development and agriculture) report that approximately 45,000 horses are kept in Berlin and Brandenburg combined (Landesamt für Ländliche Entwicklung, Landwirtschaft und Flurneuordnung (LELF), 2026). Given that there is no publicly available census of equids in Berlin, we use this statistic as the baseline regional susceptible equid population, while exposed, infected, recovered, and deceased are initialised to zero. Susceptible equids are recruited at a birth rate of $b_E = 0.00016$ and die at a natural mortality rate of $\mu_E = 0.00011$ adopted from Laperriere et al. (2011). Mosquitoes can bite either unvaccinated or vaccinated equids, with a force of infection

$$\lambda_{ME} = \frac{\delta_M k(T) p_M \phi_E I_E}{K_M}. \tag{16}$$

A successful bite from an infectious mosquito on susceptible equids moves them to the exposed compartment. The force of infection for vaccinated equids is controlled by the threshold $(1 - c_E)$, where c_E is the vaccine effectiveness. When $c_E = 0$, the vaccine is ineffective, and vaccinated equids progress to the exposed compartment just like unvaccinated ones. Conversely, when $c_E = 1$, the vaccine is 100% effective, and no vaccinated equids will be infected with WNV. The population of exposed equids is then increased via a combined force infection: $\lambda_{ME} S_E + (1-c_E)\lambda_{ME} V_E$, and exposed equids can die naturally at a rate of μ_E. The intrinsic incubation period of equids is $\frac{1}{\gamma_E}$, where $\gamma_E = 0.05$. Equids in all compartments may die naturally at a rate μ_E, while a proportion $\nu_E = 0.04$ of infected equids may die due to WNV and progress to the D_E compartment at a rate $\alpha_E = 0.2$. A proportion $1 - \nu_E$ recover at a rate of α_E. The mosquito to bird ratio is assumed to be $\phi_E = 3$, while the vaccination rate ranges from 0 to 1, as we aim to investigate different levels of vaccination rates. The vaccine waning rate is estimated as 0.00190 per day (full derivation shown in Section S3 of the Supplementary material).

2.5. Model flowchart and system of equations

The flowchart diagram of our model is shown in Fig. 4, and the complete set of equations for system (17) is given.

$$\begin{aligned}
\text{Mosquitoes:}\quad & \begin{cases}
\frac{dL_M}{dt} &= \left[(1-\boldsymbol{u_1})b_L(T)\delta_M N_M - (\mu_L + \boldsymbol{u_1} + \boldsymbol{u_2})L_M\right] \\
&\quad \times \left[1 - \frac{L_M}{K_M}\right] - b_M(T)L_M, \\
\frac{dS_M}{dt} &= b_M(T)L_M - [\lambda_{BM}(T) + \mu_M(T) + \boldsymbol{u_3}]S_M, \\
\frac{dE_M}{dt} &= \lambda_{BM}(T)S_M - [\gamma_M(T) + \mu_M(T) + \boldsymbol{u_3}]E_M, \\
\frac{dI_M}{dt} &= \gamma_M(T)E_M - [\mu_M(T) + \boldsymbol{u_3}]I_M,
\end{cases} \\
\text{Birds:}\quad & \begin{cases}
\frac{dS_B}{dt} &= b_B\left[1 - \frac{N_B}{K_B}\right]N_B - \left[\lambda_{MB}(T) + \mu_B\right]S_B, \\
\frac{dE_B}{dt} &= \lambda_{MB}(T)S_B - [\gamma_B + \mu_B]E_B, \\
\frac{dI_B}{dt} &= \gamma_B E_B - [\alpha_B + \mu_B]I_B, \\
\frac{dR_B}{dt} &= (1-\nu_B)\alpha_B I_B - \mu_B R_B, \\
\frac{dD_B}{dt} &= \alpha_B \nu_B I_B,
\end{cases} \\
\text{Humans:}\quad & \begin{cases}
\frac{dS_H}{dt} &= b_H N_H - (1-\boldsymbol{x})\lambda_{MH}(T)S_H - \mu_H S_H, \\
\frac{dE_H}{dt} &= (1-\boldsymbol{x})\lambda_{MH}(T)S_H - (\mu_H + \gamma_H)E_H, \\
\frac{dI_H}{dt} &= \gamma_H E_H - (\alpha_H + \mu_H)I_H, \\
\frac{dR_H}{dt} &= (1-\nu_H)\alpha_H I_H - \mu_H R_H, \\
\frac{dD_H}{dt} &= \nu_H \alpha_H I_H, \\
\frac{d\boldsymbol{x}}{dt} &= \kappa \boldsymbol{x}(1-\boldsymbol{x})\left[-1+\omega I_B\right],
\end{cases} \\
\text{Equids:}\quad & \begin{cases}
\frac{dS_E}{dt} &= b_E N_E + \omega_E V_E - \lambda_{ME}(T)S_E - (\mu_E + \boldsymbol{\theta_E})S_E, \\
\frac{dV_E}{dt} &= \boldsymbol{\theta_E} S_E - (\omega_E + \mu_E)V_E - (1-c_E)\lambda_{ME}(T)V_E, \\
\frac{dE_E}{dt} &= \lambda_{ME}(T)S_E + (1-c_E)\lambda_{ME}(T)V_E - [\gamma_E + \mu_E]E_E, \\
\frac{dI_E}{dt} &= \gamma_E E_E - [\alpha_E + \mu_E]I_E, \\
\frac{dR_E}{dt} &= (1-\nu_E)\alpha_E I_E - \mu_E R_E, \\
\frac{dD_E}{dt} &= \nu_E \alpha_E I_E,
\end{cases}
\end{aligned} \tag{17}$$

with $N_M = L_M + S_M + E_M + I_M$, $N_B = S_B + E_B + I_B + R_B$, $N_H = S_H + E_H + I_H + R_H$, $N_E = S_E + V_E + E_E + I_E + R_E$. Initial values used and a summary of the description of the state variables are shown in Table (S1) of the Supplementary material, while parameter values are summarised in Table 2.

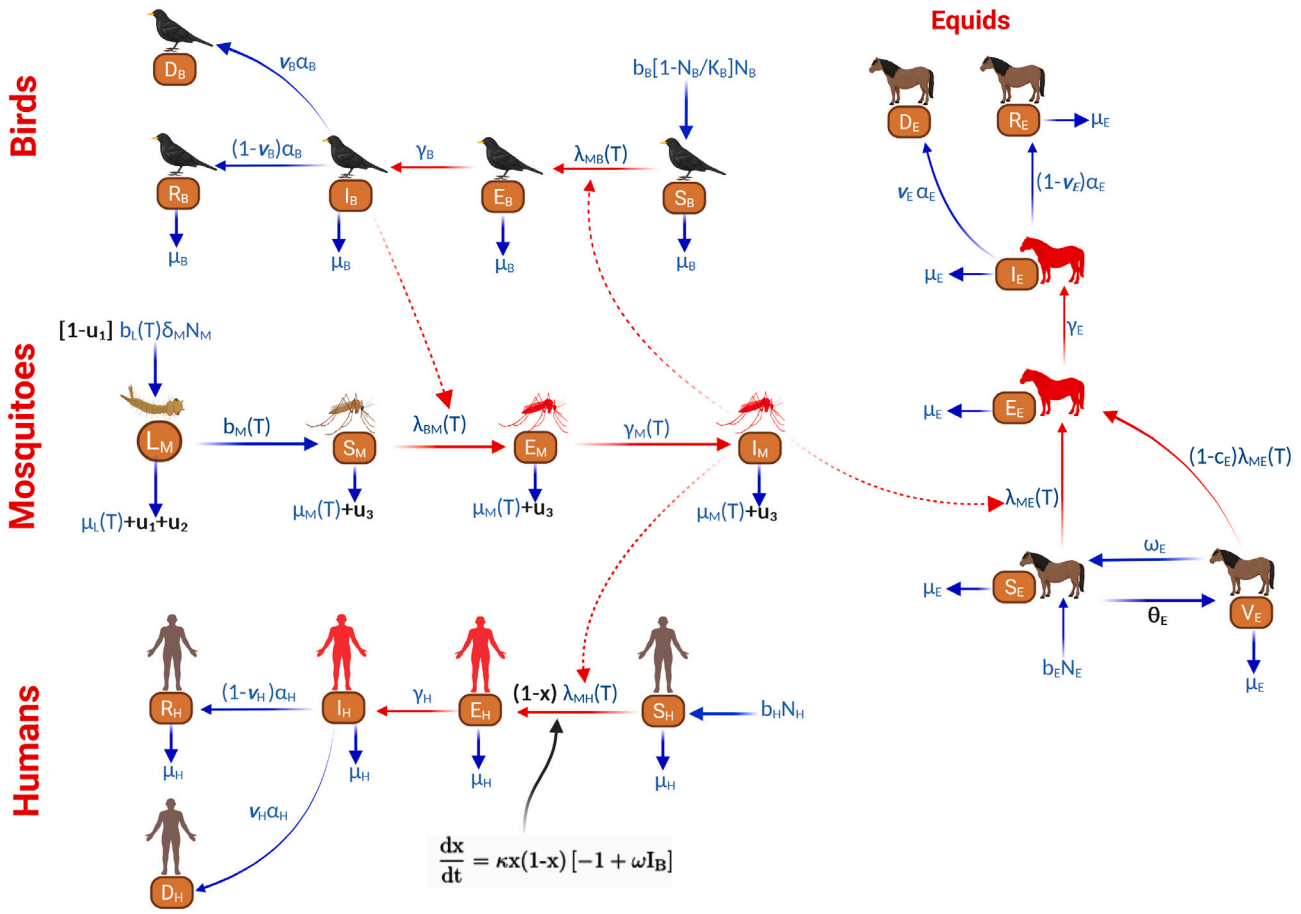


Fig. 4. Flow chart diagram for the process-based model of WNV with control interventions in bold black colour. Red arrows and compartments indicate infected classes. Diagram created in BioRender with license Arbovirologie (2026) (https://BioRender.com/8a0gfj1). Content not licensed under the Creative Commons Attribution (CC BY) license.

3. Methods

A global sensitivity analysis was conducted to evaluate the influence of control parameters on WNV transmission dynamics. Sensitivity indices were determined using the Partial Rank Correlation Coefficient (PRCC) method (Blower and Dowlatabadi, 1994; Marino et al., 2008), which measures the strength of monotonic relationships between model inputs and outputs. Parameter values were sampled via Latin Hypercube Sampling, a stratified Monte Carlo technique, with 1000 simulations per run (Fig. 7).

The model was then simulated for the period 2018–2025 using temperature data derived from the ERA5-Land Monthly Averaged Data from 1950 to Present for Berlin, obtained through the Copernicus Climate Data Store (CDS) (S.J., 2019) (Figs. 5(a)–5(c)). The data were first interpolated to daily resolution to provide temperature inputs for the model's temperature-dependent parameters, aligning with the solver's daily time step. Linear interpolation along the temporal dimension was performed using `xarray.interpolate_na()` function in Python (Hoyer and Hamman, 2017). Model solutions were scaled to the observed data, and Spearman's correlation coefficient was calculated between the monthly observed and simulated time series for each year to assess the similarity in seasonal epidemic dynamics.

Control parameters were varied within their reasonable ranges to examine the impact of increased interventions on WNV dynamics. To explore different control scenarios, an interactive web-based Shiny application was developed to enable users to test different combinations of intervention strategies and their epidemiological outcomes in real time. Firstly, climate projections from the CMIP6 dataset in the CDS (Copernicus Climate Change Service, 2021) were used to simulate the model for the years 2026–2046. Three shared socioeconomic pathway scenarios were considered, i.e., SSP1-2.6, SSP2-4.5, and SSP5-8.5, representing low, intermediate, and high greenhouse gas emission factors. These scenarios were included, to assess how different climate predictions may influence temperature-driven WNV dynamics, which has an impact on control intensity and timing. For each SSP scenario, controls can be implemented over user-defined time intervals and explored under each scenario. Our application was implemented using the `RShiny` package in R (Chang et al., 2025), and is freely available as a free open-source tool at or via the link: https://zero-west-nile-virus.bnitm.de/.

In the app, users can specify the simulation period, and the start and end dates for implementing the controls (default: 1 January 2026 to 31 December 2046), and run the model by clicking the ▶ button. The model is then solved dynamically, and simulations of infectious mosquitoes and birds, humans, and equids are immediately displayed. A 10% threshold, defined as 10% of the maximum simulated value for each compartment, is included to help users explore intervention combinations that lower epidemic curves below this level.

Table 1
Interpretation of the weight parameters and control costs in the objective functional, and their assumed values.

Parameter	Description	Interpretation	Value
A_1	Weight associated with mosquito larvae (L_M)	Represents the epidemiological cost associated with high mosquito larval abundance.	0.0001/max(LM)
A_2	Weight associated with adult mosquito population (N_M)	Represents the epidemiological cost associated with the large number of adult mosquitoes that influence WNV transmition.	0.0001/max(NM)
A_3	Weight associated with infectious birds (I_B)	Represents the epidemiological cost of WNV infection in birds.	0.1/max(IB)
c_1	Cost coefficient for breeding-site removal (u_1)	Represents the economic and operational costs associated with environmental management interventions such as habitat modification and removal of standing water.	50
c_2	Cost coefficient for larviciding (u_2)	Represents the cost associated with the application of larval control measures.	50
c_3	Cost coefficient for adult mosquito control (u_3)	Represents the economic and operational cost of adult mosquito control measures.	10^4

To determine the necessary conditions for the optimal timing and effort level of mosquito controls under temperature forcing, an optimal control framework was formulated. For this, an objective functional (Eq. (18)) was defined to minimise both the eco-epidemiological burden of WNV and the economic costs associated with implementing mosquito control over a 24-month period. This functional penalises high mosquito abundance (both larval and adults) and bird infections while also accounting for the costs of applying control strategies. The objective functional (Eq. (18)) integrates three components: mosquito larvae, adult population, and infectious birds, together with quadratic costs associated with the three control measures: breeding-site removal (u_1), larviciding (u_2), and adult mosquito control (u_3). Such a formulation helps us understand the necessary conditions under which mosquito control is most effective, based on temperature predictions, thereby minimising mosquito larvae, adult mosquitoes, and infectious bird populations at the minimum possible cost. The optimal control problem was formulated using Pontryagin's Maximum Principle (Pontryagin, 1987), which introduces adjoint (costate) equations associated with the state variables by minimising the objective functional:

$$J = \int_0^{T_F} A_1 L_M + A_2 N_M + A_3 I_B + \frac{1}{2}\left[c_1 u_1^2(t) + c_2 u_2^2(t) + c_3 u_3^2(t)\right]\, dt, \quad (18)$$

subject to the state system (17), without dead-end hosts, and the admissible control set

$$\mathcal{U} = \left\{(u_1(t), u_2(t), u_3(t)) : 0 \le u_i(t) \le 0.5,\ t \in [0, T_F],\ i = 1, 2, 3\right\}.$$

Here, A_1, A_2, A_3 are normalised weight constants of the state variables, while c_1, c_2, c_3 are cost coefficients associated with the control variables, whose values are defined in Table 1. The functions $u_1(t), u_2(t), u_3(t)$ represent bounded Lebesgue measurable controls on the interval $[0, T_F]$, with T_F indicating the terminal time of controls. An upper bound of 0.5 was imposed on the control functions, assuming that the interventions may not be fully effective (Blayneh et al., 2010). The full derivation and proof are provided in Section S6 of the Supplementary material. The optimal control problem was then solved numerically using the forward–backward sweep method (Lenhart and Workman, 2007; Rodrigues et al., 2014), where the state system (17) was solved forward in time and the co-state system (S6 in the Supplementary material) backward in time using a forward Euler scheme, together with the control characterisations (Eq. (19)), until convergence. A_1, A_2, A_3 were normalised using maximum values from the uncontrolled simulation, and their values chosen such that $A_1 > A_2;\ A_1,\ A_2 < A_3$, indicating that reducing infectious birds is more important than reducing mosquito abundance. Similarly, the cost coefficients c_1, c_2, c_3 are such that $c_3 > c_1, c_2$, reflecting the very high costs associated with adult control methods compared to larviciding and breeding site removal (Table 1).

4. Results

4.1. Model fit

The observed data used in this study are very sparse because no systematic WNV surveillance was conducted in Germany during the study period. As a result, reported cases are sporadic and unevenly distributed over time. To enable a meaningful comparison between the model results and observations, both the simulated and observed data were aggregated into monthly totals to minimise daily fluctuations and highlight the overall seasonal patterns of WNV transmission (Laperriere et al., 2011; Rubel et al., 2008).

4.2. Sensitivity analysis of the control variables

Sensitivity analysis was performed to assess the contribution of each control parameter to the host populations (Fig. 7). Negative PRCC values indicate that increasing the control effort is associated with a decrease in the corresponding infectious/infected host population. Conversely, positive PRCC values indicate that increasing the control effort increases the infected host population (Marino et al., 2008).

4.3. Behavioural dynamics of PPE adoption

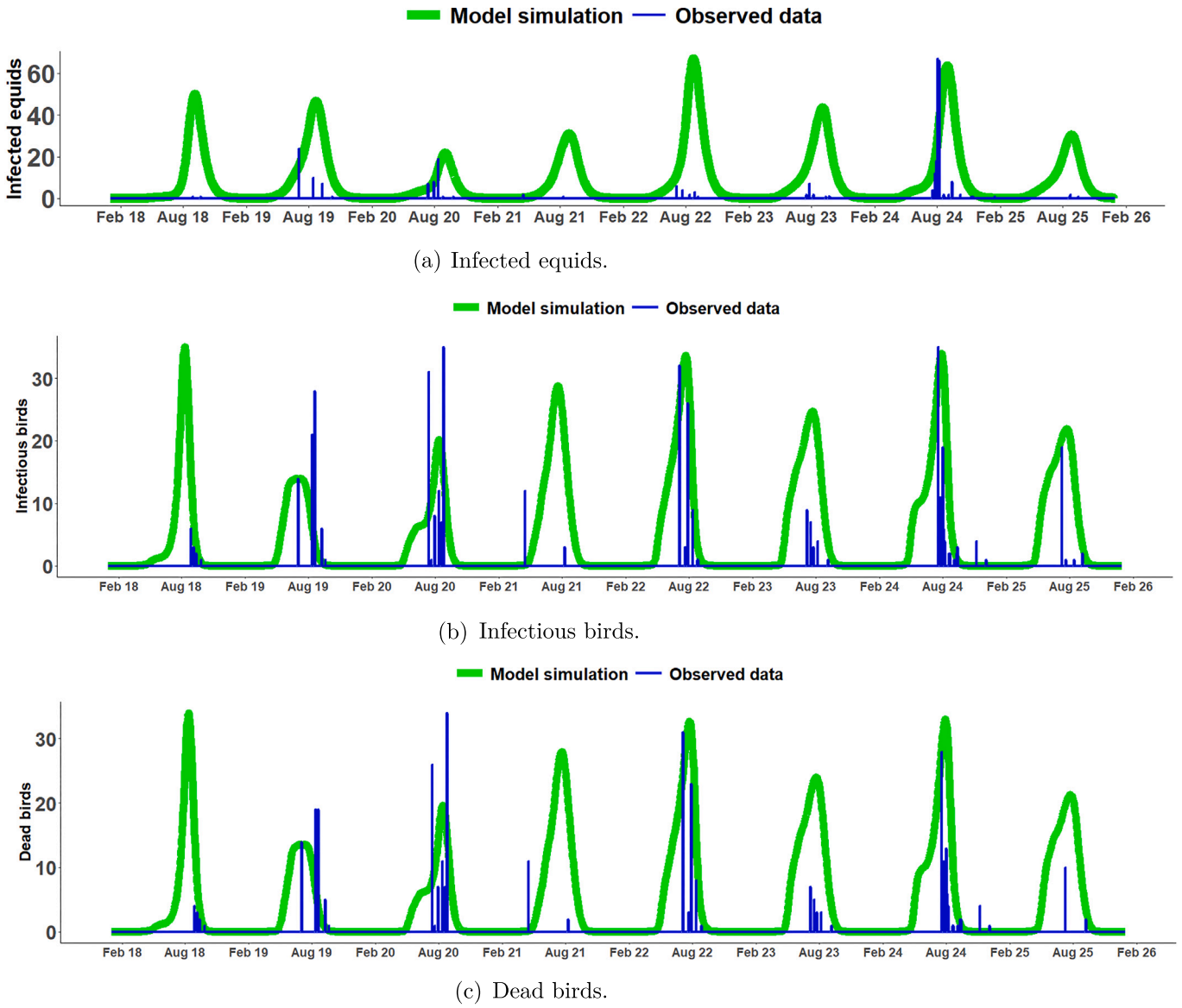
Human adoption of PPE was examined in relation to WNV prevalence in birds (Fig. 8). The parameter ω, which represents the sensitivity of human behavioural response to increases in the infectious bird population, was varied such that PPE adoption begins to increase when $I_B > \frac{1}{\omega}$. Simulations were performed for $\kappa = 4 \times 10^{-4}$ and $\omega = 0.001,\ 0.005,\ 0.008$. These values correspond to behavioural response thresholds of approximately 1000, 200, and 125 infectious birds, respectively. Smaller values of ω therefore represent a delayed behavioural response, in which PPE adoption occurs only when the outbreak becomes relatively large, whereas larger values represent earlier adoption of PPE as the infectious bird population begins to rise.

4.4. Impact of vaccinating equids

The effect of the vaccination rate on WNV control was assessed by varying the vaccination rate between 0 and 1 (Fig. 9).

4.5. Optimal control problem

The control functions for the optimal control problem were derived analytically using Pontryagin's Maximum Principle, together with the characterisation and adjoint system (Section S6 of the Supplementary material). Simulations (Fig. 10) indicate that intervention efforts are concentrated early in the transmission season. Breeding site removal



(a) Infected equids.

(b) Infectious birds.

(c) Dead birds.

Fig. 5. Temporal dynamics of WNV compared to the observed cases for the period 2018–2025.

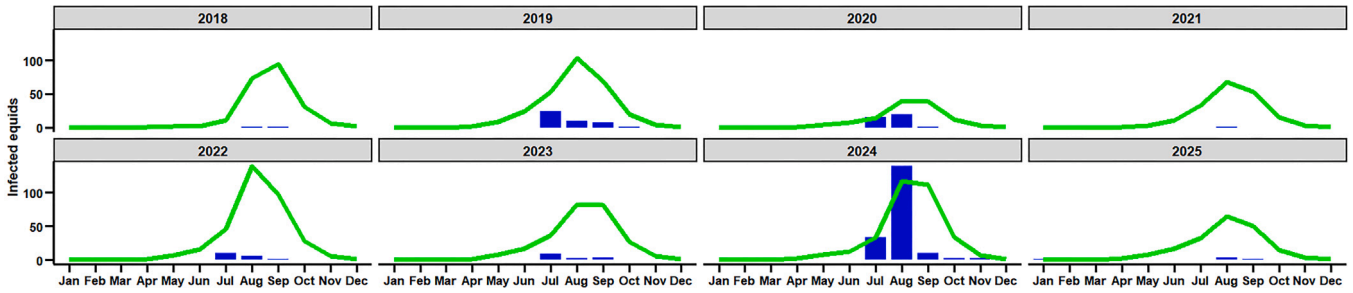
and larviciding and adult control reach their maximum peak values on 11 May, 10 May and 24 April of the first year of simulation (Fig. 10), respectively. In contrast, the peak number of infectious birds occurs later on 13 August. Thus, the maximum effect of control by breeding-site removal occurs approximately 13 weeks before the peak in infectious birds. Given that the objective was to minimise mosquito populations and infectious birds, while penalising adulticiding, the average control intensities remained relatively low throughout the season (with $\bar{u}_1 = 0.0031$, $\bar{u}_2 = 0.0024$, $\bar{u}_3 = 0.00059$), highlighting that the optimal control strategy relies mainly on breeding site removal and larviciding, while the adult control is applied only at lower levels.

$$\begin{cases} u_1^\star(t) = \min\left\{0.5, \max\left\{0, \dfrac{(b_L\delta_M N_M + L_M)(1 - L_M/K_M)\lambda_1}{c_1}\right\}\right\}, \\ u_2^\star(t) = \min\left\{0.5, \max\left\{0, \dfrac{L_M(1 - L_M/K_M)\lambda_1}{c_2}\right\}\right\}, \\ u_3^\star(t) = \min\left\{0.5, \max\left\{0, \dfrac{S_M\lambda_2 + E_M\lambda_3 + I_M\lambda_4}{c_3}\right\}\right\}, \end{cases} \tag{19}$$

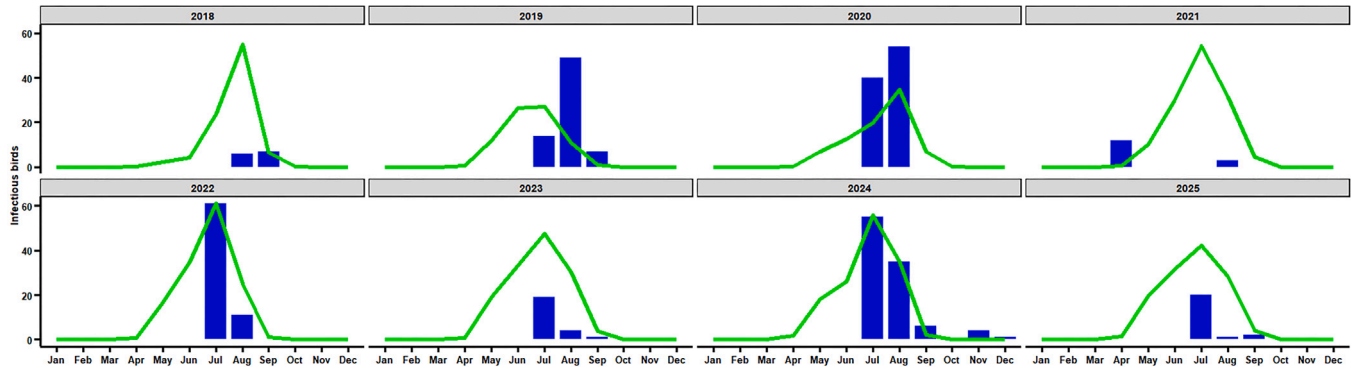
5. Discussion and conclusions

We investigated the impact of different control measures against WNV. We adapted the model originally developed by Rubel et al. (2008) to describe the dynamics of Usutu virus in Austria and later extended by Laperriere et al. (2011) to capture the transmission dynamics of WNV among birds, humans, and equids. Recent advances in interdisciplinary research have enabled the incorporation of human behavioural responses into epidemiological models. In particular, we modelled the adoption of PPE using imitation dynamics derived from evolutionary game theory (Bauch, 2005). This framework allows the integration of mosquito ecology, epidemiological dynamics, and human behavioural responses, while accounting for factors such as perceived inconvenience, limited awareness, or misinformation that may reduce the willingness to adopt protective measures.

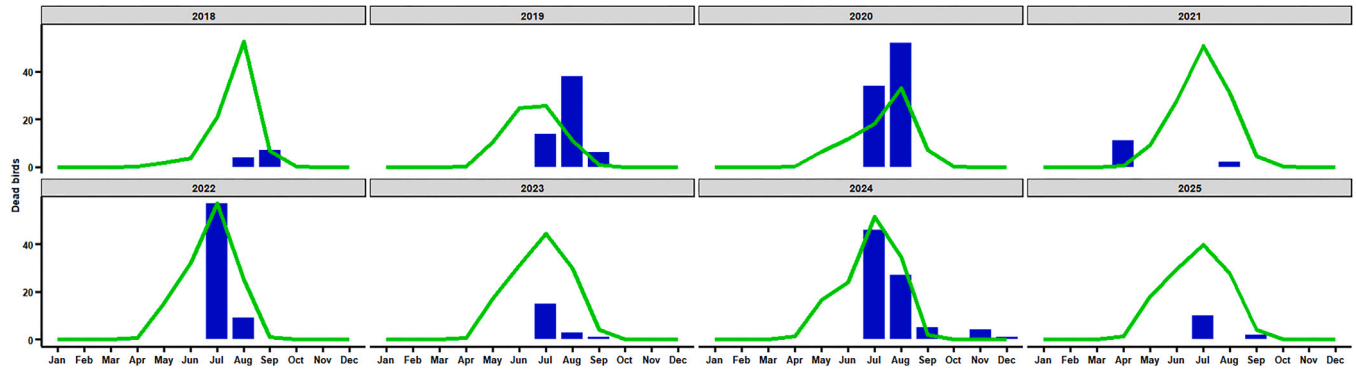
Using temperature data for Berlin, we simulated the population dynamics of infectious birds, dead birds and infected equids, for the period 2018–2025 (Fig. 5). Our model accurately predicted the known seasonal pattern for WNV dynamics in temperate regions. Some years



(a) Infected equids ($\rho = 0.63$).



(b) Infectious birds ($\rho = 0.53$).



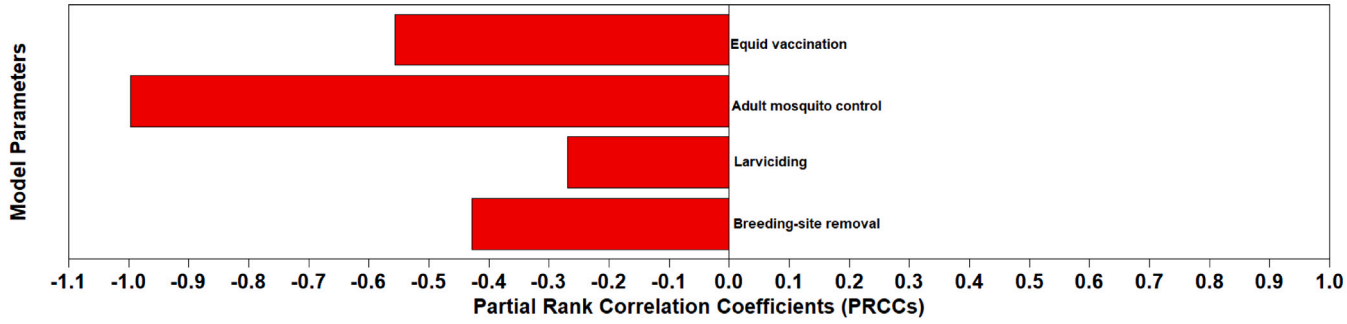
(c) Dead birds ($\rho = 0.52$).

Fig. 6. Temporal comparison of observed and simulated WNV infections in birds (2018–2025). Blue bars show monthly observed cases, while the green line represents the corresponding monthly model simulations.

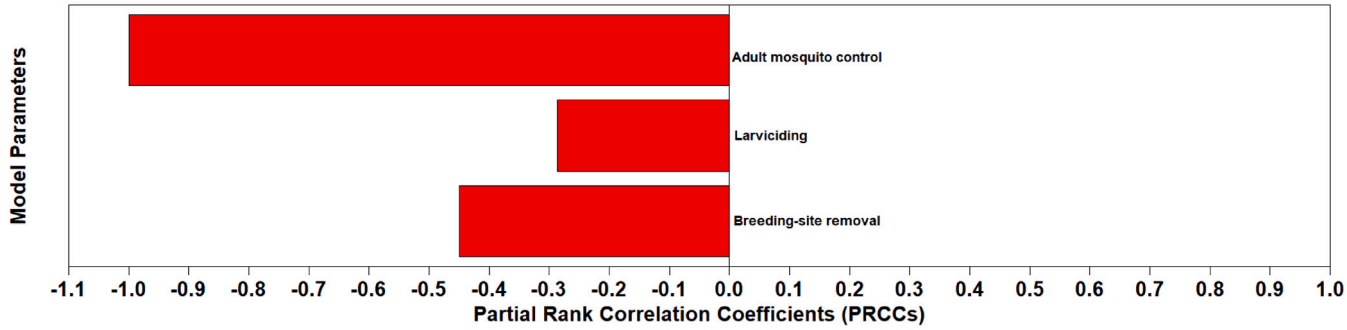
had more cases than others, highlighting the impact of seasonal variation in yearly temperatures. To assess the model's performance, monthly averaged predictions were compared with observed surveillance data over the study period (Fig. 6). The model successfully reproduced the seasonal dynamics of WNV transmission, capturing the overall seasonal timing and monthly peaks of occurrences. Particularly in 2020 and 2022–2025, the model correctly identified peak months for both infectious and dead birds, yielding average Spearman correlation coefficients of 0.53 and 0.52, respectively, between observed and predicted seasonal patterns. For equids, the model identified the July peak in 2020 and the August peaks in 2024 and 2025, yielding $\rho = 0.63$ for the overall WNV dynamics. Although agreements are evident in some years, discrepancies between observed and predicted patterns may partly be attributed to the lack of systematic WNV surveillance in Germany.

We explored different levels of individuals' reactions to disease prevalence in birds (ω) and how these influence PPE adoption and WNV infections in humans (Fig. 8). The simulations show that when individuals adopt PPE promptly following reports of WNV cases in birds, the number of human infections can be substantially reduced (Section 4.3). In particular, when individuals respond quickly to increases in WNV prevalence in birds (larger ω), PPE adoption occurs earlier and reduces spillover transmission to humans. This result is consistent with several studies indicating that WNV infections in mosquitoes and amplifying hosts are typically detected at least two weeks before human cases are reported (Angelini et al., 2010; Petrović et al., 2018; Veksler et al., 2009). Conversely, delayed responses (smaller ω) prolong periods of unprotected human exposure to infectious mosquitoes before protective behaviour increases, leading to higher numbers of human infections. This result further highlights the importance of early risk communication based on bird surveillance, which can encourage the timely adoption of PPE and reduce human infections.

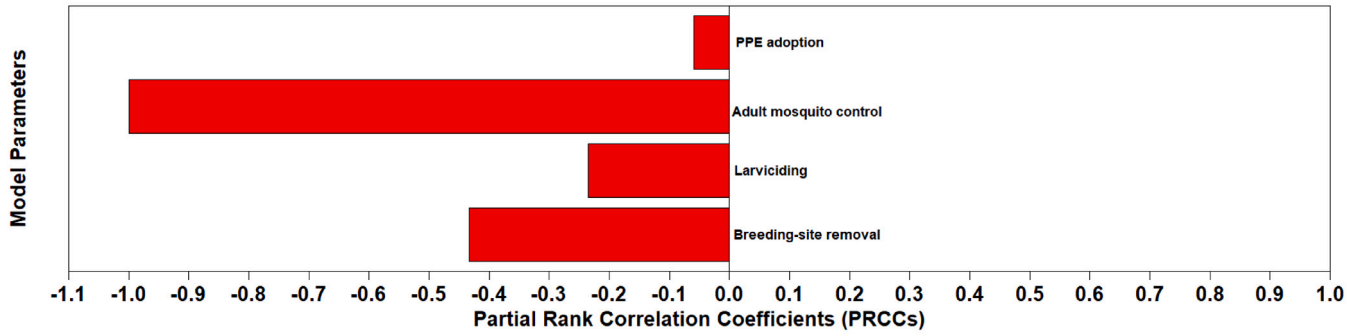
Simulations of equid vaccination indicate that increasing the vaccination rate leads to a substantial reduction in WNV infections among equids. As shown in Fig. 9, higher vaccination rate results in a decline in the number of infected equids. However, even at relatively high



(a) PRCC values for WNV-infected equids.



(b) PRCC values for infectious birds.



(c) PRCC values for WNV-infected humans.

Fig. 7. Tornado plots showing the PRCC values for the control variables of the population dynamics of WNV infectious birds, WNV infected humans, and WNV infected equids.

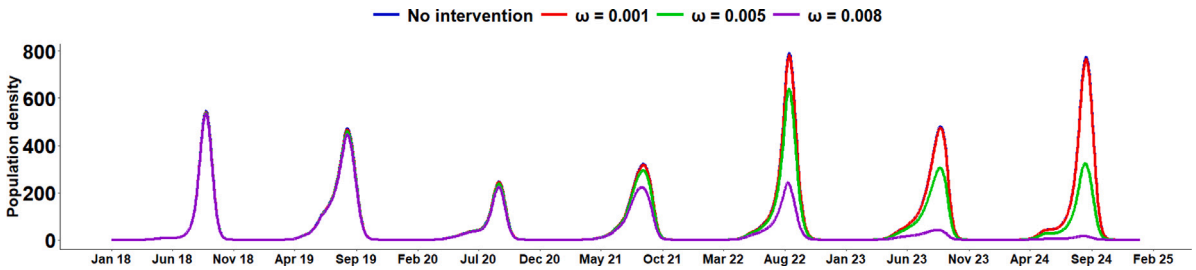


Fig. 8. Population of infected humans for different values of the parameter ω, representing the sensitivity of human behavioural response to WNV prevalence in birds.

vaccination rates, the vaccine alone may not eliminate equid infections completely as some vaccines mainly reduce the number of viremic horses, duration and severity of clinical signs and WNV-mortality (Bowen et al., 2014). Indeed, when vaccination is complemented with mosquito-reduction strategies (mosquito reduction methods + equid vaccination in the control app), the model with interventions predicts a larger decline in equid infections, a result supported by Cendejas and Goodman (2024).

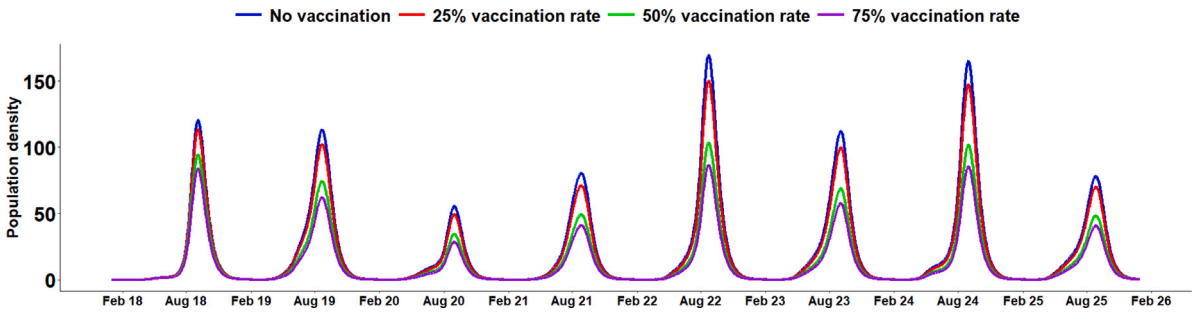
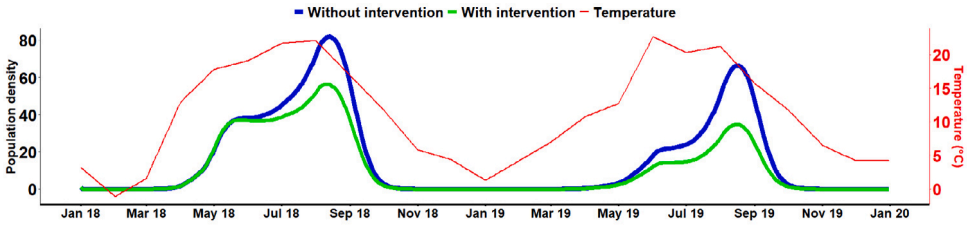
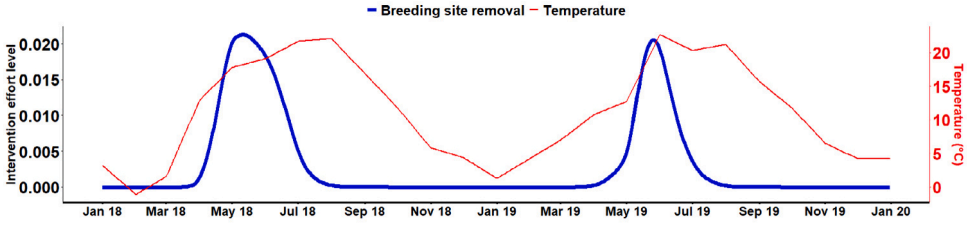


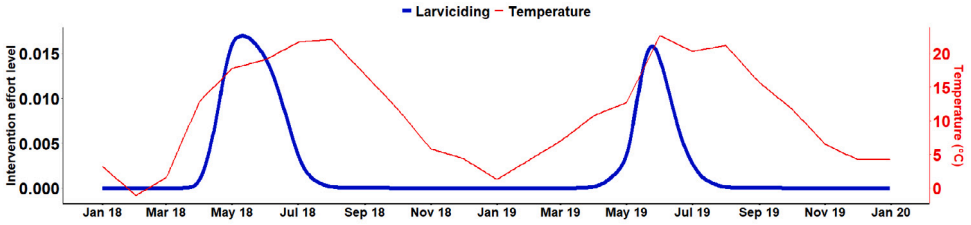
Fig. 9. Population dynamics of infected equids under different vaccination rates. The blue curve represents the scenario without vaccination. The red, green, and purple curves correspond to annual vaccination rates of 25%, 50%, and 75%, implemented as daily rates of 0.25/365, 0.5/365, and 0.75/365, respectively.



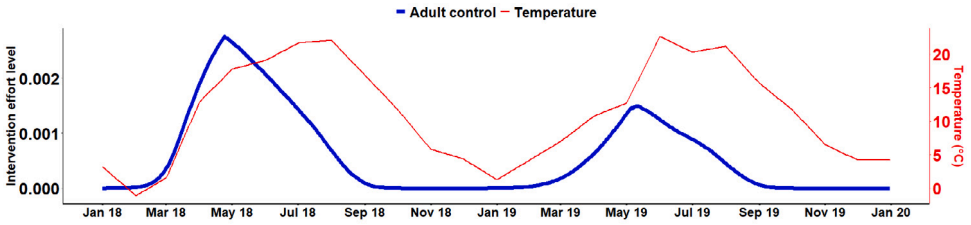
(a) Infectious birds with and without interventions.



(b) Physical removal and destruction of potential mosquito breeding sites (u_1).



(c) Larviciding (u_2).



(d) Adult control (u_3).

Fig. 10. Simulation of the infectious bird population compared to the control profile.

Sensitivity analysis of the seasonal recruitment function revealed that the simulated epidemic dynamics were better reproduced for values of p close to one (Fig. 3). This suggests that recruitment functions with a temporal timing and magnitudes similar to those observed for northern goshawks may produce epidemic patterns that more closely match the observed dynamics. Importantly, this result does not imply that northern goshawks dominate the avian community, but instead demonstrates how recruitment timing and magnitude shape the availability of susceptible hosts.

Results from the sensitivity analysis of the control parameters (Fig. 7) indicate that the most effective control method is the use of adult controls, as it yields the highest PRCC values across all hosts. This result

is consistent with the conclusion of Bowman et al. (2005), who stated that on average adult control methods such as adulticiding are more effective at preventing WNV spread in humans than personal protection. Breeding site removal follows on the list. Larviciding and PPE are also negatively correlated with the infected human population, highlighting that larviciding with perfect seasonal timing is highly effective, as also indicated by Abdelrazec et al. (2015). The adoption of PPE by humans reduces the population of infected humans, further complementing mosquito control efforts. On the other hand, vaccination of equids is also highly negatively correlated with the population of infected equids, indicating the need to intensify vaccination campaigns and efforts to curb WNV infections in equids.

Temperature fluctuations may also have economic implications, as larger outbreaks may require increased resources for control, whereas smaller outbreaks may require comparatively fewer resources (Barber et al., 2010). For this reason, an optimal control problem that considers temperature- time-dependent controls was studied. Results obtained suggest that breeding site removal and larviciding started before 1 April, aligning with rising spring temperatures, and maximised around 11 May, may have the potential to reduce the August peak in bird infections. Because the optimal controls reach their highest levels several weeks before the peak in infectious birds, the model results indicate that preventive measures may be implemented well before the epidemic peak, when mosquito populations begin to increase. This aligns with the suggestions from the European Centre for Disease Prevention and Control (2023), of preventively applying mosquito control methods before and during the transmission season, while starting awareness campaigns and other protective measures at the start of the WNV transmission season. On the other hand, adult control methods such as modifying overwintering sites may be implemented earlier (before March). While this result is theoretical, it is supported by other modelling studies, including Fesce et al. (2025) and Thomas et al. (2009). However, it should be noted that some adult mosquito control methods, such as winter adulticiding, are not yet well-established and may raise questions regarding their practical feasibility; therefore, further research is needed to evaluate their applicability. Additionally, this analysis indicates that temperature monitoring and forecasts can act as early warning indicators for the timely deployment of control measures.

Finally, a Shiny application was developed to explore the potential impact of future climate projections on WNV transmission and control. The app enables users to evaluate various intervention strategies under different climate scenarios without requiring mathematical/computational skills, thereby supporting climate-informed surveillance and control planning. Users can define the start and end of both the simulation and the control implementations. From the app, users can explore the effects of different control combinations at different time periods. Explorations indicate that although interventions reduce early-season transmission, they may also delay the epidemic peak within the same period. This occurs because early control suppresses infections and preserves a larger susceptible population, which can enable a later resurgence once interventions end and environmental conditions remain favourable for transmission. These rebound dynamics can be seen in the app, and they are mainly because, in uncontrolled scenarios, high infection levels naturally decrease the number of susceptible hosts, whereas control measures reduce infections and preserve a larger susceptible population. A similar pattern occurs in host species, given that infected birds often die from WNV, whereas humans and equids typically recover with prolonged immunity (Papa et al., 2011; Tolnai et al., 2025).

Mosquito reduction methods alone may not fully reduce the risk of arbovirus transmission, but they remain important for suppressing WNV risk across different host groups. To complement them, an integrated approach that combines mosquito control methods, human PPE adoption, and equid vaccination may be the best strategy to reduce the WNV burden in humans and equids. For bird infections, more research is still needed to determine which methods can complement mosquito reduction efforts to lower infection rates. A study by Malik (2018) provided a theoretical framework that considers bird vaccination and other methods to reduce contact between mosquitoes and birds, as birds are the amplifying hosts of WNV. This suggests that mosquito reduction efforts remain an important strategy for disrupting the WNV transmission cycle.

Our WNV control model can be further improved in the future, e.g., by considering other mosquito control efforts, such as the use of modified mosquitoes, including sterile insect techniques and *Wolbachia* mosquitoes (Atyame et al., 2015; Lees et al., 2015). Furthermore, other environmental factors, such as precipitation, wind speed, and direction, can be incorporated to support temperature in long term predictions under climate change (Bhowmick et al., 2025; Mbaoma et al., 2024). In recent years, advanced epidemiological modelling approaches, including system identification techniques and artificial intelligence-based adaptive policy frameworks, have been developed to improve the prediction and control of epidemic outbreaks (Farooq et al., 2022; Tutsoy, 2021). These approaches support the growing role of data-driven methods in complementing traditional mechanistic epidemic models, and this forms a possible direction for the extension of this work.

6. Limitations of the study

The lack of a system surveillance for WNV in Germany limits the reliability of observed cases. For model fitting, we relied on the WNV data from World Organisation for Animal Health (WOAH) (2018 - 2025), which are spatially and temporally sparse and subject to under-reporting, particularly regarding the large proportion of asymptomatic cases, resulting in incomplete detection of local WNV activity. In a real-world situation, uncertainty is a natural part of epidemiological modelling. It can range from incomplete knowledge of model parameters (parametric uncertainty), assumptions made in the model structure, and external factors like climate variability. Both the size and form of these uncertainties is often unknown, and hence, they must be taken into account when interpreting model predictions (He et al., 2009; King et al., 2015; Li et al., 2024). Moreover, our WNV control strategies are scenario-based. Thus, due to the absence of field-tested intervention data in Germany, the study aims to provide a qualitative assessment of some of the available WNV control strategies.

CRediT authorship contribution statement

Pride Duve: Writing – review & editing, Writing – original draft, Validation, Methodology, Formal analysis, Conceptualization. **Felix Gregor Sauer:** Writing – review & editing, Supervision, Methodology, Conceptualization. **Renke Lühken:** Writing – review & editing, Supervision, Methodology, Conceptualization.

Declaration of competing interest

All authors declare that they have no competing interests.

Acknowledgements

The authors would like to thank the Federal Ministry of Education and Research of Germany (BMBF), Germany under the project NEED (Grant Number 01Kl2022), the Federal Ministry for the Environment, Nature Conservation, Germany, Nuclear Safety and Consumer Protection, Germany (Grant Number 3721484020), and the German Research Foundation (JO 1276/51) for funding this project. Moreover, the authors would like to thank Markus Jansen for his support in running our app in a Docker container on the BNITM website.

Table 2
Definition of parameters used in system (17).

Parameter	Definition	Value	Source
$\delta_M(D)$	fraction of non-overwintering mosquitoes	Eq. (1)	Rubel et al. (2008)
$b_L(T)$	birth rate of mosquito larvae	Eq. (2)	Rubel et al. (2008)
$\mu_L(T)$	mortality rate of mosquito larvae	Eq. (3)	Rubel et al. (2008)
$b_M(T)$	birth rate of adult mosquitoes	Eq. (4)	Rubel et al. (2008)
$k(T)$	mosquito biting rate	Eq. (5)	Rubel et al. (2008)
$\lambda_{BM}(T)$	force of infection on mosquitoes	Eq. (6)	Rubel et al. (2008)
$\mu_M(T)$	mortality rate of adult mosquitoes	Eq. (7)	Rubel et al. (2008)
$\gamma_M(T)$	latency rate of mosquitoes	Eq. (8)	Rubel et al. (2008)
p_M	transition probability by infectious mosquitoes	1.0	Laperriere et al. (2011)
K_M	carrying capacity of mosquito population	3,300,000	Laperriere et al. (2011)
$N_{V\,min}$	minimum number of adult mosquitoes	500,000	Laperriere et al. (2011)
b_B	crude per-capita daily recruitment rate of susceptible birds	Eq. (11)	defined by the authors
μ_B	crude per-capita natural mortality rate of birds	0.0005	Mbaoma et al. (2024)
γ_B	latency rate of birds	0.196	Mbaoma et al. (2024)
$\lambda_{MB}(T)$	force of infection on birds	Eq. (12)	Rubel et al. (2008)
ϕ_B	mosquito to bird ratio	50–300	defined by the authors
ν_B	proportion of infectious birds that die due to WNV	0.655	Mbaoma et al. (2024)
α_B	removal rate of infectious birds	0.867	Mbaoma et al. (2024)
p_B	transition probability by infectious birds	0.125	Laperriere et al. (2011)
K_B	carrying capacity of bird population	1,159,340	defined by the authors
b_H	recruitment rate of susceptible humans	0.0000452	defined by the authors
μ_H	natural mortality rate of humans	0.0000287	defined by the authors
γ_H	latency rate of humans	0.25	Laperriere et al. (2011)
$\lambda_{MH}(T)$	force of infection on humans	Eq. (15)	Laperriere et al. (2011)
ϕ_H	mosquito to human ratio	0.3–3	defined by the authors
ν_H	proportion of infected humans that die due to WNV	0.004	Laperriere et al. (2011)
α_H	removal rate of infected humans	0.5	Laperriere et al. (2011)
κ	imitation rate	0.00001	defined by the authors
ω	individuals' sensitivity to the WNV prevalence in birds	varies	defined by the authors
b_E	birth rate of susceptible equids	0.00016	Laperriere et al. (2011)
μ_E	natural mortality rate of equids	0.00011	Laperriere et al. (2011)
γ_E	latency rate of equids	0.05	Laperriere et al. (2011)
$\lambda_{ME}(T)$	force of infection on equids	Eq. (16)	Laperriere et al. (2011)
ϕ_E	mosquito to equid ratio	3	defined by the authors
ν_E	proportion of infected equids that die due to WNV	0.04	Laperriere et al. (2011)
α_E	removal rate of infected equids	0.2	Laperriere et al. (2011)
θ_E	vaccination rate of equids	[0–1]	defined by the authors
ω_E	vaccine waning rate	0.0019	defined by the authors
c_E	vaccine effectiveness	0.5	defined by the authors
u_1	removal and destruction of potential mosquito breeding sites	varies	defined by the authors
u_2	larvicides	varies	defined by the authors
u_3	adult control	varies	defined by the authors

Appendix A. Supplementary data

Supplementary material related to this article can be found online at https://doi.org/10.1016/j.ecolmodel.2026.111605.

Data availability

The cleaned West Nile virus data and the code for our app are freely available at https://github.com/Pride1234/West-Nile-virus-control. The original datasets can be requested from the World Organisation for Animal Health (WOAH) (2018 - 2025) website.

References

Abdelrazec, Ahmed, Lenhart, Suzanne, Zhu, Huaiping, 2015. Dynamics and optimal control of a west nile virus model with seasonality. Can. Appl. Math. Q. 23 (4), 12–33.

Amt für Statistik Berlin-Brandenburg, 2024. Berlin population 2024. URL https://www.statistik-berlin-brandenburg.de/bevoelkerung.

Amt für Statistik Berlin-Brandenburg, 2025a. Geburten, Sterbefälle und Eheschließungen in Berlin und Brandenburg. URL https://www.statistik-berlin-brandenburg.de/a-ii-1-j.

Amt für Statistik Berlin-Brandenburg, 2025b. Migration statistics 2024 Berlin – migration gains for the capital. URL https://www.statistik-berlin-brandenburg.de/106-2025.

Andreadis, S.S., Dimotsiou, O.C., Savopoulou-Soultani, M., 2014. Variation in adult longevity of *Culex pipiens f. pipiens*, vector of the West Nile virus. Parasitol. Res. (ISSN: 1432-1955) 113 (11), 4315–4319. http://dx.doi.org/10.1007/s00436-014-4152-x.

Angelini, P., Tamba, M., Finarelli, A.C., Bellini, R., Albieri, A., Bonilauri, P., Cavrini, F., Dottori, M., Gaibani, P., Martini, E., Mattivi, A., Pierro, A.M., Rugna, G., Sambri, V., Squintani, G., Macini, P., 2010. West Nile virus circulation in Emilia-Romagna, Italy: The integrated surveillance system 2009. Eurosurveillance (ISSN: 1560-7917) 15 (16), http://dx.doi.org/10.2807/ese.15.16.19547-en.

Atyame, C.M., Cattel, J., Lebon, C., Flores, O., Dehecq, J.S., Weill, M., Gouagna, L.C., Tortosa, P., 2015. *Wolbachia*-based population control strategy targeting *Culex quinquefasciatus* mosquitoes proves efficient under semi-field conditions. PLoS One (ISSN: 1932-6203) 10 (3), e0119288. http://dx.doi.org/10.1371/journal.pone.0119288.

Bakonyi, T., Haussig, J.M., 2020. West Nile virus keeps on moving up in Europe. Eurosurveillance (ISSN: 1560-7917) 25 (46), http://dx.doi.org/10.2807/1560-7917.es.2020.25.46.2001938.

Barber, L.M., Schleier, J.J., Peterson, R.K.D., 2010. Economic cost analysis of West Nile virus outbreak, Sacramento county, California, USA, 2005. Emerg. Infect. Dis. (ISSN: 1080-6059) 16 (3), 480–486. http://dx.doi.org/10.3201/eid1603.090667.

Bauch, C.T., 2005. Imitation dynamics predict vaccinating behaviour. Proc. R. Soc. B: Biological Sci. (ISSN: 1471-2954) 272 (1573), 1669–1675. http://dx.doi.org/10.1098/rspb.2005.3153.

Bellini, R., Zeller, H., Van Bortel, W., 2014. A review of the vector management methods to prevent and control outbreaks of West Nile virus infection and the challenge for Europe. Parasites & Vectors (ISSN: 1756-3305) 7 (1), 323. http://dx.doi.org/10.1186/1756-3305-7-323.

Bhowmick, S., Fritz, M.L., Smith, R.L., 2024. Host-feeding preferences and temperature shape the dynamics of West Nile virus: A mathematical model to predict the impacts of vector-host interactions and vector management on R_0. Acta Trop. (ISSN: 0001-706X) 258, 107346. http://dx.doi.org/10.1016/j.actatropica.2024.107346.

Bhowmick, S., Irwin, P., Lopez, K., Fritz, M.L., Smith, R.L., 2025. A weather-driven mathematical model of *Culex* population abundance and the impact of vector control interventions. Ecol. Informatics (ISSN: 1574-9541) 89, 103163. http://dx.doi.org/10.1016/j.ecoinf.2025.103163.

Blayneh, K.W., Gumel, A.B., Lenhart, S., Clayton, T., 2010. Backward bifurcation and optimal control in transmission dynamics of West Nile virus. Bull. Math. Biol. (ISSN: 1522-9602) 72 (4), 1006–1028. http://dx.doi.org/10.1007/s11538-009-9480-0.

Blower, S.M., Dowlatabadi, H., 1994. Sensitivity and uncertainty analysis of complex models of disease transmission: An HIV model, as an example. Int. Stat. Rev. / Rev. Int. Stat. (ISSN: 0306-7734) 62 (2), 229. http://dx.doi.org/10.2307/1403510.

Bowen, R.A., Bosco-Lauth, A., Syvrud, K., Thomas, A., Meinert, T.R., Ludlow, D.R., Cook, C., Salt, J., Ons, E., 2014. Protection of horses from West Nile virus lineage 2 challenge following immunization with a whole, inactivated WNV lineage 1 vaccine. Vaccine (ISSN: 0264-410X) 32 (42), 5455–5459. http://dx.doi.org/10.1016/j.vaccine.2014.07.093.

Bowman, C., Gumel, A., van den Driessche, P., Wu, J., Zhu, H., 2005. A mathematical model for assessing control strategies against West Nile virus. Bull. Math. Biol. (ISSN: 0092-8240) 67 (5), 1107–1133. http://dx.doi.org/10.1016/j.bulm.2005.01.002.

Cailly, P., Tran, A., Balenghien, T., L'Ambert, G., Toty, C., Ezanno, P., 2012. A climate-driven abundance model to assess mosquito control strategies. Ecol. Model. (ISSN: 0304-3800) 227, 7–17. http://dx.doi.org/10.1016/j.ecolmodel.2011.10.027.

Cendejas, P.M., Goodman, A.G., 2024. Vaccination and control methods of West Nile virus infection in equids and humans. Vaccines (ISSN: 2076-393X) 12 (5), 485. http://dx.doi.org/10.3390/vaccines12050485.

Chang, W., Cheng, J., Allaire, J.J., Sievert, C., Schloerke, B., Xie, Y., Allen, J., McPherson, J., Dipert, A., B., Borges, 2025. shiny: Web application framework for R. R package version 1.10.0.9000, https://github.com/rstudio/shiny, URL https://shiny.posit.co/.

Colpitts, T.M., Conway, M.J., Montgomery, R.R., Fikrig, E., 2012. West Nile virus: Biology, transmission, and human infection. Clin. Microbiol. Rev. (ISSN: 1098-6618) 25 (4), 635–648. http://dx.doi.org/10.1128/cmr.00045-12.

Copernicus Climate Change Service, 2021. CMIP6 climate projections. http://dx.doi.org/10.24381/cds.c866074c, Accessed 07 March 2026.

Courtiol, A., 2020. Courtiol/accipiter: Phantom of the forest or successful citizen? analysing how Northern goshawks (Accipiter gentilis) cope with the urban environment. http://dx.doi.org/10.5281/zenodo.4271624.

Eldridge, B.F., 1968. The effect of temperature and photoperiod on blood-feeding and ovarian development in mosquitoes of the *Culex pipiens* complex. Am. J. Trop. Med. Hyg. (ISSN: 0002-9637) 17 (1), 133–140. http://dx.doi.org/10.4269/ajtmh.1968.17.133.

Erazo, D., Grant, L., Ghisbain, G., Marini, G., Colón-González, F.J., Wint, W., Rizzoli, A., Van Bortel, W., Vogels, C. B.F., Grubaugh, N.D., Mengel, M., Frieler, K., Thiery, W., Dellicour, S., 2024. Contribution of climate change to the spatial expansion of West Nile virus in Europe. Nat. Commun. (ISSN: 2041-1723) 15 (1), http://dx.doi.org/10.1038/s41467-024-45290-3.

European Centre for Disease Prevention and Control, 2023. Prevention and control of West Nile virus and Usutu virus infections in the EU/EEA_2023. EFSA Support. Publ. (ISSN: 2397-8325) 20 (9), http://dx.doi.org/10.2903/sp.efsa.2023.en-8242.

European Centre for Disease Prevention and Control, 2024. West Nile virus infection. https://www.ecdc.europa.eu/en/west-nile-virus-infection. (Accessed 15 December 2024).

Farooq, Z., Rocklöv, J., Wallin, J., Abiri, N., Sewe, M.O., Sjödin, H., Semenza, J.C., 2022. Artificial intelligence to predict West Nile virus outbreaks with eco-climatic drivers. Lancet Reg. Health - Eur. (ISSN: 2666-7762) 17, 100370. http://dx.doi.org/10.1016/j.lanepe.2022.100370.

Ferede, G., Tiruneh, M., Abate, E., Kassa, W.J., Wondimeneh, Y., Damtie, D., Tessema, B., 2018. Distribution and larval breeding habitats of *Aedes* mosquito species in residential areas of northwest Ethiopia. Epidemiology Health (ISSN: 2092-7193) 40, e2018015. http://dx.doi.org/10.4178/epih.e2018015.

Fesce, E., Marini, G., Rosà, R., Lelli, D., Cerioli, M.P., Chiari, M., Farioli, M., Ferrari, N., 2025. Are we doing our best to contain the spread of West Nile virus? Evaluating intervention efficacy through mathematical modelling. Parasites & Vectors (ISSN: 1756-3305) 18 (1), http://dx.doi.org/10.1186/s13071-025-07128-9.

Field, E.N., Shepard, J.J., Clifton, M.E., Price, K.J., Witmier, B.J., Johnson, K., Boze, B., Abadam, C., Ebel, G.D., Armstrong, P.M., Barker, C.M., Smith, R.C., 2022. Semi-field and surveillance data define the natural diapause timeline for *Culex pipiens* across the United States. Commun. Biology (ISSN: 2399-3642) 5 (1), http://dx.doi.org/10.1038/s42003-022-04276-x.

Gerlach, B., Dröschmeister, R., Langgemach, T., Borkenhagen, K., Busch, M., Hauswirth, M., Heinicke, T., Kamp, J., Karthäuser, J., König, C., et al., 2019. Vögel in Deutschland–Übersichten zur Bestandssituation. DDA, BfN, LAG VSW, Münster, 152.

He, D., Ionides, E.L., King, A.A., 2009. Plug-and-play inference for disease dynamics: measles in large and small populations as a case study. J. R. Soc. Interface (ISSN: 1742-5662) 7 (43), 271–283. http://dx.doi.org/10.1098/rsif.2009.0151.

Heider, B., Stroms, P., Koch, J., Siedentop, S., 2020. Where do immigrants move in Germany? The role of international migration in regional disparities in population development. Popul. Space Place (ISSN: 1544-8452) 26 (8), http://dx.doi.org/10.1002/psp.2363.

Hoyer, S., Hamman, J., 2017. xarray: N-D labeled arrays and datasets in Python. J. Open Res. Softw. (ISSN: 2049-9647) 5 (1), 10. http://dx.doi.org/10.5334/jors.148.

King, A.A., Domenech de Cellès, M., Magpantay, F.M.G., Rohani, P., 2015. Avoidable errors in the modelling of outbreaks of emerging pathogens, with special reference to Ebola. Proc. R. Soc. B: Biological Sci. (ISSN: 1471-2954) 282 (1806), 20150347. http://dx.doi.org/10.1098/rspb.2015.0347.

Kobayashi, M., Kasai, S., Isawa, H., Hayashi, T., Sawabe, K., Tsuda, Y., 2012. Overwintering site of *Culex pipiens* pallens in an urban environment of Saitama Prefecture in Japan. Med. Èntomol. Zoöl. (ISSN: 2185-5609) 63 (4), 319–323. http://dx.doi.org/10.7601/mez.63.319.

Landesamt für Ländliche Entwicklung, Landwirtschaft und Flurneuordnung (LELF), 2026. Pferde. URL https://lelf.brandenburg.de/lelf/de/landwirtschaft/tierzucht-und-tierhaltung/pferde/.

Laperriere, V., Brugger, K., Rubel, F., 2011. Simulation of the seasonal cycles of bird, equine and human West Nile virus cases. Prev. Vet. Med. (ISSN: 0167-5877) 98 (2–3), 99–110. http://dx.doi.org/10.1016/j.prevetmed.2010.10.013.

Lees, R.S., Gilles, J.R.L., Hendrichs, J., Vreysen, M.J.B., Bourtzis, K., 2015. Back to the future: the sterile insect technique against mosquito disease vectors. Curr. Opin. Insect Sci. (ISSN: 2214-5745) 10, 156–162. http://dx.doi.org/10.1016/j.cois.2015.05.011.

Lenhart, S., Workman, J.T., 2007. Optimal Control Applied to Biological Models. Chapman and Hall/CRC, ISBN: 9781420011418, http://dx.doi.org/10.1201/9781420011418.

Li, J., Ionides, E.L., King, A.A., Pascual, M., Ning, N., 2024. Inference on spatiotemporal dynamics for coupled biological populations. J. R. Soc. Interface (ISSN: 1742-5662) 21 (216), http://dx.doi.org/10.1098/rsif.2024.0217.

Liu, L., Zhang, B., Cheng, P., Wang, H., Guo, X., Zhang, C., Wang, H., Zhao, Y., Gong, M., 2016. Overwintering of *Culex pipiens pallens* (diptera: *Culicidae*) in Shandong, China. J. Èntomol. Sci. (ISSN: 0749-8004) 51 (4), 314–320. http://dx.doi.org/10.18474/jes15-38.1.

Malik, T., 2018. A discrete time West Nile virus transmission model with optimal bird- and vector-specific controls. Math. Biosci. (ISSN: 0025-5564) 305, 60–70. http://dx.doi.org/10.1016/j.mbs.2018.08.008.

Marino, S., Hogue, I.B., Ray, C.J., Kirschner, D.E., 2008. A methodology for performing global uncertainty and sensitivity analysis in systems biology. J. Theoret. Biol. (ISSN: 0022-5193) 254 (1), 178–196. http://dx.doi.org/10.1016/j.jtbi.2008.04.011.

Mbaoma, O.C., Thomas, S.M., Beierkuhnlein, C., 2024. Spatiotemporally explicit epidemic model for West Nile virus outbreak in Germany: An inversely calibrated approach. J. Epidemiology Glob. Health (ISSN: 2210-6014) 14 (3), 1052–1070. http://dx.doi.org/10.1007/s44197-024-00254-0.

Merling de Chapa, M., Courtiol, A., Engler, M., Giese, L., Rutz, C., Lakermann, M., Müskens, G., van der Horst, Y., Zollinger, R., Wirth, H., Kenntner, N., Krüger, O., Chakarov, N., Müller, A.K., Looft, V., Grünkorn, T., Hallau, A., Altenkamp, R., Krone, O., 2020. Phantom of the forest or successful citizen? Analysing how Northern Goshawks (*Accipiter gentilis*) cope with the urban environment. R. Soc. Open Sci. (ISSN: 2054-5703) 7 (12), 201356. http://dx.doi.org/10.1098/rsos.201356.

Michel, F., Fischer, D., Eiden, M., Fast, C., Reuschel, M., Müller, K., Rinder, M., Urbaniak, S., Brandes, F., Schwehn, R., Lühken, R., Groschup, M., Ziegler, U., 2018. West Nile virus and Usutu virus monitoring of wild birds in Germany. Int. J. Environ. Res. Public Health (ISSN: 1660-4601) 15 (1), 171. http://dx.doi.org/10.3390/ijerph15010171.

Nemeth, N., Kratz, G., Edwards, E., Scherpelz, J., Bowen, R., Komar, N., 2007. Surveillance for West Nile virus in clinic-admitted raptors, Colorado. Emerg. Infect. Dis. (ISSN: 1080-6059) 13 (2), 305–307. http://dx.doi.org/10.3201/eid1302.051626.

N'konzi, J.P.N., Chukwu, C.W., Nyabadza, F., 2022. Effect of time-varying adherence to non-pharmaceutical interventions on the occurrence of multiple epidemic waves: A modeling study. Front. Public Health (ISSN: 2296-2565) 10, http://dx.doi.org/10.3389/fpubh.2022.1087683.

Offergeld, R., Frank, C., Schmidt-Chanasit, J., Ziegler, U., Preußel, K., Lachmann, R., 2025. West Nile virus infections in Germany: Update 2022-2024. Transfus. Med. Hemotherapy (ISSN: 1660-3818) 53 (1), 13–22. http://dx.doi.org/10.1159/000549166.

Papa, A., Danis, K., Athanasiadou, A., Delianidou, M., Panagiotopoulos, T., 2011. Persistence of West Nile virus immunoglobulin M antibodies, Greece. J. Med. Virol. (ISSN: 1096-9071) 83 (10), 1857–1860. http://dx.doi.org/10.1002/jmv.22190.

Paz, S., 2015. Climate change impacts on West Nile virus transmission in a global context. Phil. Trans. R. Soc. B (ISSN: 1471-2970) 370 (1665), 20130561. http://dx.doi.org/10.1098/rstb.2013.0561.

Petersen, L.R., Brault, A.C., Nasci, R.S., 2013. West Nile Virus: Review of the literature. JAMA (ISSN: 0098-7484) 310 (3), 308. http://dx.doi.org/10.1001/jama.2013.8042.

Petrović, T., Šekler, M., Petrić, D., Lazić, S., Debeljak, Z., Vidanović, D., Ignjatović Ćupina, A., Lazić, G., Lupulović, D., Kolarević, M., Plavšić, B., 2018. Methodology and results of integrated WNV surveillance programmes in Serbia. PLoS One (ISSN: 1932-6203) 13 (4), e0195439. http://dx.doi.org/10.1371/journal.pone.0195439.

Phalen, D.N., Dahlhausen, B., 2004. West Nile virus. Semin. Avian Exot. Pet Med. (ISSN: 1055-937X) 13 (2), 67–78. http://dx.doi.org/10.1053/j.saep.2004.01.002.

Pontryagin, L.S., 1987. Mathematical Theory of Optimal Processes. Routledge, ISBN: 9780203749319, http://dx.doi.org/10.1201/9780203749319.

Rodrigues, H.S., Monteiro, M.T.T., Torres, D.F.M., 2014. Optimal control and numerical software: an overview. http://dx.doi.org/10.48550/arXiv.1401.7279, arXiv preprint arXiv:1401.7279.

Rubel, F., Brugger, K., Hantel, M., Chvala-Mannsberger, S., Bakonyi, T., Weissenböck, H., Nowotny, N., 2008. Explaining Usutu virus dynamics in Austria: Model development and calibration. Prev. Vet. Med. (ISSN: 0167-5877) 85 (3–4), 166–186. http://dx.doi.org/10.1016/j.prevetmed.2008.01.006.

Salazar, P., Traub-Dargatz, J.L., Morley, P.S., Wilmot, D.D., Steffen, D.J., Cunningham, W.E., Salman, M.D., 2004. Outcome of equids with clinical signs of West Nile virus infection and factors associated with death. J. Am. Vet. Med. Assoc. (ISSN: 0003-1488) 225 (2), 267–274. http://dx.doi.org/10.2460/javma.2004.225.267.

Sambri, V., Capobianchi, M., Charrel, R., Fyodorova, M., Gaibani, P., Gould, E., Niedrig, M., Papa, A., Pierro, A., Rossini, G., Varani, S., Vocale, C., Landini, M.P., 2013. West Nile virus in Europe: emergence, epidemiology, diagnosis, treatment, and prevention. Clin. Microbiol. Infect. (ISSN: 1198-743X) 19 (8), 699–704. http://dx.doi.org/10.1111/1469-0691.12211.

Sauer, F.G., Lange, U., Schmidt-Chanasit, J., Kiel, E., Wiatrowska, B., Myczko, Ł., Lühken, R., 2023. Overwintering *Culex torrentium* in abandoned animal burrows as a reservoir for arboviruses in Central Europe. One Health (ISSN: 2352-7714) 16, 100572. http://dx.doi.org/10.1016/j.onehlt.2023.100572.

Sauer, F.G., Timmermann, E., Lange, U., Lühken, R., Kiel, E., 2022. Effects of hibernation site, temperature, and humidity on the abundance and survival of overwintering *Culex pipiens pipiens* and *Anopheles messeae* (Diptera: *Culicidae*). J. Med. Entomol. (ISSN: 1938-2928) 59 (6), 2013–2021. http://dx.doi.org/10.1093/jme/tjac139.

Schuler, L.A., Khaitsa, M.L., Dyer, N.W., Stoltenow, C.L., 2004. Evaluation of an outbreak of West Nile virus infection in horses: 569 cases (2002). J. Am. Vet. Med. Assoc. (ISSN: 0003-1488) 225 (7), 1084–1089. http://dx.doi.org/10.2460/javma.2004.225.1084.

S.J., Muñoz, 2019. ERA5-Land Monthly Averaged Data from 1950 to Present. http://dx.doi.org/10.24381/cds.68d2bb30.

Spielman, A., Wong, J., 1973. Environmental control of ovarian diapause in *Culex pipiens*. Ann. Entomol. Soc. Am. (ISSN: 0013-8746) 66 (4), 905–907. http://dx.doi.org/10.1093/aesa/66.4.905.

Takken, W., Knols, B.G.J., 2009. Malaria vector control: current and future strategies. Trends Parasitol. (ISSN: 1471-4922) 25 (3), 101–104. http://dx.doi.org/10.1016/j.pt.2008.12.002.

Tamba, M., Bonilauri, P., Galletti, G., Casadei, G., Santi, A., Rossi, A., Calzolari, M., 2024. West Nile virus surveillance using sentinel birds: results of eleven years of testing in corvids in a region of northern Italy. Front. Vet. Sci. (ISSN: 2297-1769) 11, http://dx.doi.org/10.3389/fvets.2024.1407271.

Thomas, D., Weedermann, M., Billings, L., Hoffacker, J., Washington-Allen, R.A., 2009. When to spray: a time-scale calculus approach to controlling the impact of West Nile virus. Ecol. Soc. (ISSN: 1708-3087) 14 (2), http://dx.doi.org/10.5751/es-03006-140221.

Tolnai, C., O'Sullivan, C., Lőrincz, M., Karvouni, M., Tenk, M., Marosi, A., Forgách, P., Paszerbovics, B., Wagenhoffer, Z., Kutasi, O., 2025. Cellular immune response in horses after West Nile neuroinvasive disease. Animals (ISSN: 2076-2615) 15 (16), 2352. http://dx.doi.org/10.3390/ani15162352.

Tutsoy, O., 2021. Covid-19 epidemic and opening of the schools: Artificial intelligence-based long-term adaptive policy making to control the pandemic diseases. IEEE Access (ISSN: 2169-3536) 9, 68461–68471. http://dx.doi.org/10.1109/access.2021.3078080.

Veksler, A., Eidson, M., Zurbenko, I., 2009. Assessment of methods for prediction of human West Nile virus (WNV) disease from WNV-infected dead birds. Emerg. Themes Epidemiology (ISSN: 1742-7622) 6 (1), http://dx.doi.org/10.1186/1742-7622-6-4.

Vogels, C.B.F., Fros, J.J., Göertz, G.P., Pijlman, G.P., Koenraadt, C.J.M., 2016. Vector competence of northern European *Culex pipiens* biotypes and hybrids for West Nile virus is differentially affected by temperature. Parasites & Vectors (ISSN: 1756-3305) 9 (1), http://dx.doi.org/10.1186/s13071-016-1677-0.

Vogels, C.B. F, Göertz, G.P., Pijlman, G.P., Koenraadt, C.J.M., 2017. Vector competence of European mosquitoes for West Nile virus. Emerg. Microbes Infect. (ISSN: 2222-1751) 6 (1), 1–13. http://dx.doi.org/10.1038/emi.2017.82.

Vollans, M., Day, J., Cant, S., Hood, J., Kilpatrick, A.M., Kramer, L.D., Vaux, A., Medlock, J., Ward, T., Paton, R.S., 2024. Modelling the temperature dependent extrinsic incubation period of West Nile virus using Bayesian time delay models. J. Infect. (ISSN: 0163-4453) 89 (6), 106296. http://dx.doi.org/10.1016/j.jinf.2024.106296.

Watts, M.J., Monteys, V.S.I., Mortyn, P.G., Kotsila, P., 2021. The rise of West Nile virus in southern and southeastern Europe: A spatial-temporal analysis investigating the combined effects of climate, land use and economic changes. One Health (ISSN: 2352-7714) 13, 100315. http://dx.doi.org/10.1016/j.onehlt.2021.100315.

World Organisation for Animal Health (WOAH), 2018 - 2025. WAHIS (Animal Disease Events). Retrieved on (2026-03-02) from (https://wahis.woah.org/#/event-management). Data extracted by (Pride Duve/BNITM). Reproduced with permission. "*The World Organisation for Animal Health (WOAH) bears no responsibility for the integrity or accuracy of the data contained herein, but not limited to, any deletion, manipulation, or reformatting of data that may have occurred beyond its control.*".

Ziegler, U., Keller, M., Michel, F., Globig, A., Denzin, N., Eiden, M., Fast, C., Gethmann, J., Bastian, M., Groschup, M.H., et al., 2019a. Aktuelles aus dem FLI zur West-Nil-Virus-Situation. Amtstierärztlicher Dienst Leb. 26, 78–81.

Ziegler, U., Lühken, R., Keller, M., Cadar, D., van der Grinten, E., Michel, F., Albrecht, K., Eiden, M., Rinder, M., Lachmann, L., Höper, D., Vina-Rodriguez, A., Gaede, W., Pohl, A., Schmidt-Chanasit, J., Groschup, M.H., 2019b. West Nile virus epizootic in Germany, 2018. Antiviral Res. (ISSN: 0166-3542) 162, 39–43. http://dx.doi.org/10.1016/j.antiviral.2018.12.005.

Ziegler, U., Santos, P.D., Groschup, M.H., Hattendorf, C., Eiden, M., Höper, D., Eisermann, P., Keller, M., Michel, F., Klopfleisch, R., Müller, K., Werner, D., Kampen, H., Beer, M., Frank, C., Lachmann, R., Tews, B.A., Wylezich, C., Rinder, M., Lachmann, L., Grünewald, T., Szentiks, C.A., Sieg, M., Schmidt-Chanasit, D., Lühken, R., 2020. West Nile virus epidemic in Germany triggered by epizootic emergence, 2019. Viruses (ISSN: 1999-4915) 12 (4), 448. http://dx.doi.org/10.3390/v12040448.

Supplementary File: Modelling the control of West Nile virus using mosquito reduction methods, vaccination of equids, and human behavioural adaptation to the usage of personal protective equipment

Pride Duve*, Felix Gregor Sauer, and Renke Lühken

Bernhard Nocht Institute for Tropical Medicine, Hamburg, Germany

S1 Temperature dependent functions

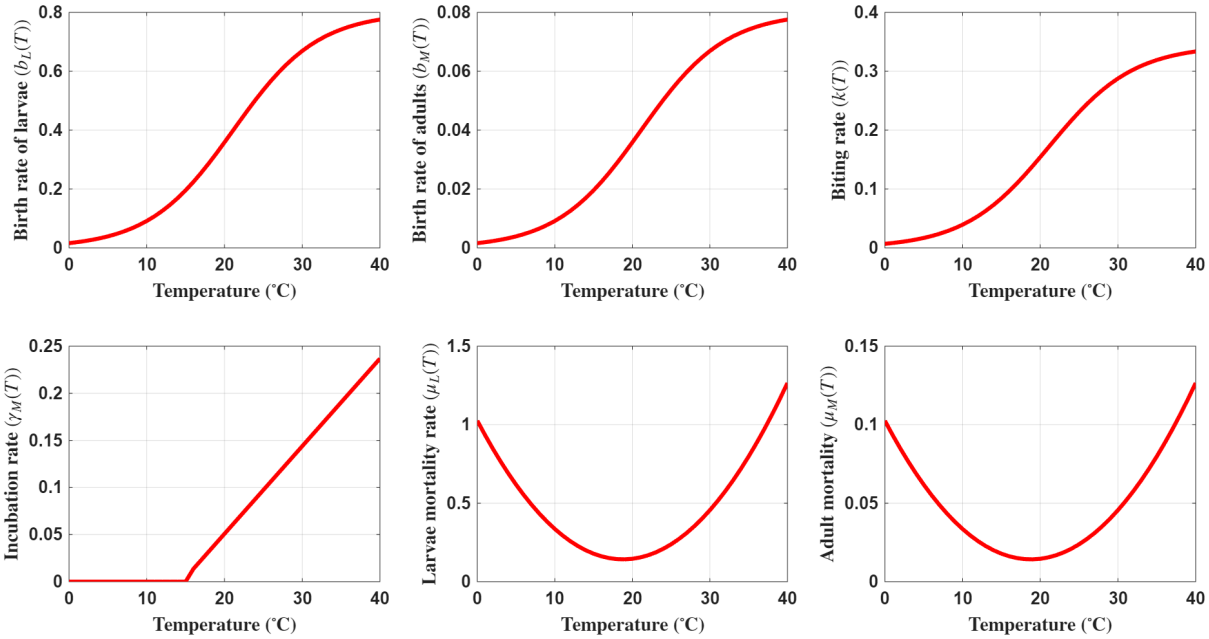


Figure S1: Temperature-dependent mosquito functions fitted in [1].

S2 PPE adoption by humans

The proportion of humans using PPE is here defined by x, while $1-x$ are those who are unprotected at any time t, with the rate of change of x described by the equation

$$\frac{dx}{dt} = qx(1-x)\left[-r_p + r_i m I_B\right]. \tag{S1}$$

In this equation, q is the imitation rate that measures how quickly people adopt PPE due to factors such as social influence, imitation, what they hear, and what they observe within their social circle.

*Corresponding author: pride.duve@bnitm.de

The parameter r_p measures the perceived inconvenience, frustration, or annoyance due to PPE use, r_i measures the perceived infection risk, and m indicates how much disease prevalence in birds affects PPE adoption by susceptible humans. Notably, when $r_i m I_B > r_p$, more people use PPE, whereas when $r_i m I_B < r_p$, fewer people do. This enables us to model PPE adoption as a game in which players are susceptible humans who are undecided about adopting PPE, considering their potential impacts on people's daily socio-economic, cultural, and emotional livelihoods [2, 3]. Setting $\kappa = \frac{q}{r_p}$, $\omega = \frac{m r_i}{r_p}$, Eq. (S1) simplifies to:

$$\frac{dx}{dt} = \kappa x(1-x)[-1+\omega I_B].$$

The new dimensionless scaling parameter $\omega \geq 0$ quantifies individuals' sensitivity to WNV prevalence in birds, indicating the strength of their response when deciding whether to use protective measures. A higher value of ω means individuals are more cautious and prioritise PPE use upon observing WNV cases in birds. Conversely, lower ω values show hesitation to adopt PPE despite increasing bird cases. This parameter captures the impact of educational initiatives, media campaigns, and other awareness efforts in informing people about WNV circulation in their communities and the benefits of PPE adoption versus the risks of not using them. The rate of PPE adoption increases whenever $\omega > \frac{1}{I_B}$. It follows that when $x = 0$, individuals do not use any PPE, whereas when $x = 1$, the entire susceptible population adopts PPE, representing the maximum level of protective behaviour in the model.

$$b_H = \frac{33,749 + 27,107}{3,685,265 \times 365} \approx 0.0000452 \text{ per day.} \tag{S2}$$

Crude death rates of humans in Berlin are calculated as:

$$\mu_H = \frac{37,686}{3,685,265 \times 365} \approx 0.0000280 \text{ per day.} \tag{S3}$$

S3 Equids: vaccination waning rate

Leading WNV vaccines are estimated to be more than 95% effective [4]. Moreover, a study by Long et al. [5] investigated whether a single immunogenic dose of a live Flavivirus chimaera WNV vaccine protects horses and concluded that this vaccine induces a protective immune response to WNV infection in horses that lasts up to 12 months. After completion of the primary vaccination course of the Equilis WNV vaccine, the European Medicines Agency [6] reported that the vaccine confers protective immunity for up to 12 months in horses. Using this evidence, and assuming no booster shots are administered to the equids, we consider the maximum duration of vaccine-induced immunity to be 12 months. At the time of vaccination ($t = 0$), immunity is assumed to be at its maximum level. Thereafter, vaccine-induced immunity in equids is assumed to wane exponentially at a rate ω_E, such that.

$$\frac{dQ}{dt} = -\omega_E Q, \tag{S4}$$

where $Q(t)$ denotes the immunity level at time t and ω_E is the vaccine waning rate.

Solving (S4) gives

$$Q(t) = Q(0)e^{-\omega_E t},$$

and therefore

$$\omega_E = -\frac{1}{t}\ln\left(\frac{Q(t)}{Q(0)}\right).$$

Assuming immunity declines from 100% at $t = 0$ to 50% after one year ($t = 365$ days), i.e. $Q(365)/Q(0) = 0.5$, we obtain

$$\omega_E = -\frac{\ln(0.5)}{365} = \approx 0.00190 \text{ day}^{-1}.$$

S4 Initial conditions

Table S1: Definition of variables used in our model and their initial conditions.

Parameter	Definition	Value	Source
L_M	mosquito larvae	1	defined by the authors
S_M	susceptible mosquitoes	500,000	[7]
E_M	exposed mosquitoes	0	[7]
I_M	infectious mosquitoes	100	[7]
S_B	susceptible birds	100,000	Defined by the authors
E_B	exposed birds	0	[7]
I_B	infectious birds	1	Defined by the authors
R_B	recovered birds	0	[7]
D_B	dead birds	0	[7]
S_H	susceptible humans	3,685,265	[8]
E_H	exposed humans	0	[7]
I_H	infected humans	0	[7]
R_H	recovered humans	0	[7]
D_H	dead humans	0	[7]
x	fraction of susceptible humans that adopt PPEs	variable	Defined by the authors
S_E	susceptible equids	45000	[9]
V_E	vaccinated equids	5	defined by the authors
E_E	exposed equids	0	[7]
I_E	infected equids	0	[7]
R_E	recovered equids	0	[7]
D_E	dead equids	0	[7]

S5 Positivity of solutions and existence of a feasible region

Our model describes a biological population. Thus, it is crucial to show that the state variables describing the populations at different compartments are always non-negative for all time $t \geq 0$.

Proof. To prove that the solutions of our model are positive, we use proof by contradiction and we show that none of the state variables will change its sign at any time $t \geq 0$.

Suppose the solutions are not positive for some time $t \geq 0$. Then there should exist a point $\tau \in (0, t)$ where any of the variables changes its sign or hits the value zero first. Suppose L_M is the first variable to hit zero, i.e., $L_M(\tau) = 0$, then for any $t \in (0, \tau)$, $L_M(t) > 0, S_M(t) > 0, E_M(t) >$

$0, I_M(t) > 0, N_M(t) > 0, S_B(t) > 0, E_B(t) > 0, I_B(t) > 0, R_B(t) > 0, D_B(t) > 0$, $S_H(t) > 0, E_H(t) > 0, I_H(t) > 0, R_H(t) > 0, D_H(t) > 0, S_E(t) > 0, V_E(t) > 0, E_E(t) > 0, I_E(t) > 0, R_E(t), D_E(t) > 0$, while $\frac{dL_M(\tau)}{dt} < 0$, i.e., is decreasing in this interval. From the first equation of our system,

$$\frac{dL_M(\tau)}{dt} = [(1-u_1)b_L\delta_M N_M(\tau) - (\mu_L+u_1+u_2)L_M(\tau)]\left[1-\frac{L_M(\tau)}{K_M}\right] - b_M L_M(\tau) = (1-u_1)b_L\delta_M N_M(\tau) > 0.$$

This contradicts the assumption that $\frac{dL_M(\tau)}{dt} < 0$, and thus $L_M(t)$ cannot hit the value zero first. Similarly, we can show that none of the variables can hit the value zero, implying that the solutions remain positive for all time $t \geq 0$. □

S6 Derivation of the optimal controls

Theorem 1. *Given the optimal control variables* $\left(u_1^\star, u_2^\star, u_3^\star\right)$ *and the objective functional:*

$$J = \int_0^{T_F} A_1 L_M + A_2 N_M + A_3 I_B + \frac{1}{2}\left[c_1 u_1^2(T) + c_2 u_2^2(T) + c_3 u_3^2(T)\right] dt, \tag{S5}$$

where the constants A_1, A_2, A_3 *are positive weight constants for the state variables,* c_1, c_2, c_3 *are weight constants or cost balancing factors over time corresponding to each control variable,* T_F *is the terminal or final time, then there exist optimal controls* $\left[u_1^\star(T), u_2^\star(T), u_3^\star(T)\right]$ *given by*

$$\begin{cases} u_1^\star(t) = \min\left\{0.5, \max\left\{0, \dfrac{(b_L\delta_M N_M + L_M)(1-L_M/K_M)\lambda_1}{c_1}\right\}\right\}, \\ u_2^\star(t) = \min\left\{0.5, \max\left\{0, \dfrac{L_M(1-L_M/K_M)\lambda_1}{c_2}\right\}\right\}, \\ u_3^\star(t) = \min\left\{0.5, \max\left\{0, \dfrac{S_M\lambda_2 + E_M\lambda_3 + I_M\lambda_4}{c_3}\right\}\right\}, \end{cases} \tag{S6}$$

Proof. The necessary conditions an optimal control problem must satisfy are defined in the Pontryagin's Maximum Principle [10]. The principle converts our optimal control problem together with the objective functional defined in Equation (S5), into a problem of minimizing pointwise the Hamiltonian ($\mathscr{H}$) with respect to the control variables $(u_1(t), u_2(t), u_3(t))$, where the Hamiltonian is given by the formula:

$$\begin{aligned} \mathscr{H} &= A_1 L_M + A_2 N_M + A_3 I_B + \frac{1}{2}c_1 u_1^2 + \frac{1}{2}c_2 u_2^2 + \frac{1}{2}c_3 u_3^2 + \lambda_1 L_M^{'} + \lambda_2 S_M^{'} + \lambda_3 E_M^{'} + \lambda_4 I_M^{'} \\ &+ \lambda_5 S_B^{'} + \lambda_6 E_B^{'} + \lambda_7 I_B^{'} + \lambda_8 R_B^{'} + \lambda_9 D_B^{'}. \end{aligned} \tag{S7}$$

Substituting the derivatives of the state variables, we get:

$$\begin{aligned}
\mathscr{H} &= A_1 L_M + A_2[S_M + E_M + I_M] + A_3 I_B + \frac{1}{2}c_1 u_1^2 + \frac{1}{2}c_2 u_2^2 + \frac{1}{2}c_3 u_3^2 \\
&+ \lambda_1 \left[\{(1-u_1) b_L \delta_M (S_M + E_M + I_M) - (\mu_L + u_1 + u_2) L_M \} \left[1 - \frac{L_M}{K_M} \right] - b_M L_M \right] \\
&+ \lambda_2 \left[b_M L_M - \frac{\delta_M \beta_B I_B S_M}{K_B} - (\mu_M + u_3) S_M \right] \\
&+ \lambda_3 \left[\frac{\delta_M \beta_B I_B S_M}{K_B} - [\gamma_M + \mu_M + u_3] E_M \right] \\
&+ \lambda_4 [\gamma_M E_M - [\mu_M + u_3] I_M] \\
&+ \lambda_5 \left[b_B \left[1 - \frac{N_B}{K_B} \right] N_B - \frac{\delta_M \beta_M \phi_B I_M S_B}{K_M} - \mu_B S_B \right] \\
&+ \lambda_6 \left[\frac{\delta_M \beta_M \phi_B I_M S_B}{K_M} - [\gamma_B + \mu_B] E_B \right] \\
&+ \lambda_7 [\gamma_B E_B - [\alpha_B + \mu_B] I_B] \\
&+ \lambda_8 [(1-\nu_B)\alpha_B I_B - \mu_B R_B] \\
&+ \lambda_9 [\alpha_B \nu_B I_B]
\end{aligned} \tag{S8}$$

The variables $\lambda_1, \lambda_2, \cdots, \lambda_9$ are the adjoints to the state variables and should satisfy

$$\lambda_1^{'} = -\frac{\partial \mathscr{H}}{\partial L_M};\ \lambda_2^{'} = -\frac{\partial \mathscr{H}}{\partial S_M};\ \lambda_3^{'} = -\frac{\partial \mathscr{H}}{\partial E_M};\ \lambda_4^{'} = -\frac{\partial \mathscr{H}}{\partial I_M};\ \lambda_5^{'} = -\frac{\partial \mathscr{H}}{\partial S_B};$$

$$\lambda_6^{'} = -\frac{\partial \mathscr{H}}{\partial E_B},\ \lambda_7^{'} = -\frac{\partial \mathscr{H}}{\partial I_B};\ \lambda_8^{'} = -\frac{\partial \mathscr{H}}{\partial R_B};\ \lambda_9^{'} = -\frac{\partial \mathscr{H}}{\partial D_B}.$$

Taking partial derivatives, we have

$$\begin{aligned}
\lambda_1^{'} &= (\mu_L + u_1 + u_2)\left[1 - \frac{2L_M}{K_M}\right]\lambda_1 + \frac{(1-u_1) b_L \delta_M N_M}{K_M}\lambda_1 + (\lambda_1 - \lambda_2) b_M - A_1, \\
\lambda_2^{'} &= \frac{\delta_M \beta_B I_B}{K_B}[\lambda_2 - \lambda_3] + (\mu_M + u_3)\lambda_2 - (1-u_1) b_L \delta_M \left[1 - \frac{L_M}{K_M}\right]\lambda_1 - A_2, \\
\lambda_3^{'} &= (\gamma_M + \mu_M + u_3)\lambda_3 - (1-u_1) b_L \delta_M \left[1 - \frac{L_M}{K_M}\right]\lambda_1 - \gamma_M \lambda_4 - A_2, \\
\lambda_4^{'} &= \frac{\delta_M \beta_M \phi_B S_B}{K_M}[\lambda_5 - \lambda_6] + (\mu_M + u_3)\lambda_4 - (1-u_1) b_L \delta_M \left[1 - \frac{L_M}{K_M}\right]\lambda_1 - A_2, \\
\lambda_5^{'} &= \frac{\delta_M \beta_M \phi_B I_M}{K_M}[\lambda_5 - \lambda_6] + \mu_B \lambda_5 + \left(\frac{2 b_B N_B}{K_B} - b_B\right)\lambda_5, \\
\lambda_6^{'} &= (\gamma_B + \mu_B)\lambda_6 - \gamma_B \lambda_7 + \left(\frac{2 b_B N_B}{K_B} - b_B\right)\lambda_5, \\
\lambda_7^{'} &= \frac{\delta_M \beta_M S_M}{K_B}[\lambda_2 - \lambda_3] + (\alpha_B + \mu_B)\lambda_7 - (1-\nu_B)\alpha_B \lambda_8 - \alpha_B \nu_B \lambda_9 + \left(\frac{2 b_B N_B}{K_B} - b_B\right)\lambda_5 - A_3, \\
\lambda_8^{'} &= \mu_B \lambda_8 + \left(\frac{2 b_B N_B}{K_B} - b_B\right)\lambda_5, \\
\lambda_9^{'} &= 0
\end{aligned} \tag{S9}$$

with transversality conditions $\lambda_1(T) = \lambda_2(T) \cdots = \lambda_9(T) = 0$. Moreover, $\left[u_1^\star(t), u_2^\star(t), u_3^\star(t)\right]$ satisfy the conditions

$$\frac{\partial \mathscr{H}}{\partial u_1} = 0, \quad \frac{\partial \mathscr{H}}{\partial u_2} = 0 \quad \frac{\partial \mathscr{H}}{\partial u_3} = 0,$$

implying that;

$$\begin{cases} c_1 u_1 - b_L \delta_M N_M \left[1 - \dfrac{L_M}{K_M}\right] \lambda_1 - L_M \left[1 - \dfrac{L_M}{K_M}\right] \lambda_1 = 0, \\ c_2 u_2 - L_M \left[1 - \dfrac{L_M}{K_M}\right] \lambda_1 = 0, \\ c_3 u_3 - \lambda_2 S_M - \lambda_3 E_M - \lambda_4 I_M = 0, \end{cases} \tag{S10}$$

in the interior of the control set $\mathscr{U}$. Solving Equation (S10) for (u_1, u_2, u_3) in $\mathscr{U}$, we get the optimal solution as:

$$\begin{cases} u_1^\star(t) = \min\left\{0.5, \max\left\{0, \dfrac{(b_L \delta_M N_M + L_M)(1 - L_M/K_M)\lambda_1}{c_1}\right\}\right\}, \\ u_2^\star(t) = \min\left\{0.5, \max\left\{0, \dfrac{L_M(1 - L_M/K_M)\lambda_1}{c_2}\right\}\right\}, \\ u_3^\star(t) = \min\left\{0.5, \max\left\{0, \dfrac{S_M \lambda_2 + E_M \lambda_3 + I_M \lambda_4}{c_3}\right\}\right\}, \end{cases} \tag{S11}$$

□

References

[1] Franz Rubel, Katharina Brugger, Michael Hantel, Sonja Chvala-Mannsberger, Tamás Bakonyi, Herbert Weissenböck, and Norbert Nowotny. Explaining usutu virus dynamics in austria: Model development and calibration. *Preventive Veterinary Medicine*, 85(3–4):166–186, July 2008. ISSN 0167-5877. doi: 10.1016/j.prevetmed.2008.01.006. URL http://dx.doi.org/10.1016/j.prevetmed.2008.01.006.

[2] Chris T Bauch. Imitation dynamics predict vaccinating behaviour. *Proceedings of the Royal Society B: Biological Sciences*, 272(1573):1669–1675, July 2005. ISSN 1471-2954. doi: 10.1098/rspb.2005.3153. URL http://dx.doi.org/10.1098/rspb.2005.3153.

[3] Joel-Pascal Ntwali N'konzi, Chidozie Williams Chukwu, and Farai Nyabadza. Effect of time-varying adherence to non-pharmaceutical interventions on the occurrence of multiple epidemic waves: A modeling study. *Frontiers in Public Health*, 10, December 2022. ISSN 2296-2565. doi: 10.3389/fpubh.2022.1087683. URL http://dx.doi.org/10.3389/fpubh.2022.1087683.

[4] T. Epp, C. Waldner, R. Corrigan, and P. Curry. Public health use of surveillance for west nile virus in horses: Saskatchewan, 2003-2005. *Transboundary and Emerging Diseases*, 55(9–10): 411–416, December 2008. ISSN 1865-1682. doi: 10.1111/j.1865-1682.2008.01051.x. URL http://dx.doi.org/10.1111/j.1865-1682.2008.01051.x.

[5] M. T. Long, E. P. J. Gibbs, M. W. Mellencamp, R. A. Bowen, K. K. Seino, S. Zhang, S. E. Beachboard, and P. P. Humphrey. Efficacy, duration, and onset of immunogenicity of a west nile virus vaccine, live flavivirus chimera, in horses with a clinical disease challenge

model. *Equine Veterinary Journal*, 39(6):491–497, November 2007. ISSN 2042-3306. doi: 10.2746/042516407x217416. URL http://dx.doi.org/10.2746/042516407x217416.

[6] European Medicines Agency. Equilis west nile: Epar – product information. https://www.ema.europa.eu/en/documents/product-information/equilis-west-nile-epar-product-information_en.pdf, 2023. Accessed: 2025-08-14.

[7] Vincent Laperriere, Katharina Brugger, and Franz Rubel. Simulation of the seasonal cycles of bird, equine and human west nile virus cases. *Preventive Veterinary Medicine*, 98(2–3): 99–110, February 2011. ISSN 0167-5877. doi: 10.1016/j.prevetmed.2010.10.013. URL http://dx.doi.org/10.1016/j.prevetmed.2010.10.013.

[8] Amt für Statistik Berlin-Brandenburg. Berlin population 2024, 2024. URL https://www.statistik-berlin-brandenburg.de/bevoelkerung.

[9] Landesamt für Ländliche Entwicklung, Landwirtschaft und Flurneuordnung (LELF). Pferde, 2026. URL https://lelf.brandenburg.de/lelf/de/landwirtschaft/tierzucht-und-tierhaltung/pferde/.

[10] L.S. Pontryagin. *Mathematical Theory of Optimal Processes*. Routledge, May 2018. ISBN 9780203749319. doi: 10.1201/9780203749319. URL http://dx.doi.org/10.1201/9780203749319.

4.3 Publication 3: *A process-based model simulating the life-cycle of Culex pipiens s.s./Cx. torrentium (Diptera: Culicidae) in Germany*

Rauhöft *et al. Parasites & Vectors* (2026) 19:207
https://doi.org/10.1186/s13071-026-07410-4

Parasites & Vectors

RESEARCH Open Access

A process-based model simulating the life-cycle of *Culex pipiens* s.s./*Cx. torrentium* (Diptera: Culicidae) in Germany

Leif Rauhöft[1*†], Pride Duve[1†], Sara M. Martins-Afonso[1], Jöst Hanna[1], Tatiana Şuleşco[1], Felix Gregor Sauer[1] and Renke Lühken[1]

Abstract

Background Mosquitoes are well known for their ability to transmit pathogens, including various arthropod-borne viruses (arboviruses) of veterinary and medical interest. In Europe, the increasing public health relevance of mosquito-borne pathogens highlights the need to understand how environmental drivers shape mosquito population dynamics relevant to transmission risk. *Culex pipiens* sensu stricto (s.s.) and *Culex torrentium* (collectively referred to here as *Cx. pipiens* s.s./*Cx. torrentium*) are the primary vectors of Usutu virus and West Nile virus in Europe and are commonly found in and around human settlements. The prediction of their spatial-temporal abundance supports early assessment of arbovirus transmission risk and the planning of effective intervention methods, such as vector control.

Methods A process-based model was developed to simulate the spatial-temporal occurrence of *Cx. pipiens* s.s./*Cx. torrentium* in Germany, with a particular focus on depicting realistic overwintering behaviour, including, diapause induced through photoperiod and temperature in the larval stage. The model output is driven by local temperature and rainfall data provided by the European re-analysis and observations for monitoring data set and evaluated with field data from 106 sampling sites in Germany.

Results A significant association between relative simulated and observed mosquito abundance was found for 75% of the sampling sites, using site-specific beta regression models. An overall beta mixed-effects model across all sites was also significant (estimate = 2.17, standard error = 0.062, Z-value = 35.03, p-value < 0.0001, marginal $R^2 = 0.4$).

Conclusions This model offers a robust framework for the depiction of the mosquito population dynamics of *Cx. pipiens* s.s./*Cx. torrentium* under current and future climate scenarios, thereby supporting vector surveillance and control strategies across Europe.

†Leif Rauhöft and Pride Duve contributed equally to this work.

*Correspondence:
Leif Rauhöft
leif.rauhoeft@bnitm.de
[1] Bernhard Nocht Institute for Tropical Medicine, Bernhard-Nocht-Straße 74, 20359 Hamburg, Hamburg, Germany

© The Author(s) 2026. **Open Access** This article is licensed under a Creative Commons Attribution 4.0 International License, which permits use, sharing, adaptation, distribution and reproduction in any medium or format, as long as you give appropriate credit to the original author(s) and the source, provide a link to the Creative Commons licence, and indicate if changes were made. The images or other third party material in this article are included in the article's Creative Commons licence, unless indicated otherwise in a credit line to the material. If material is not included in the article's Creative Commons licence and your intended use is not permitted by statutory regulation or exceeds the permitted use, you will need to obtain permission directly from the copyright holder. To view a copy of this licence, visit http://creativecommons.org/licenses/by/4.0/. The Creative Commons Public Domain Dedication waiver (http://creativecommons.org/publicdomain/zero/1.0/) applies to the data made available in this article, unless otherwise stated in a credit line to the data.

Background

Mosquitoes (Culicidae) are small dipteran insects of global importance due to their role as vectors of numerous pathogens affecting humans and animals. Their life-cycle consists of four distinct stages: egg, larva, pupa and adult. The immature stages develop in aquatic habitats. Female mosquitoes depend on blood meals for egg production, and thus pathogens can be ingested and subsequently transmitted during the next gonotrophic cycle. Male mosquitoes do not feed on blood under natural field conditions. Following a blood meal, female mosquitoes undergo a resting period during which they digest the ingested blood to develop eggs [1], which are then laid in standing water bodies. *Culex pipiens* sensu stricto (*Cx. pipiens* s.s.) and *Culex torrentium* (collectively referred to here as *Cx. pipiens* s.s./*Cx. torrentium*) are very important mosquito vectors of aboviruses of medical and veterinary relevance [2], with a high vector competence for Usutu virus and West Nile virus (WNV) [3, 4]. Since their initial emergence in Germany, where Usutu virus was first detected in 2011 and WNV in 2018, these pathogens have been detected each year in birds, mosquitoes and humans [5–8]. WNV and Usutu virus are mosquito-borne flaviviruses that are maintained in enzootic transmission cycles between mosquitoes and avian hosts, with humans and other mammals acting as incidental dead-end hosts. While most human infections are asymptomatic, both viruses can cause neuroinvasive disease, particularly in elderly and immunocompromised individuals, and they have emerged as significant public health concerns in several European countries. *Culex pipiens* s.s./*Cx. torrentium* are widely distributed and have broad host-feeding patterns, including birds, non-human mammals and humans, making them suitable bridge vectors [9]. These characteristics have resulted in these two mosquito species being a main target for surveillance and risk assessment efforts [10, 11]. However, although *Cx. pipiens* s.s./*Cx. torrentium* are separate species, the females cannot be morphologically differentiated. They are sibling species that frequently occur in sympatry across Europe, with *Cx. pipiens* s.s. being ubiquitous throughout Europe while *Cx. torrentium* abundances increase in more northern and cooler regions. However, each of these species has distinct biological and ecological characteristics. For example, *Cx. pipiens* s.s. is easily captured with CO_2-baited traps, while *Cx. torrentium* seems to be disproportionately underrepresented in such captures [12]. In addition, *Cx. torrentium* has a higher vector competence for WNV compared to *Cx. pipiens* s.s. [3]. Also, these two species use different overwintering sites, with *Cx. pipiens* s.s. predominant in anthropogenic sites, such as cellars, and *Cx. torrentium* more frequently found in abandoned animal burrows [13].

Entomological monitoring through systematic mosquito collections provides the foundation for identifying the spatial-temporal risk of mosquito-borne pathogen transmission. Field-based mosquito surveillance, including collection using CO_2-baited traps and subsequent taxonomic identification and arbovirus screening, is logistically demanding and difficult to sustain at high spatial and temporal resolution. Process-based (mechanistic) models describe dynamic systems by representing the biological processes that determine system behaviour rather than relying on statistical correlations. Building on the foundations laid by Lotka [14], these models provide a framework linking environmental drivers to population dynamics. In the study reported here, we used a process-based model to simulate the life-cycle of *Cx. pipiens* s.s./*Cx. torrentium*, using temperature-, precipitation- and photoperiod-dependent equations to capture developmental and mortality rates. This type of model enables the spatial-temporal mosquito abundance to be estimated while at the same time allowing the simulation of changing conditions, such as control measures [15]. Several process-based models for mosquitoes have been published for Europe, with a focus on the Mediterranean region (southern France or Italy [15–18]). These models showed a high level of performance in terms of estimating the temporal mosquito abundance, but they were generally only validated with field data from a few sampling sites or relatively small areas. Consequently, a process-based model for *Cx. pipiens* s.s./*Cx. torrentium*, two of the most important vectors in Central Europe, and a large-scale, site-specific evaluation is missing.

In this work, we developed and validated a process-based model for *Cx. pipiens* s.s./*Cx. torrentium* in Germany. To achieve this, we adjusted the generic model for *Aedes albopictus* originally proposed by Cailly et al. [15] and later extended to further species, including "*Culex pipiens*", by Ezanno et al. [16]. We extend the model by replacing predefined seasonal start and end dates with explicit, photoperiod- and temperature-driven diapause dynamics. The model further incorporates sex-differentiated life stages and revised temperature-dependent transition and mortality functions, allowing realistic representation of overwintering behaviour under temperate European conditions.

The aim of this study was to develop and validate, for the first time in Germany, a process-based model for *Cx. pipiens* s.s./*Cx. torrentium*, perform site-specific validation to capture local population dynamics, compare the performance of this process-based model to that of a temperature-dependent correlative model and assess the

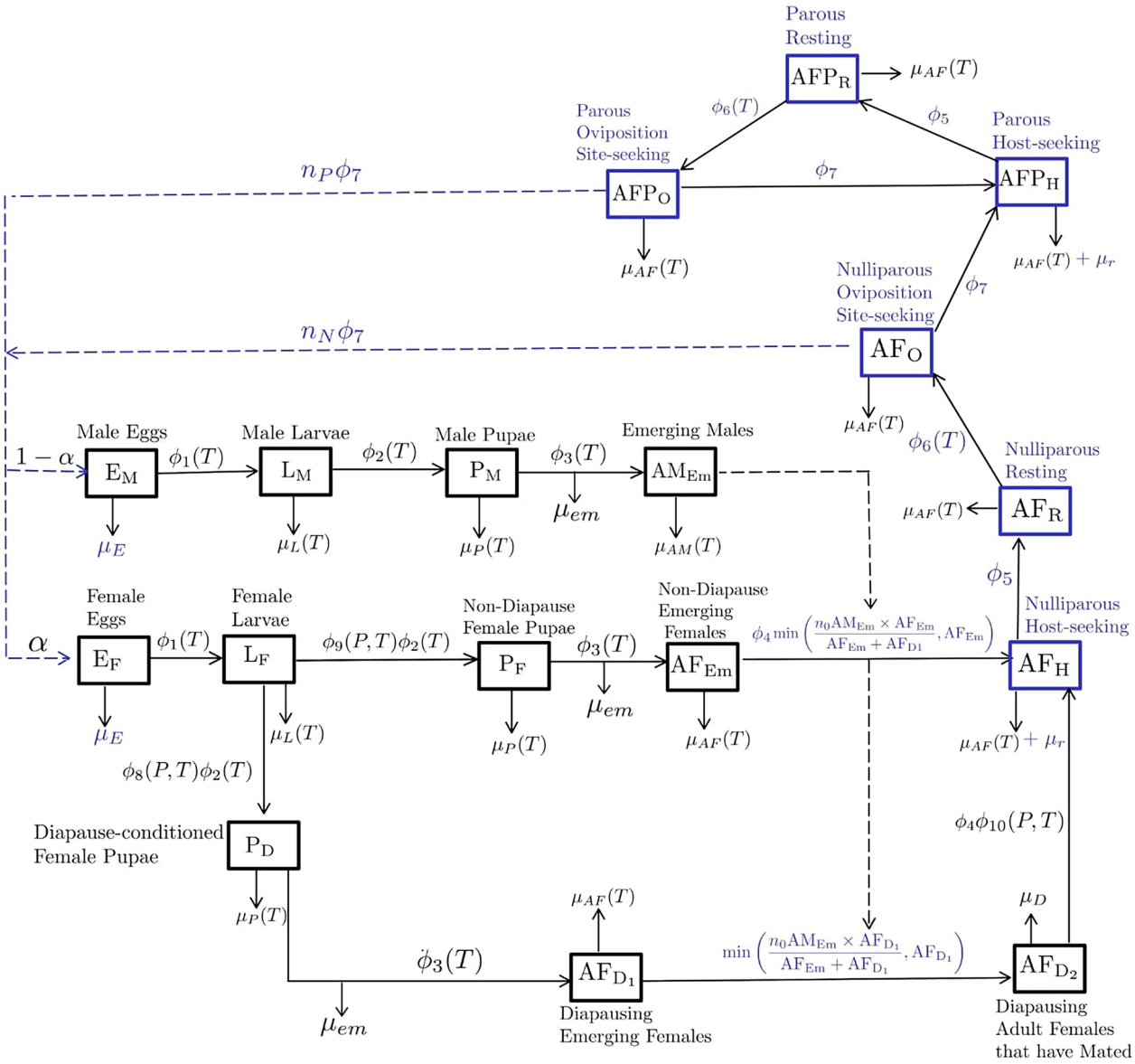


Fig. 1 Flow chart of the process-based model for the life-cycle of mosquitoes *Culex pipiens* sensu stricto and *Culex torrentium* (*Cx. pipiens* s.s./*Cx. torrentium*). Boxes represent compartments or different life stages. Solid lines represent the development from one stage to another and dashed lines represent the interactions between the different compartments. Previously published compartments, transition and mortality rates are highlighted in blue. For specific definitions, see Table 1 and section Mathematical model for the life cycle of *Cx. pipiens* s.s./*Cx. torrentium*

relative importance of model parameters on overall mosquito dynamics using a sensitivity analysis.

Methods

Mathematical model for the life cycle of *Cx. pipiens* s.s./*Cx. torrentium*

The model consists of different compartments (Fig. 1) for mosquito abundance in aquatic stages. These are male and female eggs (E_M, E_F); larvae (L_M, L_F); pupae (P_M, P_F) and diapause-conditioned pupae (P_D); and adult stages: emerging males and females (AM_{Em}; AF_{Em}), nulliparous host-seeking females (AF_H); nulliparous resting females (AF_R) and nulliparous oviposition site-seeking females (AF_O); parous host-seeking females (AFP_H); parous resting females (AFP_R) and parous oviposition site-seeking females (AFP_O); and diapausing stages: emerging adult females (AF_{D1}) and overwintering adult females (AF_{D2}; Eq. 1).

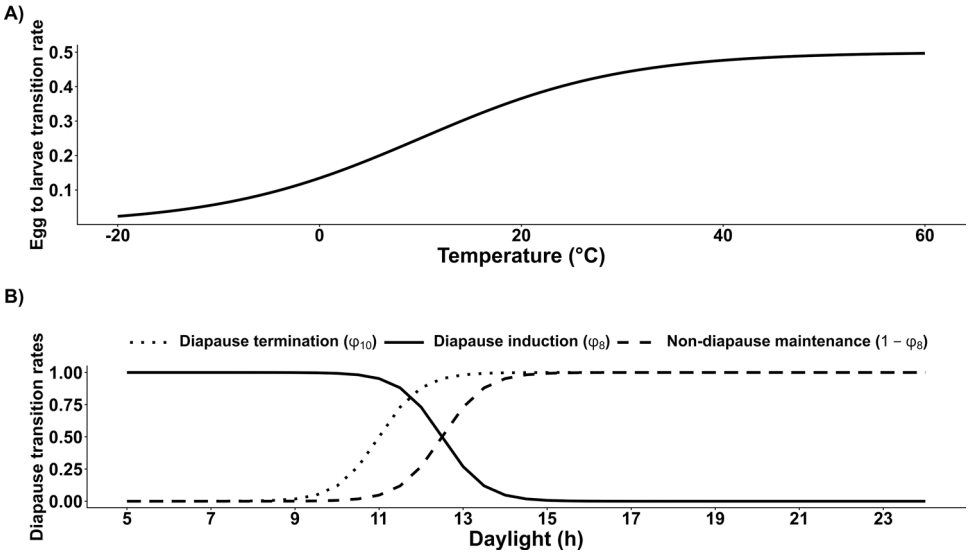


Fig. 2 **A** Newly developed temperature-dependent transition rates. **B** Newly developed photoperiod-dependent transition rates

The transition between the aquatic stages is temperature-dependent ($\phi_1(T)$, $\phi_2(T)$, $\phi_3(T)$; Eq. 2; Fig. 2a). Previous laboratory and semi-field studies suggest that diapause is induced at photoperiods < 15 h of light and temperatures lower than 20 °C [19, 20]. This is represented in our temperature- and photoperiod-dependent function $\phi_8(P, T)$ inducing diapause (Fig. 2b; Eq. 3). Adult females that do not enter diapause remain in the reproductive (non-diapausing) state, which is governed by the temperature- and photoperiod-dependent non-diapause maintenance rate $\phi_9(P, T)$. The rate of diapause termination is also temperature- and photoperiod-dependent ($\phi_{10}(P, T)$; Eq. 4; [21]). The development of eggs begins at temperatures exceeding T_{Ag}. Development is over when the cumulative daily temperatures exceeds TDD_{Ag}. Additionally, temperature-dependent mortality rates were utilised for larvae and pupae ($\mu_L(T)$, $\mu_P(T)$; Eq 5; Fig. 3). Rainfall increases the environmental carrying capacity for larvae (K_L) and pupae (K_P) by increasing the standard environmental carrying capacities (κ_l, κ_p) using the normalised rainfall over a period of 14 days (Eq 6). The competition for resources within the breeding site is taken into account by the density-dependent larval mortality of $\mu_L(T)\left[1+\frac{\mu_L(T)}{K_L}\right]$ [16, 22, 23].

The pupal density dependence was previously combined in an exponential decay function using the mortality at emergence (μ_{em}) as scaling factor. We propose that the mortality at emergence (μ_{em}) is not a matter of resources since pupae do not take up any nutrients. Consequently, the mortality at emergence can only be a stochastic event or a matter of actual space restriction by density. We thereby replaced the scaling factor with β and strongly reduced it compared to μ_{em}. The mortality at emergence was kept outside of the exponential decay function.

A proportion α of mosquito eggs are female while a proportion of $(1-\alpha)$ are male. Based on the assumption that all female mosquitoes mate before seeking a host, emerging females (AF_{Em}) and emerging diapausing females (AF_{D1}) mate before the females progress either to the host-seeking stage (AF_H) or the overwintering stage (AF_{D2}). As also implemented by Ezanno et al. [16], it is assumed that females mate only once. In contrast, males can mate several times. Asman [24] showed that under laboratory conditions male *Cx. tarsalis* mosquitoes can inseminate up to eight females over 21 days. Thereby, the number of females which get fertilised by males is highly dependent on the population density of sexually active male mosquitoes [25]. When sexually active males are scarce in the environment, the number of inseminated females that progress to the host-seeking stage is proportional to the number of available males multiplied by the number of females each male can inseminate. This is denoted as $n_0 AM_{Em}$, where n_0 is the number of females each male inseminates. After mating, female mosquitoes progress to the host-seeking stage at a rate of ϕ_4. Blood-feeding induces the resting stage at a rate of ϕ_5 before females start seeking an oviposition site to lay eggs at a rate of $\phi_6(T)$ (Eq 7). Female mosquitoes become parous after depositing eggs at a rate of ϕ_7. The cycle repeats until the mosquitoes die and are removed from the population. During the diapausing stage, the overwintering females die at a rate of μ_D. Female adult mosquitoes in

general die at a rate of $\mu_{AF}(T)$ (Eq 5), while for host-seeking females AF_H and AFP_H, an additional host seeking mortality μ_r is added. Adult males are shown to have shorter longevity especially during the highest and lowest temperatures [26]. Therefore, an additional mortality rate for males $\mu_{AM}(T)$ (Eq. 8) was generated based on the general adult mortality rate but was more constrained in the temperature range (Fig. 3).

$$
\begin{aligned}
\frac{dE_F}{dt} &= \alpha \cdot \phi_7[n_P AFP_O + n_N AF_O] - [\phi_1(T) + \mu_E(T)]E_F,\\
\frac{dE_M}{dt} &= (1-\alpha)\phi_7[n_P AFP_O + n_N AF_O] - [\phi_1(T) + \mu_E(T)]E_M,\\
\frac{dL_F}{dt} &= \phi_1(T)\cdot E_F - \left[\phi_2(T) + \mu_L(T)\left(1 + \frac{L_F + L_M}{K_L}\right)\right]L_F,\\
\frac{dL_M}{dt} &= \phi_1(T)\cdot E_M - \left[\phi_2(T) + \mu_L(T)\left(1 + \frac{L_F + L_M}{K_L}\right)\right]L_M,\\
\frac{dP_F}{dt} &= \phi_2(T)\cdot\phi_9(P,T)\cdot L_F - [\phi_3(T) + \mu_P(T)]P_F,\\
\frac{dP_M}{dt} &= \phi_2(T)\cdot L_M - [\mu_P(T) + \phi_3(T)]P_M,\\
\frac{dP_D}{dt} &= \phi_2(T)\cdot\phi_8(P,T)\cdot L_F - [\mu_P(T) + \phi_3(T)]P_D,\\
\frac{dAM_{Em}}{dt} &= \phi_3(T)\cdot P_M\cdot(1-\mu_{em})\cdot e^{-\beta\left(1 + \frac{P_M + P_D + P_F}{K_P}\right)} - \mu_{AM}(T)\cdot AM_{Em},\\
\frac{dAF_{Em}}{dt} &= \phi_3(T)\cdot P_F\cdot(1-\mu_{em})\cdot e^{-\beta\left(1 + \frac{P_M + P_D + P_F}{K_P}\right)} - \phi_4\min\left\{n_0 AM_{Em}\frac{AF_{Em}}{AF_{D1} + AF_{Em}}, AF_{Em}\right\} - \mu_{AF}(T)\cdot AF_{Em},\\
\frac{dAF_{D1}}{dt} &= \phi_3(T)\cdot P_D\cdot(1-\mu_{em})\cdot e^{-\beta\left(1 + \frac{P_M + P_D + P_F}{K_P}\right)} - \min\left\{n_0 AM_{Em}\frac{AF_{D1}}{AF_{D1} + AF_{Em}}, AF_{D1}\right\} - \mu_{AF}(T)\cdot AF_{D1},\\
\frac{dAF_{D2}}{dt} &= \min\left\{n_0 AM_{Em}\frac{AF_{D1}}{AF_{D1} + AF_{Em}}, AF_{D1}\right\} - [\phi_4\cdot\phi_{10}(P,T) + \mu_D]AF_{D2},\\
\frac{dAF_H}{dt} &= \phi_4\min\left\{n_0 AM_{Em}\frac{AF_{Em}}{AF_{D1} + AF_{Em}}, AF_{Em}\right\} + \phi_4\cdot\phi_{10}(P,T)\cdot AF_{D2} - [\phi_5 + \mu_r + \mu_{AF}(T)]AF_H,\\
\frac{dAF_R}{dt} &= \phi_5\cdot AF_H - [\phi_6(T) + \mu_{AF}(T)]AF_R,\\
\frac{dAF_O}{dt} &= \phi_6(T)\cdot AF_R - [\phi_7 + \mu_{AF}(T)]AF_O,\\
\frac{dAFP_H}{dt} &= \phi_7\cdot[AF_O + AFP_O] - [\phi_5 + \mu_r + \mu_{AF}(T)]AFP_H,\\
\frac{dAFP_R}{dt} &= \phi_5\cdot AFP_H - [\phi_6(T) + \mu_{AF}(T)]AFP_R,\\
\frac{dAFP_O}{dt} &= \phi_6(T)\cdot AFP_R - [\phi_7 + \mu_{AF}(T)]AFP_O.
\end{aligned}
\tag{1}
$$

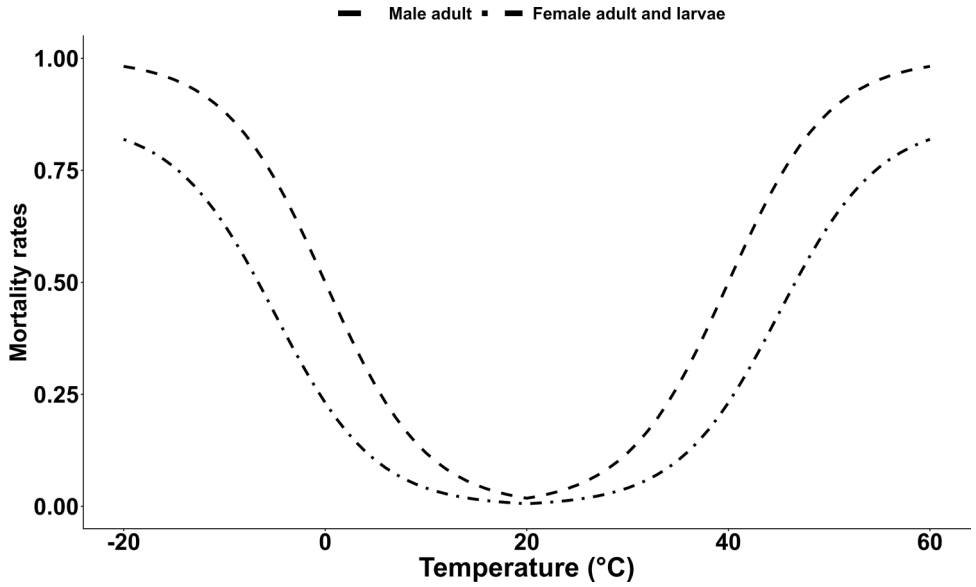


Fig. 3 Temperature-dependent mortality rates

$$\phi_1(T), \phi_2(T), \phi_3(T) = \frac{0.5}{1 + e^{0.1(10 - T)}} \quad (2)$$

$$\phi_8(P, T) = \begin{cases} \dfrac{1}{1 + e^{\frac{12.5 - P}{-0.5}}} & \text{if } T < 15^\circ\text{C} \\ 0 & \text{otherwise} \end{cases} \quad (3)$$

$$\phi_{10}(P, T) = \begin{cases} \dfrac{e^{\frac{P - 11}{0.5}}}{1 + e^{\frac{P - 11}{0.5}}} & \text{if } T > 6^\circ\text{C} \\ 0 & \text{otherwise} \end{cases} \quad (4)$$

$$\mu_L(T), \mu_P(T), \mu_{AF}(T) = \begin{cases} \dfrac{0.86}{1 + e^{0.2(45 - T)}} & \text{if } T > 20^\circ\text{C} \\ \dfrac{0.86}{1 + e^{\frac{5 + T}{5}}} & \text{otherwise} \end{cases} \quad (5)$$

$$K_L(R), K_P(R) = \kappa_X \cdot (R_{\text{norm}}(R) + 1) \quad X \in \{l, p\} \quad (6)$$

$$\phi_6(T) = \begin{cases} \dfrac{T - T_{Ag}}{TDD_{Ag}} & \text{if } T > T_{Ag} \\ 0 & \text{otherwise} \end{cases} \quad (7)$$

$$\mu_{AM}(T) = \begin{cases} \dfrac{1}{1 + e^{0.2(40 - T)}} & \text{if } T > 20^\circ\text{C} \\ \dfrac{1}{1 + e^{-\frac{T}{5}}} & \text{otherwise} \end{cases} \quad (8)$$

Model initialisation and parameterisation

Following previous implementations of climate-driven mosquito population models, simulations were initialised with 10^6 male and female eggs each (E_M, E_F) to avoid numerical extinction at the start of the simulation period [17]. In addition, small non-zero numbers (1000 specimens each) of emerging females (AF_{Em}) and emerging diapausing females (AF_{D1}) were assigned at initialisation to ensure that all coupled stage transitions in the model equations were defined from the first time step. The remaining compartments initially contain zero specimens, allowing population dynamics to develop from temperature-, rainfall-, and photoperiod-driven processes. Simulations from each sampling site were initialised using site-specific environmental data starting from 1 January 2015, which is 1 year prior to the first mosquito field sampling, to ensure that model outputs at the time of validation were not influenced by the choice of initial conditions. The simulations ended on 31 December 2023.

The majority of model parameters were derived from published literature (Table 1). Existing temperature-dependent development and mortality functions from studies conducted in Mediterranean regions led to unrealistic population collapse under temperate climatic conditions and were therefore unsuitable for Central and Northern Europe.

To address limitations of temperature-dependent mortality and developmental functions derived primarily from Mediterranean studies, biologically plausible functions were reformulated for temperate climatic conditions. The functional shape and range of the

Table 1 Table of all model parameters, their definitions, values or functional forms, and biological origin

Parameter	Definition	Value	Reference	Origin
$\phi_1(T)$	Egg development rate	Eq. 2	[16][a]	*Cx. pipiens* s.s.
$\phi_2(T)$	Larval development rate	Eq. 2	[16][a]	*Cx. pipiens* s.s.
$\phi_3(T)$	Pupal development rate	Eq. 2	[16][a]	*Cx. pipiens* s.s.
ϕ_4	Host-seeking rate	0.143	[16]	*Cx. pipiens* s.s./*Cx. torrentium*
ϕ_5	Resting rate	0.885	[16]	*Cx. pipiens* s.s./*Cx. torrentium*
$\phi_6(T)$	Oviposition site-seeking rate	Eq. 7	[16]	*Cx. pipiens* s.s./*Cx. torrentium*
ϕ_7	Egg-laying rate	0.2	[16]	*Cx. pipiens* s.s./*Cx. torrentium*
$\phi_8(P,T)$	Diapause induction rate	Eq. 3	[19, 20]	*Cx. pipiens* s.l.
$\phi_9(P,T)$	Non-diapause maintenance rate	$1-\phi_8(P,T)$	[19, 20]	*Cx. pipiens* s.l.
$\phi_{10}(P,T)$	Diapause termination rate	Eq. 4	[21]	*Cx. pipiens* s.l.
μ_E	Egg mortality rate	0.0262	[16]	*Cx. pipiens* s.s./*Cx. torrentium*
$\mu_L(T)$	Larval mortality rate	Eq. 5	[27, 28][a]	*Cx. pipiens* s.s.
$\mu_P(T)$	Pupal mortality rate	Eq. 5	[27, 28][a]	*Cx. pipiens* s.s.
$\mu_{AF}(T)$	Mortality rate of female adult mosquito	Eq. 5	[27, 28]	*Cx. pipiens* s.s.
$\mu_r(T)$	Host-seeking mortality	0.08	[16]	*Cx. pipiens* s.s./*Cx. torrentium*
$\mu_{AM}(T)$	Mortality rate of male adult mosquito	Eq. 8	[27, 28]	*Cx. pipiens* s.s.
$\mu_D(T)$	Mortality rate of diapausing female mosquito	0.02	[30]	*Cx. pipiens* s.s.
α	Sex ratio at emergence stage	0.5	[16]	*Cx. pipiens* s.s./*Cx. torrentium*
β	Strength of pupal density dependence	0.003	[a]	*Cx. pipiens* s.s.
T_E	Minimal temperature for egg maturation (°C)	9.8	[16, 31, 32]	*Cx. pipiens* s.l.
TDD_{Ag}	Degree-days for egg maturation (°C)	64.4	[16, 31, 32]	*Cx. pipiens* s.l.
κ_l	Larval standard environmental carrying capacity	8×10^8	[16, 31, 32]	*Cx. pipiens* s.l.
κ_p	Pupal standard environmental carrying capacity	10^7	[16, 31, 32]	*Cx. pipiens* s.l.

Cx. Culex, *s.l.* sensu lato, *s.s.* sensu stricto

[a] Functional forms or parameter magnitudes were informed by laboratory experiments conducted under fluctuating temperature regimes and supported by published studies

temperature–mortality relationship were informed by published experimental studies on *Cx. pipiens* s.s./*Cx. torrentium* (e.g. [27, 28]) and supported by independent survival (Additional file 1: Figure S1) and development (Additional file 1: Figure S2) experiments conducted by the authors under fluctuating temperature regimes in a climate chamber. These sources were used to define biologically realistic response shapes, while the viable temperature range was broadened to reflect survival under Europe-wide climatic conditions and heterogeneous environments.

This approach is consistent with recent assessments highlighting the limited transferability of temperature-dependent parameters derived under restricted climatic conditions and the need for biologically plausible extrapolation when applying mechanistic models across broader environmental gradients [29]. Model parameters were defined a priori to ensure biologically plausible seasonal timing, without reliance on calibration to field-derived abundance data.

Validation

Data for the validation of the process-based model were collected with CO_2-baited mosquito traps on a weekly, bi-weekly or daily basis from April to October in 2016–2017 and 2021–2023 (Fig. 4). In 2016, 41 sites were sampled; in subsequent years, 33 (2017), 22 (2021), eight (2022) and seven (2023) sites were sampled. All traps were run for approximately 24 h. For the 347 traps (of 3365 sampling events) that ran for > 24 h, the daily average was calculated. Five sampling sites were active across multiple years. All mosquitoes were identified by morphology using the taxonomic key by Becker et al. [1]. The blood-fed status of the caught mosquitoes was assessed using the Sella score [33], with mosquitoes categorised as unfed (Sella score 1) or as blood-fed (from freshly engorged to gravid; Sella score 2–7). Only female mosquitoes with a Sella score of 1 were used for validation, since these are the specimens considered to be host-seeking. Data from sampling sites were included in the analysis only if: the sites were sampled on at least six dates over 6 months per year, a total number of > 30 *Cx. pipiens* s.s./*Cx. torrentium* females were captured per year and > 10 mosquitoes were captured during the seasonal peak; this threshold

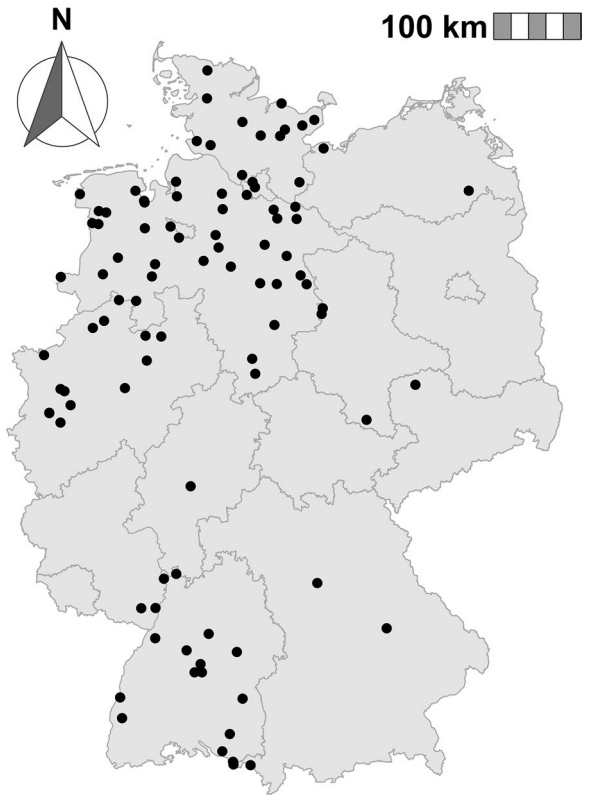


Fig. 4 Map of Germany showing all sampling sites used to validate the process-based model

was considered to be the minimum necessary to catch a representative seasonal dynamic. The final validation data set consisted of 106 sampling sites (Additional file 2: Tables S1, S2) with 73,540 *Cx. pipiens* s.s./*Cx. torrentium* females (mean per day = 26.69; 95% confidence interval [95% CI] 21.31–32.08). *Culex pipiens* s.s./*Cx. torrentium* females cannot be reliably distinguished by their morphology. Due to the ubiquitous distribution of *Cx. pipiens* s.s. and the fact that *Cx. torrentium* is less frequently captured using CO_2-baited traps, the potential inclusion of *Cx. torrentium* is expected to have little effect. However, to account for this uncertainty, we refer to these specimens collectively as *Cx. pipiens* s.s./*Cx. torrentium* throughout this manuscript.

Mean daily temperature and daily rainfall data (European Reanalysis and Observations for Monitoring [EURO4M] E-OBS v29 dataset; https://www.ecmwf.int/en/forecasts/dataset/european-reanalysis-and-observations-monitoring) were obtained from the ECA&D project (http://www.ecad.eu, [34]) and extracted for each sampling site for the period 2015–2023. For each sampling site and sampling date, the sum of simulated nulliparous and parous host-seeking females was compared with data from the field-caught samples. Therefore, smoothed rolling means were calculated for the captured mosquito counts, the process-based model output and the temperature-only baseline, using a rolling window length of 4 days to reduce short-term fluctuations. For each sampling site, all smoothed time series were subsequently normalised to relative values to remove differences in absolute magnitude and to focus on temporal dynamics. Because the response variable was bounded between 0 and 1, site-level inference was based on beta regression. Two beta regression models were fitted per site, with one model relating relative observed mosquito abundance to mechanistic model output and a second model relating relative observed abundance to daily mean temperature as a baseline comparison. Temperature-only models were included to assess how well temporal patterns could be explained without an explicit population model.

A Student's t-test was used to determine whether the correlation between the model's simulations and actual mosquito counts from field data was significantly different from the correlation between temperature alone and field data. Validation for all available data was conducted with a beta mixed-effects model, which analysed the relative number of simulated host-seeking female mosquitoes from the model and the relative number of field-collected female mosquitoes with a Sella score of 1. Hereby, the sampling site was used as a random effect. Again, we used an additional beta mixed-effects model to examine whether the process-based model provided any advantage over simply quantifying mosquito phenology based solely on temperature data. Model performance was quantified using regression coefficients, pseudo-R^2, and mean squared error (MSE) for site-specific analyses. For the pooled analysis across all sites, regression coefficients together with MSE and marginal and conditional R^2 from beta mixed-effects models were used to assess model performance. A complementary scatterplot analysis of observed versus modelled relative abundance was performed at different levels of aggregation (Additional file 1: S3). Specifically, values were first analysed at the original site-specific temporal resolution, then aggregated across sites within each year by calendar week and finally aggregated across sites and years by calendar week.

Consecutive generations per season

To account for the importance of the length of the mosquito biting season, we evaluated temperature- and photoperiod-dependent developmental transition rates within the process-based model to estimate generation turnover. For each life stage, the developmental time was calculated as the inverse of the corresponding transition

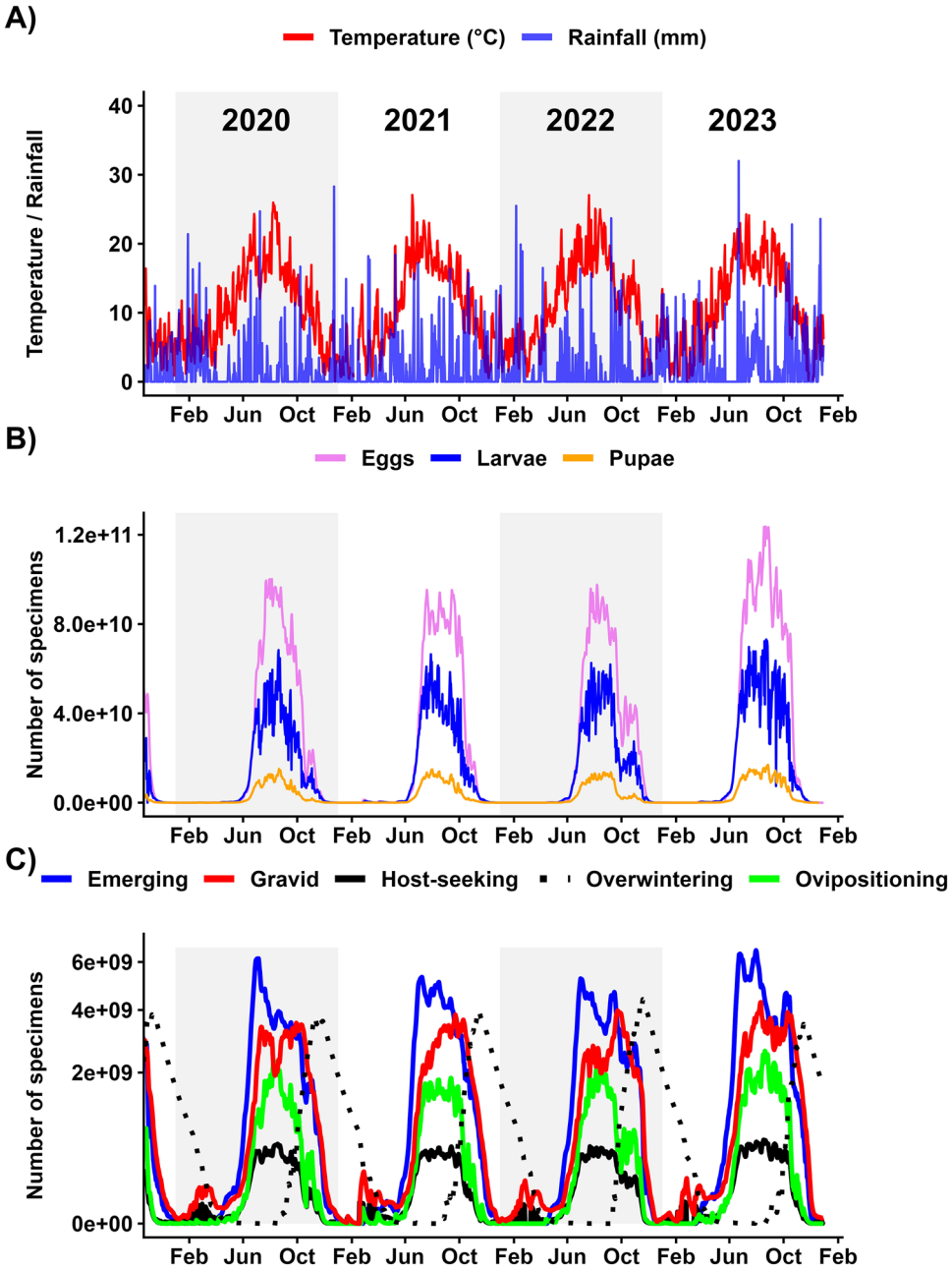


Fig. 5 Model output for a single sampling site in Hamburg, Germany, between 2020 and 2023, with corresponding environmental data (**A**), aquatic life stages (males and females summarised) (**B**) and adult life stages (nulliparous and parous females summarised; the *Y*-axis was square-root transformed for visualisation) (**C**)

rate, $\tau_i(T) = \frac{1}{\phi_i(T)}$, where $\phi_i(T)$ denotes the temperature-dependent developmental rate of each life stage. Total generation time was obtained by summing the developmental times across all life stages.

Developmental rates were evaluated using a 7-day mean temperature at the onset of each life stage. Based on the resulting total generation time, the maximum number of consecutive generations that could be completed within a season was calculated for each raster cell; these served as a proxy for the effective length of the mosquito season.

This model-based calculation was performed for each grid cell of the Europe-wide E-OBS raster for the time period 2021–2024. Due to known artefacts in the E-OBS dataset near the domain boundaries [35], maps were visually inspected and regions with implausible high or low

values were excluded prior to calculating area-weighted minimum, mean and maximum numbers of consecutive generations for Europe as a whole. In addition, a buffer zone of 50 km inside national borders was applied before calculating country-level summaries for Sweden, Germany and Spain, which represent northern, central and southern European regions, respectively.

Sensitivity analysis

We conducted a sensitivity analysis to gain insights into factors that influenced the general phenology of the population of host-seeking females (sum of nulliparous and parous females) throughout the simulation period. To this end, parameters were resampled using the Latin Hypercube Sampling, which is an efficient stratified Monte Carlo sampling method that allows for simultaneous sampling of the multidimensional parameter space [36, 37]. The simulation was carried out for 1 year, with 1000 simulations per run. Partial rank correlation coefficients (PRCCs) were computed for each selected input parameter and for the output variables (phenology of host-seeking females) for the entire simulation period.

Software

All analysis was performed in R (version: 4.5.2) using the RStudio IDE (version: 2026.01.04) [38]. Additionally, functions from the following packages were used for data preparation, visualisation and analysis: betareg [39], DHARMa [40], performance [41], dplyr [42], tidyr [43], ggplot2 [44], scales [45], rstatix [46], stringr [47], deSolve [48], sensitivity [49], lhs [50], knitr [51], plyr [52], ggpubr [53], zoo [54], raster [55], geosphere [56], lubridate [57] and xtable [58].

Results

Validation

The process-based model depicted a seasonal dynamic for every life stage for each sampling site (Fig. 5b, c). With an average pseudo-R^2-value of 0.54 (95% CI 0.49–0.59), site-specific beta regression demonstrated a significant positive association between the field data and model output for 79 sampling sites (Fig. 6; Additional file 2: Table S1); the remaining 21 sites showed no significant correlation. In contrast, site-specific beta regressions only correlating temperature with mosquito field data had an average pseudo-R^2-value of 0.37 (95% CI 0.32 - 0.41). The process-based model accounts for significantly more variation in the field data than does the daily average temperature alone ($t_{()} = 5.05$, $p < 0.0001$) and showed similar model error on the relative scale (MSE_{model} = 0.012; $MSE_{temperature}$ = 0.016). The beta mixed-effects model over all sites, which relates relative field captures to relative model predictions was significant (estimate [E] = 2.17, standard error [SE] = 0.062, $Z = 35.03$, $p < 0.0001$) and explained 40.42% of the variation for the fixed effect only (marginal [marg.] $R^2 = 0.4$) and 262.06% accounting for random variation among sampling sites (conditional [cond.] $R^2 = 0.62$). Again, the association between temperature and the field data was significant (E = 2.14, SE = 0.07, $Z = 29.55$, $p < 0.0001$), but explained less variation: 32.41% for the fixed effect (marg. $R^2 = 0.32$) and 56.71% accounting for random variation among sampling sites (cond. $R^2 = 0.57$). The process-based model showed a similar model error on the relative scale compared to the temperature ($MSE_{model} = 0.02$; $MSE_{temperature} = 0.02$).

Consecutive generations per season

Calculation of the theoretical maximum number of consecutive generations per year for *Cx. pipiens* s.s./*Cx. torrentium* resulted in a range of one to 10 generations per year across Europe, with an average of seven generations (Fig. 7). For example, in Spain, six to 10 generations were possible, with an average of nine generations; in Sweden, three to eight generations per year were calculated, with an average of six generations; and in Germany, the number of generations ranged from five to nine, with an average of eight generations.

Sensitivity analysis

In the sensitivity analysis, we observed that, in particular, the egg, larval and pupal development rates as well as the host-seeking, diapause entering rate and the number of females each male inseminates are positively correlated to the phenology of the population of host-seeking adults (PRCCs > 0.2; Fig. 8). A strong negative impact (PRCCs < − 0.2) on the phenology was found for the larval and pupal mortality rate and the mortality of adult females. The egg development rate contributed the most to the phenology (PRCCs = 0.52), followed by the larval development rate (PRCCs = 0.51). The strongest negative impact on the phenology was shown for the mortality rate of adult female mosquitoes (PRCCs = − 0.71).

Discussion

Our updated model with adapted temperature-dependent mortality and transition rates and overwintering compartment was able to depict the seasonal dynamics of *Cx. pipiens* s.s./*Cx. torrentium* for a temperate region. Although we observed strong site-specific differences in mosquito phenology, the developed process-based model was able to capture a large proportion of the observed variability. The newly added compartments, designed to integrate the overwintering period of the mosquitoes, successfully captured the mosquitoes' behaviours observed in the field. Female

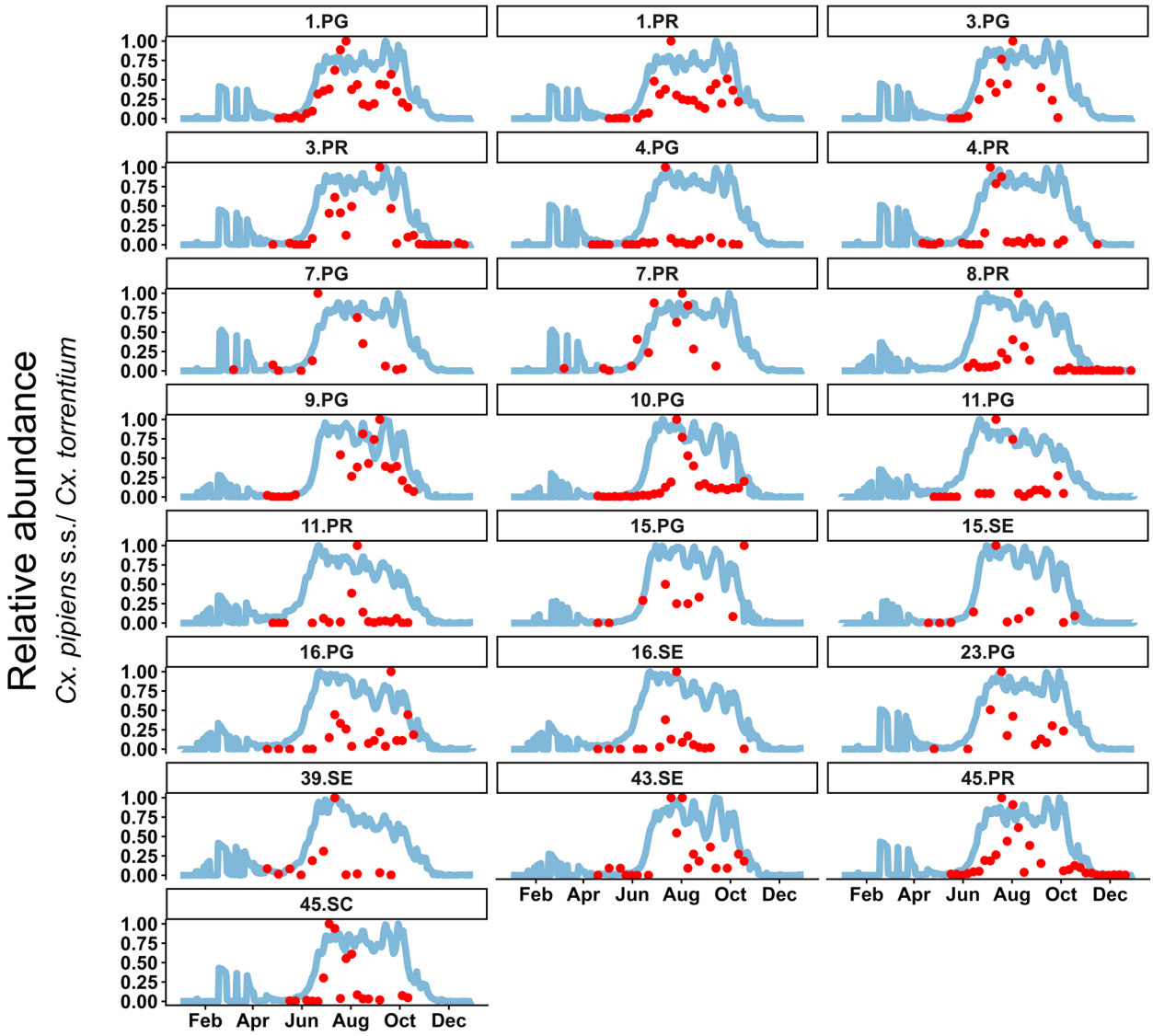


Fig. 6 Daily model output of the relative number of host-seeking *Culex pipiens* s.s./*Culex torrentium* (blue) and relative weekly averaged field data (red) for all sampling sites in 2021. Sampling site codes indicate trap types: PG = BG-Trap Station (Gravid), PR = BG-Trap Station, SE = BG-Sentinel 2, SE = VectorCube

Cx. pipiens s.s./*Cx. torrentium* overwinter, while the males do not survive [13, 30]. The inseminated females overwinter in burrows, barns and cellars and are the ones that start the new population by laying eggs in the beginning of the favourable season, after successfully feeding on a host. Photoperiod is considered to be the main trigger for the induction of the diapause [19, 20]. However, only during low temperatures was the threshold of < 15 h daylight found to induce diapause under laboratory conditions. Previous publications either relied on predefined favourable and unfavourable seasons to simulate overwintering behaviour [16] or, when diapause was explicitly modeled, it was triggered during a nulliparous stage rather than the larval stage [59]. To the authors' knowledge, this study represents the first process-based modelling approach that explicitly captures biologically realistic overwintering dynamics in *Culex* mosquitoes. However, characterisation of the overwintering ecology of *Culex* mosquitoes still contains important knowledge gaps, particularly regarding the termination of diapause at the end of the unfavourable season; in this context, more research is needed to fully grasp the relationship between temperature and photoperiod, and the termination of diapause [21, 60]. The inclusion of the overwintering stage allowed for a dynamic start and end of the season. Since natural

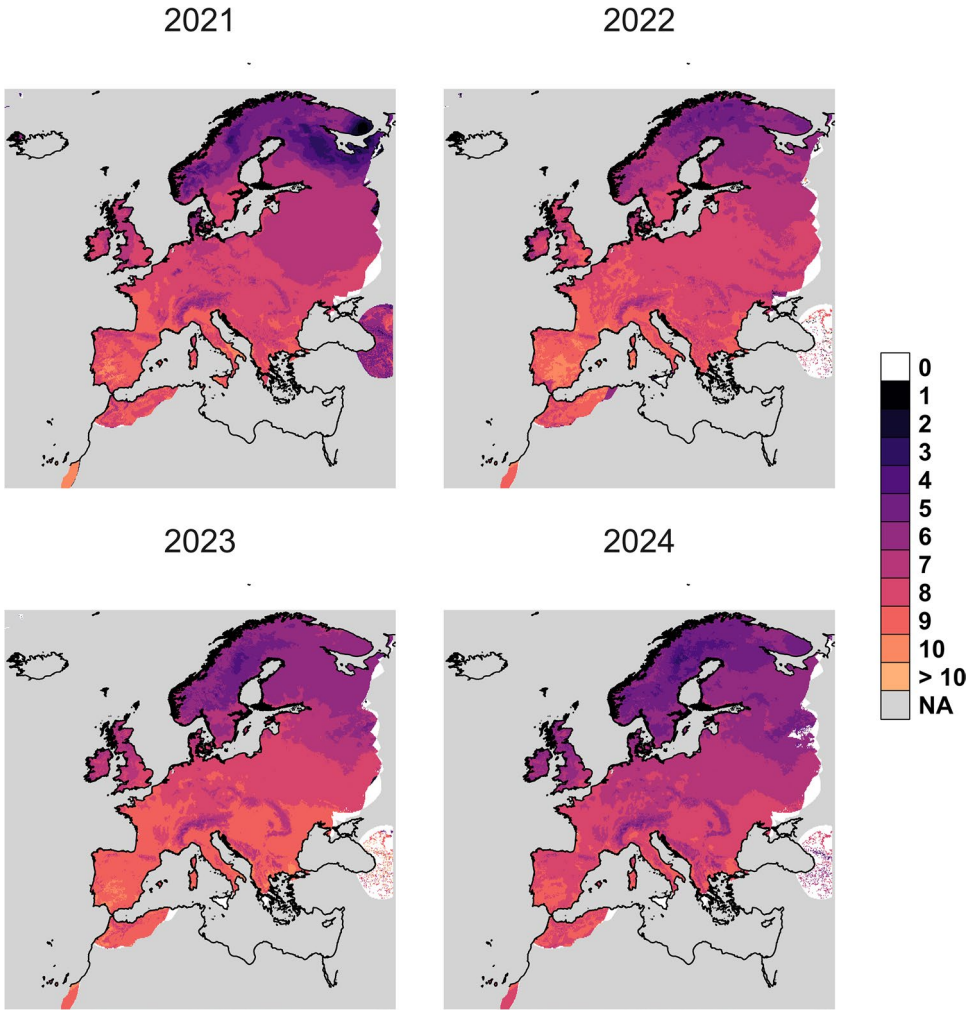


Fig. 7 Raster map of maximum number of consecutive generations per year for *Cx. pipiens* s.s./*Cx. torrentium* over Europe

photoperiod variations remain constant from year to year, only temperature thresholds can postpone the induction or termination of diapause, thereby shortening or extending favourable and unfavourable seasons. The temperature-dependent transition rates were designed to produce biologically meaningful values across the entire viable temperature range, with sigmoid functions reaching an upper plateau around the temperature optima. Previously used transition rates only delivered meaningful rates in a temperature range suitable to the respective study area. On this basis, the calculated maximum number of consecutive mosquito generations has the advantage that it does not only consider the beginning and ending of the favourable season but also incorporates meteorological data of the entire season. Previous studies have also highlighted the importance of the seasonal length in disease transmission risk [61]: a longer biting season is associated with a higher transmission risk. Also, the vertical transmission of a pathogen by an infected mosquito to its offspring plays a role in the persistence of WNV in temperate regions [62]. Therefore, this process-based model and the extracted maximum number of consecutive generations provides a framework for a more realistic assessment of the local virus transmission risk.

Although not all sampling sites showed a significant association in the site-specific beta regression models, the beta mixed-effects model across all sampling sites demonstrated a significant association between relative simulated and observed host-seeking female mosquito abundance. At the same time, mosquito phenology was shown to be strongly temperature-dependent, although temperature alone explained less variation in the data set than the process-based model. The MSE differed only marginally between the process-based model and the temperature-only baseline, reflecting the strong temperature dependence of mosquito phenology, which largely determines the timing of seasonal dynamics. In

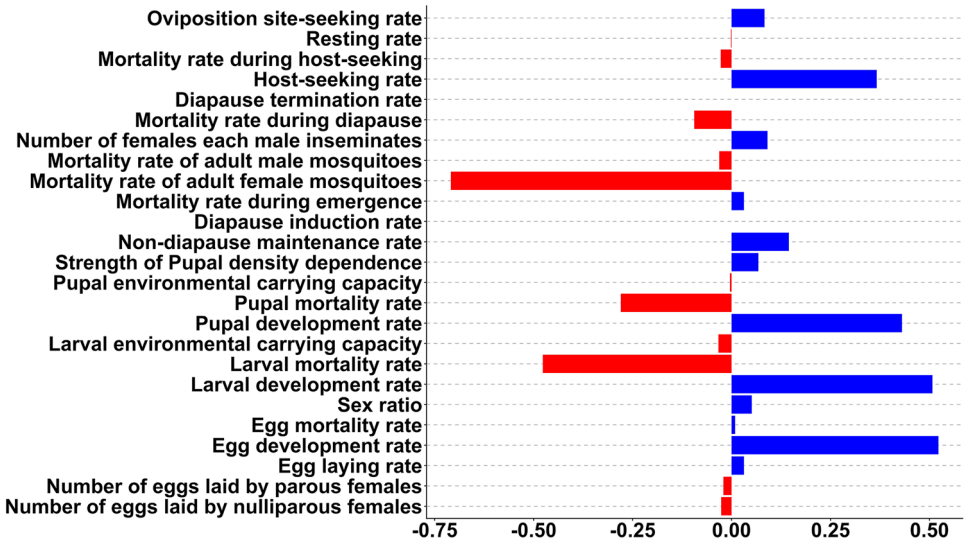


Fig. 8 Sensitivity analysis for the phenology of host-seeking females

contrast, the higher explained variance of the process-based model indicates that incorporating mechanistic life-cycle processes improves the representation of population structure and variability beyond temperature alone. The absence of a significant association at some sites likely reflects local heterogeneity in habitat structure, sampling intensity and microclimatic conditions that are not explicitly resolved by gridded environmental inputs, rather than a systematic failure of the model framework.

It should be noted that mosquito data collected from the field can be easily biased by various factors, such as sampling rhythms, weather conditions, trap position or errors by the volunteers running the trap, possibly leading to additional challenges in the validation of process-based models. Previous publications addressed such issues by averaging the mosquito collection data over several traps sampled on a weekly or biweekly basis and then using these data for validation on a regional scale [16–18]. In our study, we validated the model based on a large-scale data set from 106 sampling sites across Germany. We did not average the data from different sampling sites, thereby preserving the full variability of the mosquito collection data, allowing a detailed assessment of the model accuracy. Consistent with this, the scatterplot analysis (Additional file 1: Figure S3) shows that agreement between observed and modelled abundance increases with increasing levels of aggregation across sites, suggesting that discrepancies at fine temporal and spatial resolution are primarily driven by variability in the observational data rather than by structural limitations of the model. While stronger aggregation would likely improve apparent model performance, it would also mask site-specific variability and short-term dynamics. In addition, part of the mismatch at daily resolution likely arises from intrinsic oscillations of the model around the environmental carrying capacity that emerge from density-dependent processes. The remaining discrepancies therefore reflect a combination of model-inherent dynamics and environmental and sampling-related noise, including weather conditions (e.g. wind, rainfall) and variation in trap performance. Incorporating such processes explicitly, for example through an observation model or by accounting for trap success and environmental constraints, represents an important direction for future model development.

A process-based mosquito population model can be a very useful tool as it can provide valuable ecological insights, e.g. seasonal dynamics of the population or the potential maximum number of consecutive generations per season. Several parameters need further investigation to improve the accuracy of our process-based model. On the one hand, factors such as host-seeking rate or environmental carrying capacities rely on expert estimation, in contrast to temperature-dependent transition rates and mortality rates during the aquatic life stages, which could be at least experimentally measured in climate chambers. The sensitivity analysis indicates that mosquito phenology in the model is primarily driven by temperature-dependent development and mortality processes, while parameters related to host-seeking behaviour and density dependence introduce additional variability, highlighting both the biological realism of the model and key targets for future empirical

refinement. Future work could explore Bayesian calibration approaches for selected parameters, potentially using reduced-form or surrogate versions of the model, to formally quantify parameter uncertainty while retaining the mechanistic structure [63]. Additional compartments for process-based mosquito population models could be considered, i.e. life stages such as resting adult male mosquitoes, however, we still lack the necessary ecological knowledge.

While precipitation was represented in the model through its effect on aquatic habitat availability, heavy rainfall events can also negatively affect immature mosquito stages through the flushing or washout of breeding sites [64]. The magnitude of such effects depend strongly on the characteristics of the breeding site (e.g. size of container habitats) and the intensity of short-term rainfall, which cannot be captured by daily mean gridded precipitation data. Incorporating rainfall-induced flushing effects therefore represents an important direction for future model development, particularly in the context of increasing rainfall variability and extreme precipitation events under climate change scenarios.

In addition, the model does not differentiate between *Cx. pipiens* s.s. and *Cx. torrentium*, two closely related sibling species which probably have different temperature dependencies [65]. Knowledge of the thermal biology of *Cx. torrentium*, in particular, is scarce, and it is not yet possible to separate these two species in our model approach. In Central and Northern Europe, these species occur sympatrically and females can only be reliably distinguished using molecular methods, as morphological characteristics alone are insufficient for female identification [1], which limits the availability of species-specific field data for model validation. Although not stated as such, previous modelling approaches for "*Culex pipiens*" in Europe treated both species collectively as *Cx. pipiens* s.s./*Cx. torrentium* because field collections were based on CO_2-baited traps targeting females that can not be distinguished by morphological means [16, 18]. Given the predominance of *Cx. pipiens* s.s. in most regions, the potential inclusion of *Cx. torrentium* is expected to have little influence on model outcomes. This expectation is also supported by the fact that *Cx. torrentium* is disproportionately less captured by CO_2-baited traps compared to *Cx. pipiens* s.s. [12]. Nonetheless, this simplification introduces uncertainty, especially in regions such as Northern Europe where *Cx. torrentium* occurs in high abundance [66]. Future versions of this model could benefit from integrating species-specific thermal and developmental parameters once sufficient experimental and field data become available. Such data would enable a more accurate assessment of the species' respective ecological niches, overwintering behaviour and vector competence. Currently, however, the scarcity of field data on *Cx. torrentium* remains a major constraint for parameter differentiation and model validation..

Conclusions

Overall, this work shows that process-based models grounded in mechanistic thermal biology, and explicitly driven by temperature, photoperiod and rainfall, can meaningfully approximate seasonal *Cx. pipiens* s.s. and *Cx. torrentium* dynamics in temperate regions, and therefore provide a useful basis for more realistic assessments of local arbovirus transmission risk.

Supplementary Information

The online version contains supplementary material available at https://doi.org/10.1186/s13071-026-07410-4.

Additional file 1.

Additional file 2.

Additional file 3.

Acknowledgements

We gratefully acknowledge the voluntary helpers who supported the field work, and Lisa J. Winter for her help during laboratory work.

Author contributions

Conceptualisation: LR, PD, FGS, RL. Data collection: LR, PD, SMMA, HJ, TŞ, FGS, RL. Data analysis: LR, PD, FGS, RL. First draft: LR, FGS, RL. Writing and editing: all authors. All authors read and approved the final manuscript.

Funding

Open Access funding enabled and organized by Projekt DEAL. This work was supported by the Federal Ministry for the Environment, Nature Conservation, Nuclear Safety and Consumer Protection (Grant Number 3721484020), the Federal Ministry of Education and Research (Grant Number 01KI2022), and the German Research Foundation (Grant Number JO 1276/5-1).

Data availability

Validation data and a minimal reproducible example are available under https://github.com/Silence1490/A-process-based-model-simulating-the-life-cycle-of-Culex-pipiens-s.s.-Cx. -torrentium-in-Germany

Declarations

Ethics approval and consent to participate

Not applicable.

Consent for publication

Not applicable.

Competing interests

The authors declare no competing interests.

Received: 5 December 2025 Accepted: 8 April 2026
Published online: 11 May 2026

References

1. Becker N, Petrić D, Zgomba M, Boase C, Madon MB, Dahl C, et al. Mosquitoes: identification, ecology and control. 3rd ed. Berlin, London: Springer Nature; 2020.

2. Brugman VA, Hernández-Triana LM, Medlock JM, Fooks AR, Carpenter S, Johnson N. The role of *Culex pipiens* L. (Diptera: Culicidae) in virus transmission in Europe. Int J Environ Res Public Health. 2018;15:389.
3. Jansen S, Heitmann A, Lühken R, Leggewie M, Helms M, Badusche M, et al. *Culex torrentium*: a potent vector for the transmission of West Nile virus in Central Europe. Viruses. 2019;11:492.
4. Fros JJ, Miesen P, Vogels CBF, Gaibani P, Sambri V, Martina BEE, et al. Comparative Usutu and West Nile virus transmission potential by local *Culex pipiens* mosquitoes in north-western Europe. One Health. 2015;1:31–6.
5. Becker N, Jöst H, Ziegler U, Eiden M, Höper D, Emmerich P, et al. Epizootic emergence of Usutu virus in wild and captive birds in Germany. PLoS ONE. 2012;7:e32604.
6. Ziegler U, Santos PD, Groschup MH, Hattendorf C, Eiden M, Höper D, et al. West Nile virus epidemic in Germany triggered by epizootic emergence, 2019. Viruses. 2020;12:448.
7. Ziegler U, Jöst H, Müller K, Fischer D, Rinder M, Tietze DT, et al. Epidemic spread of Usutu virus in southwest Germany in 2011 to 2013 and monitoring of wild birds for Usutu and West Nile viruses. Vector-Borne Zoonotic Dis. 2015;15:481–8.
8. Orru S, Reissinger A, Filomena A, Heitmann A, Funk MB, Schmidt-Chanasit J, et al. Assessment of the effectiveness of West Nile virus screening by analysing suspected positive donations among blood donors, Germany, 2020 to 2023. Eurosurveillance. 2025;30:2400373.
9. Wehmeyer ML, Jaworski L, Jöst H, Şuleşco T, Rauhöft L, Afonso SMM, et al. Host attraction and host feeding patterns indicate generalist feeding of *Culex pipiens* s.s. and *Cx. torrentium*. Parasit Vectors. 2024;17:369.
10. Rosà R, Marini G, Bolzoni L, Neteler M, Metz M, Delucchi L, et al. Early warning of West Nile virus mosquito vector: climate and land use models successfully explain phenology and abundance of *Culex pipiens* mosquitoes in north-western Italy. Parasit Vectors. 2014;7:269.
11. Rudolf M, Czajka C, Börstler J, Melaun C, Jöst H, von Thien H, et al. First nationwide surveillance of *Culex pipiens* complex and *Culex torrentium* mosquitoes demonstrated the presence of *Culex pipiens* biotype pipiens/molestus hybrids in Germany. PLoS ONE. 2013;8:e71832.
12. Hesson JC, Ignell R, Hill SR, Östman O, Lundström JO. Trapping biases of *Culex torrentium* and *Culex pipiens* revealed by comparison of captures in CDC traps, ovitraps, and gravid traps. J Vector Ecol. 2015;40:158–63.
13. Sauer FG, Lange U, Schmidt-Chanasit J, Kiel E, Wiatrowska B, Myczko Ł, et al. Overwintering *Culex torrentium* in abandoned animal burrows as a reservoir for arboviruses in Central Europe. One Health. 2023;16:100572.
14. Lotka AJ. Elements of physical biology. Philadelphia: Williams & Wilkins; 1925.
15. Cailly P, Tran A, Balenghien T, L'Ambert G, Toty C, Ezanno P. A climate-driven abundance model to assess mosquito control strategies. Ecol Modell. 2012;227:7–17.
16. Ezanno P, Aubry-Kientz M, Arnoux S, Cailly P, L'Ambert G, Toty C, et al. A generic weather-driven model to predict mosquito population dynamics applied to species of *Anopheles*, *Culex* and *Aedes* genera of southern France. Prev Vet Med. 2015;120:39–50.
17. Tran A, L'Ambert G, Lacour G, Benoît R, Demarchi M, Cros M, et al. A rainfall-and temperature-driven abundance model for *Aedes albopictus* populations. Int J Environ Res Public Health. 2013;10:1698–719.
18. Marini G, Poletti P, Giacobini M, Pugliese A, Merler S, Rosà R. The role of climatic and density-dependent factors in shaping mosquito population dynamics: the case of *Culex pipiens* in northwestern Italy. PLoS ONE. 2016;11:e0154018.
19. Spielman A, Wong J. Environmental control of ovarian diapause in *Culex pipiens*. Ann Entomol Soc Am. 1973;66:905–7.
20. Field EN, Shepard JJ, Clifton ME, Price KJ, Witmier BJ, Johnson K, et al. Semi-field and surveillance data define the natural diapause timeline for *Culex pipiens* across the United States. Commun Biol. 2022;5:1300.
21. Nelms BM, Fechter-Leggett E, Carroll BD, Macedo P, Kluh S, Reisen WK. Overwintering biology of *Culex* (Diptera: Culicidae) mosquitoes in the Sacramento Valley of California. J Med Entomol. 2013;50:773–90.
22. Legros M, Lloyd AL, Huang Y, Gould F. Density-dependent intraspecific competition in the larval stage of *Aedes aegypti* (Diptera: Culicidae): revisiting the current paradigm. J Med Entomol. 2009;46:409–19.
23. Lutambi AM, Penny MA, Smith T, Chitnis N. Mathematical modelling of mosquito dispersal in a heterogeneous environment. Math Biosci. 2013;241:198–216.
24. Asman M. Observations of mating behavior in *Culex tarsalis*. Ann Entomol Soc Am. 1975;68:777–8.
25. Anguelov R, Dufourd C, Dumont Y. Mathematical model for pest–insect control using mating disruption and trapping. Appl Math Modell. 2017;52:437–57.
26. Andreadis SS, Dimotsiou OC, Savopoulou-Soultani M. Variation in adult longevity of *Culex pipiens* f. *pipiens*, vector of the West Nile Virus. Parasitol Res. 2014;113:4315–9.
27. Moser SK, Barnard M, Frantz RM, Spencer JA, Rodarte KA, Crooker IK, et al. Scoping review of *Culex* mosquito life history trait heterogeneity in response to temperature. Parasit Vectors. 2023;16:200. https://doi.org/10.1186/s13071-023-05792-3.
28. Rinehart JP, Robich RM, Denlinger DL. Enhanced cold and desiccation tolerance in diapausing adults of *Culex pipiens*, and a role for Hsp70 in response to cold shock but not as a component of the diapause program. J Med Entomol. 2006;43:713–22. https://doi.org/10.1093/jmedent/43.4.713.
29. de Wit MM, Martins AD, Delecroix C, Heesterbeek H, ten Bosch QA. Mechanistic models for West Nile virus transmission: a systematic review of features, aims and parametrization. Proc Biol Sci. 2024;291:20232432. https://doi.org/10.1098/rspb.2023.2432.
30. Sauer FG, Timmermann E, Lange U, Lühken R, Kiel E. Effects of hibernation site, temperature, and humidity on the abundance and survival of overwintering *Culex pipiens pipiens* and *Anopheles messeae* (Diptera: Culicidae). J Med Entomol. 2022;59:2013–21.
31. Ahumada JA, LaPointe DA, Samuel MD. Modeling the population dynamics of *Culex quinquefasciatus* (Diptera: Culicidae), along an elevational gradient in Hawaii. J Med Entomol. 2004;41:1157–70.
32. Balenghien T, Vazeille M, Grandadam M, Schaffner F, Zeller H, Reiter P, et al. Vector competence of some French *Culex* and *Aedes* mosquitoes for West Nile virus. Vector-Borne Zoonotic Dis. 2008;8:589–96.
33. Detinova TS. Age-grouping methods in Diptera of medical importance with special reference to some vectors of malaria. Monogr Ser World Health Organ. 1962:47:13–191.
34. Cornes RC, van der Schrier G, van den Besselaar EJM, Jones PD. An ensemble version of the E-OBS temperature and precipitation data sets. J Geophys Res Atmos. 2018;123:9391–409.
35. Copernicus—Climate Change Service. Known issues in E-OBS. 2024. https://surfobs.climate.copernicus.eu/userguidance/known_issues_eobs.php. Accessed 30 Apr 2024.
36. Blower SM, Dowlatabadi H. Sensitivity and uncertainty analysis of complex models of disease transmission: an HIV model, as an example. Int Stat Rev/Rev Int Stat. 1994;62:229–43.
37. Hoare A, Regan DG, Wilson DP. Sampling and sensitivity analyses tools (SaSAT) for computational modelling. Theor Biol Med Modell. 2008;5:1–18.
38. R Core Team. R: a language and environment for statistical computing. 2024. Vienna: R Foundation for Statistical Computing. https://www.R-project.org/.
39. Cribari-Neto F, Zeileis A. Beta regression in R. J Stat Softw. 2010;34:1–24.
40. Hartig F. DHARMa: residual diagnostics for hierarchical (multi-level / mixed) regression models; 2024. R package version 0.4.7. Available from: https://CRAN.R-project.org/package=DHARMa.
41. Lüdecke D, Ben-Shachar MS, Patil I, Waggoner P, Makowski D. performance: an R package for assessment, comparison and testing of statistical models. J Open Source Softw. 2021;6:3139.
42. Wickham H, François R, Henry L, Müller K, Vaughan D. dplyr: a grammar of data manipulation. 2026. R package version 1.2.1. https://CRAN.R-project.org/package=dplyr.
43. Wickham H, Vaughan D, Girlich M. tidyr: tidy messy data; 2025. R package version 1.3.2. https://CRAN.R-project.org/package=tidyr.
44. Wickham H. ggplot2: elegant graphics for data analysis. New York: Springer; 2016. https://ggplot2.tidyverse.org.
45. Wickham H, Pedersen TL, Seidel D. scales: scale functions for visualization. 2023. R package version 1.3.0. https://CRAN.R-project.org/package=scales.
46. Kassambara A. rstatix: pipe-friendly framework for basic statistical tests. 2025. R package version 0.7.3. https://CRAN.R-project.org/package=rstatix.

47. Wickham H. stringr: simple, consistent wrappers for common string operations. 2025. R package version 1.6.0. https://CRAN.R-project.org/package=stringr.
48. Soetaert K, Petzoldt T, Setzer RW. Solving differential equations in R: package deSolve. J Stat Softw. 2010;33:1–25.
49. Pujol G, Iooss B, Janon A, Sobieczky F, Da Veiga S, Delage T, et al. sensitivity: an R package for sensitivity analysis. J Stat Softw. 2008;62:1–25.
50. Carnell R. lhs: an R package for Latin hypercube sampling. J Stat Softw. 2012;46:1–7.
51. Xie Y. knitr: a general-purpose package for dynamic report generation in R. 2025. R package version 1.51. https://yihui.org/knitr/.
52. Wickham H. plyr: tools for splitting, applying and combining data. R J. 2011;3:29–32.
53. Kassambara A. ggpubr: 'ggplot2'-based publication-ready plots. R package version 0.6.3. 2026. https://CRAN.R-project.org/package=ggpubr.
54. Zeileis A, Grothendieck G. zoo: S3 infrastructure for regular and irregular time series. J Stat Softw. 2005;14:1–27.
55. Hijmans RJ. raster: geographic data analysis and modeling. R package version 3.6-32. 2025. https://CRAN.R-project.org/package=raster.
56. Hijmans RJ. geosphere: spherical trigonometry. R package version 1.6-8. 2026. https://CRAN.R-project.org/package=geosphere.
57. Grolemund G, Wickham H. Dates and times made easy with lubridate. J Stat Softw. 2011;40:1–25. https://www.jstatsoft.org/v40/i03/.
58. Dahl DB, Scott D, Roosen C, Magnusson A, Swinton J. xtable: export tables to LaTeX or HTML. 2019. R package version 1.8-4. https://CRAN.R-project.org/package=xtable.
59. Andrade R, White SM, Cobbold CA. Incorporating adult age into mosquito population models: implications for predicting abundances in changing climates. J Theor Biol. 2025;604:112084.
60. Onyeka JOA, Boreham PFL. Population studies, physiological state and mortality factors of overwintering adult populations of females of *Culex pipiens* L. (Diptera: Culicidae). Bull Entomol Res. 1987;77:99–111.
61. Ewing DA, Cobbold CA, Purse BV, Nunn MA, White SM. Modelling the effect of temperature on the seasonal population dynamics of temperate mosquitoes. J Theor Biol. 2016;400:65–79.
62. Anderson JF, Main AJ. Importance of vertical and horizontal transmission of West Nile virus by *Culex pipiens* in the Northeastern United States. J Infect Dis. 2006;194:1577–9.
63. Kennedy MC, O'Hagan A. Bayesian calibration of computer models. J R Stat Soc Series B Stat Methodol. 2001;63:425–64. https://doi.org/10.1111/1467-9868.00294.
64. Koenraadt CJM, Harrington LC. Flushing effect of rain on container-inhabiting mosquitoes *Aedes aegypti* and *Culex pipiens* (Diptera: Culicidae). J Med Entomol. 2008;45:28–35. https://doi.org/10.1093/jmedent/45.1.28.
65. Zittra C, Flechl E, Kothmayer M, Vitecek S, Rossiter H, Zechmeister T, et al. Ecological characterization and molecular differentiation of *Culex pipiens* complex taxa and *Culex torrentium* in eastern Austria. Parasit Vectors. 2016;9:1–9.
66. Hesson JC, Rettich F, Merdić E, Vignjević G, Östman O, Schäfer M, et al. The arbovirus vector *Culex torrentium* is more prevalent than *Culex pipiens* in northern and central Europe. Med Vet Entomol. 2014;28:179–86.

Publisher's Note

Springer Nature remains neutral with regard to jurisdictional claims in published maps and institutional affiliations.

4.4 Publication 4: *A temperature-driven diffusion model of Usutu virus spread in Germany with spillover into neighbouring countries*

arXiv:2605.03146v1 [q-bio.PE] 4 May 2026

A temperature-driven diffusion model of Usutu virus spread in Germany with spillover into neighbouring countries

Pride Duve[a,*], Dániel Cadar[a], Norbert Becker[b,c], Jonas Schmidt-Chanasit[a,d], Felix Gregor Sauer[a], and Renke Lühken[a]

[a]*Bernhard Nocht Institute for Tropical Medicine, Bernhard-Nocht-Straße 74, 20359 Hamburg, Germany*
[b]*Institute for Dipterology, Georg-Peter-Süß-Straße 3, 67346 Speyer, Germany*
[c]*University of Heidelberg, Grabengasse 1, 69117 Heidelberg, Germany*
[d]*University of Hamburg, Faculty of Mathematics, Informatics and Natural Sciences, Mittelweg 177, 20148 Hamburg, Germany*

Abstract

Usutu virus (USUV) is a flavivirus of the Japanese encephalitis complex transmitted between *Culex* mosquitoes and birds, a transmission pattern similar to that of the West Nile virus (WNV). In Germany, the first case of USUV was detected in 2010 in mosquitoes collected in the town of Weinheim, and by 2018 the virus had spread to almost the entire country. Interestingly, the infection front exhibited a clockwise rotational spread pattern throughout the years, a pattern completely different from that of the WNV. This clockwise progression corresponded closely with the spatial temperature gradient, suggesting that warmer regions probably facilitated faster viral amplification and onward transmission. Understanding the drivers that influence the spreading patterns of arboviruses is important as it guides surveillance and implementation of control strategies. In this study, we develop a reaction-diffusion partial differential equation (PDE) model to investigate the spatial spread of USUV in Germany within an extended domain that includes some neighbouring countries (Belgium, the Netherlands, and Luxembourg), thereby capturing cross-border transmission processes. Mosquito parameters, i.e., extrinsic incubation rate, mortality and biting rates, are temperature-driven, as temperature plays an important role in the activity of mosquitoes. Our model qualitatively reproduced the main spatial trends of USUV in Germany and surrounding countries. The heterogeneous spread pattern arises from the interplay of diffusion and spatially varying temperature, which together may influence determine regions with higher transmission potential.

Keywords: Usutu virus, diffusion, spread, birds, partial differential equations

1 Introduction

Mosquito-borne arboviruses are a global health concern. Despite their main relevance in tropical countries, Europe has recorded an increased number of mosquito-borne disease cases, both imported and autochthonous (Calzolari, 2016). Factors such as climate and land-use change, or long-distance travel, among others, have been closely linked to the expansion of several medically relevant mosquito species in the European continent (Cheng et al., 2018; Kolimenakis et al., 2021; Mangili and Gendreau, 2005; Semenza and Paz, 2021). Among the tropical viruses in Europe, the Usutu virus (USUV) has stood out in recent years as a particularly lethal pathogen for birds, especially blackbirds (*Turdus merula*) (Lühken et al., 2017). USUV is a mosquito-borne flavivirus of the

*Corresponding author: pride.duve@bnitm.de

Japanese encephalitis complex and circulates between birds and transmitted by mosquitoes, especially of the *Culex* genus (De Madrid and Porterfield, 1974; Jöst et al., 2011; Lühken et al., 2017). European blackbirds have been identified as the most susceptible amplifying host, while humans, equids, and other mammals are considered dead-end hosts, a transmission cycle similar to that of West Nile virus (WNV) (Nikolay, 2015).

USUV was first isolated from *Cx. neavei* mosquitoes in South Africa in 1959 near the Usutu river (Woodall, 1964). More than five decades later, the virus was retrospectively detected to have caused an extensive die-off of common blackbirds in the Tuscany region of Italy, in 1996 (Weissenböck et al., 2013). Since then, USUV has been confirmed in Austria, Hungary, Germany, the United Kingdom and other European countries (Simonin, 2024).

In Germany, the first case of USUV in mosquitoes was isolated from a pool of *Cx. pipiens* biotype *pipiens* trapped in August 2010 in South West Germany (Jöst et al., 2011). The phylogenetic analysis of this strain showed a close relationship with the USUV strain from Italy (Engel et al., 2016), indicating the spread within the European continent. Soon after, Germany experienced high blackbird mortality events (Becker et al., 2012b; Cadar et al., 2017a), and at least two cases of human infections were recorded among healthy blood donors (Allering et al., 2012; Cadar et al., 2017b). Infected blackbirds often show neurological clinical signs such as overturning, pedalling, and incoordination (Musto et al., 2022). On the other hand, infected humans may exhibit mild symptoms ranging from rash, jaundice, fever, and many more (Cadar and Simonin, 2022; Roesch et al., 2019). However, the emergence of neuroinvasive USUV disease has been also documented, including a recent fatal autochthonous case in an immunocompromised patient in Hungary in 2025 (Tóth et al., 2025; Szabó et al., 2025).

To date, USUV remains a major concern, with its re-emergence continuously threatening the avian population, and a potential to cause disease to humans (Vilibić-Čavlek et al., 2025). Despite its growing public health and veterinary importance, USUV remains understudied compared to other arboviruses (Cheng et al., 2018). Its genetic similarity with WNV and co-circulation in the same ecological niche further complicates its diagnosis and can have negative effects on its epidemiology (Nikolay, 2015). Thus, a further understanding of its spreading pattern, climate drivers, and spillover risks to mammals is required (Lühken et al., 2017). Moreover, a deeper understanding of the underlying factors influencing transmission patterns and the geographical spread of USUV can help to develop effective early warning systems. Therefore, in this study, we formulate and study a PDE model for USUV with an aim of mechanistically linking local transmission processes with spatial movement of mosquitoes and birds, and environmental heterogeneity via temperature gradients, in order to explain and model the spread of USUV.

Although the primary focus of this study is Germany, the inclusion of neighbouring regions such as the Netherlands, Belgium, and Luxembourg helps us better capture cross-border transmission dynamics, particularly in border areas where reported cases indicate possible spillover driven by ecological connectivity and host movement.

Several models have been studied to understand the transmission dynamics of USUV. Rubel et al. (2008) developed and calibrated the first model to explain USUV dynamics in Austria. The compartmental model consists of bird and mosquito populations, with temperature-dependent mosquito parameters. This model draws insights on how temperature patterns can be coupled with traditional process-based models to explain the USUV transmission cycle. Since then, many models have been studied, extended from this initial model considering further epidemiological and ecological factors. Reiczigel et al. (2009) extended this model into a hierarchical Bayesian model which adds stochasticity to deterministic models. The stochastic version improved the fitting to real-world USUV data, revealing the structure of inter-dependencies between different model parameters.

Brugger and Rubel (2009) modelled USUV using five global climate models with temperature-dependent parameters. The model considered four different climate-warming scenarios defined by

the Intergovernmental Panel on Climate Change, IPCC (20 different model-scenario combinations). Results from the simulation of the worst-case scenarios identified an endemic equilibrium with a decline of the blackbird population of about 24%. Machine learning models such as Maxent, are well known for their high predictive accuracy, especially when there is presence-only data. Therefore, Cheng et al. (2018) compared an environmental niche model with the compartmental model by Rubel et al. (2008) to evaluate the risk of USUV circulation in Europe. The study showed that the mechanistic model was able to capture the transmission potential but could overestimate the local transmission risk. On the other hand, the environmental niche models reproduced observed patterns yet underestimated emergence risk for new, previously uninfected regions. Lühken et al. (2017) studied a boosted regression tree-based model to identify areas suitable for USUV circulation and the effects of the virus on breeding bird populations in Germany. This modelling approach identified the southwestern region of Germany as the high-risk zone of USUV, although the virus circulation affected all federal states by the year 2018 (Michel et al., 2019).

While USUV models have been useful in identifying risk areas and potential outbreak drivers, such as temperature and rainfall, key uncertainties remain. Most existing models focus on the fixed spatial-temporal distribution of USUV. In fact, some models only explain the spatial distribution pattern in specific years without considering movement of USUV-infected specimens in time and space. However, in reality, hosts and vectors are not stationary but move locally roughly random manner in search of food, shelter and other dispersal factors (Hamer et al., 2014; Michel et al., 2019). Mathematically, this movement can be described by the diffusion process, represented by the Laplacian operator (Δ) added to each equation, which causes the population densities to flow from initially infected areas to more suitable ones across the domain. As a result, such a model becomes a reaction-diffusion PDE model, which can better depict real spatial patterns of USUV. Therefore, in this study, we extend the ordinary differential equation based model originally developed by Rubel et al. (2008) for the dynamics of USUV in Austria and we formulate a reaction-diffusion PDE model that includes bird and mosquito populations. This model incorporates the diffusion process, to simulate the random movement of birds and mosquitoes, while the reaction terms describe their interactions at each point in time and space.

2 Model description

In this study, we adopted the ordinary differential equation model by Rubel et al. (2008). This model is extended to include the diffusion process representing the random movement of both mosquitoes and birds, and mosquito parameters depend on the spatial temperature data for Germany, Netherlands, Belgium and Luxembourg. Our extended version consists of a system of PDEs with populations of mosquitoes and birds (Figure 1 and system 6). The mosquito population at any given time t and location $\boldsymbol{x} \in (x, y)$ is divided into susceptible: S_V, exposed: E_V, and infectious mosquitoes: I_V, with a total population $N_V = S_V + E_V + I_V$. Mosquitoes are recruited into the susceptible class via a logistic recruitment term: $b_V N_V \left[1 - \frac{N_V}{K_V}\right]$. Susceptible mosquitoes that interact with infectious birds progress to the exposed class, with a temperature dependent mosquito biting rate:

$$\beta(T, \boldsymbol{x}) = \frac{0.344}{1 + 1.231e^{-0.184(T-20)}}, \tag{1}$$

and a probability of acquiring an infection from a successful bite of an infectious bird of p_v. The force of infection on mosquitoes is given by

$$\lambda_{BV}(T, \boldsymbol{x}) = \frac{p_v \beta(T, \boldsymbol{x}) I_B}{N_B}. \tag{2}$$

In the exposed class, mosquitoes are infected but not yet infectious. Only after an incubation period of $\frac{1}{\gamma_V(T,\boldsymbol{x})}$ days they become infectious at a latency rate:

$$\gamma_V(T,\boldsymbol{x}) = \frac{1}{e^{-0.09T+5.36}}, \tag{3}$$

which was fitted for WNV in *Cx. pipiens* by Heidecke et al. (2025). A WNV latency rate is adopted because suitable USUV data to estimate the USUV extrinsic incubation period is unavailable. However, given the similarities between the two viruses, this assumption is reasonable (Rubel et al., 2008). Mosquitoes in all health states die at a natural death rate:

$$\mu_V(T,\boldsymbol{x}) = \frac{0.0025T^2 - 0.094T + 1.0257}{10}, \tag{4}$$

fitted in Rubel et al. (2008).

The population of birds under study is divided into susceptible: S_B, exposed: E_B, infectious: I_B, recovered: R_B, and dead birds: D_B. Birds are recruited into the susceptible class through a logistic recruitment rate of $b_B N_B\left[1-\frac{N_B}{K_B}\right]$, where $N_B = S_B + E_B + I_B + R_B$ is the total bird population. With a force of infection

$$\lambda_{VB}(T,\boldsymbol{x}) = \frac{\phi_B(\boldsymbol{x})p_b(\boldsymbol{x})\beta(T,\boldsymbol{x})I_V}{N_V} \tag{5}$$

susceptible birds (S_B) move to the exposed class (E_B). The parameter p_b measures the probability that a successful bite by an infectious mosquito leads to a new bird infection, while $\beta(T,\boldsymbol{x})$ is the mosquito biting rate and ϕ_B is the mosquito to bird ratio. Similar to WNV models (Bhowmick et al., 2020, 2023; Laperriere et al., 2011; Mbaoma et al., 2024), the mosquito to bird ratio is an important factor that determines the per biting pressure each bird receives, and therefore how efficiently a virus can spread.

Birds leave the exposed class (E_B) at a latency rate of γ_B, where they become infectious. A proportion ν_B of infectious birds (I_B) die due to the USUV at a rate α_B, while a proportion $1-\nu_B$ recovers at the same rate. The natural mortality rate of birds at all life stages is denoted by μ_B. The schematic diagram of the model under study is shown in Figure (1), while the corresponding system of equations is described by system (6).

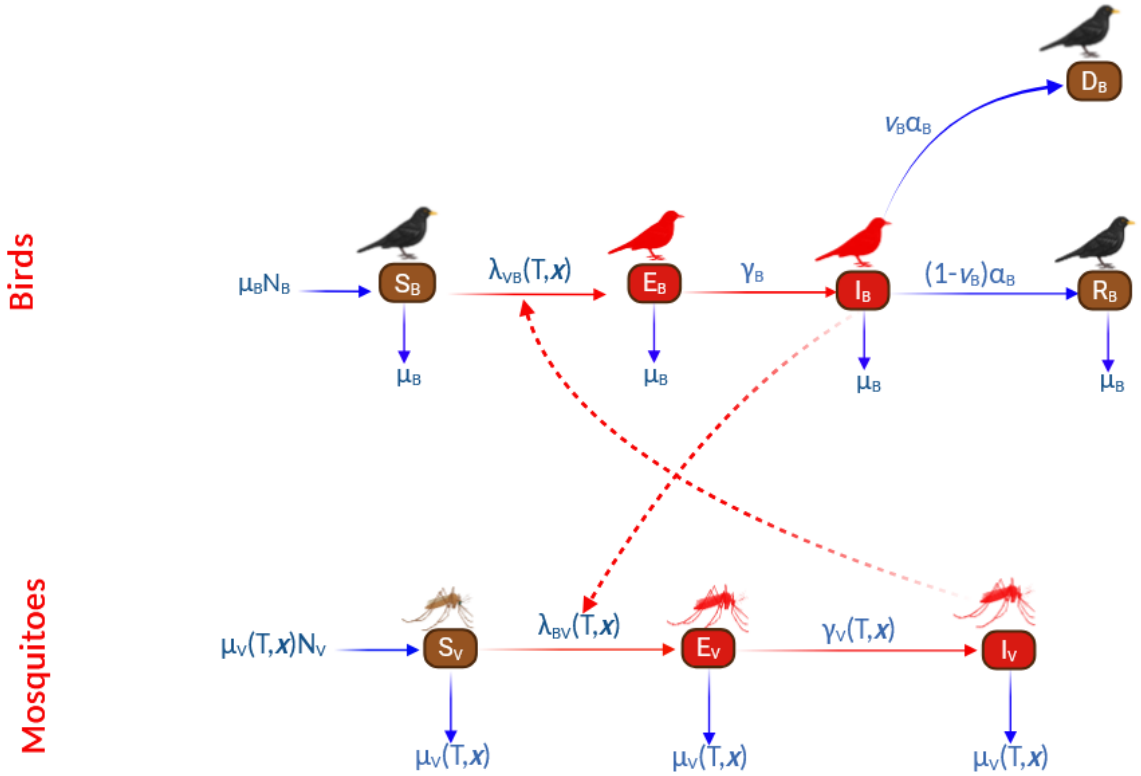


Figure 1: Flow chart diagram for the transmission dynamics of USUV. Red colours indicate infected classes, while dotted lines indicate cross-infection between birds and mosquitoes. Figure created using BioRender. Arbovirologie (2025), https://BioRender.com/r9wek95. Content not licensed under the Creative Commons Attribution (CC BY) license.

The system of equations becomes:

$$
\begin{aligned}
\frac{\partial S_V}{\partial t} &= D_1 \Delta S_V + b_V N_V \left[1 - \frac{N_V}{K_V}\right] - [\lambda_{BV}(T,\boldsymbol{x}) + \mu_V(T,\boldsymbol{x})] S_V, \\
\frac{\partial E_V}{\partial t} &= D_1 \Delta E_V + \lambda_{BV}(T,\boldsymbol{x}) S_V - [\gamma_V(T,\boldsymbol{x}) + \mu_V(T,\boldsymbol{x})] E_V, \\
\frac{\partial I_V}{\partial t} &= D_1 \Delta I_V + \gamma_V(T,\boldsymbol{x}) E_V - \mu_V(T,\boldsymbol{x}) I_V, \\
\frac{\partial S_B}{\partial t} &= D_2 \Delta S_B + b_B N_B \left[1 - \frac{N_B}{K_B}\right] - [\lambda_{VB}(T,\boldsymbol{x}) + \mu_B] S_B, \\
\frac{\partial E_B}{\partial t} &= D_2 \Delta E_B + \lambda_{VB}(T,\boldsymbol{x}) S_B - [\gamma_B + \mu_B] E_B, \\
\frac{\partial I_B}{\partial t} &= D_2 \Delta I_B + \gamma_B E_B - [\alpha_B + \mu_B] I_B, \\
\frac{\partial R_B}{\partial t} &= D_2 \Delta R_B + (1 - \nu_B)\alpha_B I_B - \mu_B R_B, \\
\frac{\partial D_B}{\partial t} &= \nu_B \alpha_B I_B,
\end{aligned}
\tag{6}
$$

subject to the initial conditions: $S_V(0,x) = \psi_1(x)$, $E_V(0,x) = \psi_2(x)$, $I_V(0,x) = \psi_3(x)$, $S_B(0,x) = \psi_4(x)$, $E_B(0,x) = \psi_5(x)$, $I_B(0,x) = \psi_6(x)$ $R_B(0,x) = \psi_7(x)$, $D_B(0,x) = D_{B_0}$, where $\boldsymbol{x} = (x,y) \in \Omega$, and $\Delta = \frac{\partial^2(\cdot)}{\partial x^2} + \frac{\partial^2(\cdot)}{\partial y^2}$. We assume the system moves in a region $\Omega \subset \mathbb{R}^2$, with a smooth boundary $\partial\Omega$

according to Fick's law (Fick, 1855), so that in the initial conditions, $\boldsymbol{x} \in \Omega$, where $\psi_i \in C^2(\Omega) \cap C(\bar{\Omega})$ and subject to the homogeneous Neumann boundary conditions:

$$\frac{\partial S_V}{\partial \nu} = \frac{\partial E_V}{\partial \nu} = \frac{\partial I_V}{\partial \nu} = \frac{\partial S_B}{\partial \nu} = \frac{\partial E_B}{\partial \nu} = \frac{\partial I_B}{\partial \nu} = \frac{\partial R_B}{\partial \nu} = 0,$$

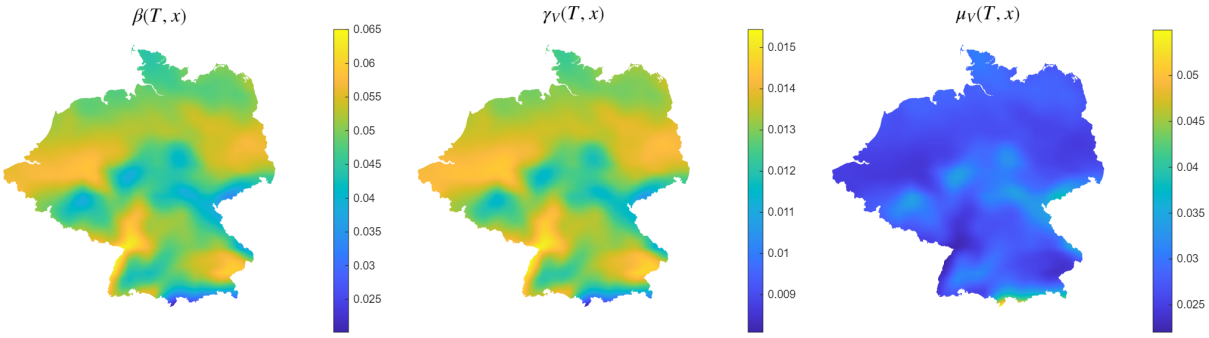
for $\boldsymbol{x} \in \partial\Omega$, $t > 0$, and ν is the unit outer normal to Ω. Variables and parameters used in the model are summarized in Table (1).

Detailed proofs of the existence, positivity, and boundedness of solutions to the PDE model are presented in Appendix (6.1).

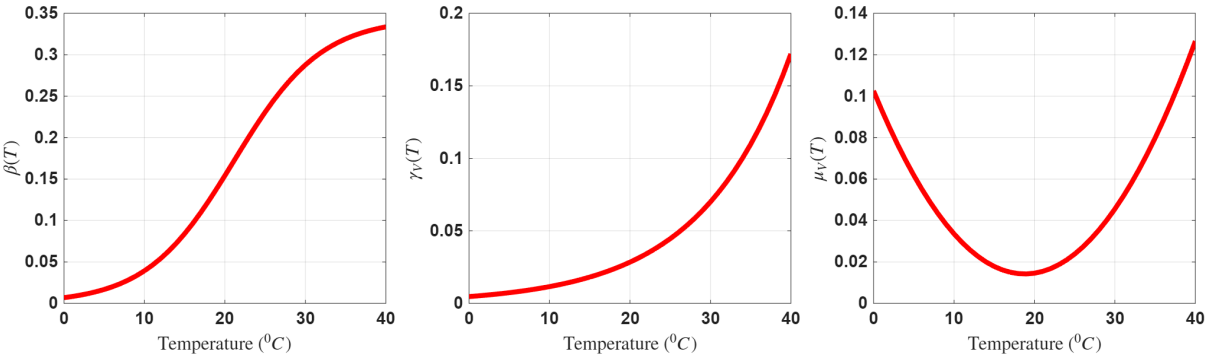
3 Methods

3.1 Temperature forcing

Temperature is a key environmental variable for USUV transmission and spread (Rubel et al., 2008). It is known for its influence on the mosquito life-history traits, including biting rate, development time, survival, and dispersal. In addition, viral processes such as the extrinsic incubation period within the mosquito shorten at higher temperatures, increasing transmission potential. Consequently, temperature directly modulates the effective transmission rate and can create seasonal windows when outbreaks are possible, especially in temperate regions such as Germany. In this study, temperature-dependent parameters, i.e., mosquito biting rate, latency rate and mortality rate, are adopted from experimental studies (Rubel et al., 2008) and (Heidecke et al., 2025). The thermal functions are defined in Eqn. (1, 3, 4) and their spatio-temporal plots in Fig. (2).



(a) Space-dependent thermal mosquito parameters for the year 2018.



(b) Temperature evolution for mosquito parameters.

Figure 2: Spatio-temporal mosquito biting rate $\beta(T,x)$, mortality rate $\mu_V(T,x)$ and extrinsic incubation rate $\gamma_V(T,x)$ over the geometry (merged maps of Belgium, Germany, Luxembourg and the Netherlands).

3.2 USUV free equilibrium point and the local reproduction number

System (6) admits an USUV-free equilibrium point $\mathscr{E}_0$:

$$\mathscr{E}_0: \quad \left[S_V^0, E_V^0, I_V^0, S_B^0, E_B^0, I_B^0, R_B^0, D_B^0\right] = \left[K_V\left[1-\frac{\mu_V}{b_V}\right], 0, 0, K_B\left[1-\frac{\mu_B}{b_B}\right], 0, 0, 0, 0\right]. \tag{7}$$

The uniqueness of $\mathscr{E}_0$ follows from [(Wang et al., 2018), Lemma 2.1]. The local basic reproductive number denoted by $R_0(\boldsymbol{x})$ is the average number of new infections produced by a single infectious mosquito or bird. In this case, we use it to create spatial USUV risk maps such that regions where $R_0(\boldsymbol{x})$ imply a higher risk, compared to regions where it is low. $R_0(\boldsymbol{x})$ is computed using the next generation matrix method defined by (Diekmann et al., 2009), and applied in an USUV model by (Rubel et al., 2008). Infected terms of system (6) are re-written in terms of the rate of appearance of new infections in compartment i, denoted F_i, and the rate of transfer into and out of compartment i, denoted V_i, where $i = E_V, I_V, E_B, I_B$ (van den Driessche and Watmough, 2002), such that:

$$\mathscr{F}(\boldsymbol{x}) = \begin{bmatrix} \frac{p_v\beta(\boldsymbol{x})I_B S_V}{N_B} \\ 0 \\ \frac{\phi_B p_b \beta(\boldsymbol{x}) I_V S_B}{N_V} \\ 0 \end{bmatrix}, \quad \text{and} \quad \mathscr{V}(\boldsymbol{x}) = \begin{bmatrix} (\gamma_V(\boldsymbol{x}) + \mu_V(\boldsymbol{x}))E_V \\ -\gamma_V(\boldsymbol{x})E_V + \mu_V(\boldsymbol{x})I_V \\ (\gamma_B + \mu_B)E_B \\ -\gamma_B E_B + (\alpha_B + \mu_B)I_B \end{bmatrix}.$$

Taking partial derivatives, we have:

$$F(\boldsymbol{x}) = \begin{bmatrix} 0 & 0 & 0 & \frac{p_v\beta(\boldsymbol{x})S_V^0}{N_B^0} \\ 0 & 0 & 0 & 0 \\ 0 & \frac{\phi_B p_b \beta(\boldsymbol{x}) S_B^0}{N_V^0} & 0 & 0 \\ 0 & 0 & 0 & 0 \end{bmatrix}, \quad \text{and} \quad V(\boldsymbol{x}) = \begin{bmatrix} \gamma_V(\boldsymbol{x}) + \mu_V(\boldsymbol{x}) & 0 & 0 & 0 \\ -\gamma_V & \mu_V & 0 & 0 \\ 0 & 0 & \gamma_B + \mu_B & 0 \\ 0 & 0 & -\gamma_B & \alpha_B + \mu_B \end{bmatrix}.$$

The basic USUV reproductive number is given by the largest eigenvalue of the matrix FV^{-1}, and is given by

$$R_0(\boldsymbol{x}) = \sqrt{\left(\frac{\beta(\boldsymbol{x})p_v(\boldsymbol{x})\gamma_B(\boldsymbol{x})}{[\gamma_B(\boldsymbol{x}) + \mu_B(\boldsymbol{x})][\alpha_B(\boldsymbol{x}) + \mu_B(\boldsymbol{x})]}\right) \times \left(\frac{\phi_B(\boldsymbol{x})\beta(\boldsymbol{x})p_b(\boldsymbol{x})\gamma_V(\boldsymbol{x})}{[\gamma_V(\boldsymbol{x}) + \mu_V(\boldsymbol{x})]\mu_V(\boldsymbol{x})}\right)}. \tag{8}$$

The USUV reproductive number ($R_0(\boldsymbol{x})$) represents the average number of new infections caused by a single infected mosquito or bird, in a completely susceptible population. In precise, ($R_0(\boldsymbol{x})$) can be written as

$$R_0(\boldsymbol{x}) = \sqrt{r_b \times r_m}, \text{ where } r_b = \frac{\beta(\boldsymbol{x}) p_v \gamma_B}{(\gamma_B + \mu_B)(\alpha_B + \mu_B)} \text{ and } r_m = \frac{\beta(\boldsymbol{x}) p_b \gamma_V(\boldsymbol{x})}{(\gamma_V(\boldsymbol{x}) + \mu_V(\boldsymbol{x}))\mu_V(\boldsymbol{x})}$$

can be interpreted as the average number of new bird infections per infectious mosquito, and the average number of new mosquito infections per infectious birds, respectively. $(R_0(\boldsymbol{x}))$ shows the spatial variation of USUV across different regions (Figure 4). For a specific location in Germany, higher values of $(R_0(\boldsymbol{x}))$ indicate a heightened USUV risk compared to regions with lower values. The spatial heterogeneity in $(R_0(\boldsymbol{x}))$ further reflects temperature associated geographical variation of USUV transmission and spread.

3.3 USUV data

Unlike many human and animal (pet and livestock) infectious diseases, USUV circulation is not easy to detect because it primarily affects wild bird populations, which are more challenging to monitor. Human clinical surveillance is limited because infections in humans are usually asymptomatic. In some instances, infections have been identified incidentally through blood donor screening (Angeloni et al., 2023), but such detections may not reliably reflect broader infection patterns.

As a result, a nationwide surveillance programme was established in Germany, encouraging citizens to report and submit dead birds for laboratory testing. This citizen science initiative, led by the Bernhard Nocht Institute for Tropical Medicine, enabled large-scale spatial and temporal monitoring of USUV circulation nationwide. However, as with most passive surveillance systems, certain limitations need to be recognised, including potential reporting bias towards urban areas, variation in carcass condition caused by shipping delays and decomposition, and occasional inaccuracies in recorded collection locations. Despite these challenges, USUV data for Germany indicated a widespread presence across the country by 2018 (Figure 4), with regions in the southwest (along the Upper Rhine valley) and Hamburg showing high circulation.

While the available German surveillance data largely depend on passive monitoring of dead birds, the available data from the Netherlands were collected within a comprehensive One Health active surveillance program for USUV in 2016. This nationwide monitoring system included sampling of live, free-ranging birds and dead birds until 2022. Live birds were captured by trained volunteer bird ringers across the country and sampled via throat and cloacal swabs, as well as blood, for serological testing. Dead birds were mainly reported through citizen submissions and examined at the Dutch Wildlife Health Centre, where necropsies were performed, and brain tissue was tested for USUV. From 2019, mosquitoes were also sampled for USUV, and all submitted birds underwent systematic testing regardless of the suspected cause of death (Münger et al., 2025).

The increased USUV circulation in both birds and humans in the neighbouring Luxembourg prompted the initiation of passive surveillance as an early warning system (Snoeck et al., 2022; Vilibic-Cavlek et al., 2020). A total of 61 samples were tested as part of surveillance based dead-bird monitoring. During the surveillance period, 33 birds were examined, and only one Eurasian blackbird (*Turdus merula*) detected in September 2020 tested positive for USUV, marking the first confirmed case in the country.

In Belgium, USUV circulation has also been documented primarily through regional passive surveillance, rather than a continuous nationwide monitoring program similar to that in Germany and the Netherlands. Following unusual bird mortality events, USUV was first detected in southern Belgium in 2016, with confirmed cases identified through RT-qPCR testing of dead wild birds submitted to wildlife rehabilitation centres (Benzarti et al., 2020; Cadar et al., 2017a). Between 2017 and 2018, expanded passive monitoring detected numerous USUV-positive birds across several species, particularly Eurasian blackbirds (*Turdus merula*), indicating active local transmission and suggesting the virus had become established (Benzarti et al., 2020).

Our data for fitting the model thus comes from various heterogeneous sources. More precisely, the German and Dutch data mainly originate from citizen science projects conducted in those countries. Cases from the Netherlands are published in Münger et al. (2025) and van den Brand et al. (2025), while the single case observed in Luxembourg in 2020 has been documented in (Snoeck et al., 2022), and the Belgian cases were reported in several studies, including (Cheng et al., 2018; Qiu et al., 2025). Citizen science data from Germany are published along with this study. Consequently, the data are only intended for reference to help identify regions with higher circulation risks.

3.4 Simulation framework

In the model simulation, the densities of susceptible birds and mosquitoes are assumed to be spatially homogeneously distributed across the entire domain. An estimated area for mainland Germany, Netherlands, Belgium and Luxembourg from our simplified geometry is A=426,840 km^2 $\approx 4.2684 \times 10^{11}$ m^2. Thus, assuming a total bird population of 110 million all over Germany, we estimate a bird density of $110 \times 10^6/A \approx 2.6 \times 10^{-4}$ susceptible birds per square meter. Given the high abundance of *Culex* mosquitoes (Becker et al., 2012a; Rudolf et al., 2013; Walther and Kampen, 2017), we assume an initial susceptible mosquito population of $2 \times 10^9/A$ yielding a density of 0.00467 susceptible mosquitoes per square meter.

Diffusion coefficients are estimated using inverse modelling, by adjusting them within the species reasonable mobility rates per day. The selected values are then interpreted using the root-mean-square displacement (RMSD), a metric that describes the dispersal distance species move from the initial source under diffusion after a time τ (Einstein, 1905; Metelmann, 2019). The RMSD is calculated using the formula:

$$\text{RMSD} = \sqrt{2pD\tau},$$

where p = 2 is the spatial dimension, D is the diffusion coefficient and τ is the time step.

Although reported cases likely under-represent the true extent of circulation due to a risk of under-reporting, they nevertheless serve as reliable indicators of regions where transmission is active. Because of this, we seed initial conditions for the infected classes in the Southwestern (around Weinheim) and Western regions (around Bonn), as described in the observed dataset. Infections were confirmed in these regions and their surroundings by the end of 2011, and thus the initial condition distribution is centred at these regions, according to a Gaussian distribution:

$$f(t, \boldsymbol{x}) = e^{-\frac{(x-x_0)^2 + (y-y_0)^2}{2\sigma^2}}. \tag{9}$$

In eq (9), (x_0, y_0) are the central nodes of the infected regions, and $\sigma = 40$ km is the standard deviation which controls the spatial radius over which the initial infection is present. Integrating eq (9) over the mesh gives the total mass B, which normalizes initial conditions for infected classes defined by the Gaussian. To ensure effective interaction of reaction terms during the simulation process, we choose initial infected populations in such a way that $S_V/A - E_V/B - I_V/B > 0$ and $S_B/A - E_B/B - I_B/B - R_B/B > 0$. The model variables and initial conditions are summarized in Table (1).

Our PDE model is solved numerically using the Matlab PDEToolbox (The MathWorks, Inc., 2025), which solves PDEs of the form:

$$m\frac{\partial^2 u}{\partial t^2} + d\frac{\partial u}{\partial t} - \nabla \cdot (c\nabla u) + au = f. \tag{10}$$

Table 1: Definition of state variables and parameters.

Variable/Parameter	Definition	Value	Source
S_V	susceptible mosquitoes (mosquitoes/m^2)	$2 \times 10^9/A$	defined by the authors
E_V	exposed mosquitoes (mosquitoes/m^2)	$10 \times 10^6/B$	defined by the authors
I_V	infectious mosquitoes (mosquitoes/m^2)	$10 \times 10^6/B$	defined by the authors
S_B	susceptible birds (birds/m^2)	$110 \times 10^6/A$	defined by the authors
E_B	exposed birds (birds/m^2)	$1 \times 10^6/B$	defined by the authors
I_B	infectious birds (birds/m^2)	$1 \times 10^6/B$	defined by the authors
R_B	recovered birds (birds/m^2)	$1 \times 10^6/B$	defined by the authors
D_B	dead birds (birds/m^2)	$1 \times 10^6/B$	Defined by the authors
$\beta(T, \boldsymbol{x})$	mosquito biting rate	Eq (1)	(Rubel et al., 2008)
$\gamma_V(T, \boldsymbol{x})$	latency rate of mosquitoes	Eq (3)	(Heidecke et al., 2025)
$\mu_V(T, \boldsymbol{x})$	mortality rate of mosquitoes	Eq (4)	(Rubel et al., 2008)
$\gamma_B(\boldsymbol{x})$	latency rate of birds	0.667	(Rubel et al., 2008)
$\alpha_B(\boldsymbol{x})$	removal rate of birds	0.0182	(Rubel et al., 2008)
$\nu_B(\boldsymbol{x})$	fraction of birds dying due to the infection	0.3	(Rubel et al., 2008)
$\mu_B(\boldsymbol{x})$	mortality rate of birds	0.0012	(Rubel et al., 2008)
$p_\nu(\boldsymbol{x})$	probability of virus transmission by infectious birds	0.125	(Rubel et al., 2008)
$p_b(\boldsymbol{x})$	probability of virus transmission by infectious mosquitoes	1.000	(Rubel et al., 2008)
$\phi_B(\boldsymbol{x})$	mosquito to bird ratio	Table (2)	defined by the authors
K_V	environmental carrying capacity of mosquitoes	$S_V(0, \boldsymbol{x})$	(Rubel et al., 2008)
K_B	environmental carrying capacity of birds	$S_B(0, \boldsymbol{x})$	(Rubel et al., 2008)
$D_1(\boldsymbol{x})$	diffusion coefficient for mosquitoes	Table (2)	defined by the authors
$D_2(\boldsymbol{x})$	diffusion coefficient for birds	Table (2)	defined by the authors

In our case, $m = 0, d = 1, a = 0$, and matrices c and f are defined in Appendix (6.3). The matrix c consists of the diffusion coefficients, while f stores reaction terms. The full algorithm for the solver is fully explained in our West Nile virus study (Duve et al., 2026). It is important to compare our model results with the observed data. However, given that the PDE model produces a continuous solution, while the observed data is discrete, fitting the model is not straightforward. We fitted our model predictions by aggregating our annual PDE solution and the annual observed data into the GADM level-2 administrative units of Germany (Global Administrative Areas, 2024), comprising 356 rural districts (Landkreise) and urban districts (kreisfreie Städte). We then tested for a Spearman's correlation between the simulated districts and observed, by checking if high predicted regions correspond to regions with high observed cases.

4 Results

With USUV initially detected in Weinheim and Bonn in 2011, a notable range expansion is observed towards Belgium, the Netherlands, and northern Germany (Figure 5). Cases increased since 2011, although the spread has been slower over the years. The root mean squared displacement (RMSD) in both mosquitoes and birds increased steadily during this period. The Spearman's correlation values, reported as ρ, ranged from 0.29 to 0.44 across all years (2011-2018), indicating a weak positive monotonic relationship between the observed data and the model predictions (Figure 8). This could be because the PDE solution is continuous and highly sensitive to small values, similar to noise, which may be present in regions without confirmed cases. On the other hand, under-reporting cannot be ruled out either. However, despite this, there is some visual agreement between the observed distributions and the predicted cases, with the main circulation area remaining in the south-west (around the Rhein valley) (Figures 5, 6, 7, 8). In 2016, an isolated case was recorded in the eastern part of Germany, within Berlin, and more cases were observed in the Netherlands. Since

Table 2: Values for the diffusion coefficients for mosquitoes and birds (D_1, D_2) in km^2 per day, root mean squared displacement (RMSD) in km, mosquito to bird ratio (ϕ_B) Spearman's rank correlation coefficient (ρ), and p-values.

Year	D_1	D_2	$RMSD_1$	$RMSD_2$	ϕ_B	ρ	p-value
2012	3.0	6.0	57.4	81.2	30	0.37	5.5×10^{-13}
2013	8.0	10.0	93.8	104.9	40	0.38	1.8×10^{-13}
2014	3.0	6.0	57.4	81.2	40	0.40	6.1×10^{-15}
2015	6.0	9.0	81.2	99.5	30	0.41	1.4×10^{-15}
2016	5.0	8.0	74.2	93.8	50	0.44	5.7×10^{-18}
2017	5.0	8.0	74.2	93.8	30	0.41	3.4×10^{-16}
2018	5.0	8.0	74.2	93.8	40	0.29	4.4×10^{-8}

then, a rising number of new cases has been detected in Belgium, the Netherlands, and subsequently across Germany. Luxembourg lies in a low-risk area (Figure 4), and the first case in this country was reported in 2020.

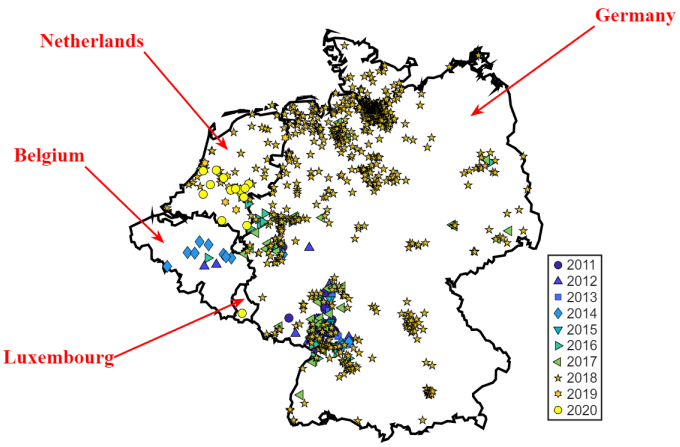


Figure 3: Observed data.

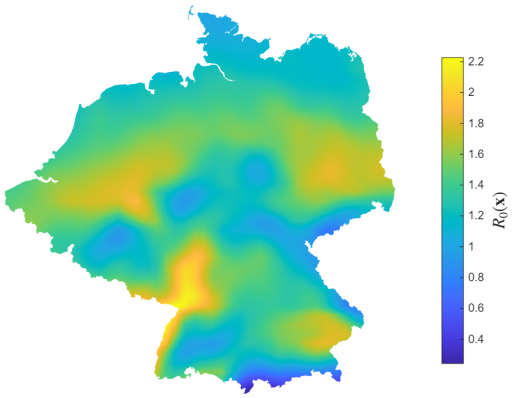
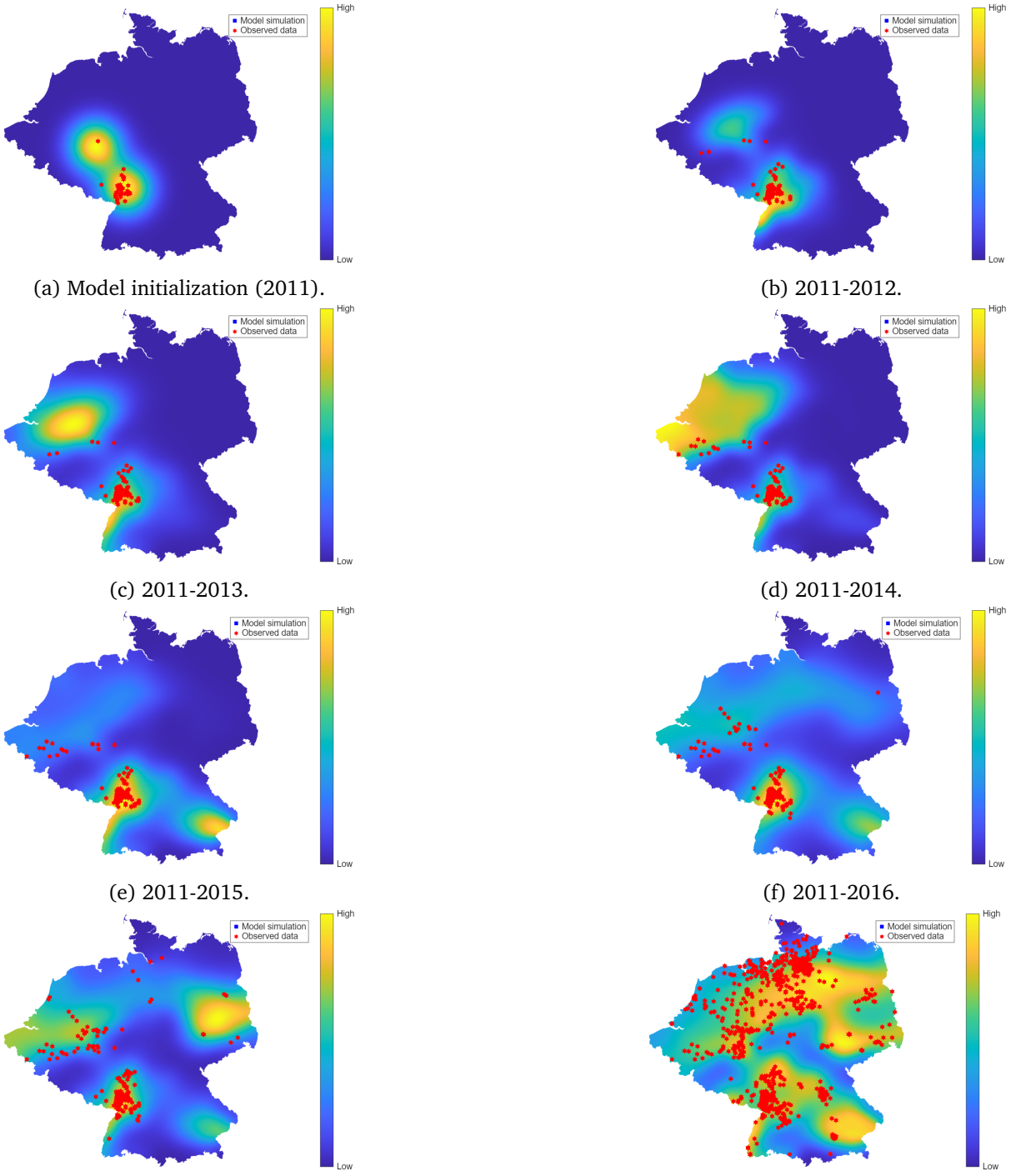


Figure 4: USUV data for the years 2011-2020 (Left) and the basic reproductive number $R_0(\boldsymbol{x})$ (Right), for the year 2018.



(a) Model initialization (2011).

(b) 2011-2012.

(c) 2011-2013.

(d) 2011-2014.

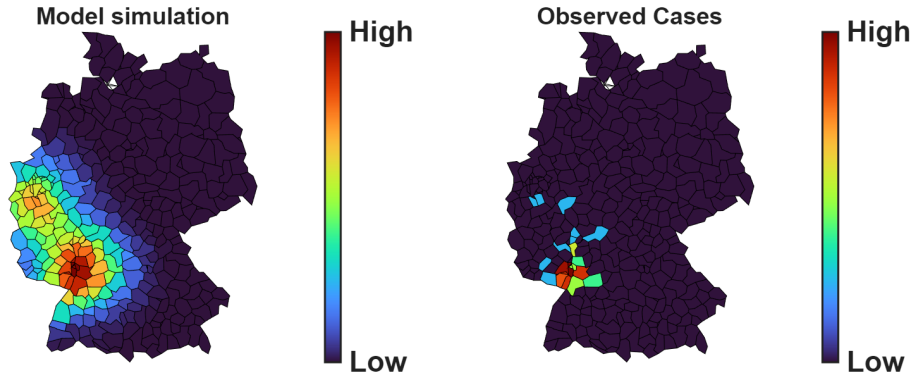
(e) 2011-2015.

(f) 2011-2016.

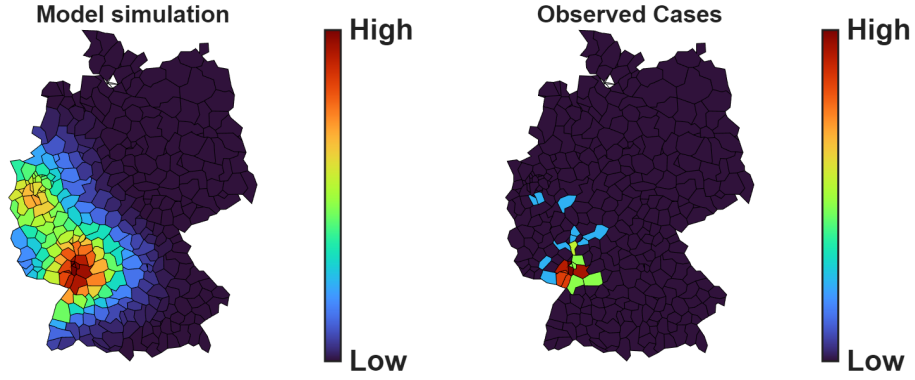
(g) 2011-2017.

(h) 2011-2018.

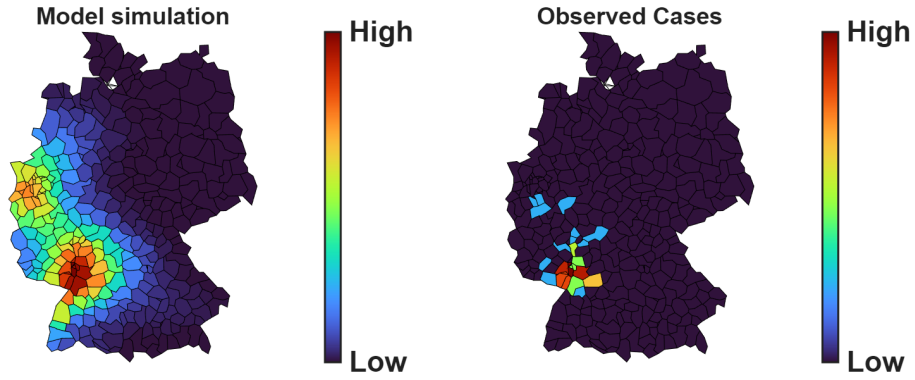
Figure 5: Model simulation compared to observed USUV data during the years 2011-2018.



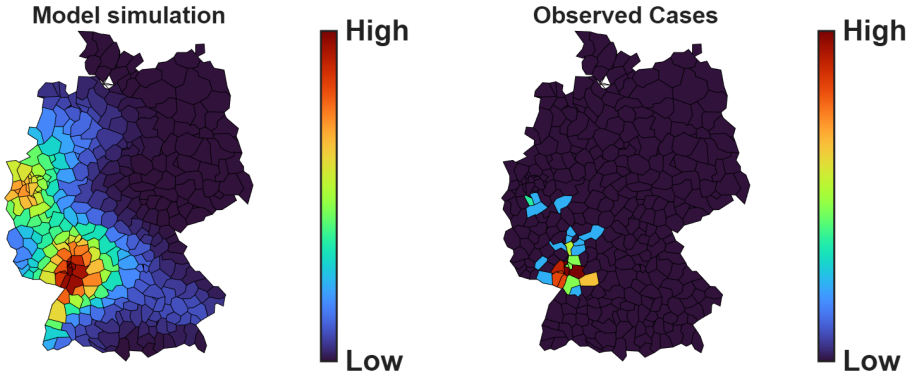
(a) 2011-2012.



(b) 2011-2013.

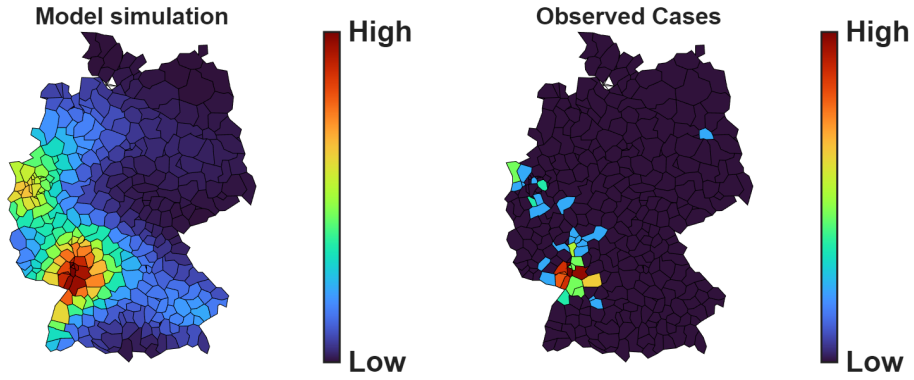


(c) 2011-2014.

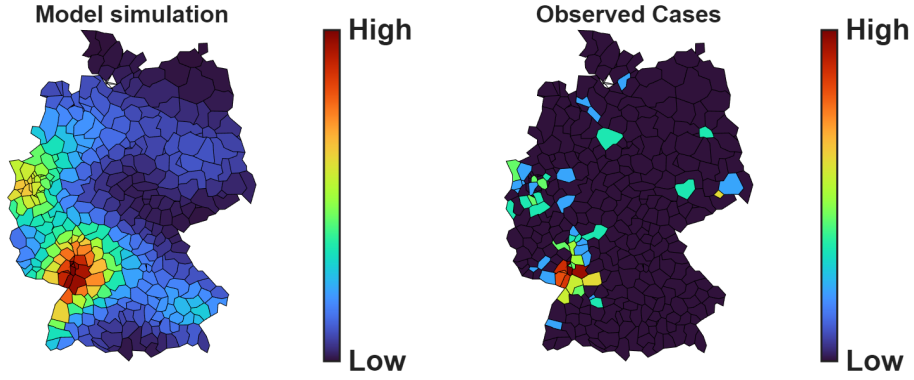


(d) 2011-2015.

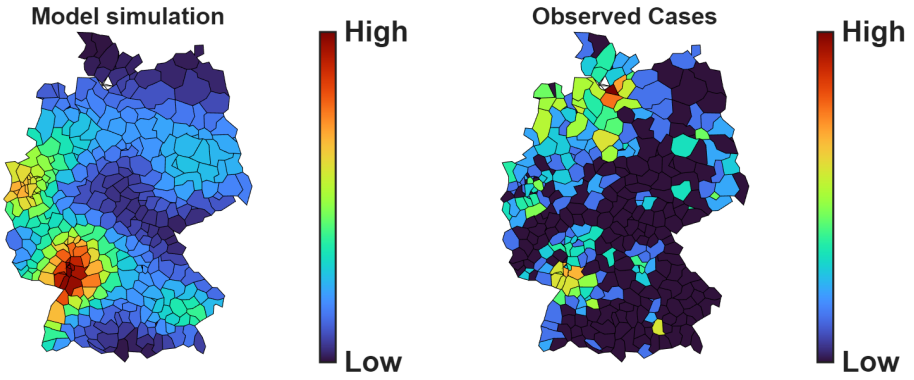
Figure 6: Spatial comparison between simulated and observed USUV cases in Germany (2012-2018), on a $\log_{10}$ scale.



(a) 2011-2016.

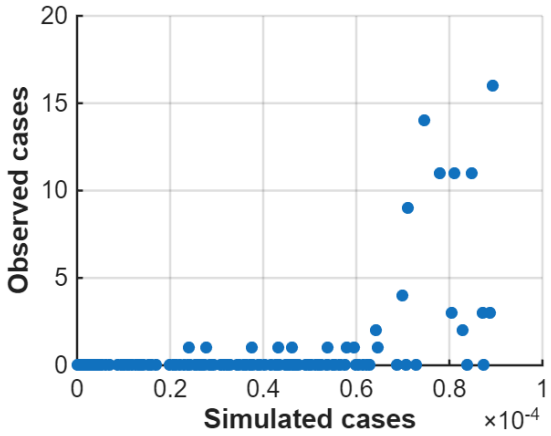


(b) 2011-2017.

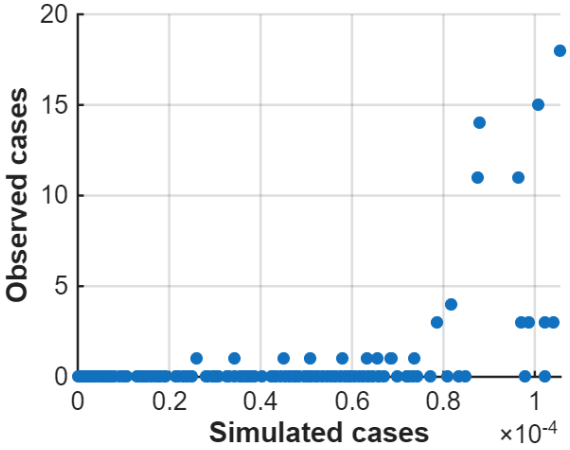


(c) 2011-2018.

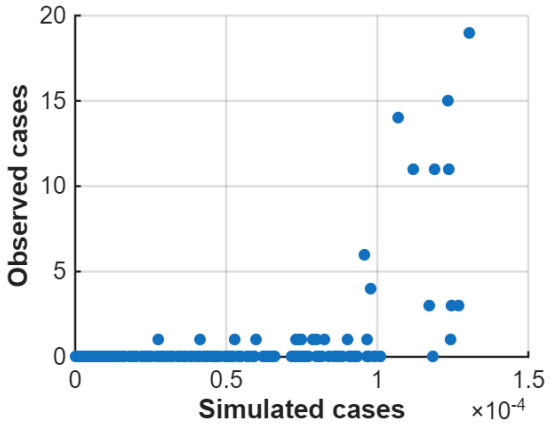
Figure 7: Spatial comparison between simulated and observed USUV cases in Germany (2012-2018), on a $\log_{10}$ scale.



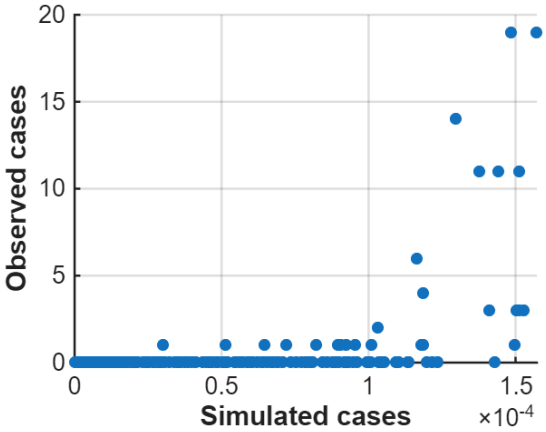
(a) 2011-2012.



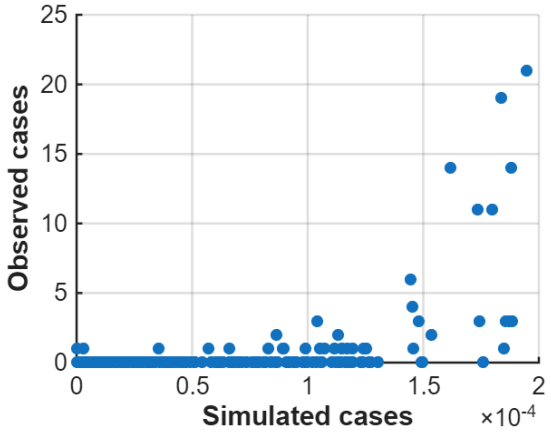
(b) 2011-2013.



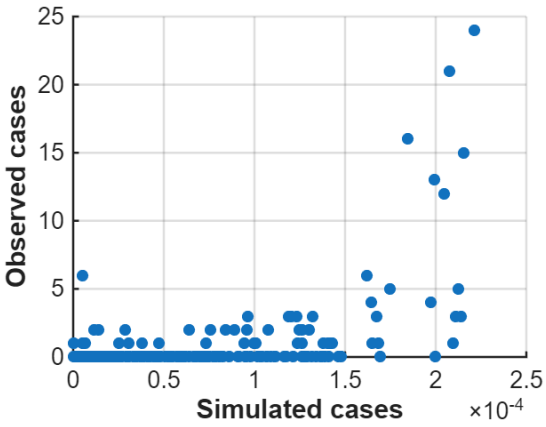
(c) 2011-2014.



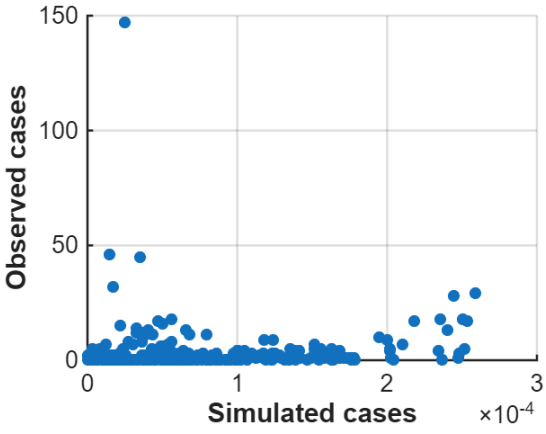
(d) 2011-2015.



(e) 2011-2016.



(f) 2011-2017.



(g) 2011-2018.

Figure 8: Scatter plots of simulated (x-axis) versus observed (y-axis) case numbers.

5 Discussions

This study provides new insights into the spread of USUV in Germany, taking into account cross-border dynamics with the Netherlands, Belgium, and Luxembourg since its first detection in Germany in 2010. We developed a reaction-diffusion PDE model for mosquitoes and birds, incorporating temperature-dependent mosquito parameters. We proved mathematical properties such as non-negativity, uniqueness of solutions and the well-posedness of the model (Appendix 6.1). The basic reproductive number $R_0(\boldsymbol{x})$ is used to assess low- and high-risk regions, with high $R_0(\boldsymbol{x})$ values indicating heightened risk. $R_0(\boldsymbol{x})$ values ranged between 0.3 and 2.2 (Figure 4), and regions with higher values indicate a heightened risk of USUV transmission. Our $R_0(\boldsymbol{x})$ is primarily driven by temperature, thereby providing a spatially explicit transmission risk map for USUV, especially since *Cx. pipiens* are ectothermic insects (Ciota et al., 2014; Vinogradova, 2000). The $R_0(\boldsymbol{x})$ map aligned well with observed data and findings from Cheng et al. (2018), identifying high-risk areas and further supporting the role of temperature in mapping USUV risk.

Notably, $R_0(\boldsymbol{x})$ identifies areas around central Germany as having a lower risk for USUV circulation, whereas regions in the south-west (around the Rhine valley) are classified as high risk. This is mainly due to the region's favourable temperature for the establishment of USUV. Although other factors, such as landscape structure or reduced anthropogenic breeding habitats, may influence risk, the model's capacity to replicate observed patterns using only temperature suggests that temperature is a key variable, a conclusion supported by Rubel et al. (2008).

Our PDE model successfully traced the spread pattern of USUV from Weinheim and Bonn, along with their surrounding regions, in 2011, and continued through 2018, when the virus was confirmed in almost all parts of Germany, parts of the Netherlands, and Belgium. USUV spread in a clockwise direction, entirely opposite to the spread pattern observed for WNV (Duve et al., 2026), despite both viruses sharing the same vector. Model simulations suggest that the differing spatial spread patterns of the two viruses mainly result from variations in their introduction pathways. Specifically, USUV was first introduced to southwest Germany, while WNV in Germany spread from the east. These distinct entry points influenced the subsequent direction and timing of spread, producing different spatial trajectories despite similar transmission mechanisms.

Although the spreading patterns of WNV and USUV differ, it is notable that both viruses spread along the same transmission corridor which is mainly shaped by regional temperatures (Figure 5 and Duve et al. (2026)). This result is supported by some studies that highlight the shared ecological niches between the two viruses (Simonin, 2024). Moreover, the transmission corridor is also in agreement with areas of high USUV suitability identified by Cheng et al. (2018) using a combination of mechanistic and the Maxent models. However, a PDE model further provides detailed information about the spreading patterns and speeds without being limited to suitability only. Because both viruses are now co-circulating in Germany (Schopf et al., 2024) and the same temperature-driven corridor, surveillance and control measures can be concentrated in this zone to improve early season detection and interventions. Therefore, interventions aimed at controlling mosquito populations, such as habitat reduction and larval source management, may reduce the transmission of both viruses simultaneously. Consequently, vector control strategies implemented for WNV in Germany are likely to offer parallel benefits in limiting the spread of USUV.

A mosquito to bird ratio ranging between 30 and 50 was chosen as it produced a realistic spread pattern that biologically meaningful diffusion alone could not reproduce. Lower ratios failed to generate sufficient biting pressure to sustain transmission spread across the country, whereas higher ratios lead to unrealistically rapid spread. Given that bird sampling was not systematic across locations, the observed data probably contain sampling biases that might affect the true spatial pattern. This affected our model fit procedure, as we obtained low correlations in the model fit process. Furthermore, our modelling work can be improved by the use of spatially varying diffusion coefficients than will further support the spatial heterogeneity of the landscapes. A systematic method

for estimating diffusion coefficients can further improve the uncertainties in the choice of diffusion coefficients.

CRediT authorship contribution statement

Pride Duve: Conceptualization, Writing - Original draft, Formal analysis, Visualization;

Dániel Cadar: Investigation, Resources;

Norbert Becker: Investigation, Resources;

Jonas Schmidt-Chanasit: Investigation, Resources;

Felix Gregor Sauer: Conceptualization, Supervision, Writing - Review & Editing;

Renke Lühken: Conceptualization, Supervision, Writing - Review & Editing

Declaration of competing interests

The authors declare that they have no known competing financial interests or personal relationships that could have appeared to influence the work reported in this paper.

Data availability

The citizen science project data used in this study will be made freely available in Zenodo upon publication of this study.

6 Appendix

6.1 Mathematical analysis of the model

Theorem 1. *System (6) has non-negative and unique solutions that are bounded in* $[0, \infty)$.

Proof. We write system (6) together with the corresponding initial conditions, in the Banach space of continuous functions that include the boundary, $\mathscr{B} = C(\bar{\Omega})$, as follows:

$$\begin{cases} \dfrac{\partial X(t,\boldsymbol{x})}{\partial t} = & \mathscr{L}X(t,\boldsymbol{x}) + f(X(t,\boldsymbol{x})),\ t > 0, \\ X(t,0) = & X_0 \geq 0_{\mathbb{R}^7}, \end{cases}$$

where

$$X(t,\boldsymbol{x}) = \begin{bmatrix} S_V(t,\boldsymbol{x}) \\ E_V(t,\boldsymbol{x}) \\ I_V(t,\boldsymbol{x}) \\ S_B(t,\boldsymbol{x}) \\ E_B(t,\boldsymbol{x}) \\ I_B(t,\boldsymbol{x}) \\ R_B(t,\boldsymbol{x}) \end{bmatrix}, X(0,\boldsymbol{x}) = \begin{bmatrix} S_V(0,\boldsymbol{x}) \\ E_V(0,\boldsymbol{x}) \\ I_V(0,\boldsymbol{x}) \\ S_B(0,\boldsymbol{x}) \\ E_B(0,\boldsymbol{x}) \\ I_B(0,\boldsymbol{x}) \\ R_B(0,\boldsymbol{x}) \end{bmatrix}, \mathscr{L}X(t,\boldsymbol{x}) = \begin{bmatrix} D_1\Delta S_V(t,\boldsymbol{x}) \\ D_1\Delta E_V(t,\boldsymbol{x}) \\ D_1\Delta I_V(t,\boldsymbol{x}) \\ D_2\Delta S_B(t,\boldsymbol{x}) \\ D_2\Delta E_B(t,\boldsymbol{x}) \\ D_2\Delta I_B(t,\boldsymbol{x}) \\ D_2\Delta R_B(t,\boldsymbol{x}) \end{bmatrix},$$

and

$$f = \begin{cases} f_1 = & b_V N_V \left[1 - \dfrac{N_V}{K_V}\right] - [\lambda_{BV}(T) + \mu_V(T)]S_V, \\ f_2 = & \lambda_{BV}(T)S_V - (\gamma_V(T) + \mu_V(T))E_V, \\ f_3 = & \gamma_V(T)E_V - \mu_V(T)I_V, \\ f_4 = & b_B N_B \left[1 - \dfrac{N_B}{K_B}\right] - [\lambda_{VB}(T) + \mu_B]S_B, \\ f_5 = & \lambda_{VB}(T)S_B - [\gamma_B + \mu_B]E_B, \\ f_6 = & \gamma_B E_B - [\alpha_B + \mu_B]I_B, \\ f_7 = & (1 - \nu_B)\alpha_B I_B - \mu_B R_B. \end{cases}$$

Next, we show that f is locally Lipschitz in $\mathscr{B}$. Thus, we show that

$$\forall\, K \subset \mathscr{B},\ \exists L: \quad \|f(X_1) - f(X_2)\|_\infty \leq L\|X_1 - X_2\|_\infty,\ \forall X_1, X_2 \in K,$$

where L is the Lipschitz constant. Setting $\Lambda_V = b_V N_V \left[1 - \dfrac{N_V}{K_V}\right]$ and $\Lambda_B = b_B N_B \left[1 - \dfrac{N_B}{K_B}\right]$, we

observe that $X_1 - X_2 =$

$$\begin{bmatrix} [\Lambda_{V_1} - \Lambda_{V_2}] - [\lambda_{BV_1} S_{V_1} - \lambda_{BV_2} S_{V_2}] - \mu_V (S_{V_1} - S_{V_2}) \\ [\lambda_{BV_1} S_{V_1} - \lambda_{BV_2} S_{V_2}] - (\gamma_V + \mu_V)[E_{V_1} - E_{V_2}] \\ \gamma_V [E_{V_1} - E_{V_2}] - \mu_V [I_{V_1} - I_{V_2}] \\ [\Lambda_{B_1} - \Lambda_{B_2}] - (\lambda_{VB_1} S_{B_1} - \lambda_{VB_2} S_{B_2}) - \mu_B [S_{B_1} - S_{B_2}] \\ \lambda_{VB_1} S_{B_1} - \lambda_{VB_2} S_{B_2} - (\gamma_B + \mu_B)[E_{B_1} - E_{B_2}] \\ \gamma_B [E_{B_1} - E_{B_2}] - (\alpha_B + \mu_B)[I_{B_1} - I_{B_2}] \\ (1 - \nu_B)\alpha_B [I_{B_1} - I_{B_2}] - \mu_B [R_{B_1} - R_{B_2}] \end{bmatrix}.$$

Simplifying, we obtain $\|f(X_1) - f(X_2)\|_\infty =$

$$\begin{aligned} = & \sup_{x \in \bar{\Omega}} |\left[\Lambda_{V_1} - \Lambda_{V_2}\right] - S_{V_1}[\lambda_{BV_1} - \lambda_{BV_2}]| \\ \vee & \sup_{x \in \bar{\Omega}} |-\lambda_{BV_2}[S_{V_1} - S_{V_2}] - \mu_V (S_{V_1} - S_{V_2})| \\ \vee & \sup_{x \in \bar{\Omega}} |\gamma_V [E_{V_1} - E_{V_2}] - \mu_V [I_{V_1} - I_{V_2}]| \\ \vee & \sup_{x \in \bar{\Omega}} |[\Lambda_{B_1} - \Lambda_{B_2}] - \lambda_{VB_1}[S_{B_1} - S_{B_2}] - S_{B_2}[\lambda_{VB_1} - \lambda_{VB_2}] - \mu_B [S_{B_1} - S_{B_2}]| \\ \vee & \sup_{x \in \bar{\Omega}} |\lambda_{VB_1}[S_{B_1} - S_{B_2}] + S_{B_2}[\lambda_{VB_1} - \lambda_{VB_2}] - (\gamma_B + \mu_B)[E_{B_1} - E_{B_2}]| \\ \vee & \sup_{x \in \bar{\Omega}} |\gamma_B [E_{B_1} - E_{B_2}] - (\alpha_B + \mu_B)[I_{B_1} - I_{B_2}]| \\ \vee & \sup_{x \in \bar{\Omega}} |(1 - \nu_B)\alpha_B [I_{B_1} - I_{B_2}] - \mu_B [R_{B_1} - R_{B_2}]|. \end{aligned}$$

By the triangular inequality, and some simplifications, we arrive at

$$\|f(X_1) - f(X_2)\|_\infty \leq (\mu_V + \nu_B \alpha_B) \|X_1 - X_2\|_\infty,$$

and thus f is locally Lipschitz in $\mathscr{B}$. By [(Capasso, 1993), Theorem B.17], (Mora, 1983), and [(Smoller, 1983), Theorem 14.4], there exist a local smooth and unique solution of system (6) in Ω. We observe that system (6) can be written in the form of system (14.12) in the book (Smoller, 1983), together with initial data defined in system (14.13). By [(Smoller, 1983), Theorem (14.14)], the solutions of system (6) are always positive. □

6.2 Well-posedness of the model in a feasible region

Theorem 2. *system (6) is well-posed mathematically and biologically, and for any* $(S_V(0,x), E_V(0,x), I_V(0,x), S_B(0,x), E_B(0,x), I_B(0,x), R_B(0,x)) \in \mathbb{X}$, *system (6) admits a unique positive solution:* $(S_V(t,x), E_V(t,x), I_V(t,x), S_B(t,x), E_B(t,x), I_B(t,x), R_B(t,x)) \in \mathbb{X}$, *satisfying:*

$(S_V(t,x), E_V(t,x), I_V(t,x), S_B(t,x), E_B(t,x), I_B(t,x), R_B(t,x) \in C^{1,2}((0,\infty) \times \bar{\Omega}) \times C^{1,2}((0,\infty) \times \bar{\Omega})$, *where* $\mathbb{X} := C(\bar{\Omega}) \times C(\bar{\Omega})$.

Moreover, there exist another constant $C_1 > 0$ *independent of initial data, such that the solution* $(S_V(t,x), E_V(t,x), I_V(t,x), S_B(t,x), E_B(t,x), I_B(t,x), R_B(t,x)(t,x))$ *satisfies:*

$\|S_V(t,x)\|_{L^\infty(\Omega)} + \|E_V(t,x)\|_{L^\infty(\Omega)} + \|I_V(t,x)\|_{L^\infty(\Omega)} + \|S_B(t,x)\|_{L^\infty(\Omega)} + \|E_B(t,x)\|_{L^\infty(\Omega)} + \|I_B(t,x)\|_{L^\infty(\Omega)} + \|R_B(t,x)\|_{L^\infty(\Omega)} \leq C_1$, *for all* $t > T_0 > 0$.

Proof. We follow the approach presented in (Peng and Zhao, 2012; Wang and Dai, 2022). Using the regularity theory of parabolic PDEs (Pao, 1993), system (6) admits a unique non-negative classical solution

$$(S_B(t,x), E_B(t,x), I_B(t,x), R_B(t,x)) \in C^{1,2}((0,T_m)\times\bar{\Omega}) \times C^{1,2}((0,T_m)\times\bar{\Omega}),$$

where T_m represents the maximal existence time of the solution. By the strong maximum principle (Protter and Weinberger, 1984), then $S_B(t,x), E_B(t,x), I_B(t,x), R_B(t,x)$ are positive in $(0,T_m)\times\bar{\Omega}$.

Summing up the equations gives

$$\frac{\partial N_B}{\partial t} = \mathscr{D}_B \Delta N_B + b_B N_B\left[1-\frac{N_B}{K_B}\right] - \mu_B N_B - \alpha_B \nu_B I_B,$$

subject to homogeneous Neumann boundary conditions $\nabla N_B \cdot n = 0$ on $\partial\Omega$ and non-negative initial data $N_B(x,0) = N_B(x) \geq 0$. Integrating over Ω, we get

$$\frac{d}{dt}\int_\Omega N_B(x,t)\,dx = \int_\Omega [b_B - \mu_B] N_B\,dx - \int_\Omega b_B \frac{N_B}{K_B}\,dx \leq \bar{r}\int_\Omega N_B(x,t)\,dx,\ x\in\Omega,\ t>0, \bar{r}\leq b_{B,max},$$

yielding

$$\int_\Omega N_B(x,t)\,dx \leq \int_\Omega e^{t b_{B,max}} N_{B0}(x)\,dx, \quad x\in\Omega,\ t\geq 0.$$

Thus, $\|S_B(t,\cdot)\|_{L^1(\Omega)}$, $\|E_B(t,\cdot)\|_{L^1(\Omega)}$, $\|I_B(t,\cdot)\|_{L^1(\Omega)}$, and $\|R_B(t,\cdot)\|_{L^1(\Omega)}$ are bounded for all $0<t<T_m$. By the positivity of $S_B(t,\cdot)$, $E_B(t,\cdot)$, $I_B(t,\cdot)$, $R_B(t,\cdot)$, and [(Peng and Zhao, 2012), Lemma (3.1)], with $\sigma = p_0 = 1$, we conclude that there exist a positive constant C_1 that does not depend on initial data such that the solution S_B, E_B, I_B, R_B satisfies

$$\|S_B(t,\cdot)\|_{L^\infty(\Omega)} + \|E_B(t,\cdot)\|_{L^\infty(\Omega)} + \|I_B(t,\cdot)\|_{L^\infty(\Omega)} + \|R_B(t,\cdot)\|_{L^\infty(\Omega)} \leq C_1,\ \forall t > T_0.$$

Similar arguments can be made for the mosquito population, thus we conclude that system (6) is well-posed. □

6.3 Matrices used in the PDEToolbox

$$c = [D_1; D_1; D_1; D_2; D_2; D_2; 0],$$

while

$$f = \begin{cases} b_V N_V\left[1-\frac{N_V}{K_V}\right] - [\lambda_{BV}(T,\boldsymbol{x}) + \mu_V(T,\boldsymbol{x})]S_V, \\ \lambda_{BV}(T,\boldsymbol{x})S_V - [\gamma_V(T,\boldsymbol{x}) + \mu_V(T,\boldsymbol{x})]E_V, \\ \gamma_V(T,\boldsymbol{x})E_V - \mu_V(T,\boldsymbol{x})I_V, \\ b_B N_B\left[1-\frac{N_B}{K_B}\right] - [\lambda_{VB}(T,\boldsymbol{x}) + \mu_B]S_B, \\ \lambda_{VB}(T,\boldsymbol{x})S_B - [\gamma_B + \mu_B]E_B, \\ \gamma_B E_B - [\alpha_B + \mu_B]I_B, \\ (1-\nu_B)\alpha_B I_B - \mu_B R_B, \\ \alpha_B \nu_B I_B. \end{cases} \tag{11}$$

References

L Allering, H Jöst, P Emmerich, S Günther, E Lattwein, M Schmidt, E Seifried, V Sambri, K Hourfar, and J Schmidt-Chanasit. Detection of Usutu virus infection in a healthy blood donor from south-west Germany, 2012. *Eurosurveillance*, 17(50), December 2012. ISSN 1560-7917. doi: 10.2807/ese.17.50.20341-en. URL http://dx.doi.org/10.2807/ese.17.50.20341-en.

Giorgia Angeloni, Michela Bertola, Elena Lazzaro, Matteo Morini, Giulia Masi, Alessandro Sinigaglia, Marta Trevisan, Céline M. Gossner, Joana M. Haussig, Tamas Bakonyi, Gioia Capelli, and Luisa Barzon. Epidemiology, surveillance and diagnosis of Usutu virus infection in the EU/EEA, 2012 to 2021. *Eurosurveillance*, 28(33), August 2023. ISSN 1560-7917. doi: 10.2807/1560-7917.es.2023.28.33.2200929. URL http://dx.doi.org/10.2807/1560-7917.es.2023.28.33.2200929.

Norbert Becker, Artur Jöst, and Thomas Weitzel. The *Culex pipiens* complex in Europe. *Journal of the American Mosquito Control Association*, 28(4s):53–67, December 2012a. ISSN 8756-971X. doi: 10.2987/8756-971x-28.4s.53. URL http://dx.doi.org/10.2987/8756-971x-28.4s.53.

Norbert Becker, Hanna Jöst, Ute Ziegler, Martin Eiden, Dirk Höper, Petra Emmerich, Elisabeth Fichet-Calvet, Deborah U. Ehichioya, Christina Czajka, Martin Gabriel, Bernd Hoffmann, Martin Beer, Klara Tenner-Racz, Paul Racz, Stephan Günther, Michael Wink, Stefan Bosch, Armin Konrad, Martin Pfeffer, Martin H. Groschup, and Jonas Schmidt-Chanasit. Epizootic emergence of Usutu virus in wild and captive birds in Germany. *PLoS ONE*, 7(2):e32604, February 2012b. ISSN 1932-6203. doi: 10.1371/journal.pone.0032604. URL http://dx.doi.org/10.1371/journal.pone.0032604.

Emna Benzarti, Michaël Sarlet, Mathieu Franssen, Daniel Cadar, Jonas Schmidt-Chanasit, Jose Felipe Rivas, Annick Linden, Daniel Desmecht, and Mutien Garigliany. Usutu virus epizootic in Belgium in 2017 and 2018: Evidence of virus endemization and ongoing introduction events. *Vector-Borne and Zoonotic Diseases*, 20(1):43–50, January 2020. ISSN 1557-7759. doi: 10.1089/vbz.2019.2469. URL http://dx.doi.org/10.1089/vbz.2019.2469.

Suman Bhowmick, Jörn Gethmann, Franz J. Conraths, Igor M. Sokolov, and Hartmut H.K. Lentz. Locally temperature-driven mathematical model of West Nile virus spread in Germany. *Journal of Theoretical Biology*, 488:110117, March 2020. ISSN 0022-5193. doi: 10.1016/j.jtbi.2019.110117. URL http://dx.doi.org/10.1016/j.jtbi.2019.110117.

Suman Bhowmick, Megan Lindsay Fritz, and Rebecca Smith. A novel temperature-dependent mathematical model of West Nile virus transmission dynamics to predict the impacts of vector-host interactions and vector management on R0. 2023. doi: 10.2139/ssrn.4642272. URL http://dx.doi.org/10.2139/ssrn.4642272.

Katharina Brugger and Franz Rubel. Simulation of climate-change scenarios to explain Usutu-virus dynamics in Austria. *Preventive Veterinary Medicine*, 88(1):24–31, January 2009. ISSN 0167-5877. doi: 10.1016/j.prevetmed.2008.06.023. URL http://dx.doi.org/10.1016/j.prevetmed.2008.06.023.

Daniel Cadar, Renke Lühken, Henk van der Jeugd, Mutien Garigliany, Ute Ziegler, Markus Keller, Jennifer Lahoreau, Lars Lachmann, Norbert Becker, Marja Kik, Bas B Oude Munnink, Stefan Bosch, Egbert Tannich, Annick Linden, Volker Schmidt, Marion P Koopmans, Jolianne Rijks, Daniel Desmecht, Martin H Groschup, Chantal Reusken, and Jonas Schmidt-Chanasit. Widespread activity of multiple lineages of Usutu virus, western Europe, 2016. *Eurosurveillance*, 22(4), January 2017a. ISSN 1560-7917. doi: 10.2807/1560-7917.es.2017.22.4.30452. URL http://dx.doi.org/10.2807/1560-7917.es.2017.22.4.30452.

Daniel Cadar, Philipp Maier, Susanne Müller, Julia Kress, Michael Chudy, Alexandra Bialonski, Alexander Schlaphof, Stephanie Jansen, Hanna Jöst, Egbert Tannich, et al. Blood donor screening for West Nile virus (WNV) revealed acute Usutu virus (USUV) infection, Germany, september 2016. *Eurosurveillance*, 22(14):30501, 2017b.

Dániel Cadar and Yannick Simonin. Human Usutu virus infections in Europe: A new risk on horizon? *Viruses*, 15(1):77, December 2022. ISSN 1999-4915. doi: 10.3390/v15010077. URL http://dx.doi.org/10.3390/v15010077.

Mattia Calzolari. Mosquito-borne diseases in Europe: an emerging public health threat. *Reports in Parasitology*, page 1, February 2016. ISSN 2230-3162. doi: 10.2147/rip.s56780. URL http://dx.doi.org/10.2147/rip.s56780.

Vincenzo Capasso. *Mathematical Structures of Epidemic Systems*. Springer Berlin Heidelberg, 1993. ISBN 9783540705147. https://dx.doi.org/10.1007/978-3-540-70514-7.

Yanchao Cheng, Nils Benjamin Tjaden, Anja Jaeschke, Renke Lühken, Ute Ziegler, Stephanie Margarete Thomas, and Carl Beierkuhnlein. Evaluating the risk for Usutu virus circulation in Europe: comparison of environmental niche models and epidemiological models. *International Journal of Health Geographics*, 17(1), October 2018. ISSN 1476-072X. doi: 10.1186/s12942-018-0155-7. URL http://dx.doi.org/10.1186/s12942-018-0155-7.

Alexander T. Ciota, Amy C. Matacchiero, A. Marm Kilpatrick, and Laura D. Kramer. The effect of temperature on life history traits of *Culex* mosquitoes. *Journal of Medical Entomology*, 51(1): 55–62, January 2014. ISSN 1938-2928. doi: 10.1603/me13003. URL http://dx.doi.org/10.1603/me13003.

A. T. De Madrid and J. S. Porterfield. The flaviviruses (group b arboviruses): a cross-neutralization study. *Journal of General Virology*, 23(1):91–96, April 1974. ISSN 1465-2099. doi: 10.1099/0022-1317-23-1-91. URL http://dx.doi.org/10.1099/0022-1317-23-1-91.

O. Diekmann, J. A. P. Heesterbeek, and M. G. Roberts. The construction of next-generation matrices for compartmental epidemic models. *Journal of The Royal Society Interface*, 7(47):873–885, November 2009. ISSN 1742-5662. doi: 10.1098/rsif.2009.0386. URL http://dx.doi.org/10.1098/rsif.2009.0386.

Pride Duve, Felix Gregor Sauer, and Renke Lühken. Modelling the impact of temperature and bird migration on the spread of West Nile virus. *One Health*, 22:101386, June 2026. ISSN 2352-7714. doi: 10.1016/j.onehlt.2026.101386. URL http://dx.doi.org/10.1016/j.onehlt.2026.101386.

A. Einstein. Über die von der molekularkinetischen theorie der wärme geforderte bewegung von in ruhenden flüssigkeiten suspendierten teilchen. *Annalen der Physik*, 322(8):549–560, January 1905. ISSN 1521-3889. doi: 10.1002/andp.19053220806. URL http://dx.doi.org/10.1002/andp.19053220806.

Dimitri Engel, Hanna Jöst, Michael Wink, Jessica Börstler, Stefan Bosch, Mutien-Marie Garigliany, Artur Jöst, Christina Czajka, Renke Lühken, Ute Ziegler, Martin H. Groschup, Martin Pfeffer, Norbert Becker, Daniel Cadar, and Jonas Schmidt-Chanasit. Reconstruction of the evolutionary history and dispersal of Usutu virus, a neglected emerging arbovirus in Europe and Africa. *mBio*, 7(1), March 2016. ISSN 2150-7511. doi: 10.1128/mbio.01938-15. URL http://dx.doi.org/10.1128/mbio.01938-15.

Adolf Fick. Ueber diffusion. *Annalen der Physik*, 170(1):59–86, January 1855. ISSN 1521-3889. doi: 10.1002/andp.18551700105. URL http://dx.doi.org/10.1002/andp.18551700105.

Global Administrative Areas. Gadm database of Global Administrative Areas (version 4.1). [digital geospatial data], 2024. Available online: https://gadm.org [Accessed: 20 October 2025].

Gabriel L. Hamer, Tavis K. Anderson, Danielle J. Donovan, Jeffrey D. Brawn, Bethany L. Krebs, Allison M. Gardner, Marilyn O. Ruiz, William M. Brown, Uriel D. Kitron, Christina M. Newman, Tony L. Goldberg, and Edward D. Walker. Dispersal of adult *Culex* mosquitoes in an urban West Nile virus hotspot: A mark-capture study incorporating stable isotope enrichment of natural larval habitats. *PLoS Neglected Tropical Diseases*, 8(3):e2768, March 2014. ISSN 1935-2735. doi: 10.1371/journal.pntd.0002768. URL http://dx.doi.org/10.1371/journal.pntd.0002768.

Julian Heidecke, Jonas Wallin, Peter Fransson, Pratik Singh, Henrik Sjödin, Pascale Claire Stiles, Marina Treskova, and Joacim Rocklöv. Uncovering temperature sensitivity of West Nile virus transmission: Novel computational approaches to mosquito-pathogen trait responses. *PLOS Computational Biology*, 21(3):e1012866, March 2025. ISSN 1553-7358. doi: 10.1371/journal.pcbi.1012866. URL http://dx.doi.org/10.1371/journal.pcbi.1012866.

Hanna Jöst, Alexandra Bialonski, Deborah Maus, Vittorio Sambri, Martin Eiden, Martin H Groschup, Stephan Günther, Norbert Becker, and Jonas Schmidt-Chanasit. Isolation of Usutu virus in Germany. *The American journal of tropical medicine and hygiene*, 85(3):551, 2011.

Antonios Kolimenakis, Sabine Heinz, Michael Lowery Wilson, Volker Winkler, Laith Yakob, Antonios Michaelakis, Dimitrios Papachristos, Clive Richardson, and Olaf Horstick. The role of urbanisation in the spread of *Aedes* mosquitoes and the diseases they transmit-a systematic review. *PLOS Neglected Tropical Diseases*, 15(9):e0009631, September 2021. ISSN 1935-2735. doi: 10.1371/journal.pntd.0009631. URL http://dx.doi.org/10.1371/journal.pntd.0009631.

Vincent Laperriere, Katharina Brugger, and Franz Rubel. Simulation of the seasonal cycles of bird, equine and human West Nile virus cases. *Preventive Veterinary Medicine*, 98(2–3):99–110, February 2011. ISSN 0167-5877. doi: 10.1016/j.prevetmed.2010.10.013. URL http://dx.doi.org/10.1016/j.prevetmed.2010.10.013.

Renke Lühken, Hanna Jöst, Daniel Cadar, Stephanie Margarete Thomas, Stefan Bosch, Egbert Tannich, Norbert Becker, Ute Ziegler, Lars Lachmann, and Jonas Schmidt-Chanasit. Distribution of Usutu virus in germany and its effect on breeding bird populations. *Emerging Infectious Diseases*, 23(12):1994–2001, December 2017. ISSN 1080-6059. doi: 10.3201/eid2312.171257. URL http://dx.doi.org/10.3201/eid2312.171257.

Alexandra Mangili and Mark A Gendreau. Transmission of infectious diseases during commercial air travel. *The Lancet*, 365(9463):989–996, March 2005. ISSN 0140-6736. doi: 10.1016/s0140-6736(05)71089-8. URL http://dx.doi.org/10.1016/s0140-6736(05)71089-8.

Oliver Chinonso Mbaoma, Stephanie Margarete Thomas, and Carl Beierkuhnlein. Spatiotemporally explicit epidemic model for West Nile virus outbreak in Germany: An inversely calibrated approach. *Journal of Epidemiology and Global Health*, 14(3):1052–1070, July 2024. ISSN 2210-6014. doi: 10.1007/s44197-024-00254-0. URL http://dx.doi.org/10.1007/s44197-024-00254-0.

Soeren Metelmann. *Development of Climate-driven Models for Mosquito-borne Disease Risk in the UK*. The University of Liverpool (United Kingdom), 2019.

Friederike Michel, Michael Sieg, Dominik Fischer, Markus Keller, Martin Eiden, Maximilian Reuschel, Volker Schmidt, Rebekka Schwehn, Monika Rinder, Sylvia Urbaniak, Kerstin Müller, Martina Schmoock, Renke Lühken, Patrick Wysocki, Christine Fast, Michael Lierz, Rüdiger Korbel, Thomas Vahlenkamp, Martin Groschup, and Ute Ziegler. Evidence for West Nile virus and Usutu virus infections in wild and resident birds in Germany, 2017 and 2018. *Viruses*, 11(7):674, July 2019. ISSN 1999-4915. doi: 10.3390/v11070674. URL http://dx.doi.org/10.3390/v11070674.

Xavier Mora. Semilinear parabolic problems define semiflows on c k spaces. *Transactions of the American Mathematical Society*, 278(1):21, July 1983. ISSN 0002-9947. https://dx.doi.org/10.2307/1999300.

C. Musto, M. Tamba, M. Calzolari, D. Torri, K. Marzani, J. Cerri, P. Bonilauri, and M. Delogu. Usutu virus in blackbirds (*Turdus merula*) with clinical signs, a case study from northern Italy. *European Journal of Wildlife Research*, 68(2), March 2022. ISSN 1439-0574. doi: 10.1007/s10344-022-01572-z. URL http://dx.doi.org/10.1007/s10344-022-01572-z.

Emmanuelle Münger, Nnomzie C. Atama, Jurrian van Irsel, Rody Blom, Louie Krol, Tjomme van Mastrigt, Tijs J. van den Berg, Marieta Braks, Ankje de Vries, Anne van der Linden, Irina Chestakova, Marjan Boter, Felicity D. Chandler, Robert Kohl, David F. Nieuwenhuijse, Mathilde Uiterwijk, Ron A. M. Fouchier, Hein Sprong, Andrea Gröne, Constantianus J. M. Koenraadt, Maarten Schrama, Chantal B. E. M. Reusken, Arjan Stroo, Judith M. A. van den Brand, Henk P. van der Jeugd, Bas B. Oude Munnink, Reina S. Sikkema, and Marion P. G. Koopmans. One health approach uncovers emergence and dynamics of Usutu and West Nile viruses in the Netherlands. *Nature Communications*, 16(1), August 2025. ISSN 2041-1723. doi: 10.1038/s41467-025-63122-w. URL http://dx.doi.org/10.1038/s41467-025-63122-w.

Birgit Nikolay. A review of West Nile and Usutu virus co-circulation in Europe: how much do transmission cycles overlap. *Transactions of The Royal Society of Tropical Medicine and Hygiene*, 109(10):609–618, August 2015. ISSN 1878-3503. doi: 10.1093/trstmh/trv066. URL http://dx.doi.org/10.1093/trstmh/trv066.

C. V. Pao. *Nonlinear parabolic and elliptic equations*. Springer US, 1993. ISBN 9781461530343. https://dx.doi.org/10.1007/978-1-4615-3034-3.

Rui Peng and Xiao-Qiang Zhao. A reaction–diffusion sis epidemic model in a time-periodic environment. *Nonlinearity*, 25(5):1451–1471, April 2012. ISSN 1361-6544. https://dx.doi.org/10.1088/0951-7715/25/5/1451.

Murray H. Protter and Hans F. Weinberger. *Maximum principles in differential equations*. Springer New York, 1984. ISBN 9781461252825. https://dx.doi.org/10.1007/978-1-4612-5282-5.

Yunbo Qiu, Chenlong Lv, Jinjin Chen, Yanqun Sun, Tian Tang, Yuanyuan Zhang, Yufeng Yang, Guolin Wang, Qiang Xu, Xiaoai Zhang, Feng Hong, Simon I. Hay, Liqun Fang, and Wei Liu. The global distribution and diversity of wild-bird-associated pathogens: An integrated data analysis and modeling study. *Med*, 6(4):100553, April 2025. ISSN 2666-6340. doi: 10.1016/j.medj.2024.11.006. URL http://dx.doi.org/10.1016/j.medj.2024.11.006.

Jenő Reiczigel, Katharina Brugger, Franz Rubel, Norbert Solymosi, and Zsolt Lang. Bayesian analysis of a dynamical model for the spread of the Usutu virus. *Stochastic Environmental Research and Risk Assessment*, 24(3):455–462, August 2009. ISSN 1436-3259. doi: 10.1007/s00477-009-0333-z. URL http://dx.doi.org/10.1007/s00477-009-0333-z.

Ferdinand Roesch, Alvaro Fajardo, Gonzalo Moratorio, and Marco Vignuzzi. Usutu virus: An arbovirus on the rise. *Viruses*, 11(7):640, July 2019. ISSN 1999-4915. doi: 10.3390/v11070640. URL http://dx.doi.org/10.3390/v11070640.

Franz Rubel, Katharina Brugger, Michael Hantel, Sonja Chvala-Mannsberger, Tamás Bakonyi, Herbert Weissenböck, and Norbert Nowotny. Explaining Usutu virus dynamics in Austria: Model development and calibration. *Preventive Veterinary Medicine*, 85(3–4):166–186, July 2008. ISSN 0167-5877. doi: 10.1016/j.prevetmed.2008.01.006. URL http://dx.doi.org/10.1016/j.prevetmed.2008.01.006.

Martin Rudolf, Christina Czajka, Jessica Börstler, Christian Melaun, Hanna Jöst, Heidrun von Thien, Marlis Badusche, Norbert Becker, Jonas Schmidt-Chanasit, Andreas Krüger, Egbert Tannich, and Stefanie Becker. First nationwide surveillance of *Culex pipiens* complex and *Culex torrentium* mosquitoes demonstrated the presence of *Culex pipiens* biotype *pipiens/molestus* hybrids in Germany. *PLoS ONE*, 8(9):e71832, September 2013. ISSN 1932-6203. doi: 10.1371/journal.pone.0071832. URL http://dx.doi.org/10.1371/journal.pone.0071832.

Franziska Schopf, Balal Sadeghi, Felicitas Bergmann, Dominik Fischer, Ronja Rahner, Kerstin Müller, Anne Günther, Anja Globig, Markus Keller, Rebekka Schwehn, Vanessa Guddorf, Maximilian Reuschel, Luisa Fischer, Oliver Krone, Monika Rinder, Karolin Schütte, Volker Schmidt, Kristin Heenemann, Anne Schwarzer, Christine Fast, Carola Sauter-Louis, Christoph Staubach, Renke Lühken, Jonas Schmidt-Chanasit, Florian Brandes, Michael Lierz, Rüdiger Korbel, Thomas W. Vahlenkamp, Martin H. Groschup, and Ute Ziegler. Circulation of West Nile virus and Usutu virus in birds in Germany, 2021 and 2022. *Infectious Diseases*, 57(3):256–277, November 2024. ISSN 2374-4243. doi: 10.1080/23744235.2024.2419859. URL http://dx.doi.org/10.1080/23744235.2024.2419859.

Jan C. Semenza and Shlomit Paz. Climate change and infectious disease in Europe: Impact, projection and adaptation. *The Lancet Regional Health - Europe*, 9:100230, October 2021. ISSN 2666-7762. doi: 10.1016/j.lanepe.2021.100230. URL http://dx.doi.org/10.1016/j.lanepe.2021.100230.

Yannick Simonin. Circulation of West Nile virus and Usutu virus in Europe: Overview and challenges. *Viruses*, 16(4):599, April 2024. ISSN 1999-4915. doi: 10.3390/v16040599. URL http://dx.doi.org/10.3390/v16040599.

Joel Smoller. *Shock Waves and Reaction—Diffusion Equations*. Springer US, 1983. ISBN 9781468401523. https://dx.doi.org/10.1007/978-1-4684-0152-3.

Chantal J. Snoeck, Aurélie Sausy, Serge Losch, Félix Wildschutz, Manon Bourg, and Judith M. Hübschen. Usutu virus africa 3 lineage, Luxembourg, 2020. *Emerging Infectious Diseases*, 28(5):1076–1079, May 2022. ISSN 1080-6059. doi: 10.3201/eid2805.212012. URL http://dx.doi.org/10.3201/eid2805.212012.

Bálint Gergely Szabó, Anna Nagy, Orsolya Nagy, Anita Koroknai, Nikolett Csonka, Dorina Korózs, Krisztina Jeszenszky, Apor Hardi, Nóra Deézsi-Magyar, János Sztikler, Zoltán Bódi, Dániel Cadar, Gábor Endre Tóth, Liliána Veres, Erzsébet Barcsay, Mária Takács, and János Sinkó. First documented case of a fatal autochthonous Usutu virus infection in an immunocompromised patient in Hungary: a clinical-virological report and implications from the literature. *Virology Journal*, 22(1), July 2025. ISSN 1743-422X. doi: 10.1186/s12985-025-02890-9. URL http://dx.doi.org/10.1186/s12985-025-02890-9.

The MathWorks, Inc. *MATLAB*. Natick, Massachusetts, United States, 2025. Available from https://www.mathworks.com/help/pde/pde-problem-setup.html?s_tid=CRUX_topnav.

Gábor Endre Tóth, Marike Petersen, Francois Chevenet, Marcy Sikora, Alexandru Tomazatos, Alexandra Bialonski, Heike Baum, Balázs Horváth, Padet Siriyasatien, Anna Heitmann, Stephanie Jansen, Ruth Offergeld, Raskit Lachmann, Michael Schmidt, Jonas Schmidt-Chanasit, and Dániel Cadar. Blood donors as sentinels for genomic surveillance of West Nile virus in Germany (2020-2024) using a sensitive amplicon-based sequencing approach. June 2025. doi: 10.1101/2025.06.24.25329984. URL http://dx.doi.org/10.1101/2025.06.24.25329984.

J. M. A. van den Brand, R. S. Sikkema, E. Münger, B. Oude Munnink, A. Gröne, and M. P. G. Koopmans. Surveillance for arboviruses in free ranging dead birds in the Netherlands, 2016–2022. https://www.ebi.ac.uk/biostudies/studies/S-BSST1523, 2025.

P. van den Driessche and James Watmough. Reproduction numbers and sub-threshold endemic equilibria for compartmental models of disease transmission. *Mathematical Biosciences*, 180(1–2): 29–48, November 2002. ISSN 0025-5564. doi: 10.1016/s0025-5564(02)00108-6. URL http://dx.doi.org/10.1016/s0025-5564(02)00108-6.

Tatjana Vilibic-Cavlek, Tamas Petrovic, Vladimir Savic, Ljubo Barbic, Irena Tabain, Vladimir Stevanovic, Ana Klobucar, Anna Mrzljak, Maja Ilic, Maja Bogdanic, Iva Benvin, Marija Santini, Krunoslav Capak, Federica Monaco, Eddy Listes, and Giovanni Savini. Epidemiology of Usutu virus: The European scenario. *Pathogens*, 9(9):699, August 2020. ISSN 2076-0817. doi: 10.3390/pathogens9090699. URL http://dx.doi.org/10.3390/pathogens9090699.

Tatjana Vilibić-Čavlek, Ljubo Barbić, Ana Klobučar, Marko Vucelja, Maja Bogdanić, Dario Sabadi, Marko Kutleša, Branimir Gjurašin, Vladimir Stevanović, Marcela Curman Posavec, Linda Bjedov, Marko Boljfetić, Tonka Jozić-Novinc, Robert Škara, Morana Tomljenović, Željka Hruškar, Mahmoud Al-Mufleh, Tanja Potočnik-Hunjadi, Ivana Rončević, and Vladimir Savić. Re-emergence of Usutu virus and spreading of West Nile virus neuroinvasive infections during the 2024 transmission season in Croatia. *Viruses*, 17(6):846, June 2025. ISSN 1999-4915. doi: 10.3390/v17060846. URL http://dx.doi.org/10.3390/v17060846.

Elena Borisovna Vinogradova. *Culex pipiens pipiens mosquitoes: taxonomy, distribution, ecology, physiology, genetic, applied importance and control*. Number 2. Pensoft Publishers, 2000.

Doreen Walther and Helge Kampen. The citizen science project 'Mueckenatlas' helps monitor the distribution and spread of invasive mosquito species in Germany. *Journal of Medical Entomology*, 54(6):1790–1794, September 2017. ISSN 1938-2928. doi: 10.1093/jme/tjx166. URL http://dx.doi.org/10.1093/jme/tjx166.

Jianpeng Wang and Binxiang Dai. Qualitative analysis on a reaction-diffusion host-pathogen model with incubation period and nonlinear incidence rate. *Journal of Mathematical Analysis and Applications*, 514(2):126322, October 2022. ISSN 0022-247X. https://dx.doi.org/10.1016/j.jmaa.2022.126322.

Xueying Wang, Xiao-Qiang Zhao, and Jin Wang. A cholera epidemic model in a spatiotemporally heterogeneous environment. *Journal of Mathematical Analysis and Applications*, 468(2):893–912, December 2018. ISSN 0022-247X. https://dx.doi.org/10.1016/j.jmaa.2018.08.039.

Herbert Weissenböck, Tamás Bakonyi, Giacomo Rossi, Paolo Mani, and Norbert Nowotny. Usutu virus, Italy, 1996. *Emerging Infectious Diseases*, 19(2):274–277, February 2013. ISSN 1080-6059. doi: 10.3201/eid1902.121191. URL http://dx.doi.org/10.3201/eid1902.121191.

JP Woodall. The viruses isolated from arthropods at the East African virus research institute in the 26 years ending december 1963. *Proc E Afr Acad*, 2:141–146, 1964.